APPENDIX E

Trajectory Modelling in Support of the
Bay du Nord Development Project (RPS 2020)

equinor


equinor

Trajectory Modelling in Support of the Bay du Nord Development Project

Prepared for: Equinor Canada Ltd.

Project Number:
2018-P-022447

Date Submitted:
06/23/2020

Version:
Final Report

Project Manager
Matthew Horn, Ph.D.

RPS
55 Village Square Dr.
South Kingstown, RI USA
02879-8248

Release	File Name	Date Submitted	Notes
Revised Final	Equinor– RPS Technical Report_20200623.docx	06/23/2020	RPS Final version of report for review by Equinor
Revised Final	Equinor– RPS Technical Report_20190206.docx	02/06/2019	RPS Final version of report for review by Equinor
Revised Final	Equinor– RPS Technical Report_20181012.docx	11/30/2018	RPS Final version of report for review by Equinor
Final	Equinor– RPS Technical Report_20181012.docx	10/19/2018	RPS Final version of report for review by Equinor
Draft	Equinor– RPS Technical Report_20180824.docx	08/24/2018	RPS Draft version of report for review by Equinor
Draft	Equinor– RPS Technical Report_20180823.docx	08/23/2018	RPS Draft version of report for review by Equinor
Draft	Equinor– RPS Technical Report_20180822.docx	08/22/2018	RPS Draft version of report following senior technical review
Draft	Equinor– RPS Technical Report_20180817.docx	08/17/2018	RPS Draft version of report
Draft	Equinor – RPS Technical Report_20180814.docx	8/14/2018	RPS Draft version of report following team review
Draft	Equinor – RPS Technical Report_20180810.docx	8/10/2018	RPS Draft version of report

List of Contributors

Matthew Horn, Ph.D. – Project Lead and Senior Scientist

matt.horn@rpsgroup.com

Lisa McStay – Ocean Engineer, oil spill modeller and report preparation

Jenna Ducharme – GIS Specialist, figure generation

Steven Tadros – Scientist, Oil spill modeller and report preparation

Matthew Frediani – GIS Analyst, oil spill modeller and figure generation

Jeremy Fontenault – Senior GIS Specialist, report preparation

Deborah Crowley – Senior Scientist, Modeller

Mahmud Monim – Oceanographer, Metocean data preparation

Daniel Torre – Environmental Chemist, Data preparation

Deborah French McCay – Senior Scientist, Report review

Cheryl Morse – Programmer/Developer

Timothy Giguere – Programmer/Developer

Gabrielle McGrath – Report review

Tara Franey – Report review

Executive Summary

Study Summary

Oil spill trajectory and fate modelling was performed, as per EIS guidelines, to support an Environmental Impact Statement (EIS) for Equinor Canada Ltd. Bay du Nord Development Project in the Flemish Pass. The Project Area includes portions of the easternmost edge of the Flemish Pass, as well as the northwestern portion of the Flemish Cap. Modelling was performed at representative sites that were located approximately 450-500 km east of St. John's, Newfoundland and Labrador, with drilling and production activities anticipated in waters that range in depth from <500 m to >1200 m. Hypothetical continuous unmitigated subsurface blowout scenarios of Bay du Nord crude oil (BdN – a representative crude oil for this region) were developed at two locations within the Project Area – Site 1 is in the Core Bay du Nord Development Area and Site 2 is in the larger Project Area. The water depths are approximately 1,134 m for Site 1 and 500 m for Site 2. Unmitigated subsurface blowouts of BdN crude oil were modelled as continuous releases for 36 days and 115 days at both hypothetical release locations, with total simulation times of 160 days. The 36-day releases represent the successful mobilization and implementation of a capping stack to contain a release, while the 115-day releases represent the anticipated time to drill a relief well. The modelled release rate of 10,500 m^3/day was the same for both the 36- and 115-day releases at both sites. The estimated release rate of hydrocarbons in the subsurface blowout scenarios are conservative (i.e., high) based on the current knowledge of the reservoir and other subsurface properties associated with the blowout scenarios. These scenarios represent the range of water depths, release rates, and the anticipated time required to contain a release. In addition, several shorter duration and smaller volume releases were modelled to be representative of spills that could occur from different sources. Releases from the floating production storage and offloading unit (FPSO) were investigated as surface releases of BdN totaling 8,300 m^3 over a two-day period. The shuttle tanker was modelled as a surface release during offloading totaling 1,000 m^3 over a one-hour period. Additional surface releases from bunkering operations (i.e., transfer from a vessel) were modelled as 6 m^3 of marine diesel. An additional seabed batch spill was modelled to be representative of a failure in the production flowline with 500 m^3 of BdN being released over one day. Mitigation modelling that included the application of subsea dispersant injection (SSDI) and surface dispersants from airplanes and vessels was also performed on the 36-day capping stack releases at Sites 1 and 2.

Study Goals

There were several goals of the modelling study. A stochastic assessment was used to provide an understanding of the probability and minimum time to exposure, based upon highly conservative thresholds for shoreline oiling, concentrations of hydrocarbons in the water column, and oil on the water surface. The goal was to identify the likely areas where oil exposure may occur as well as the likelihood and minimum time based upon the variable environmental conditions. To determine the level of potential concentrations (i.e. actual time varying concentrations rather than simply the knowledge of a threshold exceedance), individual deterministic scenarios were selected to represent 95th percentile maximum potential effects. These highly conservative 95th percentile scenarios were identified from area of surface oil, length of shoreline oiled, and mass of oil in the water column. In essence, very low probability spill events were used to identify even lower probability credible “worst case” (i.e., highly conservative subset of all modelled scenarios) to maximize potential effects and ensure that spill planning and preparedness is sufficient to respond to nearly any situation that may arise at the release location.

Study Use

It is understood that the hypothetical releases modelled in spill trajectory studies are in no way intended to predict a specific future event. Rather, they are used as a planning tool for application in environmental assessments and spill contingency planning. The results presented in this document demonstrate that there are a range of potential trajectories and fates that may result following a release of crude oil, based upon the environmental variability that may occur over the course of a year or many years. If there were any event such as a subsurface blowout or topside release, it is likely that a different volume of oil may be released from a different location and under different environmental conditions than modelled here. While it is impossible to know the exact trajectory and fate of an oil release in the future, inferences may be made from this study.

Models

In order to reproduce the dynamic and complex processes associated with deep subsea blowout releases, two models were used. The OILMAPDeep near-field model was used to characterize the dynamics of the jet and buoyant-plume phases of a subsurface blowout. It contains two sub-models, a plume model and a droplet size model. The plume model predicts the evolution of plume position, geometry, centerline velocity, and oil and gas concentrations until the plume either surfaces or reaches a terminal height, at which point the plume is trapped. The droplet size model is used to characterize the size and distribution of oil droplets, including the associated mass of oil being released at specific

water depths, where the plume became neutrally buoyant. The output data from OILMAPDeep was then used to initialize the SIMAP model, which simulates the far-field trajectory, fate, and potential exposure in the marine environment following a release.

Geographical Data

Geographical data including habitat mapping and shoreline identification and classification were obtained from multiple data sources. For Canadian areas, province-specific data from the New Brunswick Department of Natural Resources and Nova Scotia Department of Natural Resources were used, as well as high-resolution data covering a broad area from Environment and Climate Change Canada. For the U.S. shoreline, the U.S. National Oceanic and Atmospheric Administration's Environmental Sensitivity Index and Maine Department of Environmental Protection's Environmental Vulnerability Index were used. Bathymetry was characterized using databases provided by NOAA National Geophysical Data Center and GEBCO (General Bathymetric Chart of the Oceans).

Wind and Currents

Wind data for this study were obtained from the U.S. National Centers for Environmental Prediction (NCEP) Climate Forecast System Reanalysis (CFSR) model. Currents for the North Atlantic region were acquired from the U.S. Navy Global HYCOM (HYbrid Coordinate Ocean Model) circulation model. All data were acquired and used for the period between January 2006 and December 2012.

Stochastic Analysis

A stochastic analysis was conducted for each hypothetical release location, consisting of either 171 or 172 individual model runs per stochastic scenario depending on the release duration. Each simulation was initialized with a different start date/time between 2006-2012 to sample a range of environmental conditions. However, the same set of start dates/times were used in each stochastic assessment to ensure comparability. The dates and times were selected randomly from within 14-day intervals spanning the entire seven years of data. Results of the stochastic analysis included probability footprints above specified thresholds for surface, water column, and shoreline contact and minimum time to oil exposure. Because the runs spanned seven full years and included the associated seasonal variability, the complete set was referred to as annual summaries. To investigate seasonality, results from stochastic analyses were broken into two seasons depending on the majority of modelled days falling within either ice free conditions (summer) from May through October or periods with ice-cover (winter) from November through April

It is important to note that although large footprints of oil are depicted for stochastic analyses, they are not the expected distribution of oil from any single release. These maps do not provide any information on the quantity of oil in a given area. They simply denote the probability of oil exceeding the specific threshold passing through each grid cell location in the model domain over the entire model duration (160 days), based on the entire ensemble of runs (171 and 172 individual releases for both locations). Only probabilities of 1% or greater were included in the map output, as lesser probabilities represent random noise in each set of 171 and 172 trajectories. Stochastic maps of water column exposure depict the likelihood that dissolved and total hydrocarbon concentrations will exceed the identified threshold at any depth within the water column. However, these figures do not specify the depth at which this threshold exceedance occurs and do not imply that the entire water column (i.e., from surface to bottom) will experience a concentration above the identified threshold.

Deterministic Analysis

Representative deterministic scenarios (i.e., single trajectory) were identified from each set of stochastic subsurface blowout results. Individual scenarios were selected based upon the size of the surface oil footprint, the length of shoreline contacted with oil, and the concentration of dissolved hydrocarbons in the water column, based upon a set of highly conservative socio-economic thresholds:

- Surface oil average thickness >0.04 µm,
- Shore oil average concentration >1.0 g/m^2,
- Subsurface (within the water column) dissolved hydrocarbon concentrations >1.0 µg/L.

The selected cases for deterministic analysis included the identified 95th percentile scenarios for surface oil footprint, water column concentration, and shoreline oil length identified for each release location. In addition to these twelve deterministic scenarios (2 locations, 2 release volumes, and 3 percentiles), batch spills of BdN and marine diesel were modelled, including release volumes ranging from 6 m^3 to 8,300 m^3 at Site 1 in the Core BdN Development Area to be representative of potential releases that could occur during production activities.

Results

Oil Trajectory and Fate

Stochastic results are useful in planning for oil spill response, as they characterize the probability that regions may experience oil exposure above specified thresholds, taking into account the environmental variability that is expected from many release scenarios over time that would experience different environmental forcing (e.g., variable wind and current speed and direction) over the course of many years. Stochastic footprints of predicted surface oil exceeding a conservative socio-economic threshold

of 0.04 µm (the thickness of a barely visible sheen) were between 3,217,000 and 3,565,000 km^2 for the modelled 160-day simulations. Within the footprints, the highest predicted likelihood of oil above 0.04 µm (75-90%) occurred to the east and south of the release site, while there was a much lower probability (<25%) for oil being transported to the north or west towards Canadian waters. Footprints depicting higher probability contours (90%) are much smaller than the total footprint (>1%), which range from 526,900 – 1,436,000 km^2 of the modelled domain, depending on the scenario. Seasonal variations were evaluated yielding different surface oil predictions for summer versus winter scenarios based upon the environmental conditions and prevailing winds and currents. For both the 36- and 115-day releases, larger surface oil footprints associated with >90% probability contours were predicted for summer scenarios at both sites indicating lower wind speeds and less entrainment of surface oil into the water column from wind induced surface breaking waves. However, the areas associated with lower probabilities (i.e., 1% and 10%) are larger in the winter, indicating more extensive and variable transport with a higher likelihood of entrainment and eventual resurfacing.

The probability of oil making contact with the shoreline was less than a 22-25% for all scenarios, with the longest lengths of susceptible shoreline predicted for the 115-day winter release scenarios. Oil has the potential to reach shore in as little as 13-15 days for winter scenarios and 31-35 days for summer scenarios. Therefore, the oil that was predicted to make contact with shorelines was expected to be highly weathered (i.e. less toxic), patchy, and discontinuous, as minimum time estimates ranged from weeks to over a month. Based upon 171 or 172 individual trajectories, it was predicted that as much as 3,933 km (Site 1) and 3,635 km (Site 2) of shoreline may be susceptible following a release. Most of the shoreline contact was predicted to occur on the southern shore of the Avalon Peninsula of the island of Newfoundland (10-25% probability), and as far north as Labrador.

Shoreline contact at the end of the 160-day simulation was less than 2% of the total released volume for all simulations. The amount of evaporation and degradation was relatively consistent between model runs. Approximately 45-51% of the BdN released was predicted to evaporate and another 27-36% to degrade by the end of the 160-day simulation. Most of the variability in the mass balances were associated with the amount of oil found either on the surface or entrained within the water column based upon the spatially and temporally variable winds, which induce surface breaking waves that force surface oil into the water column.

Accidental discharges which result in small volume near-instantaneous batch spills of BdN and marine diesel resulted in smaller areas and volumes of potential hydrocarbon exposure, when compared to the blowout scenarios. At the end of the 30-day BdN surface batch spill simulations (8,300 m^3 and 1,000 m^3), 29% of the released volume was predicted to remain floating on the water surface, 37-39% evaporated into the atmosphere, 10-11% remained entrained in the water column, 0.01% adhered to suspended

sediment, 0% contacted the shore, and 22-24% degraded. At the end of the marine diesel surface batch spill, <1% was predicted to remain on the water surface, 58% evaporated, 12% entrained into the water column, and 30% degraded. At the end of the 30-day simulation of the seafloor batch spill of BdN at Site 1, 32% was predicted to remain on the water surface, while 42% evaporated, 6% entrained, and 20% degraded.

Spill Response Mitigation Modelling

Oil spill response mitigation modelling that included subsurface dispersant injection (SSDI) and surface dispersant application from aircrafts and vessels was performed on the 36-day surface oil exposure cases. The SIMAP model was used to predict the changes in the dynamics and ultimate trajectory and fate of the releases. The SSDI was effective in reducing the droplet size distribution of the subsurface oil released from the blowout. This reduction in droplet size results in a larger surface area to volume ratio which reduces the rise velocity of the oil and increases the amount of dissolution and resulting biodegradation, when compared to the larger droplets in the unmitigated scenarios. For a fraction of the released oil, droplet sizes were reduced to a level that resulted in their permanent entrainment. Due to these changes, nearly half as much of the released oil was predicted to evaporate to the atmosphere (averaging 48 vs 27%) and a much larger proportion was predicted to degrade in the water column (averaging 35 vs 55%) in the mitigated scenarios.

Document Summary

This report includes an introduction describing the region, the modelling approach, the methodology, and finally the results of the study. The model results are summarized in figures and tables in the main body of this document, describing the potential for oil exposure within the water column, on the water surface, and along shorelines. This document is broken down into several sections.

- Section 1 – Introduction
- Section 2 – Background and Scenarios, including description of project area, modelling approach with the OILMAPDeep and SIMAP models, scenarios, and uncertainty
- Section 3 – Model Input Data.
- Section 4 – Model Results, including both stochastic and deterministic oil trajectory and fate model runs
- Section 5 – Discussion and Conclusions
- Section 6 – References
- Appendix A – additional information including a detailed description of the OILMAPDeep and SIMAP models, fate processes, and algorithms used.

Table of Contents

List of Figures

List of Tables

List of Acronyms and Abbreviations

3D	Three dimensional, referring to the vertical and horizontal, as in x, y, and z directions
AL	In modelling terms, the aliphatic portion of the total hydrocarbon is modelled as a volatile but insoluble fraction within the SIMAP model and can therefore evaporate but will not dissolve. Note that this is different than the chemical definition of aliphatics.
AR	In modelling terms, the aromatic portion of the total hydrocarbon is modelled as a volatile and soluble fraction within the SIMAP model and can therefore evaporate and dissolve. Note that this is different than the chemical definition of aromatics and as an example AR may contain low molecular weight aliphatics that may be soluble.
BAOAC	Bonn Agreement Oil Appearance Code
BdN	Bay du Nord crude oil
BTEX	Benzene, toluene, ethylbenzene, and xylene
CERCLA	The U.S. Superfund or Comprehensive Environmental Response, Compensation, and Liability Act of 1980
EIS	Environmental Impact Statements
FPSO	Floating production storage and offloading unit
GEBCO	The General Bathymetric Chart of the Oceans operated by the International Hydrographic Organization (IHO) and Intergovernmental Oceanographic Commission (IOC) of UNESCO.
HYCOM	The U.S. Navy HYbrid Coordinate Ocean Model used for currents
MAH	Monocyclic aromatic hydrocarbons (monoaromatic), with only one six carbon ring
MICOM	Miami Isopycnic-Coordinate Ocean Model
NCODA	U.S. Navy Coupled Ocean Data Assimilation
NOAA	U.S. National Oceanic and Atmospheric Administration
NRC	U.S. National Research Council
NRDA	U.S. Natural Resource Damage Assessment
NRDAM/CME	Natural Resource Damage Assessment Model for Coastal and Marine Environments

PAH	Polycyclic aromatic hydrocarbons (polyaromatic), with two or more six-carbon rings
PPB	Part per billion, as referring to concentration. Roughly equivalent to µg/L
PPM	Part per million, as referring to concentration
SIMAP	Spill Impact Model Application Package, a 3D trajectory and fate model developed by RPS
Site 1 / Site 2	Bay du Nord Development Project hypothetical release locations
THC	Total hydrocarbon concentrations

1 Introduction

RPS (previously Applied Science Associates, Inc.) conducted trajectory and fate modelling in support of an Environmental Impact Statement (EIS) for the Equinor Canada Ltd (Equinor Canada) Bay du Nord Development Project (the Project). The EIS Project Area is located approximately 450 km east of the Newfoundland coast in the Flemish Pass area. Water depths in the Project Area range from approximately 340 m to 1200 m. Major currents, including the Labrador Current and the Gulf Stream, influence the circulation and biological productivity in this region.

This modelling was conducted to evaluate hypothetical unmitigated and mitigated release events associated with production of oil and gas, including large scale deep-water blowouts of Bay du Nord (BdN) crude oil from the wellhead at the seafloor and smaller scale batch spills of BdN crude and marine diesel at the surface and at depth. Three-dimensional (3D) oil spill trajectory and fate modelling and analyses were performed to support evaluation of the potential movement and behavior of oil following hypothetical releases into the Northwest Atlantic Ocean near Newfoundland. RPS' nearfield OILMAPDeep blowout model and the far-field Spill Impact Model Application Package (SIMAP) oil trajectory and fate model were used. This report provides a description of the Project Area and modelled scenarios, an overview of the modelling approach, details about the model input data used, and a presentation and discussion of the modelled results.

2 Background and Scenarios

2.1 Project Area

Newfoundland is comprised of a series of islands off the east coast of Canada, and along with Labrador forms the easternmost Canadian province. The relatively shallow waters of the continental shelf extend eastward into the Northwest Atlantic Ocean up to 500 km off the Newfoundland coast. The Project Area (47.7-48.4 °N, 45.9-47.3 °W) contains the northwestern side of the Flemish Cap and the northeastern portion of the Flemish Pass, located east of Newfoundland (Figure 2-1). An expanded view of the Project Area highlights the location of the hypothetical release locations (Figure 2-2). Site 1 is in the Core Bay du Nord Development Area and is also within a designated Vulnerable Marine Area as it is Fishery Closure Area (NAFO). Site 2 is representative of the shallower waters in the larger Project Area. This biologically productive region sits atop substantial petroleum resources, with the Hibernia, White Rose, and Terra Nova oil fields in close proximity. Bathymetry in the area ranges from less than 100 m over the Grand Banks to greater than 4,500 m deep in the Labrador Basin. The model domain extends as from 42°N to 57°N and 72°W to 28°W, encompassing Canadian, U.S., and International waters. This modelled extent is

much larger than the Project Area, as hypothetical releases of oil will be tracked for long periods of time (160 days).

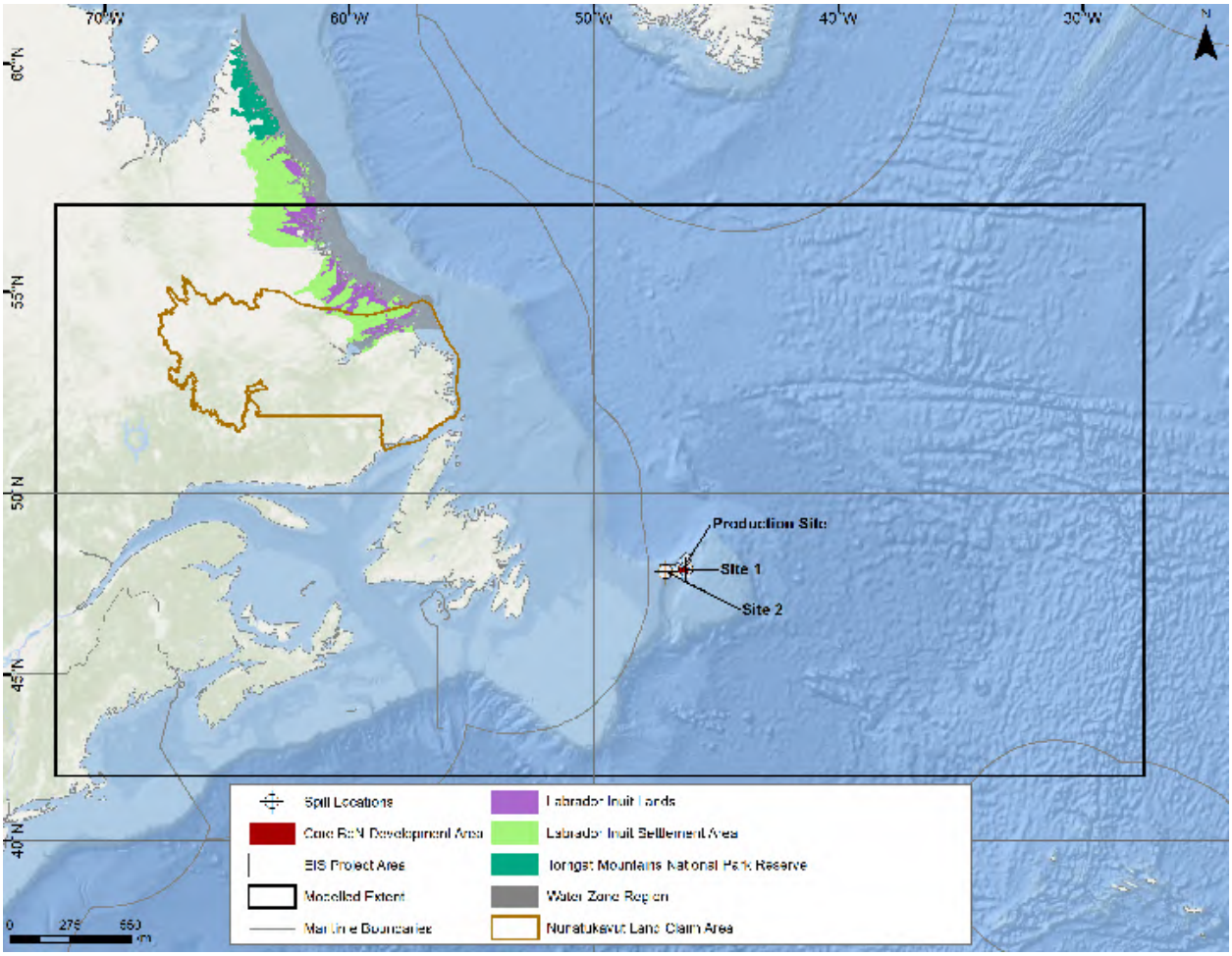

Figure 2-1. Map of the Project Area, including hypothetical release locations: Site 1, Site 2, and the proposed FPSO location (labelled Production Site). The black box represents the modelling extent, while the smaller shaded boxes represent the EIS Project Area and Core BdN Development Area.

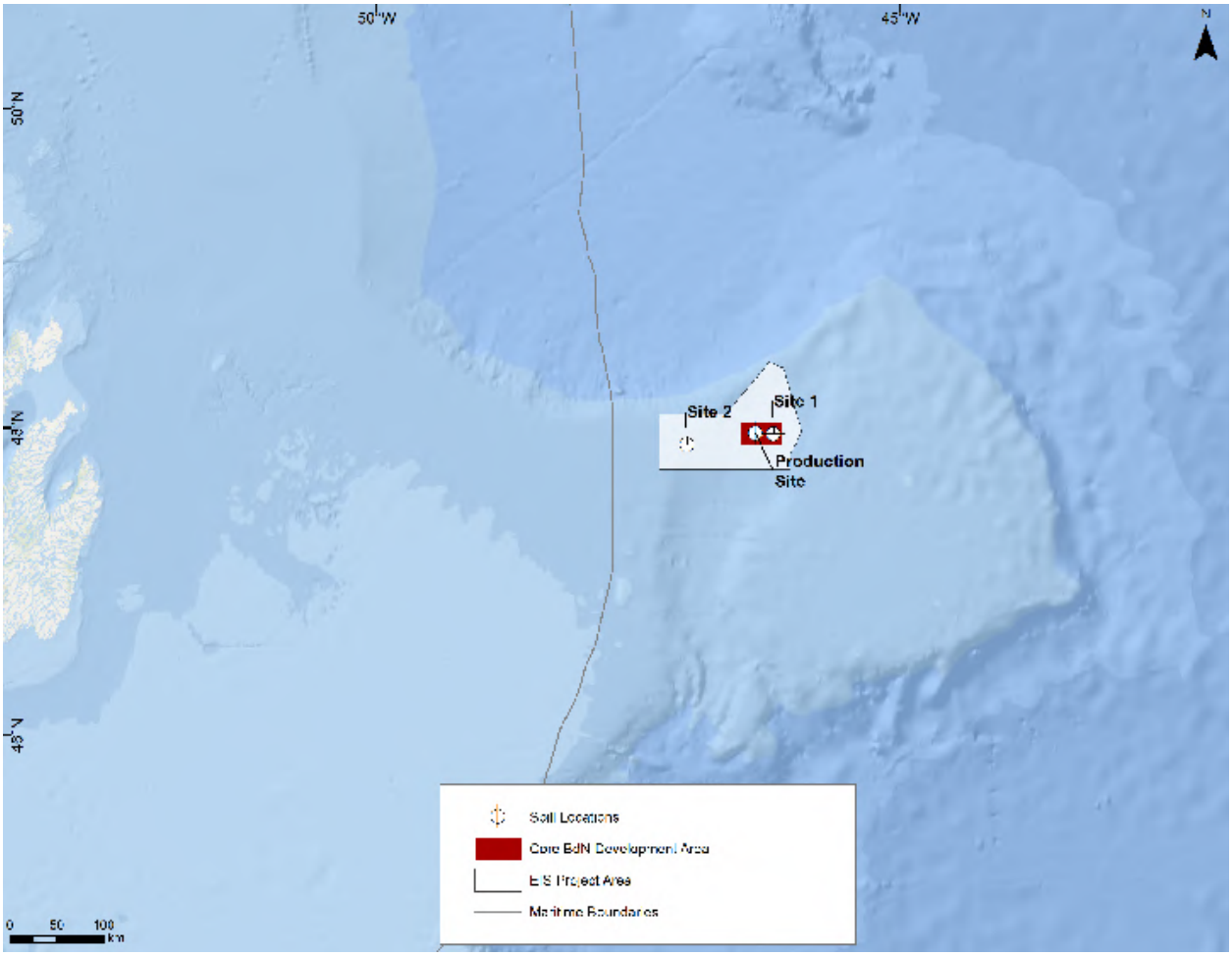

Figure 2-2. Map of the EIS Project Area and Core BdN Development Area including hypothetical release locations: Site 1, Site 2, and the proposed FPSO location (labelled Production Site).

2.2 Modelling Approach

This modelling study employed a combined stochastic and deterministic approach to determine the potential trajectory and fate of hypothetical hydrocarbon releases from two sites east of Newfoundland within the Project Area (Table 2-1). Stochastic modelling provides a probabilistic view of the likelihood that a given region might be exposed to released hydrocarbons over specified thresholds given the range of possible environmental conditions that may occur within and across multiple years. A deterministic analysis provides a view of the time history of the specific movement and behavior of released product from a given (e.g., representative) individual release. Together, these methods provide a more complete view of both the likelihood and degree of potential exposure.

For this report, stochastic information is presented for predicted surface oil thickness, shoreline oil mass, and dispersed oil in the water column exceeding the threshold concentration for the full year (i.e., annual), and for different seasons with variable ice-cover conditions (i.e., summer/ice-free and winter/ice-covered). Individual representative deterministic trajectories that characterize single release scenarios are also presented. Stochastic analyses of hypothetical blowouts were modelled at two sites using the physical-chemical properties of the specific oil type that may be released and seven years of variable environmental data, which are discussed in Section 3. Site 1 is representative of location of the production installation and is within a sensitive marine area, a fisheries closure area. Site 2 is within the larger Project Area and is representative of potential future development. At each location, a total of 171 or 172 individual oil release trajectories were modelled throughout the year, depending on the release duration (Table 2-1). The smaller number of scenarios were contained in the shorter duration release with 81 winter and 90 summer scenarios. The longer duration release included 83 winter and 89 summer scenarios. The duration of each modelled simulation was 160 days.

In addition, batch spills of BdN and marine diesel were analyzed to evaluate potential discharges between surface vessels and on the sea floor. These volumes are representative of FPSO, offloading, bunkering, and production flowline operations and were selected to bound the potential range of effects that are typical of small volume releases of crude oil and marine diesel.

Table 2-1. Release location and release information used in the stochastic and deterministic modelling approaches.

Modelling Approach	Release Location	Depth of Release	Release Duration	Model Duration	Number of Model Runs	Released Product	Release Type	Release Volume
Stochastic and Deterministic*	Site 1 (47.96°N 46.21°W)	1,134 m	36 d	160 d	171	BdN	Subsurface Blowout	378,000 m^3 (10,500 m^3/day)
	Site 1 (47.96°N 46.21°W)	1,134 m	115 d		172			1,207,500 m^3 (10,500 m^3/day)
	Site 2 (47.89°N, 47.04°W)	500 m	36 d		171			378,000 m^3 (10,500 m^3/day)
	Site 2 (47.89°N, 47.04°W)	500 m	115 d		172			1,207,500 m^3 (10,500 m^3/day)
Deterministic	Proposed FPSO location (47.96°N, 46.38°W)	Surface	2 d	30 d	1	BdN	Batch Spill - FPSO	8,300 m^3 (4,150 m^3/day)
			1 hr		1		Batch Spill-Offloading	1,000 m^3
			2 mins		1	Marine Diesel	Batch Spill - Bunkering	6 m^3
	Site 1 (47.96°N 46.21°W)	1,134 m	1 d		1	BdN	Batch Spill Production Flowline	500 m^3

*The 95th percentile "worst case" scenarios for surface, shoreline, and water column concentrations were identified for each stochastic assessment and modelled as three separate deterministic simulations.

2.2.1 Modelling Tools

Hypothetical release scenarios were simulated using the OILMAPDeep blowout model and the SIMAP, oil trajectory and fate model, both developed by RPS. OILMAPDeep was used to define the near-field dynamics of the subsurface blowout plume, which was then used to initialize the far-field modelling conducted in SIMAP. The near-field plume dynamics are modelled to predict the mass, location, and droplet size distribution of the subsurface plume of oil at the termination (i.e., trap) height of the buoyant oil and gas plume. This termination height occurs when the oil droplets pass from the jet phase through to the buoyant plume phase by diluting with enough surrounding seawater to become neutrally buoyant, based upon the environmental conditions, the specific chemical and physical properties of the oil, and other release parameters. Typically, the near-field model is considered at timescales of seconds and length scales of hundreds of meters, whereas the far-field model is on the scale of many hours/days and tens or even hundreds of kilometers.

OILMAPDeep Model

The OILMAPDeep model incorporates the basic dynamics of a subsurface oil and gas plume and the associated complexities of increased hydrostatic pressure at depths deeper than 200 m. It contains two sub-models, i.e., a plume model and a droplet size model. The plume model predicts the evolution of the plume position, geometry, centerline velocity, and oil and gas concentrations until the plume either surfaces or reaches a terminal height (i.e., trap height). At this height, the plume no longer rises by buoyant forces, and the oil contained within the plume escapes to the surrounding water and rises based on the individual buoyancies of the droplets. The jet created by the blowout is modelled by considering the momentum of the oil discharge, the density difference between the expanding gas bubbles in the plume and the receiving water, the entrainment of water into the plume, the mixing by turbulence within the plume, the hydrate formation, and the transport by local ambient currents. The droplet size model predicts the size and volume (mass) distribution of the oil droplets in the release at the trap height or at the water surface, which influences trajectory and fate processes, such as oil rise velocity and dissolution.

For oil discharged during a deep-water blowout, the oil droplet size distribution has a profound effect on how oil is transported and behaves after the initial release as a buoyant plume. The size of the individual droplets dictates buoyancy, which controls the length of time that oil will remain within the water column before surfacing. Large oil droplets surface faster than small ones, thus large droplets more quickly generate a floating oil slick, which may be transported by winds and surface currents. Small droplets remain in the water column longer than large droplets and are subjected to subsurface advection-diffusion processes and are therefore transported within the water column for a longer period of time. As oil is transported by subsurface currents away from the release location, natural dispersion of the oil droplets quickly reduces concentrations within the water column. However, the lower rise velocities associated with smaller oil droplets correspond to longer residence times of oil suspended in the water column, which can increase the dissolution of soluble components and potentially result in larger volumes of water being affected. Details of the OILMAPDeep model background theory, inputs, algorithms, and outputs can be found in Appendix A.

SIMAP Model

The SIMAP model is a state-of-the-art oil trajectory, fate, and effects model that is constantly being developed based upon the growing body of field and laboratory data associated with releases of oil in many different environments. It originated from the oil fate sub-model within the Natural Resource Damage Assessment Models for Coastal and Marine Environments (NRDAM/CME). RPS developed the NRDAM/CME in the early 1990s for the U.S. Department of the Interior for use in “type A” Natural Resource Damage Assessment (NRDA) regulations under the Comprehensive Environmental Response,

Compensation and Liability Act of 1980 (CERCLA). The most recent version of the type A models, the NRDAM/CME (Version 2.4, April 1996) was published as part of the CERCLA type A NRDA Final Rule (Federal Register, May 7, 1996, Vol. 61, No. 89, p. 20559-20614). The technical documentation for the NRDAM/CME is in French et al. (1996). While the NRDAM/CME was developed for simplified NRDAs of small releases in the U.S., SIMAP was further developed to evaluate fate and exposure of both real and hypothetical releases in marine, estuarine, and freshwater environments worldwide. Additions and modifications to SIMAP include increasing model resolution, allowing site-specific input data, incorporating spatially and temporally varying current data, evaluating subsurface releases and movements of subsurface oil, tracking multiple chemical components of the oil, enabling stochastic modelling, and facilitating analysis of results.

The 3D physical fates model estimates the distribution of whole oil and oil components on the water surface, on shorelines, in the water column, and in sediments as both mass and concentration. Because oil contains many chemicals with varying physical and chemical properties, and the environment is spatially and temporally variable, the oil rapidly separates into different environmental compartments through multiple fate processes. Oil fate processes included in SIMAP are spreading (gravitational and by shearing), evaporation, transport, randomized dispersion, emulsification, entrainment (natural and facilitated by dispersant), dissolution of the soluble fraction of oil into the water column, volatilization of dissolved hydrocarbons from the surface water, adherence of oil droplets to suspended sediments, adsorption of soluble and sparingly-soluble aromatics to suspended sediments, sedimentation, and degradation. Oil trajectory and weathering endpoints include surface oil, emulsified oil (mousse), tar balls, suspended oil droplets, oil adhered to particulate matter, dissolved hydrocarbon compounds in the water column and pore water, and oil on and in bottom sediments and shoreline surfaces. Details of the SIMAP model background theory, inputs, algorithms, and outputs can be found in Appendix A.

2.2.2 Stochastic Approach

A stochastic approach was employed to determine the footprint and probability of areas that are at increased risk of oil exposure based upon the variability of meteorological and hydrodynamic conditions that might prevail during and after a release. A stochastic scenario is a statistical analysis of results generated from many different individual trajectories of the same release scenario, with each trajectory starting at a randomized time from a relatively long-term window. For this project, individual trajectory start dates were selected randomly every 14 days throughout the window of environmental data coverage to ensure that the data was adequately sampled. This stochastic approach allows for the same type of release to be analyzed under varying environmental conditions (e.g., summer vs. winter or one year to the next). The results provide the probable behavior of the potential releases based upon this environmental variability.

In order to reproduce the natural variability of winds and currents, the model requires both spatially- and temporally-varying datasets. Historical observations and models of multiple-year wind and current records were used to perform the simulations within the coinciding time period. These datasets allow for reproduction of the natural variability of the wind and current speeds and directions. Optimally, the minimum time window for stochastic analysis is at least five years, so that various weather patterns from year to year are represented. Seven years of environmental data have been used for this modelling study. Using wind and current data from throughout this extensive period, a sufficient number of model runs will adequately sample the variability in the time sequences of wind and current speeds and directions in the region of interest and will result in a prediction of the probable oil pathways for a release at the prescribed location.

Stochastic analyses provide two types of information: 1) the areas associated with probability of oil exposure at some time during or after a release, and 2) the shortest time required for oil to reach any point within the areas predicted to be exposed above a specified threshold. The left panel of Figure 2-3 depicts four individual trajectories predicted by SIMAP for a generic example scenario. Because these trajectories were started on different dates and times, they experienced varying environmental conditions, and thus traveled in different directions. To compute the stochastic results, tens to hundreds of individual trajectories like the four depicted here were overlain and the number of times that each given location throughout the modelled domain was intersected by the different trajectories was used to calculate the probability of oil exposure for each specific location. This process is illustrated by the stacked runs in the right panel of Figure 2-3. The predicted footprint is the cumulative oil-exposed area for all of the ten to hundreds of individual releases combined. The color-coding represents a statistical analysis of all the individual trajectories to predict the probability of oil at each point in space, based upon the environmental variability. The footprint of any single release of oil, be it modelled or real, would be much smaller than the cumulative footprint of all the runs used in the stochastic analysis. Similarly, the footprint of oil from any individual release at a single time step (snapshot in time) would be even smaller than the cumulative swept area depicted here.

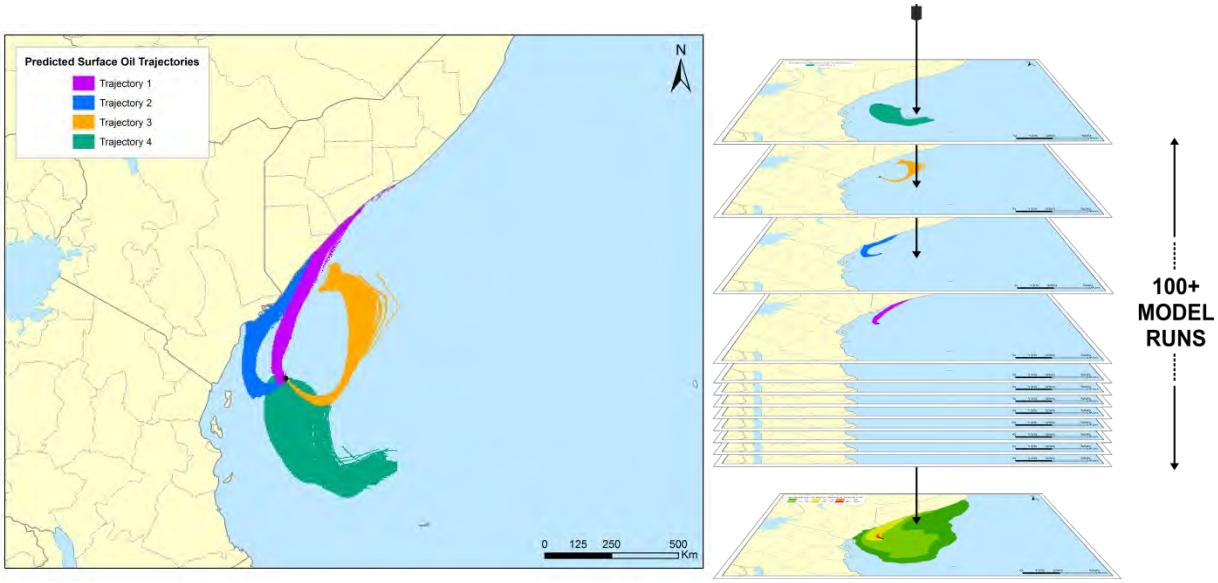

Figure 2-3. Examples of four individual release trajectories predicted by SIMAP for a generic release scenario simulated with different start dates and therefore environmental conditions. Tens to hundreds of individual trajectories are overlaid (shown as the stacked runs on the right) and the frequency of contact with given locations is used to calculate the probability of threshold exceedance during a release.

The number of individual trajectories and the timeframe of a given stochastic analysis play roles in the spatial extent of the resulting stochastic footprints. More individual runs may incorporate greater environmental variability, which may result in larger footprints. As the number of trajectories modelled increases, the confidence and resolution of reported probabilities also increase. Annual stochastic model runs resulted in the largest footprint, encompassing all environmental variability throughout the years. Seasonal footprints may be smaller, encompassing only the environmental variability expected within the smaller time period (e.g., prevailing winds, seasonal patterns, etc.). It is important to note that a single trajectory encounters only a small portion of an overall stochastic probability footprint (e.g., an individual trajectory may be less than 10% of an annual stochastic footprint). Maps of probability and minimum time to oil exceeding identified thresholds are provided in Section 4.1.

2.2.3 Thresholds of Interest

In a stochastic analysis, multiple model runs (tens to hundreds of releases) are overlaid upon one another to create a cumulative footprint of the potential trajectories. When combined with one another, the many individual deterministic footprints can be used to generate an area of probability that describes the potential areas that may be exposed to oil from the entire suite of modelled conditions. To determine the probability or likelihood of potential exposure, specific thresholds for surface oil thickness, oil on shorelines and sediments, and in-water concentrations were required (Table 2-2).

Above these conservative socio-economic thresholds, previous studies have identified that there is the potential that negative effects may occur. Figures and further analyses in this study include the more conservative lower socio-economic thresholds of concern calculated from stochastic results. The use of such conservative thresholds serves as more of a binary "yes/no" question of whether any oil has passed through each identified area. Should a higher, less conservative stochastic threshold be used (e.g., ecological threshold), the predicted probability footprint would be much smaller.

Floating surface oil is expressed as mass per unit area, averaged over a defined (grid cell) area. If the oil is evenly distributed in that area, it would be equivalent to a mean thickness, where 1 micron (µm) of thickness corresponds to a layer of oil that has a mass concentration of approximately 1 g/m^2. Surface oil thickness is typically associated with visual appearance by aerial observation for responders (NRC, 1985; Bonn Agreement, 2009, 2011; NOAA, 2016b; Table 2-3). As an example, barely visible sheens may be observed above 0.04 µm and silver sheens correspond with surface oil thickness of approximately 0.3 µm. Crude and heavy fuel oils greater than 1 mm thick typically appear as black oil while light fuels and diesels that are greater than 1 mm thick may appear brown or reddish. Because of the differences between oils and their degree of weathering, as well as the weather conditions and sea state at the time of observations, floating oil will not always have the same appearance. As oil weathers, it may be observed in the form of scattered floating tar balls and tar mats where currents converge. Typically, oil slicks in the environment would be observed as patchy and discontinuous with a range of visual appearances including silver sheen, rainbow sheen, and metallic areas simultaneously, as a combination of thicknesses may be present (Figure 2-4). Thus, a model result presented as average oil mass per unit area or "thickness" is actually a region with patches of oil of varying thickness, which when distributed evenly in the area of interest, would be on average a certain thickness.

Table 2-2. Thresholds used to define areas and volumes exposed above levels of concern.

Threshold Type	Cutoff Threshold	Rationale/Comments (Socio-economic, Response, Ecological)	Visual Appearance	References
Oil Floating on Water Surface	0.04 g/m^2	**Socio-economic:** A conservative threshold used in several risk assessments to determine effects on socio-economic resources (e.g., fishing may be prohibited when sheens are visible on the sea surface). Socio-economic resources and uses that would be affected by floating oil include commercial, recreational and subsistence fishing; aquaculture; recreational boating, port concerns such as shipping, recreation, transportation, and military uses; energy production (e.g., power plant intakes, wind farms, offshore oil and gas); water supply intakes; and aesthetics.	Fresh oil at this minimum thickness corresponds to a slick being barely visible or scattered sheen (colorless or silvery/grey), scattered tarballs, or widely scattered patches of thicker oil.	French McCay et al., 2011; French McCay et al., 2012; French McCay, 2016; Lewis, 2007, Bonn Agreement
	10 g/m^2	**Ecological:** Mortality of birds on water has been observed at and above this threshold. Sublethal effects on marine mammals, sea turtles, and floating Sargassum communities are of concern.	Fresh oil at this thickness corresponds to a slick being a dark brown or metallic sheen.	French et al., 1996; French McCay, 2009 (based on review of Engelhardt, 1983, Clark, 1984, Geraci and St. Aubin 1988, and Jenssen 1994 on oil effects on aquatic birds and marine mammals); French McCay et al., 2011; French McCay et al., 2012; French McCay, 2016
Shoreline Oil	1.0 g/m^2	**Socio-economic/Response:** A conservative threshold used in several risk assessments. This is a threshold for potential effects on socio-economic resource uses, as this amount of oil may trigger the need for shoreline cleanup on amenity beaches and affect shoreline recreation and tourism. Socio-economic resources and uses that would be affected by shoreline oil include recreational beach and shore use, wildlife viewing, nearshore recreational boating, tribal lands and subsistence uses, public parks and protected areas, tourism, coastal dependent businesses, and aesthetics.	May appear as a coat, patches or scattered tar balls, stain	French-McCay et al., 2011; French McCay et al., 2012; French McCay, 2016
	100 g/m^2	**Ecological:** This is a screening threshold for potential ecological effects on shoreline flora and fauna, based upon a synthesis of the literature showing that shoreline life has been affected by this degree of oiling. Sublethal effects on epifaunal intertidal invertebrates on hard substrates and on sediments have been observed where oiling exceeds this threshold. Assumed lethal effects threshold for birds on the shoreline.	May appear as black opaque oil.	French et al., 1996; French McCay, 2009; French McCay et al., 2011; French McCay et al., 2012; French McCay, 2016
In Water Concentration	1.0 ppb (µg/L) of dissolved PAHs; corresponds to ~100 ppb (µg/L) of whole oil (THC) in the water column (soluble PAHs are approximately 1% of the total mass of fresh oil)	Water column effects for both **ecological** and **socio-economic** (e.g., seafood) resources may occur at concentrations exceeding 1 ppb dissolved PAH or 100 ppb whole oil; this threshold is typically used as a screening threshold for potential effects on sensitive organisms.	N/A	Trudel et al. 1989; French-McCay 2004; French McCay 2002; French McCay et al. 2012

*Thresholds used in supporting stochastic results figures. For comparison, a bacterium is 1-10 µm in size, a strand of spider web silk is 3-8 µm, and paper is 70-80 µm thick. Oil averaging 1 g/m^2 is roughly equivalent to 1 µm.

Table 2-3. Oil appearances based on NOAA Job Aid (2016b) and BAOAC.

Code	Description	Layer-Thickness		Concentration	
		microns (µm)	Inches (in.)	m^3 per km^2	bbl/acre
S	Silver Sheen	0.04 - 0.30	1.6×10^{-6} - 1.2×10^{-5}	0.04 - 0.30	1×10^{-3} - 7.8×10^{-3}
R	Rainbow Sheen	0.30 - 5.0	1.2×10^{-5} - 2.0×10^{-4}	0.3 - 5.0	7.8×10^{-3} - 1.28×10^{-1}
M	Metallic Sheen	5.0 - 50	2.0×10^{-4} - 2.0×10^{-3}	5.0 - 50	1.28×10^{-1} - 1.28
T	Transitional Dark (or true) Color	50 - 200	2.0×10^{-3} - 8×10^{-3}	50 - 200	1.28 - 5.1
D	Dark (or true) Color	> 200	> 8×10^{-3}	> 200	> 5.1
E	Emulsified	Thickness range is very similar to that of dark oil.			

Chart from Bonn Agreement Oil Appearance Code (BAOAC) May 2, 2006, modified by A. Allen

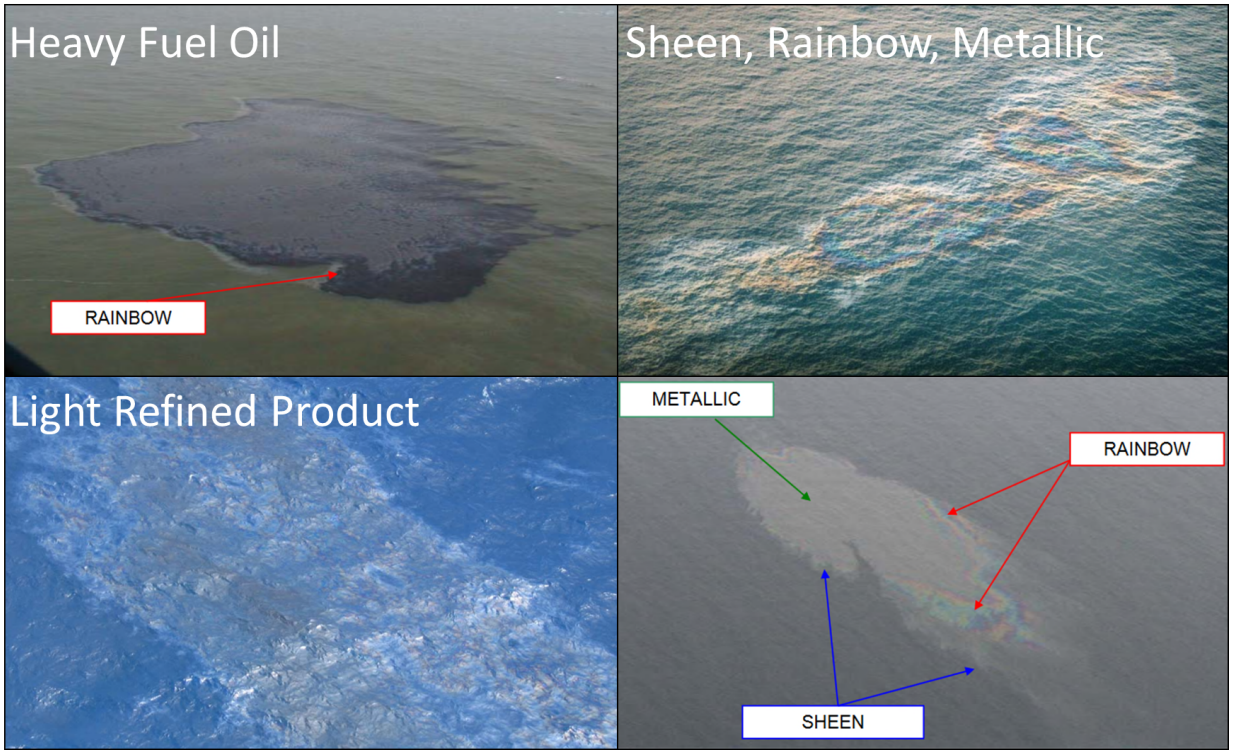

Figure 2-4. Aerial surveillance images of released oil in the environment as examples of different visual appearances based on surface oil thickness and product type (images from Bonn Agreement, 2011).

2.2.4 Deterministic Approach

Individual trajectories of interest were identified and selected from the stochastic ensemble of results for the deterministic analysis. The deterministic trajectory and fate simulations provided an estimate of the oil's transport and fate through the environment as well as its physical and chemical behavior for a specific set of environmental conditions. While the stochastic analysis provides insight into the probable behavior of oil spills given historic wind and current data for the Project Area, the deterministic analysis provides individual trajectory, oil weathering information, expected concentrations and thicknesses of oil, mass balance, and other information related to a single release at a given location and time.

Each single run within a stochastic analysis represents a specific set of wind and current conditions for the modelled time period. When analyzed together, tens to hundreds of stochastic simulations provide a range of expected exposures. The exposures between cases may differ greatly, as the trajectory of each individual modelled release is unique. Therefore, the movement and behavior, as well as the resulting area of surface oil, mass of oil along the shoreline, and mass of oil within the water column, will be different for each modelled simulation. The 95th percentile "worst" case exposure for surface, shoreline, and in-water concentration for each release location were identified based upon the area, length, or mass of oil that was predicted in each environmental compartment of interest (i.e., water surface area, shoreline length, or mass in the water column). In addition, deterministic analyses of batch spills of both BdN and marine diesel at Site 1 and the FPSO location were conducted for spill volumes ranging from 6 m^3 to 8,300 m^3. This modelling was conducted to evaluate any potential discharges from the FPSO, shuttle tanker, or production flowlines during offloading or bunkering operations (i.e., transfer of oil) between surface vessels. Scenarios were chosen to occur during the calmest wind-speed period during the summer/ice-free conditions, as they would result in the largest amount of oil on the surface. Each simulation has its own trajectory, mass balance, surface oil thickness, in-water concentration of dissolved hydrocarbons, etc. reported individually.

The results of the deterministic simulations provide a time history of the fate and weathering of oil over the duration of the release (mass balance), expressed as the percentage of released oil on the water surface, on the shoreline, evaporated, entrained in the water column, and degraded. In addition, cumulative footprints of the individual trajectories over the course of the entire modelled duration will depict the cumulative path of floating surface oil, mass of shoreline oil, and the maximum concentration of dissolved hydrocarbons in the water column at any instant in time. These results are presented in figures in Section 4.2.

2.2.5 Mitigation Response Modelling

In the event of an oil release, there are several response options available to responders that would act to contain, collect, remove, or disperse a release. Typically, these options include booming, burning, collection (e.g., skimming), and dispersant application. One of the primary response options would likely be the application of dispersants, through subsea dispersant injection (SSDI) at the well head followed by the installation of a capping stack (represented in the modelling by the 36-day release duration) and surface dispersant application (through aerial and vessel distribution). A minimum of two vessels would be initially required. The first response vessel would be utilized to spray dispersants with spray arms on the water surface at the location where the oil surfaces. This method is designed to protect workers on vessels around the well head location. The second response vessel would be utilized to operate an SSDI system at the well head. Dispersants and supplies would be transferred by Vessels of Opportunity (VOOs). The capping stack would be installed on the well head by the transport vessel and any necessary attendant vessels.

Dispersant application was modelled in this analysis as it is likely the most effective option for a subsea release at the Project Area given the distance from shore. Due to technical limitations with the use of mechanical recovery (i.e., booming and collection) and in situ burning, including sea state requirements (e.g., wind and waves), distance to shore, periods of reduced visibility (i.e., extensive fog, particularly in the late spring and summer), these options were not simulated in this analysis.

When responding to a release of oil, one of the most critical factors impacting the effectiveness of containment and cleanup operations is timing. Typically, a faster response initiation leads to a lower potential magnitude of consequences, as it reduces the volume of oil in the environment and the extent over which oil travels. This study addresses the effects that a number of different oil spill response timings would have on the ultimate trajectory and fate of hypothetical releases. Specifically, the 95th percentile “worst case” surface exposure cases from the 36-day releases at Site 1 and Site 2 were modelled with response options. Site 1 is over 400 km from shore base support in St. John’s and approximately 350-400 km from Gander International Airfield. Equinor Canada has noted that VOOs and industry support vessels are regionally located in St John’s and Halifax, Nova Scotia. Additional vessels are available in Boston. Marine and aerial response equipment would be obtained from Oil Spill Response Limited. Oil dispersants would be obtained from global supplies. Additional information on spill response options can be found in Appendix N of the EIS. The response equipment inputs that were modelled are presented in Section 3.8.

2.3 Modelled Scenarios

Two release locations were used for blowout modelling including the representative sites within the Core BdN Development area (Site 1) and the overall Project Area (Site 2) (Table 2-1;Table 2-4). Site 1 is located within a fisheries closure area and was chosen as the site for a potential subsurface blowout within the Core BdN Development Area. Batch spills are also modelled from this location as well as from a proposed location for the FPSO within the Core BdN Development Area. Site 2 is a shallower site within the overall Project Area and is representative of potential future development. Subsurface blowouts near the seafloor were modelled separately at each location in a stochastic analysis that included 171 or 172 individual model runs per location. This analysis investigated the influence of environmental variability throughout the year over multiple years, on the trajectory and fate of released oil. Results from stochastic analyses were broken into two seasons depending on the majority of modelled days falling within either ice free conditions (summer) from May through October or periods with ice-cover (winter) from November through April. Analysis of representative deterministic scenarios were conducted for individual trajectories that were identified as the 95th percentile "worst case" for surface oil exposure, water column concentration, and shoreline contact from blowouts near the seafloor modelled in the stochastic analysis, as well as for batch spills of BdN and marine diesel (Table 2-5).

Table 2-4. Hypothetical subsurface release locations and stochastic scenario information.

Scenario Parameter	Release Locations of Subsurface Blowout Scenarios			
Block	Site 1		Site 2	
Latitude	47.958818° N		47.889718° N	
Longitude	46.211357° W		47.037747° W	
Water Depth of Release	1,134 m		500 m	
Product	Bay du Nord			
Model Duration	160 d			
Gas to Oil Ratio	45.9 m^3/m^3			
Pipe Diameter	8.5 in. (21.59 cm)			
Oil Discharge Temperature	75°C			
Release Rate	10,500 m^3/d			
Release Duration	36 d	115 d	36 d	115 d
Total Released Volume	378,000 m^3	1,207,500 m^3	378,000 m^3	1,207,500 m^3
Number of Runs within Stochastic Analysis	171 annual (81 winter & 90 summer)	172 annual (83 winter & 89 summer)	171 annual (81 winter & 90 summer)	172 annual (83 winter & 89 summer)

Table 2-5. Selected representative deterministic scenarios.

Scenario Parameter	Release Parameters for Representative Deterministic Scenarios															
	95th Percentile –Site 1						95th Percentile – Site 2						Batch Spills			
Representative Scenario	Surface Oil Exposure Area	Water Column Oil Mass	Shoreline Contact Length	Surface Oil Exposure Area	Water Column Oil Mass	Shoreline Contact Length	Surface Oil Exposure Area	Water Column Oil Mass	Shoreline Contact Length	Surface Oil Exposure Area	Water Column Oil Mass	Shoreline Contact Length	FPSO Release	Offloading Release	Bunkering	Production Flowline Release
Release Site	Site 1						Site 2						Proposed FPSO Location			Site 1
Release Type	Subsurface Blowout						Subsurface Blowout						Surface Release			Subsurface Release
Depth of Release	1,134 m						500 m						Surface			1,134 m
Released Product	Bay du Nord						Bay du Nord						Bay du Nord		Marine Diesel	Bay du Nord
Release Duration	36 d			115 d			36 d			115 d			2 d	1 hr	2 mins	1 d
Release Rate	10,500 m^3/d						10,500 m^3/d						4,150 m^3/d	1,000 m^3/hr	0.05 m^3/hr	500 m^3/d
Total Released Volume	378,000 m^3			1,207,500 m^3			378,000 m^3			1,207,500 m^3			8,300 m^3	1,000 m^3	6 m^3	500 m^3
Model Duration	160 d						160 d						30 d			
Modelled Start Date and Season	2/18/2010 Winter	11/6/2010 Winter	2/27/2006 Winter	12/28/2009 Winter	5/27/2008 Summer	12/8/2010 Winter	11/29/2009 Winter	4/24/2012 Summer	4/6/2008 Summer	1/14/2010 Winter	9/8/2010 Winter	12/8/2010 Winter	6/4/2009 (calmest site-specific period identified between 2006-2012)			

The estimated volumes of hydrocarbons released in the subsurface blowout scenarios (Table 2-4) are conservative (i.e., high) based upon the current knowledge of subsurface properties and potential blowout scenarios. The durations of flow rates were determined by Equinor Canada in consideration of spill response measures to stop the flow of oil, such as installation of a capping stack (36 days) and/or drilling a relief well (115 days). It is the opinion of Equinor Canada that the most likely (although still highly unlikely) credible "worst-case" release scenario would be the shorter duration subsurface blowout that required a capping stack to contain the release. This scenario is considered "worst-case" as it is an unrestricted release of oil from the seafloor (without consideration of the BOP, riser, or other restrictions that would likely reduce flow rate) that was allowed to continue with no reduction in reservoir pressure with time. Furthermore, the anticipated water depths and release rates are conducive towards a cap and contain methodology to contain the release.

2.4 Model Uncertainty and Validation

The SIMAP model has been developed over several decades to include past and recent information from laboratory-based experiments and real-world releases to simulate the trajectory and fate of discharged oil. However, there are limits to the complexity of processes that can be modelled, as well as gaps in knowledge regarding the affected environment. Assumptions based on available scientific information and professional judgment were made in the development of the model, which represent a best assessment of the processes and potential exposures that could result from oil releases.

The major sources of uncertainty in the oil fate model are:

- Oil contains thousands of chemicals with differing physical and chemical properties that determine their fate in the environment. The model must, out of necessity, treat the oil as a mixture of a limited number of components, grouping chemicals by physical and chemical properties.
- The fate model contains a series of algorithms that are simplifications of complex physical-chemical processes. These processes are understood to varying degrees.
- The model treats each release as an isolated, singular event and does not account for any potential cumulative exposure from other sources.
- Several physical parameters, including but not limited to, hydrodynamics, water depth, total suspended solids concentration, and wind speed were not sampled extensively throughout the entire modelled domain. However, the data that did exist was sufficient for this type of modelling. When data was lacking, professional judgment and previous experience was used to refine the model inputs.

SIMAP has been validated against many real-world releases including the Deepwater Horizon oil spill, where it was used in the US Government's Natural Resource Damage Assessment. In this specific example, a small portion of the released oil may have sunk as a result of the interaction of released oil with sediments, drilling muds, and other material used in response efforts such as procedures used to seal a leaking well. These are currently areas of active research. While there are additional fate processes that may result in slight differences in the ultimate fate of oil, these processes are known to have relatively lower effects on the total volume of oil in each environmental compartment (on the order of single percentages different, depending on the release and receiving environment) as compared to the fate processes such as entrainment, which are already being modelled. The science and algorithms that may be used to model these processes have not been developed in the scientific community to the point of a consensus or use in modelling. Ongoing research topics currently underway include the formation of marine oil snow (MOS), photo-degradation, droplet size distributions, and other research areas. These and other multi-year research projects are considered for incorporation in modelling nearly constantly. Due to these topics being in the research phase, Equinor Canada is not in a position to analyze the effects on the valued components (VCs) or to develop follow-up monitoring programs at this time. However, in collaboration with research partners, Equinor Canada may consider research on this topic if prioritized as per the processes established within the collaborative research organizations, such as the Environmental Studies Research Fun (ESRF) and Petroleum Research Newfoundland and Labrador (PRNL).

In the unlikely event of an actual release of oil, the trajectory, fate, and potential biological exposure will be strongly determined by the specific environmental conditions, the precise locations, and a myriad of details related to the event and specific timeframe of the release. Modelled results are a function of the scenarios simulated and the accuracy of the input data used. The goal of this study was not to forecast every detail that could potentially occur, but to describe a range of possible consequences and exposures of oil releases under various representative scenarios.

3 Model Input Data

3.1 Oil Characterization

Two hydrocarbon products were modelled for this study at the three release locations. The two product types include Bay du Nord (BdN) crude oil and marine diesel. BdN was modelled for the subsurface blowouts at Site 1 and Site 2, the surface batch spills at the proposed FPSO location, and the subsurface batch spill at Site 1. Marine diesel was modelled for the surface vessel transfer batch spill at the proposed FPSO location. The physical and chemical data used to characterize these oils was provided by

Equinor Canada, with additional assays and measurements by S.L. Ross Environmental Research Ltd. (2016) and Intertek (2016).

BdN is a light crude oil with low viscosity and a high aromatic content (Table 3-1 & Table 3-2). The marine diesel modelled is a standard diesel that also has a low viscosity and high content of soluble hydrocarbons. The low viscosity and high soluble content of these oil products provides conservative approximations of anticipated concentrations in the water following a release, as a relatively large proportion of constituents have the potential to dissolve into the water column, when compared to oils with lower soluble content. The physical and chemical parameters of BdN are similar to those of Hibernia crude oil, which was used in previous studies (SL Ross, 2016; ESTC, 2001) as identified in Equinor Canada's response to the C-NLOPB (Statoil, 2016). BdN and Hibernia would behave similarly in the event of a release and would be more persistent than the marine diesel, which would evaporate more rapidly and be less persistent due to lower concentrations of heavy ends and residuals.

Table 3-1. Physical properties for the two oil products used in the modelling.

Physical Property	BdN Crude Oil	Marine Diesel
Density (g/cm^3)	0.84553 @16°C 0.85800 @0°C	0.83100 @25°C 0.83089 @16°C
Viscosity (cP)	5.0 @20°C 53.0 @0°C	2.76 @25°C 2.76 @15°C
API Gravity	35.85	38.8
Pour Point (°C)	-9	-50
Interface Tension (dyne/cm)	15.5	27.5
Emulsion Maximum Water Content (%)	72	0

Table 3-2. Fraction of the whole oil comprised of different distillation cuts for the two oil products. Note that the total hydrocarbon concentration (THC) is the sum of the aromatic (AR) and aliphatic (AL) groups. Numbers of carbons in the included compounds are listed.

Distillation Cut[1]	Boiling Point (°C)	Description	BdN Crude Oil	Marine Diesel
AR1	< 180	highly volatile and soluble monoaromatic hydrocarbons (BTEX[2] and MAHs C6-C9)	0.023739	0.019333
AR2	180 - 264	semi-volatile and soluble 2-ring aromatics (MAHs and PAHs C10-C12)	0.004166	0.011410
AR3	265 - 380	low volatility and solubility 3-ring aromatics (PAHs C13-C18)	0.066998	0.015605
AL1	< 180	highly volatile aliphatics (C4-C8)	0.206261	0.144667
AL2	180 - 280	semi-volatile aliphatics (C9-C16)	0.160834	0.478690
AL3	280 - 380	low volatility aliphatics (C17-C23)	0.168002	0.303295
THC1	< 180	total hydrocarbon fraction 1 (sum of AR1 and AL1)	0.230000	0.164000
THC2	180 - 280	total hydrocarbon fraction 2 (sum of AR2 and AL2)	0.165000	0.490100
THC3	280 - 380	total hydrocarbon fraction 3 (sum of AR3 and AL3)	0.235000	0.318900
Residuals	> 380	aromatics ≥ 4 rings and aliphatics > C20 that are neither volatile nor soluble	0.37000	0.02700

The “pseudo-component” approach is used to simplify the tracking of thousands of chemicals comprising oil for modelling (Payne et al., 1984; 1987; French et al., 1996; Jones, 1997; Lehr et al., 2000). Chemicals in the oil mixture are grouped by physical-chemical properties, and the resulting component category behaves as if it were a single chemical with characteristics typical of the chemical group. In this component breakdown, aromatic (AR) groups are treated as both soluble (i.e., dissolve into the water column) and volatile (i.e., evaporate to the atmosphere), while the aliphatic (AL) groups are only

[1] Note that the terms “aromatic” and “aliphatic” are used in a modelling context. “Aromatic” refers to all soluble and volatile hydrocarbons and may include actual aliphatic compounds (by chemical definition) that are soluble. In the modelling context, “aliphatic” refers to insoluble and volatile hydrocarbons. Note that Σ(AR) + Σ(AL) + residuals = Σ(THC) + residual = total hydrocarbon composition

[2] BTEX (benzene, toluene, ethylbenzene, xylene), MAHs (monocylic aromatic hydrocarbons), and PAHs (polycyclic aromatic hydrocarbons) are the more soluble, bioavailable, and potentially toxic components in oil.

volatile. The total hydrocarbon concentration (THC) within the boiling range of volatile components is the sum of all AR and AL components. The remainder of the oil is considered to be residual oil, which does not dissolve or volatilize but will degrade over time.

Degradation rates for each component and compartment (surface, upper water column, lower water column, and sediments) were based on biodegradation rates obtained from literature reviews that included estimates for compounds and/or components of crude oil generally. For the semi-volatile components, degradation in floating oil would be considerably slower than volatilization. The rates for residual oil are consistent with studies by Zahed et al. (2011) and Atlas and Bragg (2009).

Through the modelled processes, the density and viscosity of the oil tend to increase as the oil weathers. It is possible for the weathered oil, especially in the presence of suspended particulate matter in the water column, to become denser than water and sink. In addition, the oil (including the residual fraction) does continue to degrade over time within the model. In addition, one must consider that the hypothetical long-term releases of oil (many months) continues to add fresh oil, which will increase the total amount of oil through time that will degrade. As time progresses, residual oil is all that remains of the early portions of the release while whole fresh oil continues to be released in later stages. In total, this may appear as though degradation rates are increasing, but it is rather a function of the static degradation rate and the increasing amount of oil (a portion fresh oil) through time.

A recent comprehensive model update with literature review of over a dozen of the most recent studies on oil degradation rates validating the use of modelled SIMAP degradation rates was conducted for work following the Deepwater Horizon Natural Resource Damage Assessment (French et al., 2015) as well as for the United States Bureau of Ocean Energy Management (BOEM) (French et al., 2018b, c).

The long-term weathering and degradability of an oil (including microbial degradation, photo-oxidation, and other processes that may break down compounds or components of oil) may increase the tendency of an oil to sink. These processes are highly dependent upon the type of oil released and the environmental conditions of the receiving environment. A large amount of work is currently being undertaken to develop scientific consensus in this area; however, it is understood that compounds with a boiling temperature >380°C degrade slowly and that these compounds are difficult to measure. The modelled bulk disappearance is quite slow and would conservatively overestimate the effects following a release as oil would remain in the model. The inclusion of compound-specific degradation would increase the degradation and reduce the amount of oil remaining in the model, therefore skewing results towards less effects.

3.2 Geographic and Habitat Data

For geographical reference, SIMAP uses rectilinear grids to designate the location of the shoreline, the water depth (bathymetry), and the shore or habitat type. The grids were generated from a digital shoreline using ESRI geoprocessing and Spatial Analyst Extension tools, and the cells were coded for depth and habitat type. Geographical data were obtained from multiple international sources to provide the geographic and environmental information required for modelling (Table 3-3). Habitat data were used to define the bottom type and vegetation found in subtidal areas, areas of extensive mud flats and wetlands, and the shoreline type (e.g., sandy beach, rocky shoreline, etc.).

The model used these grids to identify the location of the shoreline and amount of oil that may adhere once oil contacted the shoreline (Figure 3-1). Retention of oil on a shoreline depends on the shoreline type, physical and chemical properties (e.g., viscosity) of the oil, tidal amplitude in estuarine areas, and wave energy. The resolution of the habitat grid was approximately 1.8 km north-south by 2.5 km east-west (0.02225° on each side). Bathymetry data define the water depths within the modelled extent. The General Bathymetric Chart of the Oceans (GEBCO) one arc-minute interval grid was used but was resampled into a grid with the same resolution as the habitat grid (Figure 3-1).

Table 3-3. Sources for habitat, shoreline, and bathymetry data.

Data Type	Data Source	Geographic Location	Reference
Habitat/Shoreline	Environment and Climate Change Canada	Canada	Therrien, A. 2017
	National Oceanic and Atmospheric Administration Environmental Sensitivity Index	United States (except Maine)	NOAA 2016a
	Maine Environmental Vulnerability Index	United States - Maine	MDEP 2016
	New Brunswick Department of Natural Resources	New Brunswick	NBDNR 2013
	Nova Scotia Department of Natural Resources	Nova Scotia	NSDNR 2013
Bathymetry	General Bathymetric Chart of the Oceans Digital Atlas	Global	GEBCO 2003

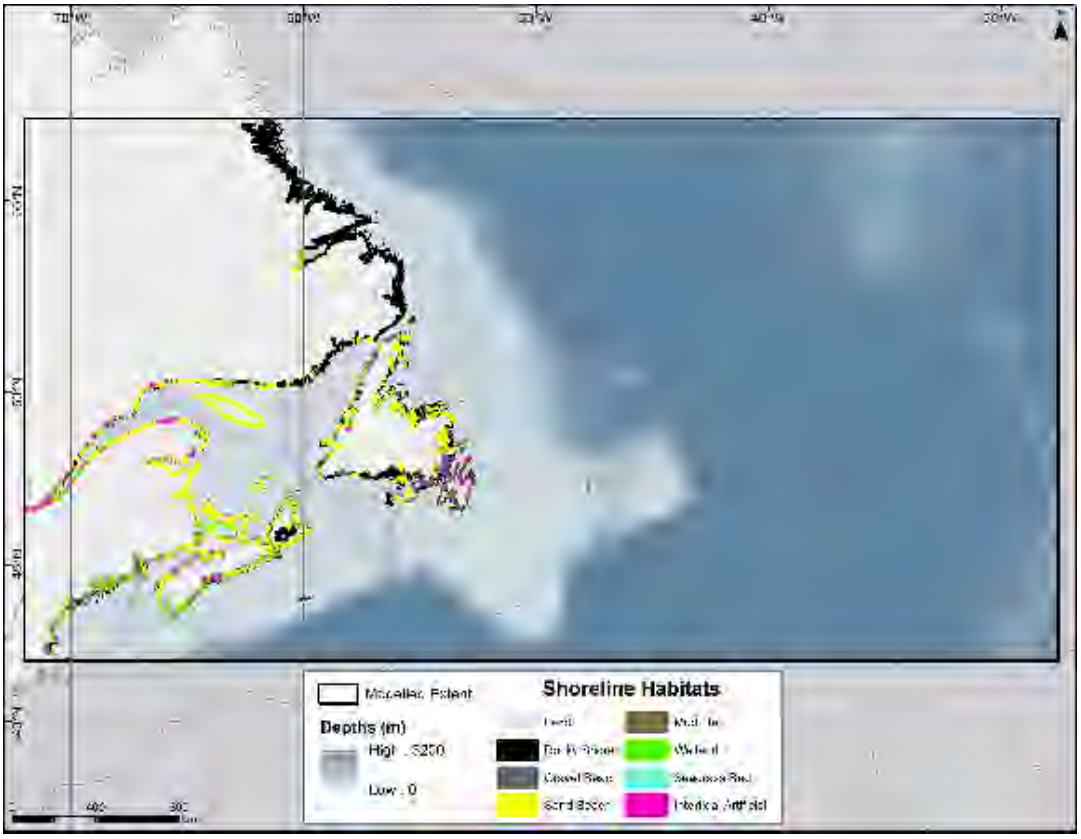

Figure 3-1. Shoreline habitat data and depth throughout the modelled domain. The black box represents the modelled extent.

3.3 Ice Cover

Sea ice is formed in the autumn in the Arctic and sub-Arctic regions of the world. The growth rate of sea ice depends on surface temperature and the heat flux in the underlying water. The formation and development of sea ice follows a progression of stages. The exact timing of these stages at any location is not the same from year to year because of subtle differences in climatic conditions. In the Northern Hemisphere during September and October, the air temperature lowers sufficiently to form a thin sheet of ice on the sea surface. The freezing temperature for average ocean salt water with a salinity of 35 ppt is about -2°C (NOAA, 2014).

The movement and behavior of released oil is greatly affected by the presence of sea ice (Figure 3-2). Oil trapped in or under sea ice will weather more slowly than oil released in open water. Algorithms in SIMAP for modelling the movement and behavior of oil in the presence of sea ice are based on the percent of ice coverage (also commonly referred to as ice concentration). From 0 to ~30% coverage, the sea ice has no effect on the advection or weathering of surface floating oil. From approximately 30 to

80% ice coverage, oil advection is forced to the right of sea ice motion in the northern hemisphere, surface oil thickness generally increases due to ice-restricted spreading, and evaporation and entrainment are both reduced by damping/shielding the water surface from wind and waves. Above 80% sea-ice coverage, surface oil moves with the sea ice, and evaporation and entrainment cease.

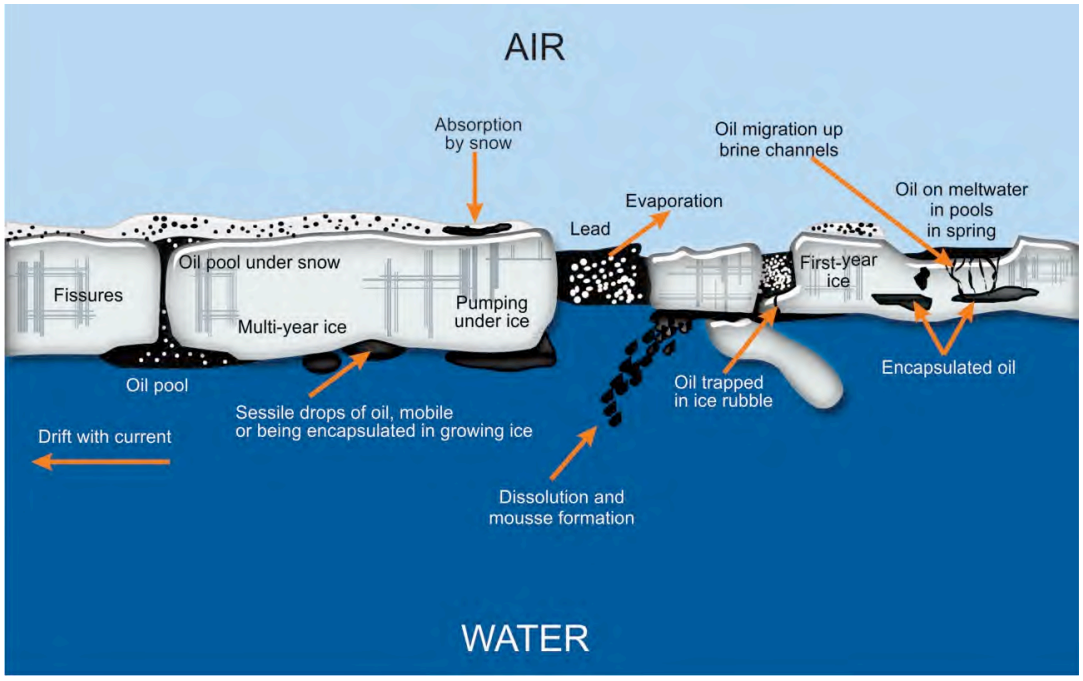

Figure 3-2. Oil and ice interactions at the water surface (Source: RPS 2017, modified from original by Alan A. Allen).

The sea-ice thickness and concentration can vary greatly based upon prevailing weather conditions. If oil is released under sea ice, water column exposures can be greater, due to the "capping" effect of the ice. Sea-ice cover limits or prevents evaporative losses and could result in substantially greater dissolution of hydrocarbons into the water column.

Sea-ice data used as modelling inputs were obtained from the Canadian Ice Service (CIS; ECCC, 2017) in weekly files spanning from January 2006 to December 2012. These data were in the form of polygon data, with information on total sea-ice concentration and stage of development. For each ice polygon, concentration codes were converted to concentration percentages. Average sea-ice thickness was calculated based on the proportional concentration of the various stages of ice present for each week of the season over seven years. The CIS data provides a range of thicknesses for each ice category and stage of development. In most cases, the mid-point of those ranges was used in the calculation of average ice thickness. If the stage was not identified, but there were concentrations provided, then sea-ice stage was assumed to be first-year medium ice (Table 3-4). The ice data was gridded at a resolution

matching the habitat grid (0.02225°). A representative map depicting percentage of sea-ice cover and thickness for the first week of February 2010 is presented (Figure 3-3).

Table 3-4. Sea-ice thickness used in the modelling characterized by CIS stage of development.

CIS Ice Category or Sea Ice Stage	Concentration	CIS Thickness Range (cm)	Model Applied Thickness (cm)
Ice Free	0%	n/a	n/a
Open Water	30%	n/a	50
Land fast Ice	100%	n/a	assumed full water depth
First year thick ice	Total concentration converted from tenths to percent ice cover	> 120	120
First year medium ice*		70 – 120	95
First year thin ice		30 – 70	50
Young ice		10 – 30	20
Grey white ice		15 – 30	22.5
Grey ice		10 – 15	12.5
New ice		< 10	5
Icebergs		unknown	100

*Default sea-ice stage assumed when none was identified in the data.

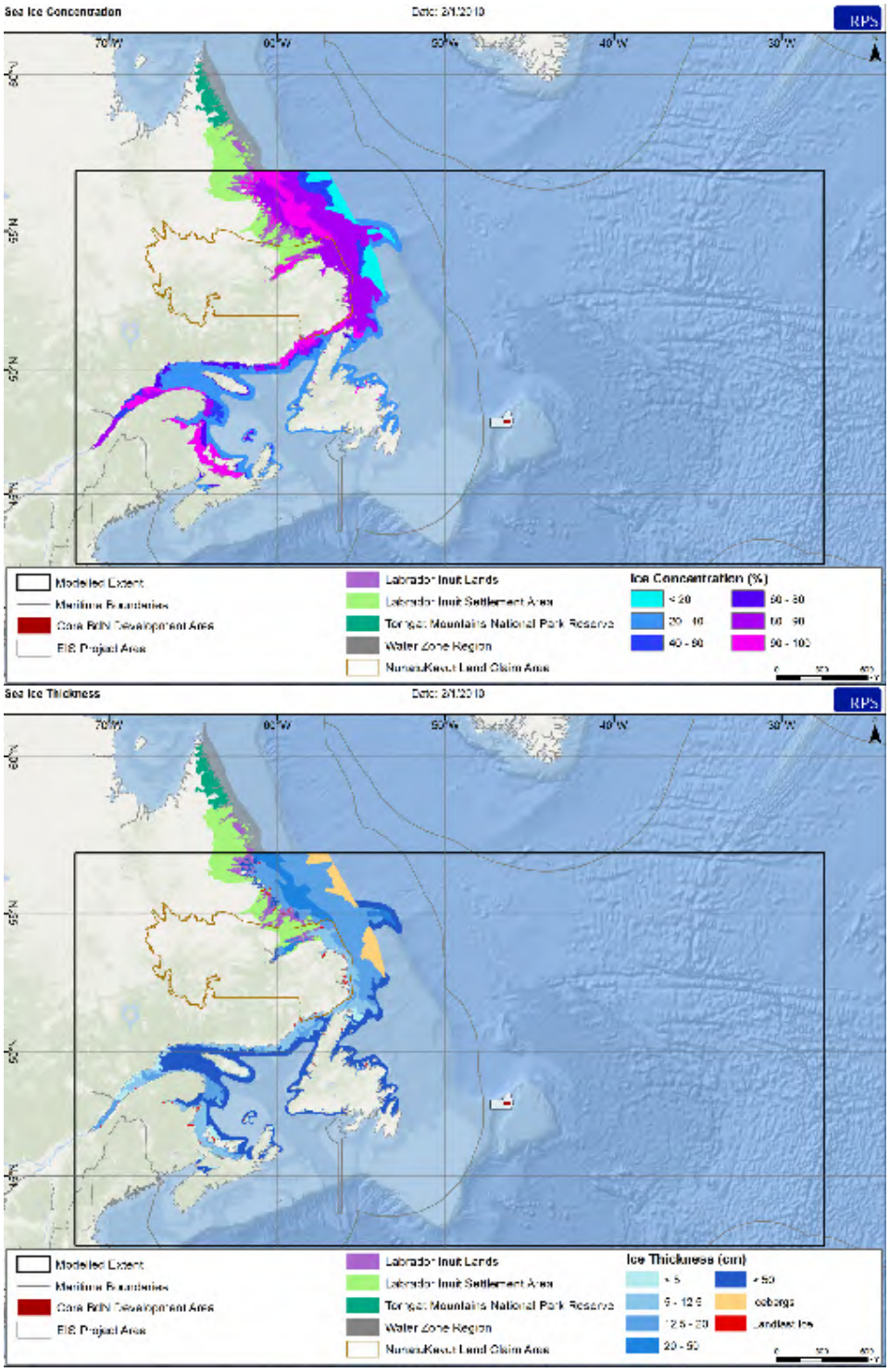

Figure 3-3. Representative percentage sea-ice cover (top) and corresponding thickness (bottom) for the first week of February 2010.

3.4 Wind Data

Winds may physically transport oil on the water surface, thus wind speed and direction at the water surface may be the driving force between a simulation with limited versus extensive transport. The SIMAP model uses time-varying wind speeds and directions for the period over which the release was simulated. A multi-year dataset of wind speed and direction was used to capture the variability that occurs on short timescales over multiple years. Oil release trajectories (simulated using long-term wind datasets) are representative of possible wind conditions at the site, assuming the temporal variability of the dataset is on similar timescales to natural variations in speed and direction that result in the transport of surface oil. Because winds can change on time scales of minutes to hours, it is best to acquire data at the highest temporal resolution possible (typically every six hours for large global models, or at the very least daily averages). Oil released over long periods of time (e.g., the 115-day blowouts modelled here for 160 days) has the potential to travel long distances by wind transport. To effectively model this, the wind speed and direction data must encompass a large geographic area in order to capture the spatial extent and any spatial variability in potential transport that may occur.

Wind data for this study were obtained for the entire model domain (Figure 2-1) from the National Centers for Environmental Prediction (NCEP) Climate Forecast System Reanalysis (CFSR) product for 2006 through 2010. Another two years (2011-2012) of wind data was added to the analysis from CFSv2, which uses the same model that was used to create CFSR and thus works as an extension of CFSR. The CFSR was designed and executed as a global, high-resolution, coupled atmosphere-ocean-land surface-sea-ice system to provide the best estimate of the state of these coupled domains (Saha et al., 2010). The CFSR includes coupling of atmosphere and ocean, as well as assimilation of satellite radiances. The CFSR global atmospheric resolution is ~38 km, with 64 vertical levels extending from the surface to 0.26 hPa. CFSR winds were also used as one of the main driving forces in the HYCOM hydrodynamic dataset used for modelling (see Section 3.5). The CFSR time series acquired for this study was available at 0.5-degree horizontal resolution at 6-hourly intervals.

Averaged annual wind data at Site 1 and Site 2 were most frequently from the west-southwest direction (Figure 3-4). Monthly average wind speeds varied between 7 and 12 m/s throughout the year, with highest speeds occurring during winter months (November – March) and lower speeds in the summer (June – August) (Figure 3-5). These winds would be expected to transport oil generally away from nearby shorelines further into the open ocean.

Winds over the Flemish Pass are predominantly from the southwest and west throughout the year. Winter season winds are most frequently from the west and northwest with higher velocity than

summer season winds, which typically come from the southwest (Statoil, 2016). Spring and autumn months are more dynamic transitional periods between the more consistent summer and winter wind regimes. Low pressure systems, tropical, and extra-tropical storms pass through the Grand Banks on a regular basis generating substantial wind speeds for short periods of time. Significant wave heights are typically highest from November through February, in regions with no ice (C-NLOPB, 2014).

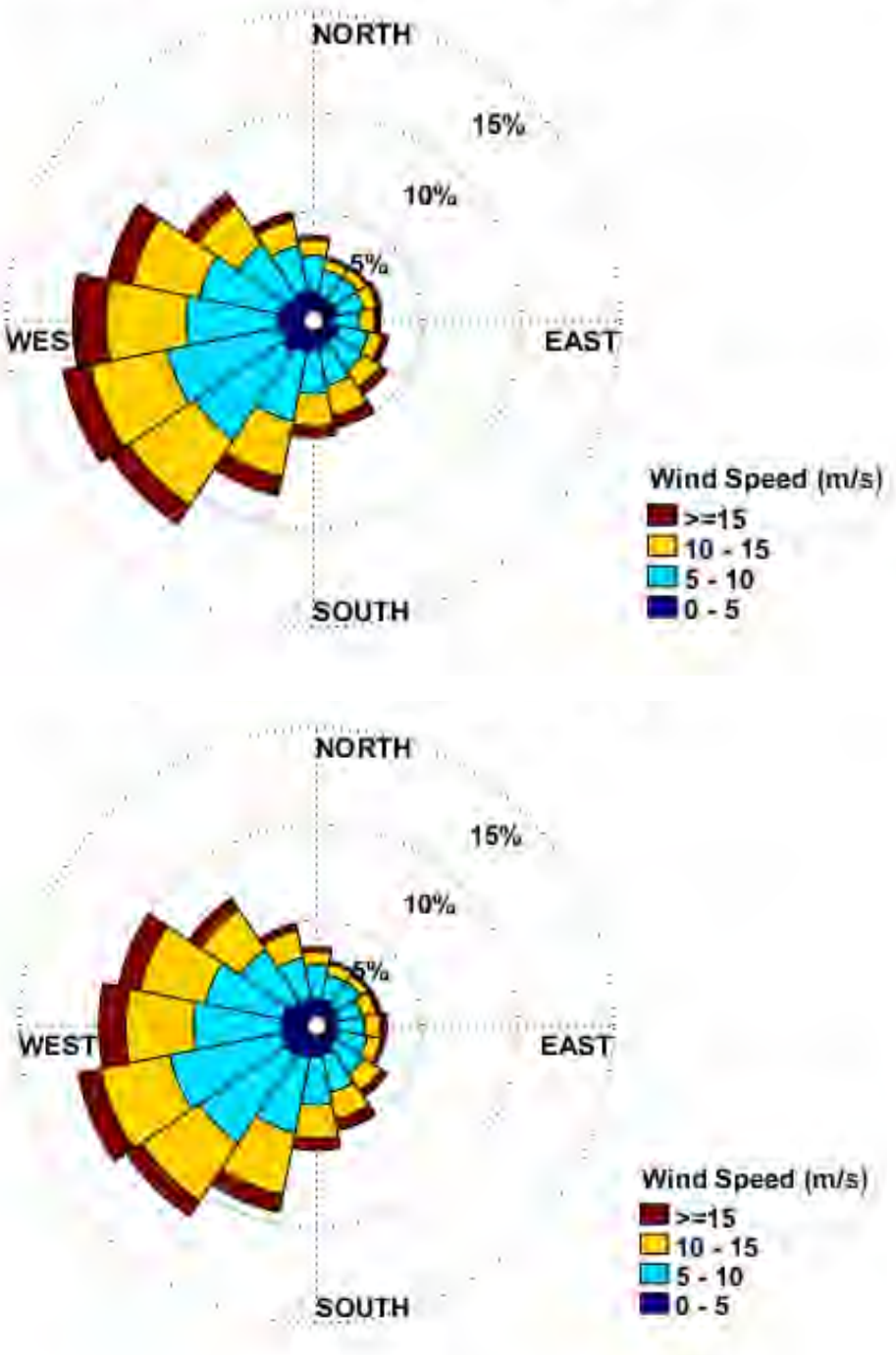

Figure 3-4. Annual CFSR wind rose near Site 1 (top) and Site 2 (bottom) release sites. Wind speeds are presented in m/s, using meteorological convention (i.e., direction wind is coming from).

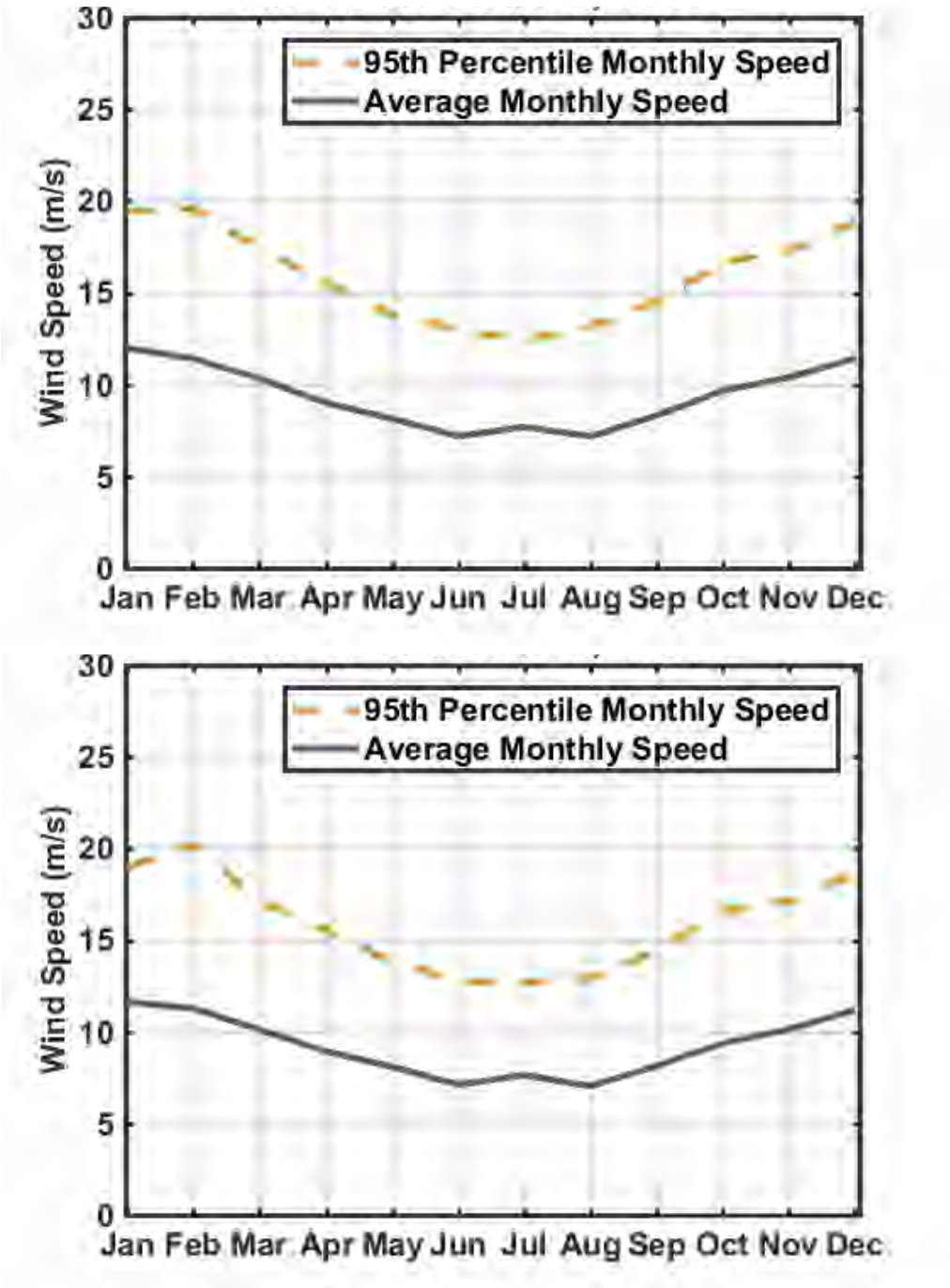

Figure 3-5. Average and 95th percentile monthly wind speeds near Site 1 (top) and Site 2 (bottom) release sites.

3.5 Currents

The Labrador Current dominates the large-scale ocean circulation in the Newfoundland region originating in the Arctic Ocean and flowing south along the coasts of Labrador and Newfoundland (Figure 3-6). This southerly current intensifies as waters funnel through the offshore branch, which follows the Flemish Pass along the 1,000 m contour between the Grand Banks and Flemish Cap. To a lesser extent, a portion of the Labrador Current flows through an inshore branch, which follows the Avalon Channel between Newfoundland and the Grand Banks. Over parts of the Grand Banks, currents can be generally weak and flow southward (Petrie and Isenor, 1985). Maximum current speeds in the upper 200 m of the water column range from 0.3 – 2.0 m/s (C-NLOPB, 2014). The strong southerly current dominates the yearly average flow, and winds may only account for approximately 10% of current variability in this region (Petrie and Isenor, 1985). South of the Flemish Pass, the Labrador Current mixes with the North Atlantic Current. The region where these two currents converge is one of the most dynamic oceanographic areas in the world. Extremely energetic and variable frontal systems and eddies are produced on smaller scales, on the order of kilometers (Volkov, 2005). Due to these eddies, local transport may advect parcels of water in nearly any direction. Satellite and drifter studies of current dynamics demonstrate this complexity; however, drifting parcels generally move to the south and east (Han and Tang, 1999; Petrie and Anderson, 1983; Richardson, 1983) where they intersect with the North Atlantic Current.

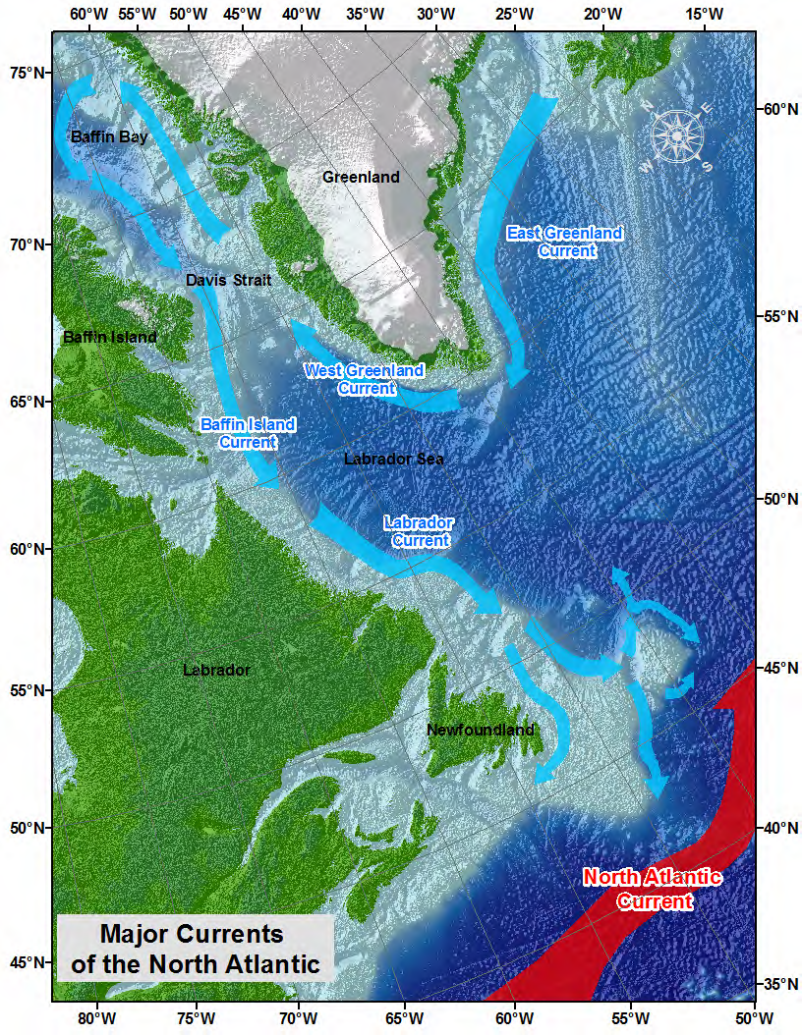

Figure 3-6. Large scale ocean currents in the Newfoundland region (USCG 2009).

Currents for the North Atlantic region were acquired from the HYCOM (HYbrid Coordinate Ocean Model) circulation model. HYCOM is a primitive-equation ocean general circulation model that evolved from the Miami Isopycnic-Coordinate Ocean Model (MICOM) (Halliwell, 2002; Halliwell et al., 1998, 2000; Bleck, 2002). MICOM has become one of the premier ocean circulation models, having been subjected to validation studies (Chassignet et al., 1996; Roberts et al., 1996; Marsh et al., 1996) and used in numerous ocean climate studies (New and Bleck, 1995; New et al., 1995; Hu, 1996; Halliwell, 1997, 1998; Bleck, 1998). The HYCOM global ocean system is a 3D dynamic model that is run each day, providing a 5-day hindcast and 5-day forecast of oceanic currents that work effectively in both deep and shallow waters. Hindcast data are used to validate the accuracy of each run to determine if modelled forcings produce results that match observational data. HYCOM uses Mercator projections between

78°S and 47°N and a bipolar patch for regions north of 47°N to avoid computational problems associated with the convergence of the meridians at the pole. The 1/12° equatorial resolution provides gridded ocean data with an average spacing of ~7 km between each point. Several studies have demonstrated that at least 1/10° horizontal resolution is required to resolve boundary currents and mesoscale variability in a realistic manner (Hurlburt and Hogan, 2000; Smith and Maltrud, 2000; Chassignet and Garaffo, 2001).

For the energetic eddies at the frontal systems discussed by Volkov (2005) that are of a smaller scale than ~7 km, the HYCOM model would not directly capture these features. However, from a broader-scale trajectory perspective, this is not required. The movement of water within an eddy is circular by nature. Therefore, while the rate of circulation (i.e. velocity of water) may be greater than that of the general circulation outside of the eddy, it is irrelevant to the broader scale modelled transport processes, as oil in the eddy would tend to be trapped, circulating within the grid cell. The general circulation (i.e., movement of the eddy itself) would be resolved by the average current within the single grid cell. In addition, the randomized advective dispersion accounts for the variability in currents below the spatial and temporal resolution of each dataset. Because HYCOM does not resolve the trapping of oil in these small-scale features, results of the modelled simulations would tend to have a higher degree of dispersion and would therefore cover larger areas. For eddies that are larger than approximately 14 km in diameter, the HYCOM gridding could capture the circular nature of the circulation in the multiple grid points that would be used to model it.

In general, the resolution of underlying forcing data has the potential to influence the results of trajectory and fate simulations. If extremely coarse resolution gridding is used, intricate flow paths may be straightened, and velocities would tend to be closer to the mean. If extremely fine resolution gridding is used, smaller-scale features will be resolved. However, there is a balance and a “law of diminishing returns” when modelling these processes. When higher spatial and temporal resolutions are used, larger amounts of data required, the number of time steps must increase (i.e., shorter time steps are required with higher spatial resolution data to account for the distance traveled in each time steps to ensure particles do not skip grid cells), and the amount of time required to model also increases.

Data is assimilated through the Navy Coupled Ocean Data Assimilation (NCODA) system (Cummings, 2005). The NCODA system employs a Multi-Variate Optimal Interpolation scheme, which uses model forecasts as a first guess and then refines estimates from available satellite and in-situ temperature and salinity data that are applied through the water column using a downward projection of surface information (Cooper and Haines, 1996). Bathymetry is derived from the U.S. Naval Research Laboratory BDB2 dataset. Surface forcing is derived from the Navy Operational Global Atmospheric Prediction System, which includes wind stress, wind speed, heat flux (using bulk formula), and precipitation.

For this study, daily HYCOM current data were obtained for the period January 2006 through December 2012 for the North Atlantic region (HYCOM, 2016). Because the data spanned seven years, the variability in winds and currents would sample daily, weekly, seasonal, and inter-annual variability, which included calm periods, seasonal variations, and the full range of environmental forcing over the entire time period. Because of the complete coverage of the bi-weekly randomized sampling within the 7-year modelled period and the 160-day duration of the models themselves, the range of calm to more energetic periods would be captured in the stochastic analysis. While this subset of data is not the most recent seven years of data, currents and winds in the study area are very similar to those from 5-10 years ago, and the data used in this study would be representative of environmental conditions present today. Similarly, while there may be questions regarding general circulation during specific time periods, it is important to note that trajectories are influenced by day to day currents, as opposed to averages. Average surface current speeds (Figure 3-7) and direction offshore Newfoundland (Figure 3-8) in the model domain from 2006 – 2012 depict larger scale features such as the Labrador Current and the North Atlantic Current, as well as bathymetric steering of currents around the Grand Banks and Flemish Cap. While these figures depict an average current speed and direction for visual purposes, oil transport was defined by the daily currents throughout each modelled simulation.

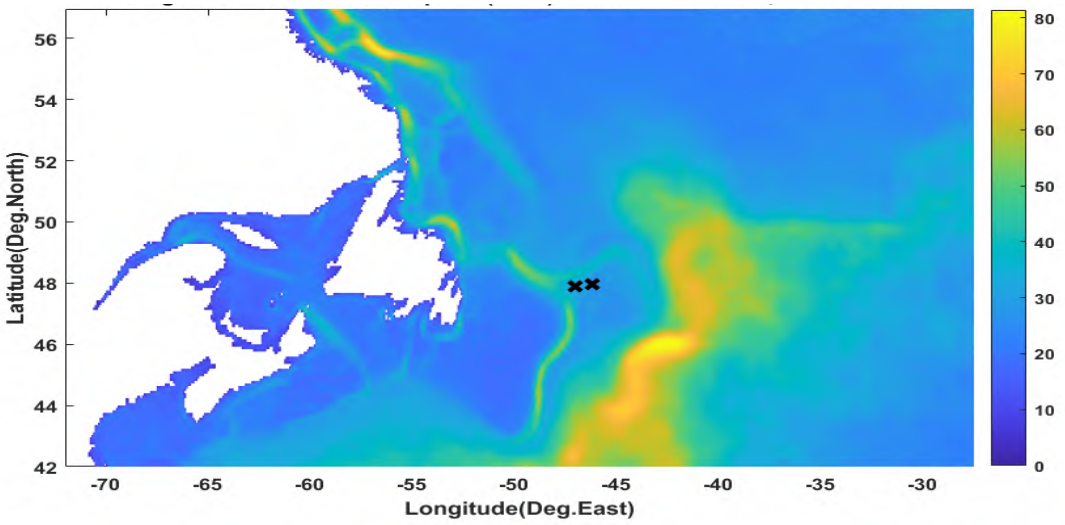

Figure 3-7. Average HYCOM surface current speeds (cm/s) off the coast of Newfoundland from 2006 – 2012.

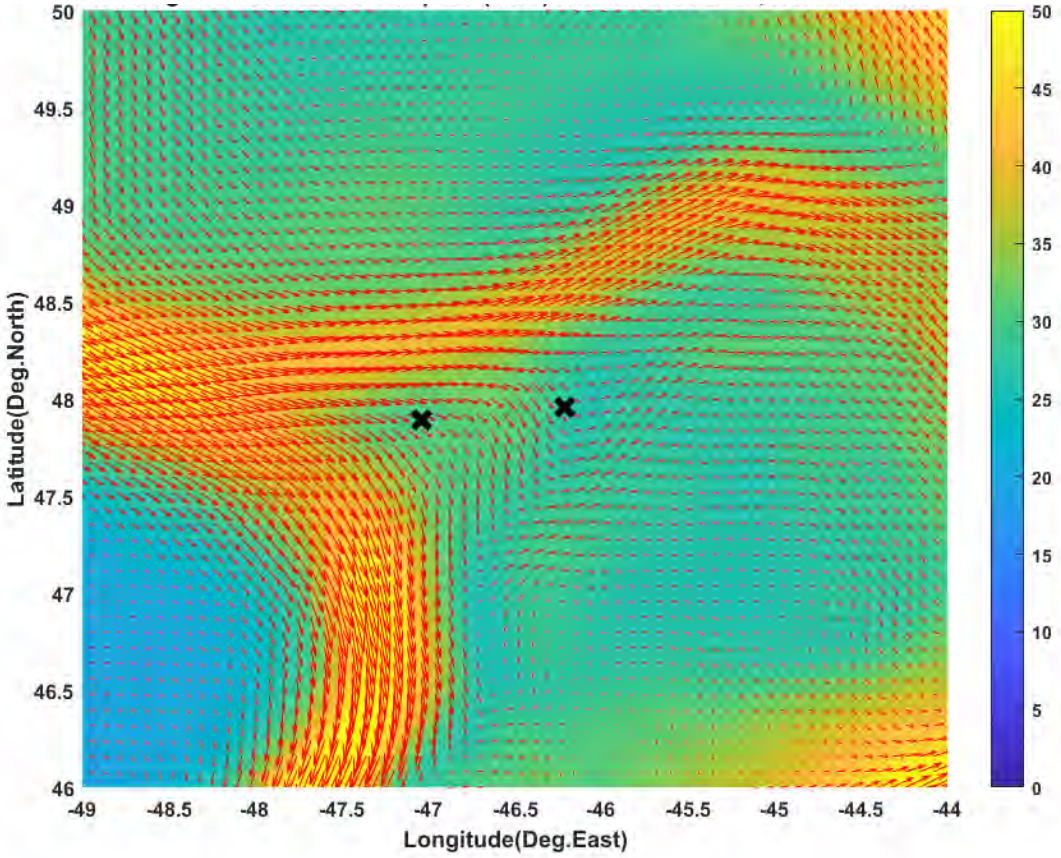

Figure 3-8. Averaged surface current speed (cm/s) in color, and direction presented as red vectors offshore Newfoundland from HYCOM (2006 – 2012).

3.6 Water Temperature & Salinity

Temperature and salinity values throughout the water column influence a number of oil transport and fate calculations. Temperature and salinity data were obtained from the World Ocean Atlas (WOA) 2013 high-resolution dataset, Version 2, which is compiled and maintained by the U.S. National Oceanographic Data Center (Levitus et al., 2014). The WOA originated from the Climatological Atlas of the World Ocean (Levitus, 1982) and was updated with new data records in 1994, 1998, 2001 (Conkright et al., 2001), and 2013. These data records consist of observations obtained from various global data management projects. The dataset includes up to 57 depth bins from the sea surface to the seabed and include averaged yearly, seasonally, and monthly data over a global grid with a 1/4° horizontal resolution.

3.7 Blowout Model Scenarios and Results

The nearfield model OILMAPDeep was used to predict the initial droplet size distribution associated with subsurface blowouts of the hydrocarbon product that was modelled across two different release locations. The droplet size model predicts the distribution of oil volume (mass) within different size ranges (measured by diameter) in response to the turbulence of the release, the gas content, the water depth, and the properties of the oil. The droplet model predicted the initial droplet size distributions for each scenario as well as the depth or "trap height" in the water column where the droplets would be released to the water column and rise according to their individual buoyancies. These values were then used to generate input files defining the size, mass, and depth of oil droplets entering the water column for use within the SIMAP far field model.

Initial droplet sizes are primarily a function of the energy of the release, the chemical and physical parameters of the released oil, the gas to oil ratio (GOR), dispersant application, and several other factors. As an example, if the energy of a release or the amount of dispersant added were to increase, or if the viscosity of the released oil were lower, the resulting droplet sizes would be smaller. In the scenarios simulated for this study, the oil was assumed not to be treated with dispersant. The energy of the release is a function of the volumetric flow rate and discharge orifice size, with higher energy releases occurring as greater volumes pass through smaller openings more quickly.

In total, four subsurface blowout release events were evaluated as part of this study. Oil and gas were introduced to the water column through an 8.5-inch orifice near the seafloor at a rate of 10,500 m3/d to simulate an uncontrolled release from the wellhead frequently referred to as a blowout. The modelled release depth ranged from 500 m (Site 2) to 1,134 m (Site 1) at the sediment/water interface at the two identified release locations. BdN was modelled to exit each wellhead for both 36 and 115 days.

The predicted droplet size distribution was represented by seven discrete size bins for each modelled release scenario (Table 3-5). The non-uniform spacing between the droplet size bins is the result of the non-linear functionality of droplet size distribution. Each of the seven bins were determined such that an equal proportion of the released oil by mass (14.29%) was within each bin. Differences in release depth resulted in different droplet size distributions for each of the two modelled release rates.

Oil droplets rise through the water column at rates based on drag, calculated using their diameter (treated as a sphere) and the buoyancy, the density difference between the oil and the water, which varies with changing temperature and salinity by depth (Figure 3-9). Rise times for oil to reach the surface varied between minutes to many hours, depending on droplet size and depth of release. Rise time estimates are approximated, based on the initial droplet size, initial droplet density, and bottom water density; neglecting dispersion, dissolution, and degradation (which were tracked within the oil

spill model and modified the rise rates). The longest rise times were associated with the smallest droplets, with some rise times exceeding a day. The longest rise times were associated with the smallest droplets, with some rise times exceeding a day. At Site 1, the smallest droplet size (397 µm) is predicted to take 1.1 days to reach the water surface from the trap depth (550 m), while the largest droplet size (3,611 µm) could take only 0.11 day (2.73 hr) to rise to the water surface. At Site 2, the smallest droplet size (273 µm) is predicted to take 0.96 day to reach the water surface from the trap depth (190 m), while the largest droplet size (2,486 µm) could take only 0.07 day (1.69 hr) to rise to the water surface.

Table 3-5. Summary of droplet size distribution results for each of two modelled subsurface blowout release sites.

Median Droplet Size in Each of Seven Equal-Mass Bins, by Diameter (µm)	
Site 1 - BdN Crude Oil (10,500 m^3/d)	**Site 2 - BdN Crude Oil (10,500 m^3/d)**
397	273
907	625
1,129	777
1,360	936
1,640	1,129
2,054	1,414
3,611	2,486

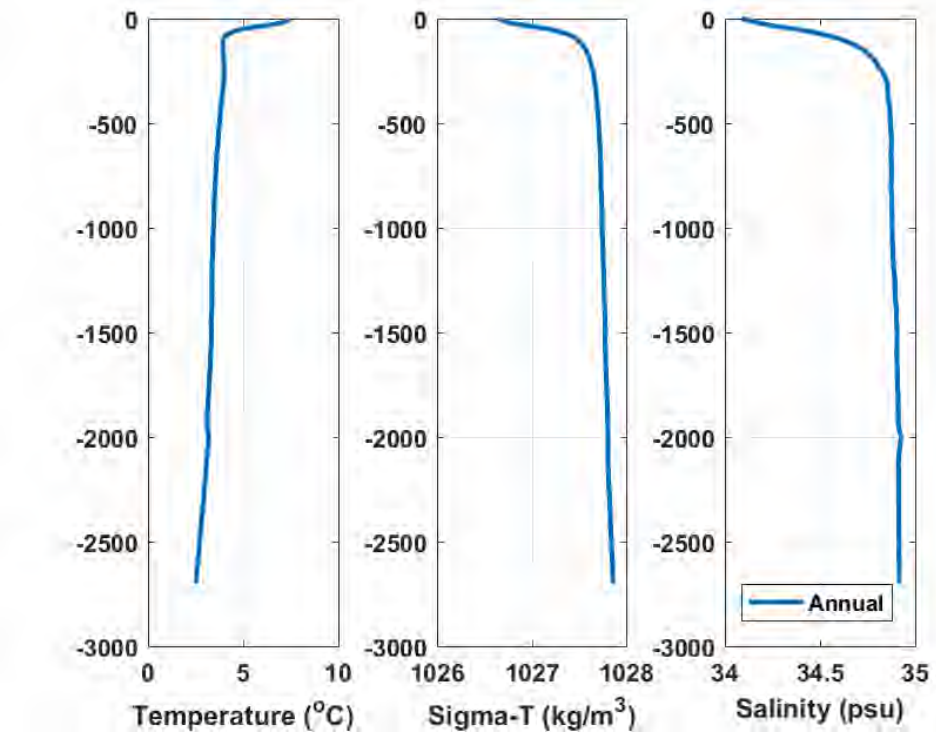

Figure 3-9. Water column profiles of temperature (left), salinity (right) and corresponding density (middle), represented as sigma-t. The density profile was generated based on the temperature and salinity profile using equations of state as published by UNESCO, 1981 (EOS-80).

3.8 Response Options Inputs

A list of the response equipment that would be available to mitigate releases in the event of a blowout in the Flemish Pass was provided by Equinor Canada. Each response type and the anticipated timing (Table 3-6), are summarized below.

- **Subsea Dispersant Injection (SSDI):** The equipment and dispersant for SSDI is located in Ft Lauderdale, FL and Southampton, UK. Given the transit time, the initiation of SSDI would begin on Day 5, assuming that the debris clearance had been completed. The modelling assumes that 100% of the discharged oil would be treated with a dispersant-to-oil-ratio (DOR) of 1:100.
- **Capping Stack Installations:** The modelled releases assume that, given a conservative transit time, the stack would be installed on Day 36 as described in the 36-day blowout scenarios described in Section 2.2.5.
- **Aerial Surface Dispersant Application:** Twin aircraft would be used to spray dispersant onto floating oil on the water surface. Both aircraft would be staged at Gander International Airport

until an alternative staging location was identified (as needed). The aircraft would only be operational during daylight hours and would begin dispersant application on Day 2.

- **Vessel Surface Dispersant Application:** A vessel fitted with spray arms would be used to apply dispersant at the water surface. It was assumed to have unlimited access to dispersant with no need to return to port daily. Vessel surface dispersant application was assumed to arrive on scene on Day 2.

Table 3-6. Timing of response options at Site 1 and Site 2. Shading indicates when the response option is operational.

	Day 1	Day 2	Day 3	Day 4	Day 5-36	Days 36-160
Capping Stack – Site 1 and Site 2						
SSDI						
Aerial Dispersant						
Vessel Dispersant						

It was assumed that response measures would continue throughout the simulation duration; however, as oil became weathered and the viscosity increased (>200,000 cP), surface dispersant application would become ineffective.

3.8.1 Modelled Response in SIMAP

This study addressed the effects of multiple response options with different response timings on the ultimate trajectory and fate of hypothetical releases. To capture the potential variability in predicted trajectory and fate of released oil, an assortment of response options was modelled with specific timings for initial response and assumptions of efficiency/effectiveness. Results from modelled response mitigated scenarios were then compared to previously modelled unmitigated releases.

The effectiveness of surface response actions modelled in SIMAP, such as dispersant application, is based on assumptions of timing, physical thresholds (e.g., wave height and wind speed), equipment efficiency, and dispersant application rates. The objective of dispersant use is to break up and dilute oil

into the water column, preventing exposure of biota to surface floating and shoreline oil, and promoting biodegradation by (1) increasing the surface area of the oil (Brakstad et al. 2014, 2015; North et al. 2015; Lee et al. 2013; Hazen et al. 2016); (2) diluting the oil below toxic levels (Lee et al. 2013); and (3) dispersing oil more widely such that nutrients (e.g., N, P, Fe) become less limiting (Bælum et al. 2012; Prince et al., 2013; Hazen et al., 2016). The surface area per volume ratio increases as oil is broken up into small droplets, which enhances microbial attack at the oil-water interface. Breaking up the oil also increases dissolution, making the soluble hydrocarbons more bioavailable to microbes. Once dissolved, the hydrocarbons are not expected to biodegrade faster with dispersant present than they do without dispersant. Dispersing the oil into the water column allows microbes to have more access to the hydrocarbons (and associated compounds) in the oil. In the case of a blowout, SSDI breaks up the oil into smaller droplets, which slows the oil's ascent to the surface, or if small enough, disperses the oil permanently at depth. This exposes more oil for a longer time to biodegradation. SSDI disperses the oil into a large water volume at depth (diluting it and enhancing biodegradation) and reduces surface water, nearshore and shoreline exposure to floating oil, and entrained/dissolved oil in the upper water column (French-McCay et al., 2018a). In the overall mass balance, effective dispersant use is expected to increase the overall amount of oil biodegraded, as opposed to having that oil end up floating or on shorelines (French-McCay et al., 2018a).

Tradeoffs to dispersant use include (1) the dispersed oil potentially increases exposure to organisms inhabiting the water column and (2) the dispersant may be an additional stressor added to the environment. However, modern dispersant formulations are of low toxicity, much less toxic than the hydrocarbons in the oil (NRC, 2005). Furthermore, oil in the water column may be diluted to concentrations below the toxicity threshold limits of resident biota (Lee et al., 2013). SSDI increases exposure to organisms inhabiting deep water and benthic environments. However, densities of fish and invertebrates are much lower in deep offshore waters than near the surface (DWH NRDA Trustees, 2016; French-McCay et al., 2018a), mitigating this potential impact.

A summary of the two scenarios modelled with various response options is provided (Table 3-7). The modelling results were used to evaluate the effect of a range of response option effectiveness implemented at multiple timings over the course of a release.

Table 3-7. Modelled response options and thresholds used in response mitigation scenarios.

Response Option	Response Target	Modelled Threshold			
		Wind (m/s)	Currents (kts)	Waves (m)	Surface Oil Thickness (µm)
SSDI	Well Head	18	n/a	n/a	n/a
Capping Stack	Well Head	n/a	n/a	n/a	n/a
Aerial Dispersant	Water Surface	16	n/a	n/a	13
Surface Vessel Dispersant	Water Surface	16	n/a	1	13

Every oil spill is unique, and similarly, the response to each release event is unique. The location of the release, volume of oil spilled, environment into which oil enters, and the environmental conditions at the time of the release all play a significant role in determining the ultimate trajectory and fate of oil, as well as the effectiveness of response and cleanup operations. The specific thresholds for environmental conditions (wind speed, current speed, wave height), the minimum thickness of surface oil that is predicted to be collected/dispersed, and the efficiency with which each piece of modelled response equipment was allowed to operate within the model are provided (Table 3-7). As an example, should winds at a specific location and point in time exceed the identified threshold, then the modelled mitigation would cease until winds fell below the identified threshold. For response options that targeted the water surface, efforts were focused on the areas identified to contain the greatest amount (i.e., thickest) of surface oil. In the SIMAP model, thresholds operate by effectively shutting off specific collection or containment potential when conditions at each location in space and time exceed the identified thresholds. As an example, if wave height exceeds 1 m at a specific location, the surface vessel dispersant at that location will not function at that location in the model until the conditions improve, and wave height falls below 1 m. Response efforts at the water surface were limited to daylight hours (Table 3-8), as effective operations are less likely during the darkness of night.

Table 3-8. Daylight hours for the 95th Percentile Surface Exposure Cases.

Scenario	Release Date	Sunrise	Sunset	Daylight Hours
Site 1 36 d	18 February 2010	7:00	17:28	10 hours 28 minutes
Site 2 36 d	29 November 2009	7:26	16:12	8 hours 46 minutes

4 Model Results

This section contains written summaries and analyses of model-predicted results. In addition, graphical depictions of surface oil thickness, in-water concentrations, and shoreline and sediment concentrations have been provided for stochastic and deterministic analyses. For each stochastic scenario, results images include both probability and minimum time for specific threshold exceedances (Table 2-2). For deterministic scenarios, results images include mass balance information and cumulative footprints of surface oil thickness, in-water concentrations, and shoreline and sediment concentrations.

4.1 Stochastic Analysis Results

Stochastic analyses characterize results from many tens to hundreds of individual modelled releases of BdN crude oil. This study included modelling 171 or 172 individual releases over the course of seven years of environmental data at Site 1 and Site 2 to capture the natural variability in the environment. The duration of each model run was 160 days with continuous 36- and 115-day blowouts at both sites. In total, four stochastic analyses were conducted based upon these two release locations and two release durations.

Because ice cover can affect the trajectory and fate of oil, stochastic model runs were separated into two groups of the individual runs based upon the specific time periods modelled that included sea-ice cover or ice-free conditions. Statistics for all releases within a stochastic scenario are referred to as “annual”, as they include all releases in any month over the course of the entire seven years. Sea-ice cover in the region is present in specific regions from November through April, while May through October is mostly ice-free. Modelled releases that have the majority of their simulated days (≥ 81 of the 160-day modelled duration) experiencing mostly ice-free periods are referred to as “summer” analyses, while those that have a majority of days experiencing periods with ice cover are referred to as “winter” analyses. The 171 runs within the 36-day release scenario contained 81 winter and 90 summer scenarios, while the 172 runs within the 115-day release scenario contained 83 winter and 89 summer scenarios. The duration of each modelled simulation was 160 days (Table 2-4). Sea-ice cover very rarely extended far enough offshore to reach the release locations, and when it did, < 10% ice cover was predicted. However, sea ice was present along most of the coastline in winter months, with February typically having the largest expanses of 90-100% ice cover.

The figures presented in this stochastic modelling results section illustrate the predicted spatial extent of surface floating oil, water column concentrations of dissolved hydrocarbons (i.e., the dissolved portion of AR1-3 from Table 3-2), and shoreline contact, including both the probabilities and associated minimum times to threshold exceedance (Table 2-2) for the hypothetical release scenarios. The

probability maps define the area of potential exposure and the associated probability with which sea surface oil, shoreline oil, or water column concentration are expected to exceed the specified thresholds at any point of time throughout the 160-day modelled duration. The colored contours in the stochastic map signify the outer boundary of areas that may experience oil at or above the specified threshold for given percentiles of the release scenarios. Darker color contours denote areas that are more likely to exceed the specified threshold, while lighter color contours are less likely. Note that the lightest mint-green line represents areas where oil may exceed the specified threshold in only 1% of release simulations. In other words, the likelihood that any oil exceeding the identified threshold would leave the area bounded by the mint-green line is <1%. The area between this contour and the next (10%) has between a 1-10% probability of exceeding the threshold, given a release of the modelled scenario has occurred.

The probabilities of oil exposure were calculated from a statistical analysis of the ensemble of individual unmitigated trajectories modelled for each release scenario. The fundamental assumption for this modelling was that a release did occur. Therefore, probability contours should be interpreted as “In the unlikely event of a release, the probability that any one specific area may experience oil exposure above the specified threshold is X%.” Stochastic figures do not imply that the entire contoured area would be covered with oil in the event of a single release, nor do they provide any information on the quantity of oil in a given area. Additionally, these figures do not provide the likelihood of a blowout occurring in any given year. Rather, these stochastic figures denote the probability of oil exceeding identified thresholds at any modelled time step (over 160 days) for each point within the modelled domain, assuming a release were to occur at some point in time.

In addition, stochastic maps depicting water column exposure by dissolved hydrocarbon concentrations do not specify the depth at which the threshold exceedance occurs. The maps depict the vertical maximum at any time during or after the release. Thus, images do not imply that the entire water column (i.e., from surface to bottom) will experience a concentration above the threshold, but rather a concentration may be exceeded at a specific depth (typically within the surface few meters) in the mapped location.

The minimum time footprints correspond with the associated probability of oil exposure map. Each figure illustrates the shortest amount of time required (from the initial release) for each point within the footprint to exceed the defined threshold. The time reported is the minimum value for each point considering the entire ensemble of trajectories. Together, probability and minimum time figures can be interpreted together to read: “There is a X% probability that oil is predicted to exceed the identified threshold at a specific location, and this exceedance could occur in as little as Y days.”

The Exclusive Economic Zone for Canada and the U.S., as well as the international border, are depicted on each map to provide context for the spatial extent and potentially-affected territorial waters from any potential release (VLIZ, 2014).

All figures depict data where probability of a region exceeding the conservative socio-economic threshold is > 1%. When comparing annual to seasonal results, the predicted percent exceedance depends on the total number of releases investigated in each subset of releases. Therefore, while only one scenario might be required to exceed the 1% threshold for visualization in seasonal results (containing <100 modelled simulations), two scenarios would be required to exceed the same threshold in the annual analysis (containing 171 or 172 modelled simulations), due to a greater number of modelled releases in the annual set of runs being analyzed. Figures depicting stochastic results are provided for surface oil thickness >0.04 µm, dissolved hydrocarbon concentration > 1 µg/L, and shoreline contact > 1 g/m^2 for annual, summer, and winter scenarios for Site 1 (Figure 4-1 through Figure 4-18) and Site 2 (Figure 4-19 through Figure 4-36).

4.1.1 Site 1 Subsurface Release

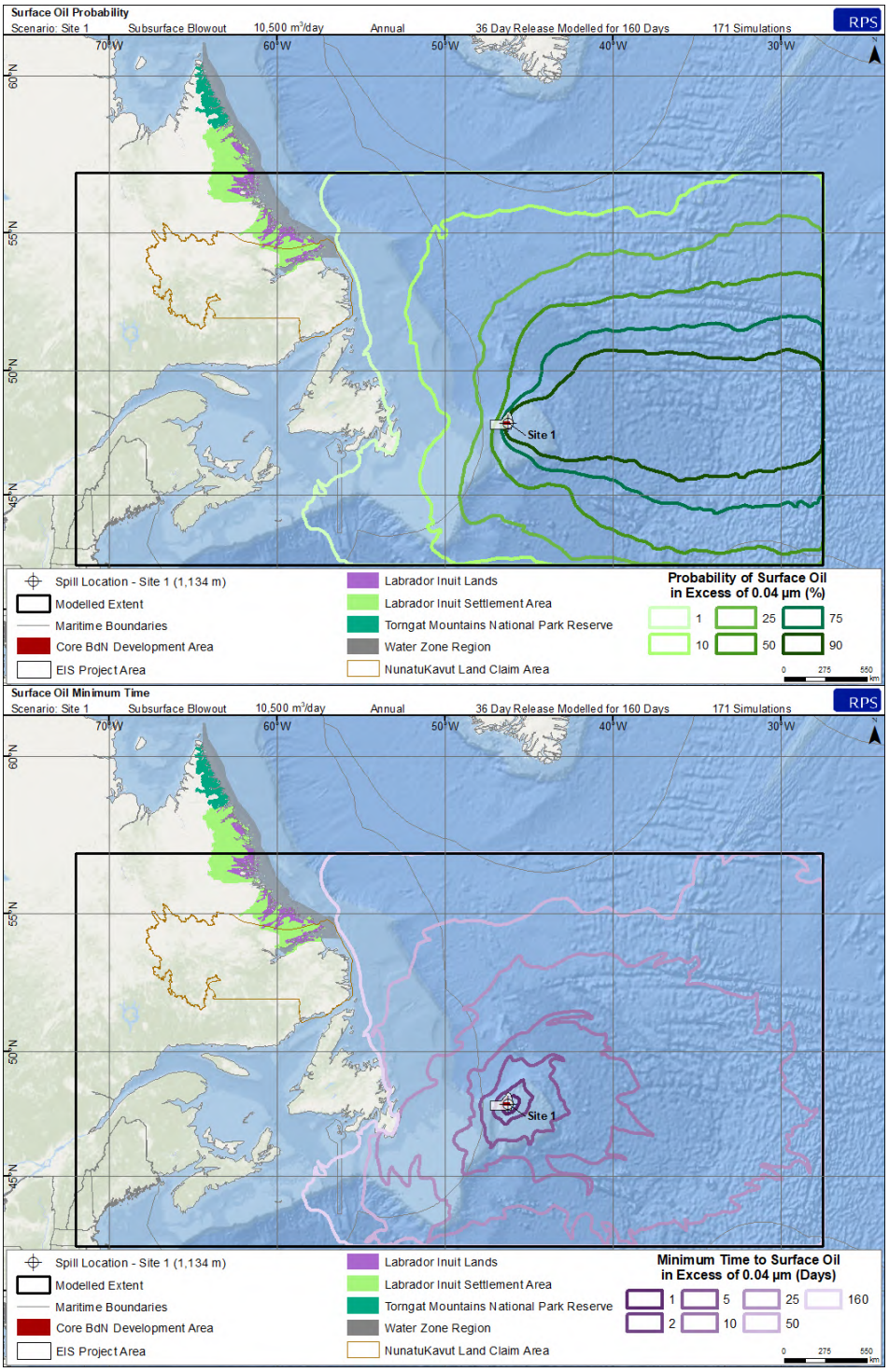

Figure 4-1. Annual probability of average surface oil thickness exceeding 0.04 µm (top) and minimum time to threshold exceedance (bottom) resulting from a 36-day subsurface blowout at Site 1.

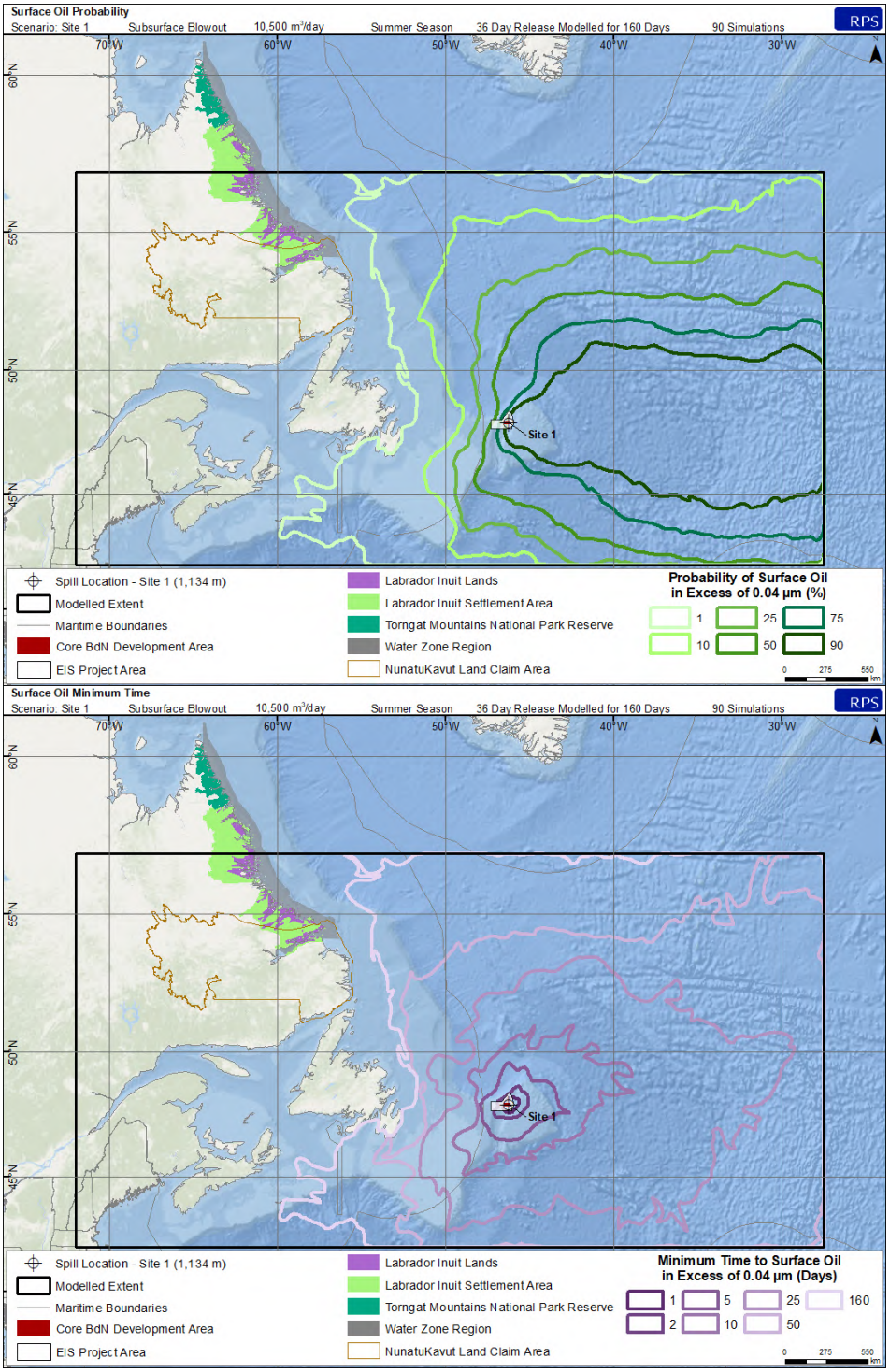

Figure 4-2. Summer probability of average surface oil thickness > 0.04 µm (top) and minimum time to threshold exceedance (bottom) resulting from a 36-day subsurface blowout at Site 1.

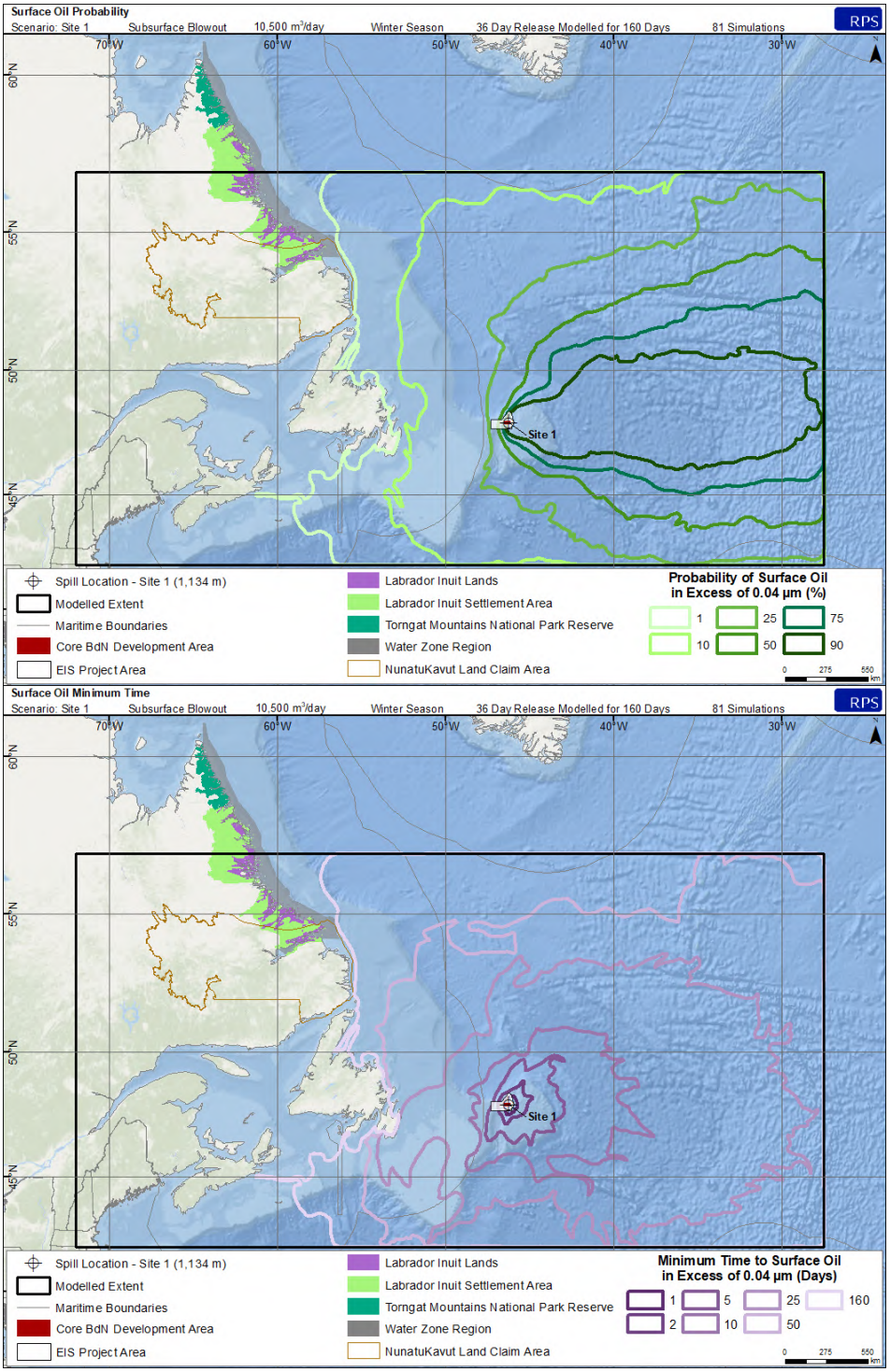

Figure 4-3. Winter probability of average surface oil thickness > 0.04 µm (top) and minimum time to threshold exceedance (bottom) resulting from a 36-day subsurface blowout at Site 1 site.

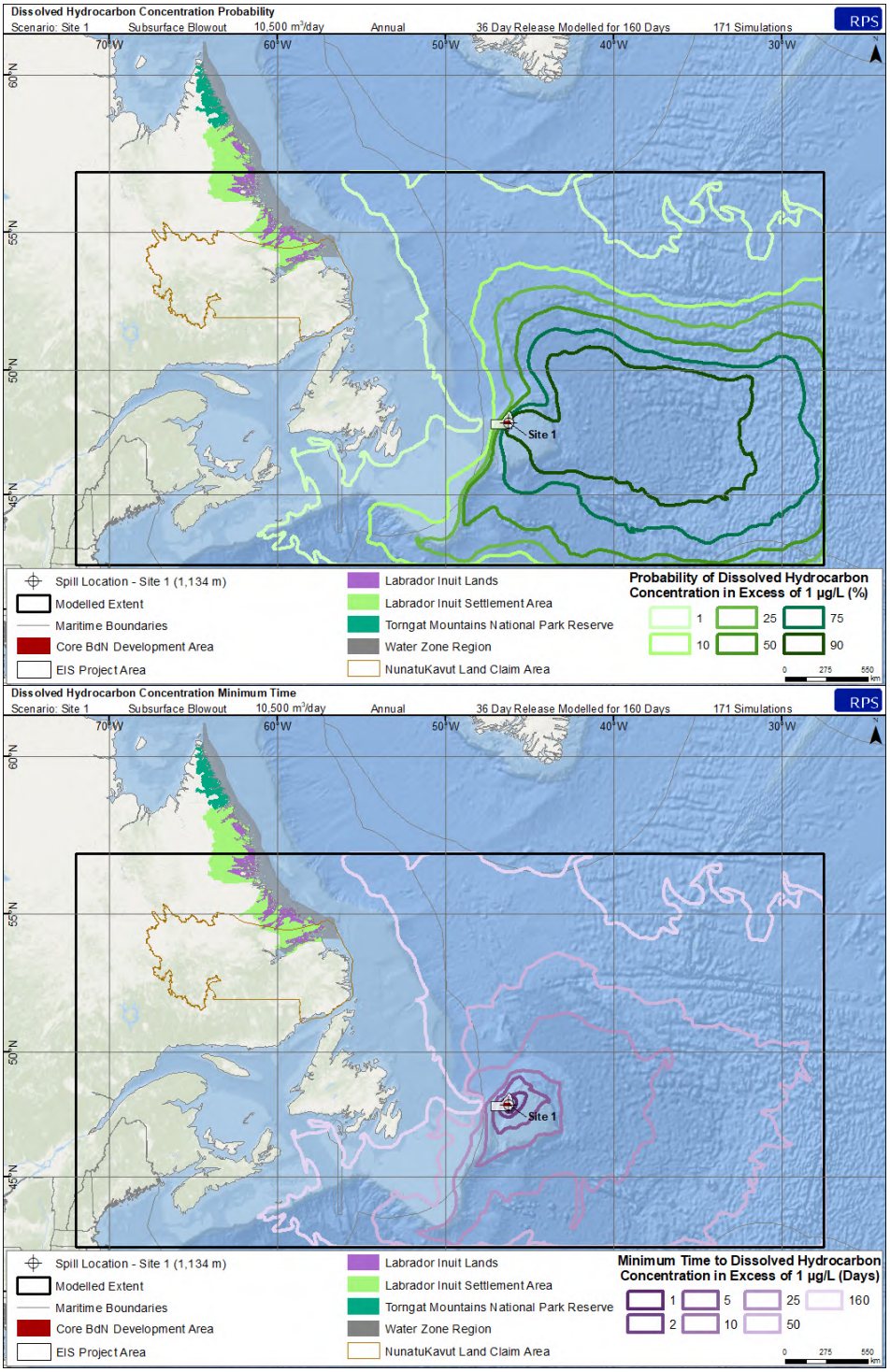

Figure 4-4. Annual probability of dissolved hydrocarbon concentrations > 1 µg/L at some depth in the water column (top) and minimum time to threshold exceedance (bottom) resulting from a 36-day subsurface blowout at Site 1.

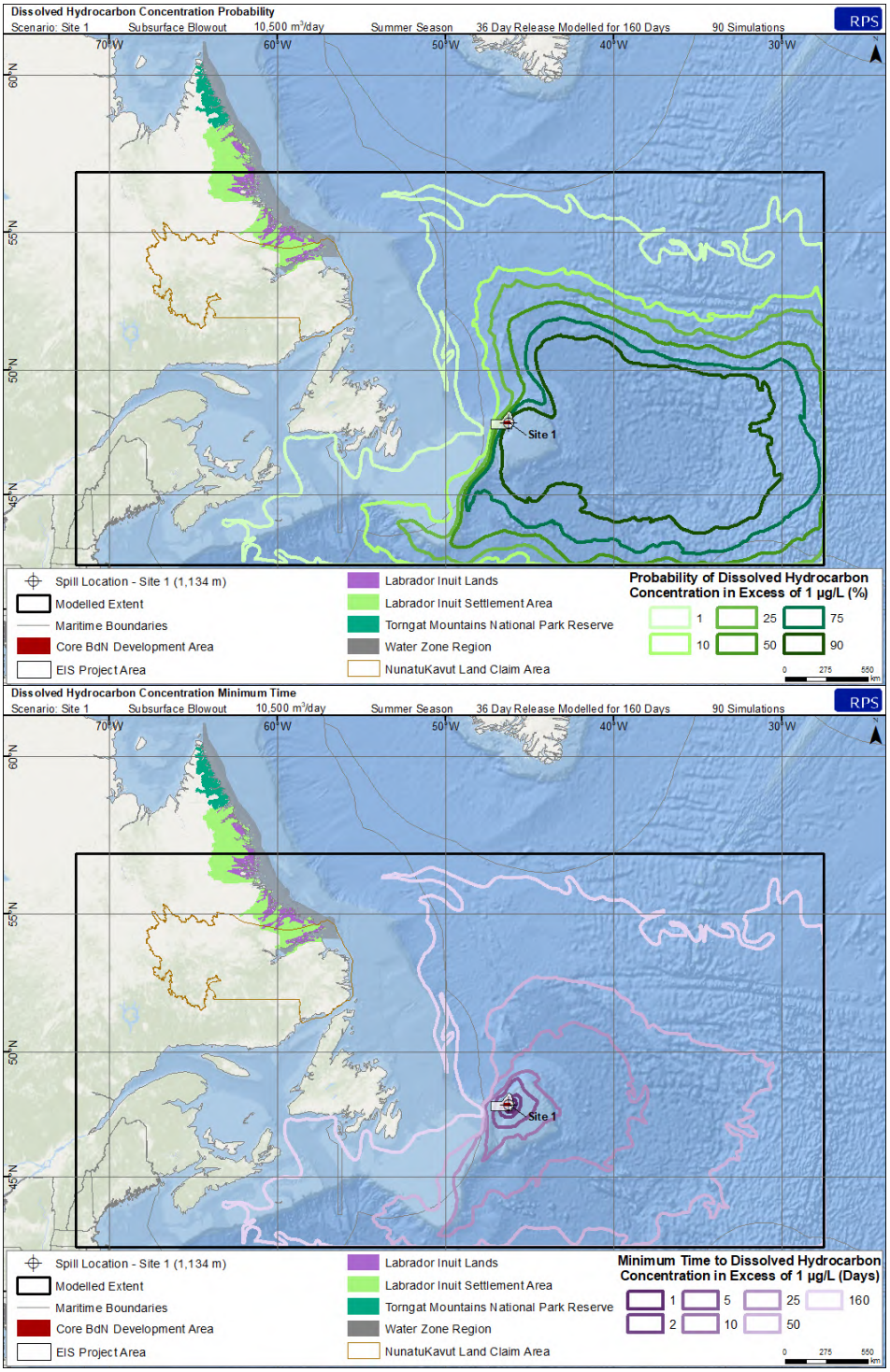

Figure 4-5. Summer probability of dissolved hydrocarbon concentrations > 1 µg/L at some depth in the water column (top) and minimum time to threshold exceedance (bottom) resulting from a 36-day subsurface blowout at Site 1.

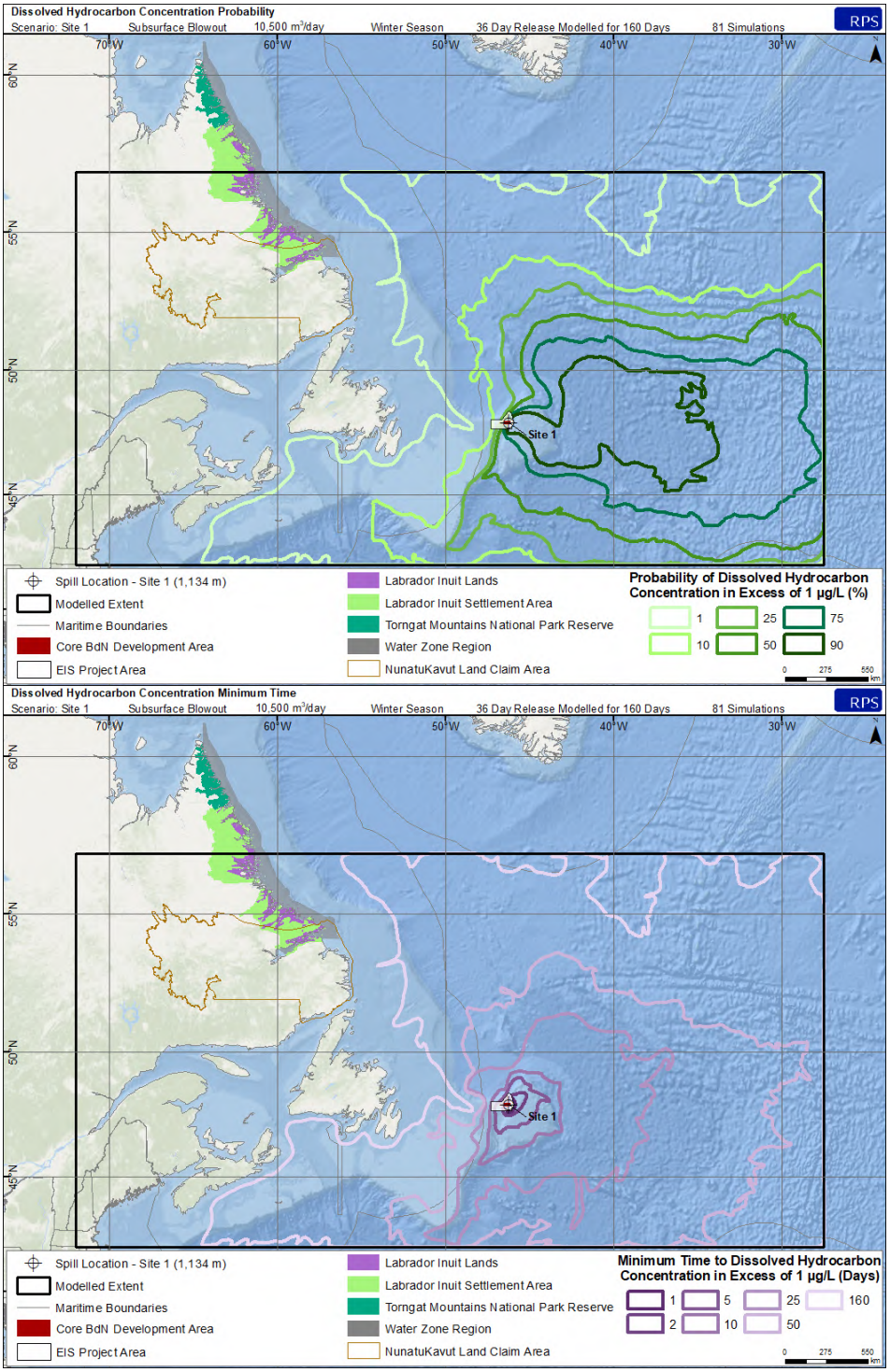

Figure 4-6. Winter probability of dissolved hydrocarbon concentrations > 1 µg/L at some depth in the water column (top) and minimum time to threshold exceedance (bottom) resulting from a 36-day subsurface blowout at Site 1.

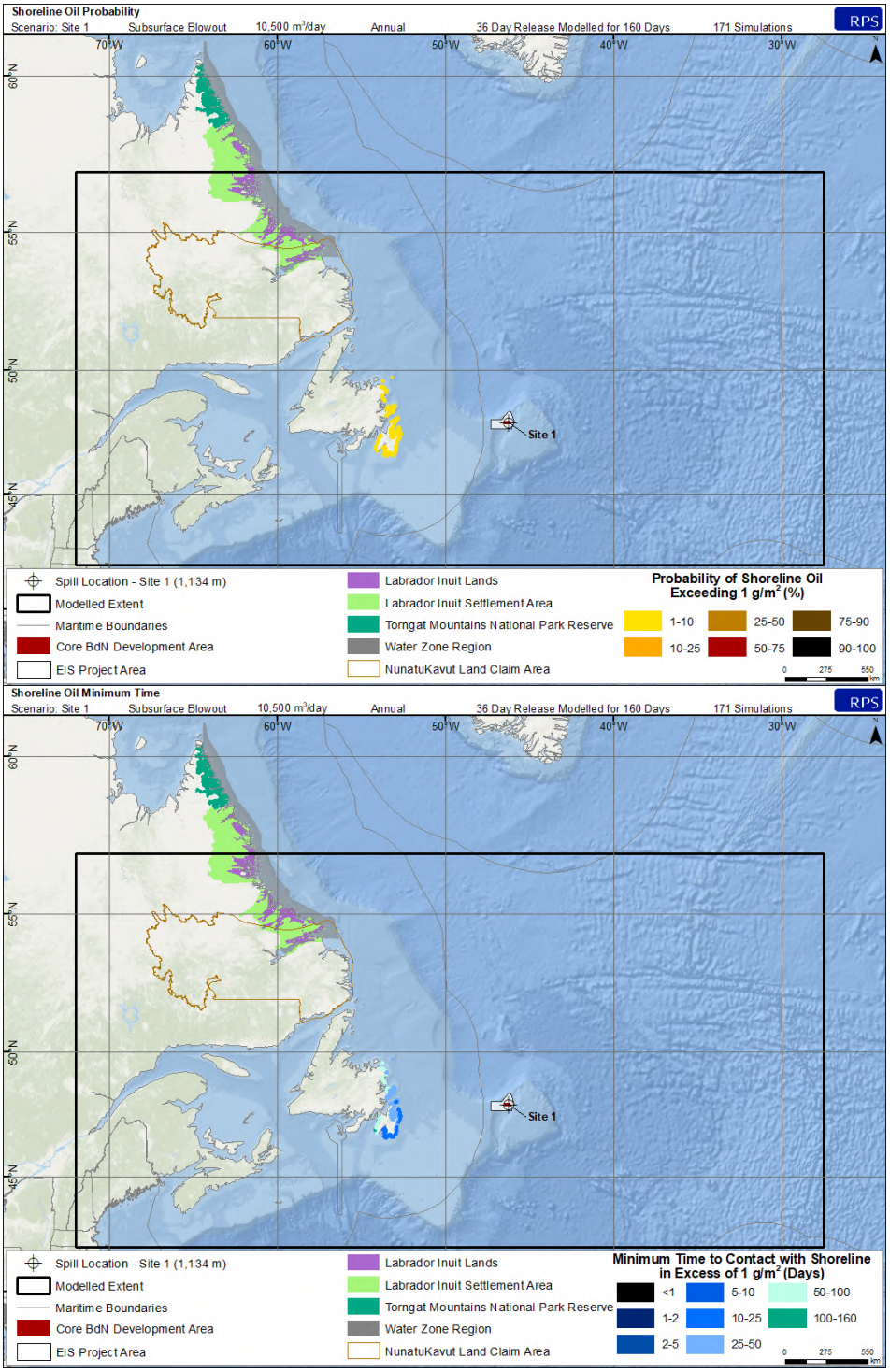

Figure 4-7. Annual probability of shoreline contact > 1 g/m² (top) and minimum time to threshold exceedance (bottom) resulting from a 36-day subsurface blowout at Site 1.

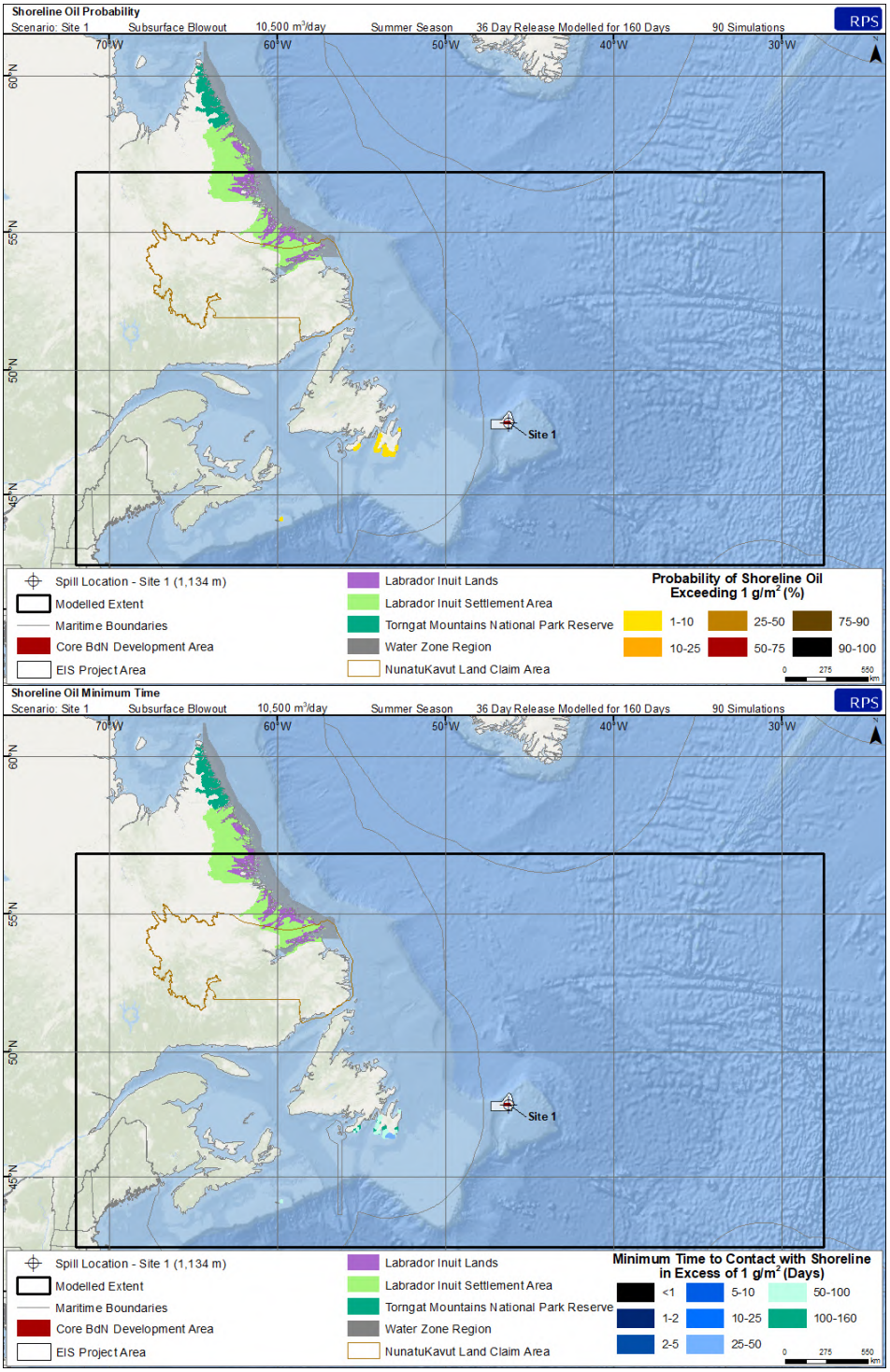

Figure 4-8. Summer probability of shoreline contact > 1 g/m² (top) and minimum time to threshold exceedance (bottom) resulting from a 36-day subsurface blowout at Site 1.

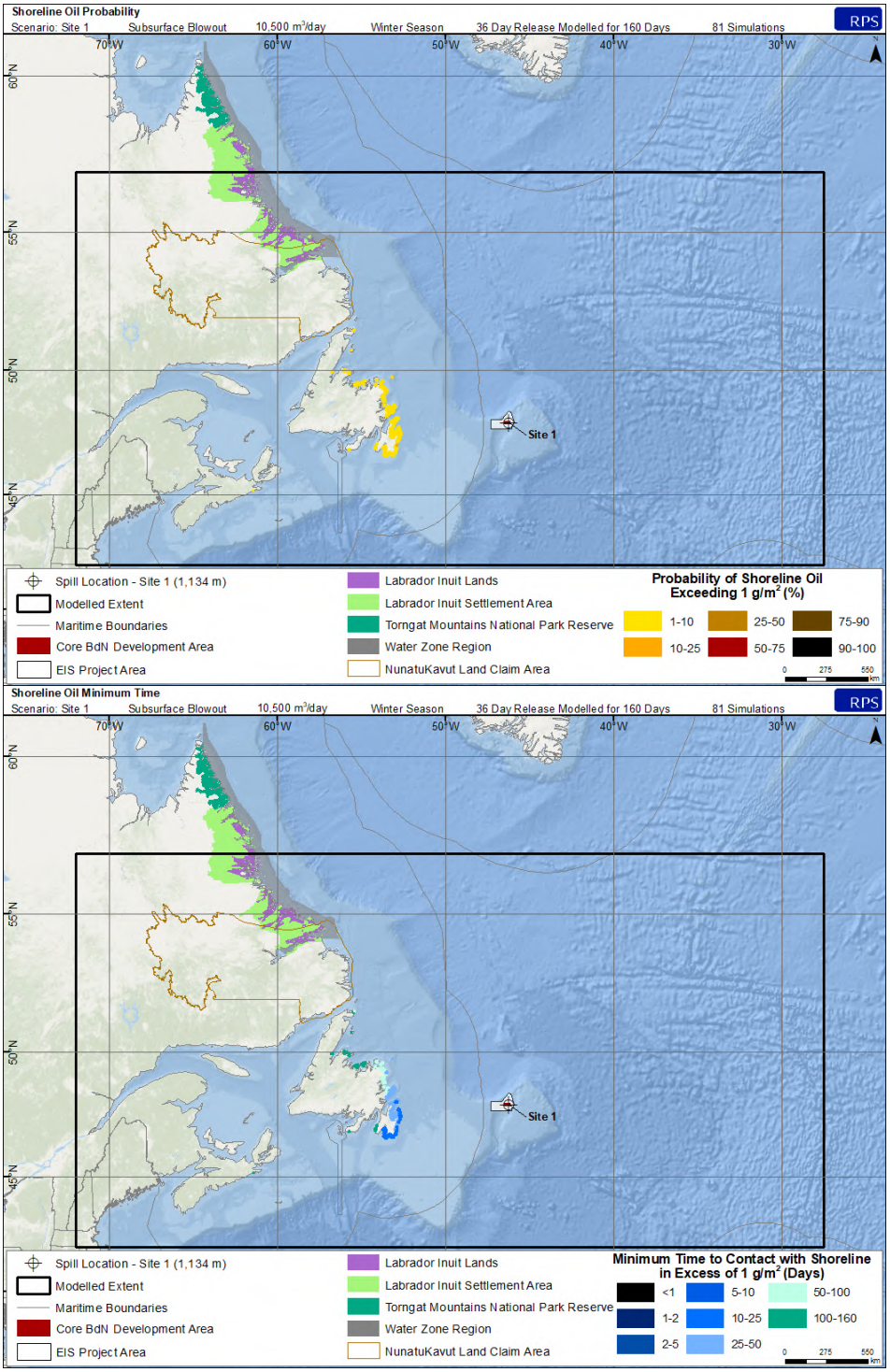

Figure 4-9. Winter probability of shoreline contact > 1 g/m² (top) and minimum time to threshold exceedance (bottom) resulting from a 36-day subsurface blowout at Site 1.

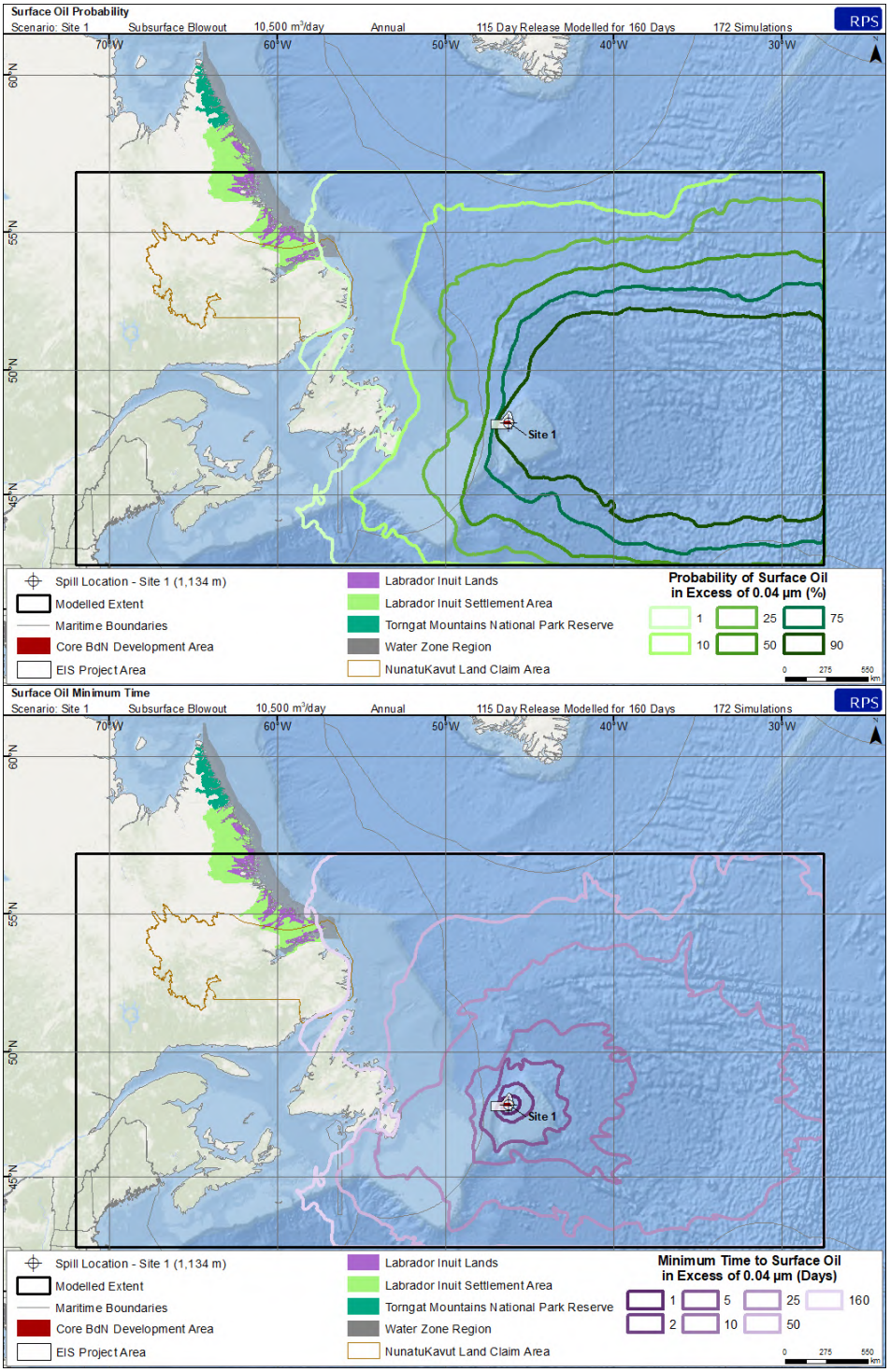

Figure 4-10. Annual probability of average surface oil thickness exceeding 0.04 µm (top) and minimum time to threshold exceedance (bottom) resulting from a 115-day subsurface blowout at Site 1.

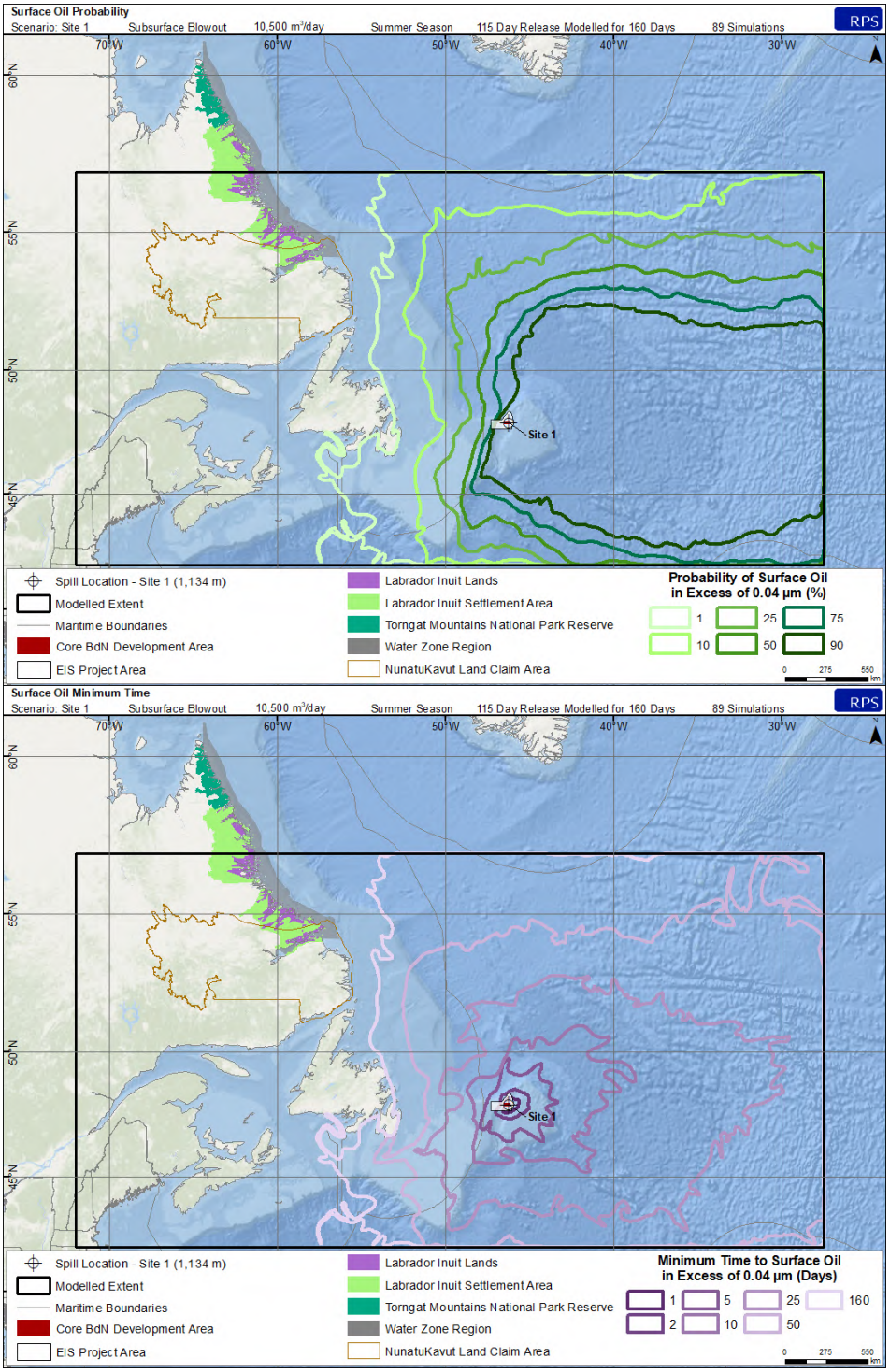

Figure 4-11. Summer probability of average surface oil thickness > 0.04 µm (top) and minimum time to threshold exceedance (bottom) resulting from a 115-day subsurface blowout at Site 1.

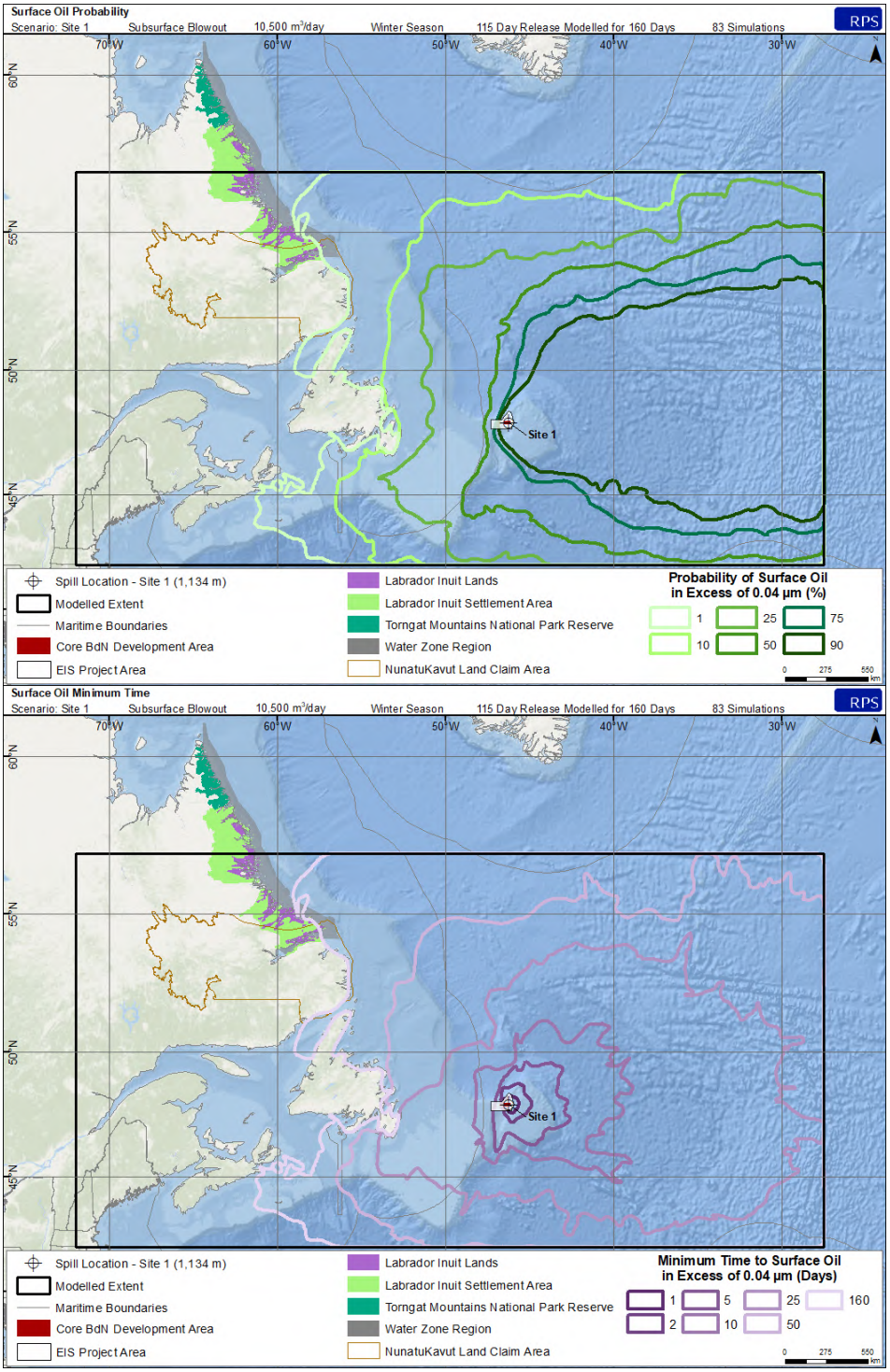

Figure 4-12. Winter probability of average surface oil thickness > 0.04 µm (top) and minimum time to threshold exceedance (bottom) resulting from a 115-day subsurface blowout at Site 1.

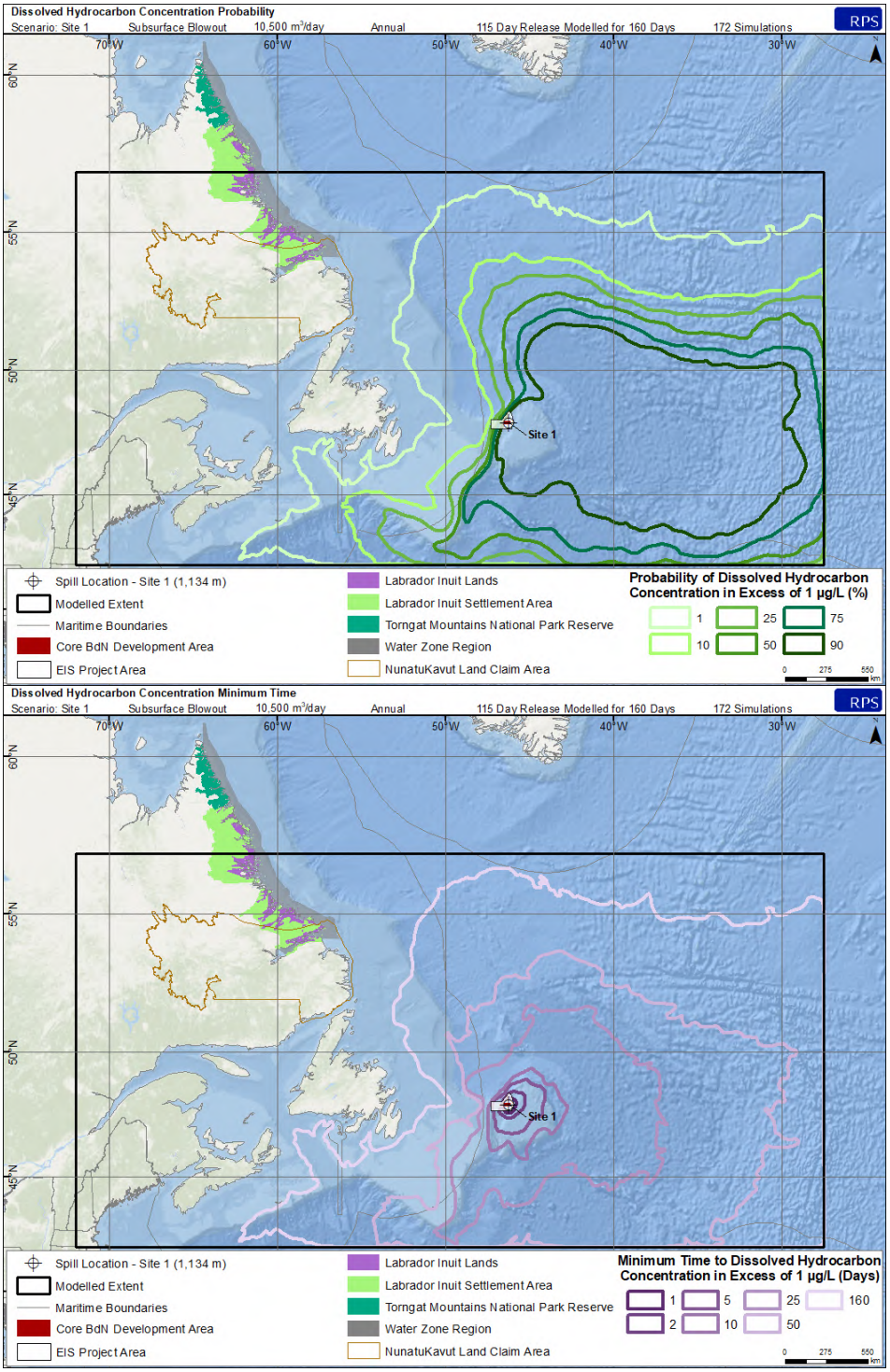

Figure 4-13. Annual probability of dissolved hydrocarbon concentrations > 1 µg/L at some depth in the water column (top) and minimum time to threshold exceedance (bottom) resulting from a 115-day subsurface blowout at Site 1.

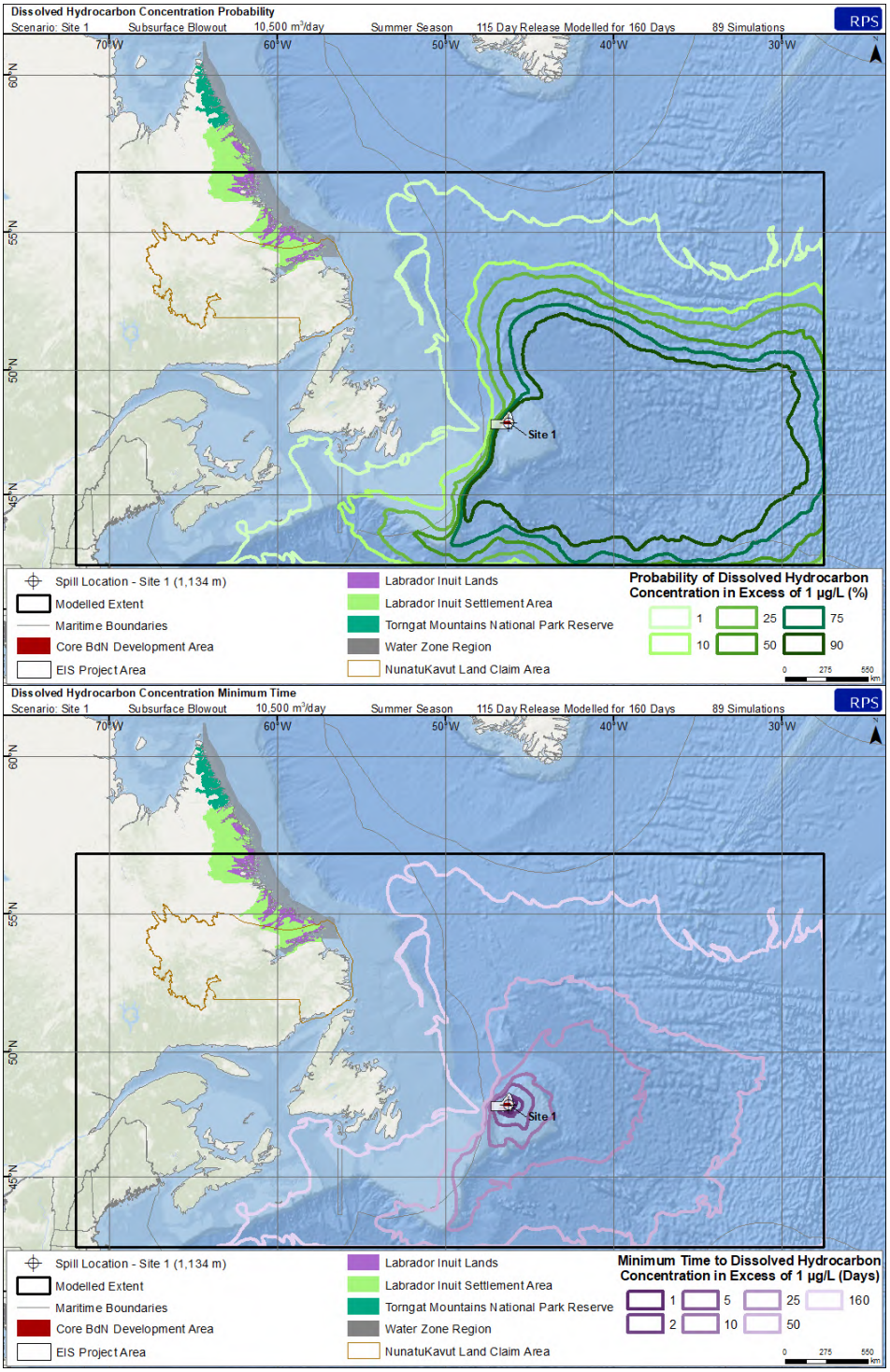

Figure 4-14. Summer probability of dissolved hydrocarbon concentrations > 1 µg/L at some depth in the water column (top) and minimum time to threshold exceedance (bottom) resulting from a 115-day subsurface blowout at Site 1.

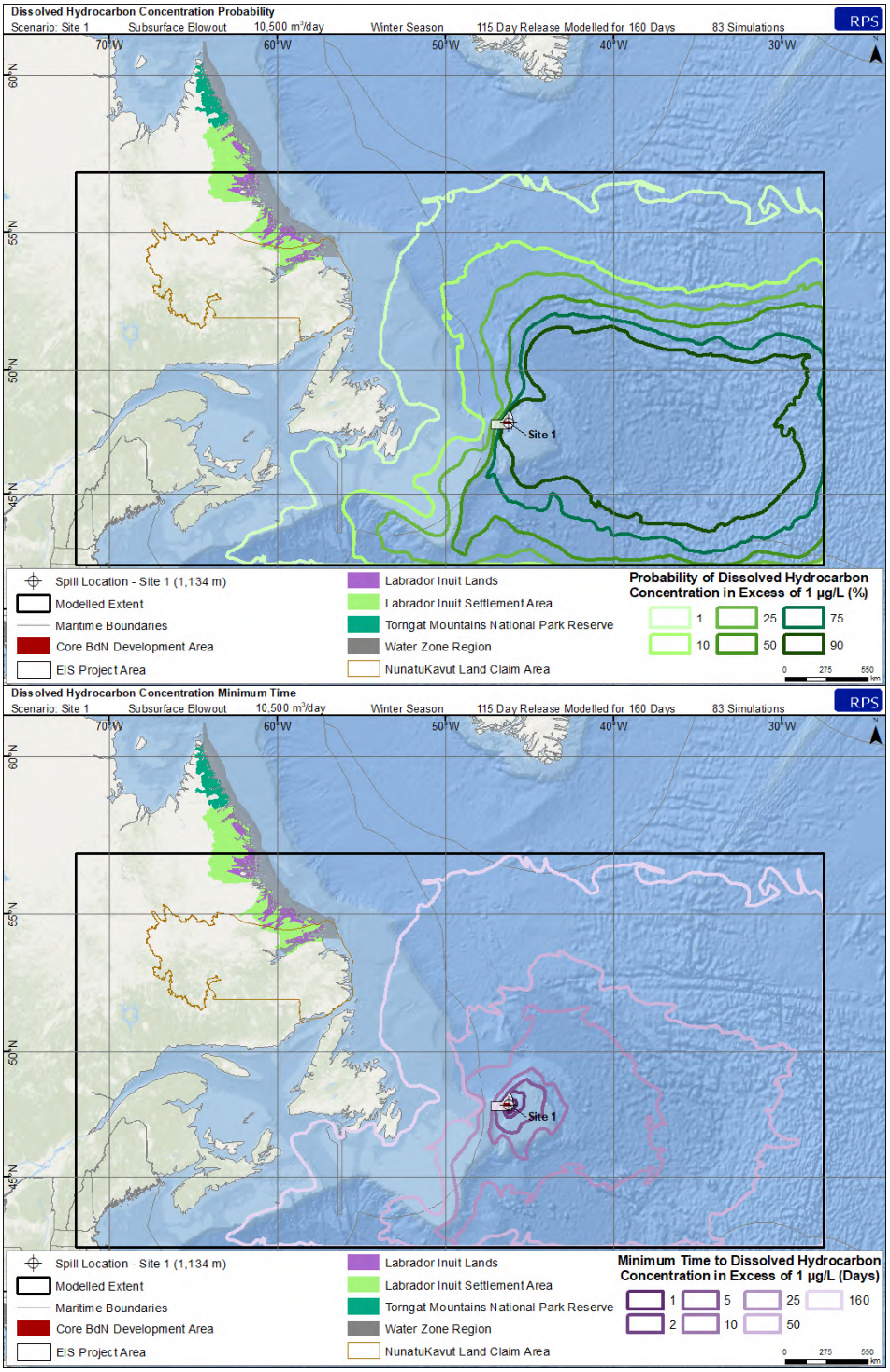

Figure 4-15. Winter probability of dissolved hydrocarbon concentrations > 1 µg/L at some depth in the water column (top) and minimum time to threshold exceedance (bottom) resulting from a 115-day subsurface blowout at Site 1.

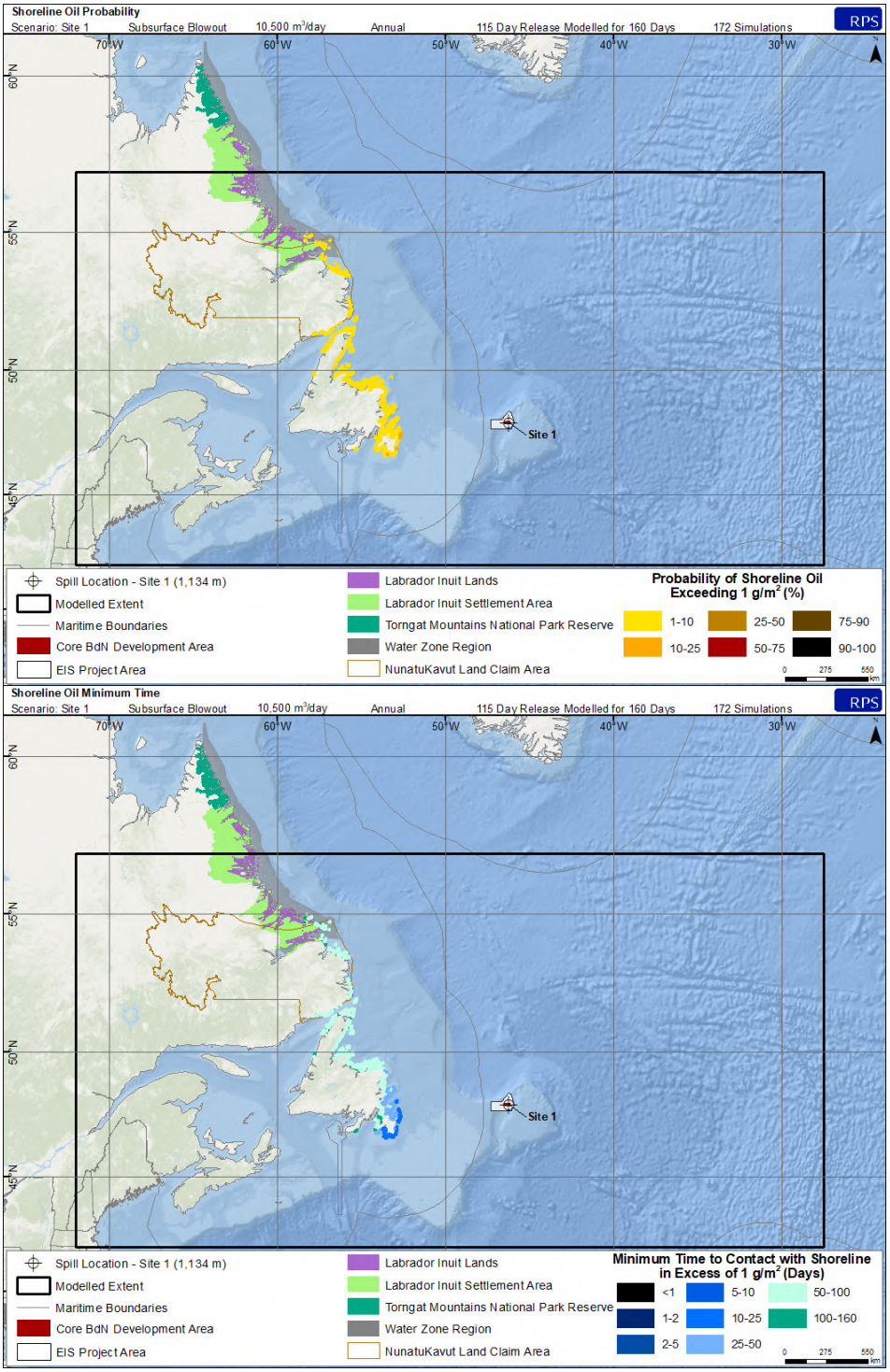

Figure 4-16. Annual probability of shoreline contact > 1 g/m² (top) and minimum time to threshold exceedance (bottom) resulting from a 115-day subsurface blowout at Site 1.

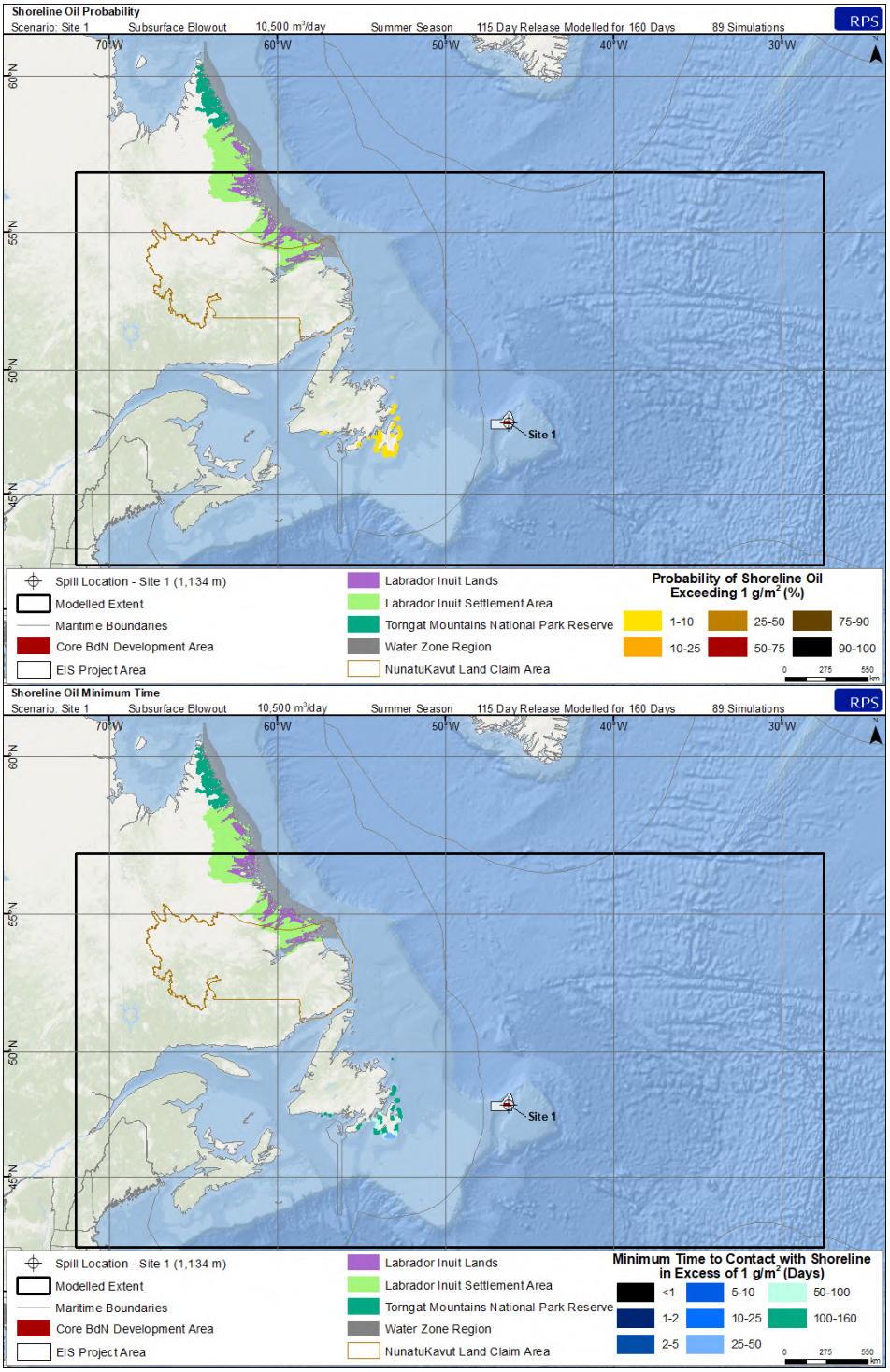

Figure 4-17. Summer probability of shoreline contact > 1 g/m² (top) and minimum time to threshold exceedance (bottom) resulting from a 115-day subsurface blowout at Site 1.

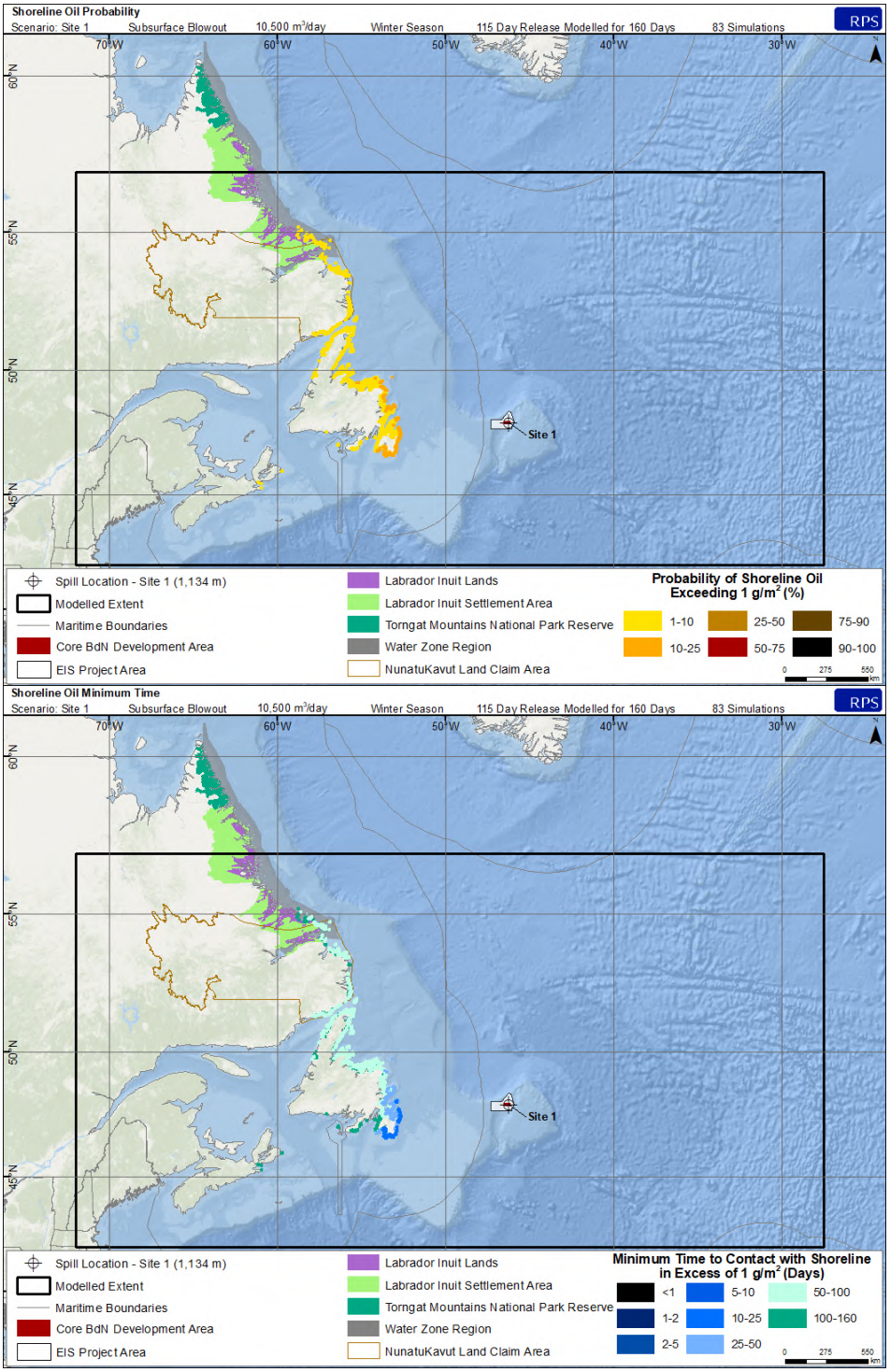

Figure 4-18. Winter probability of shoreline contact > 1 g/m² (top) and minimum time to threshold exceedance (bottom) resulting from a 115-day subsurface blowout at Site 1.

4.1.2 Site 2 Subsurface Release

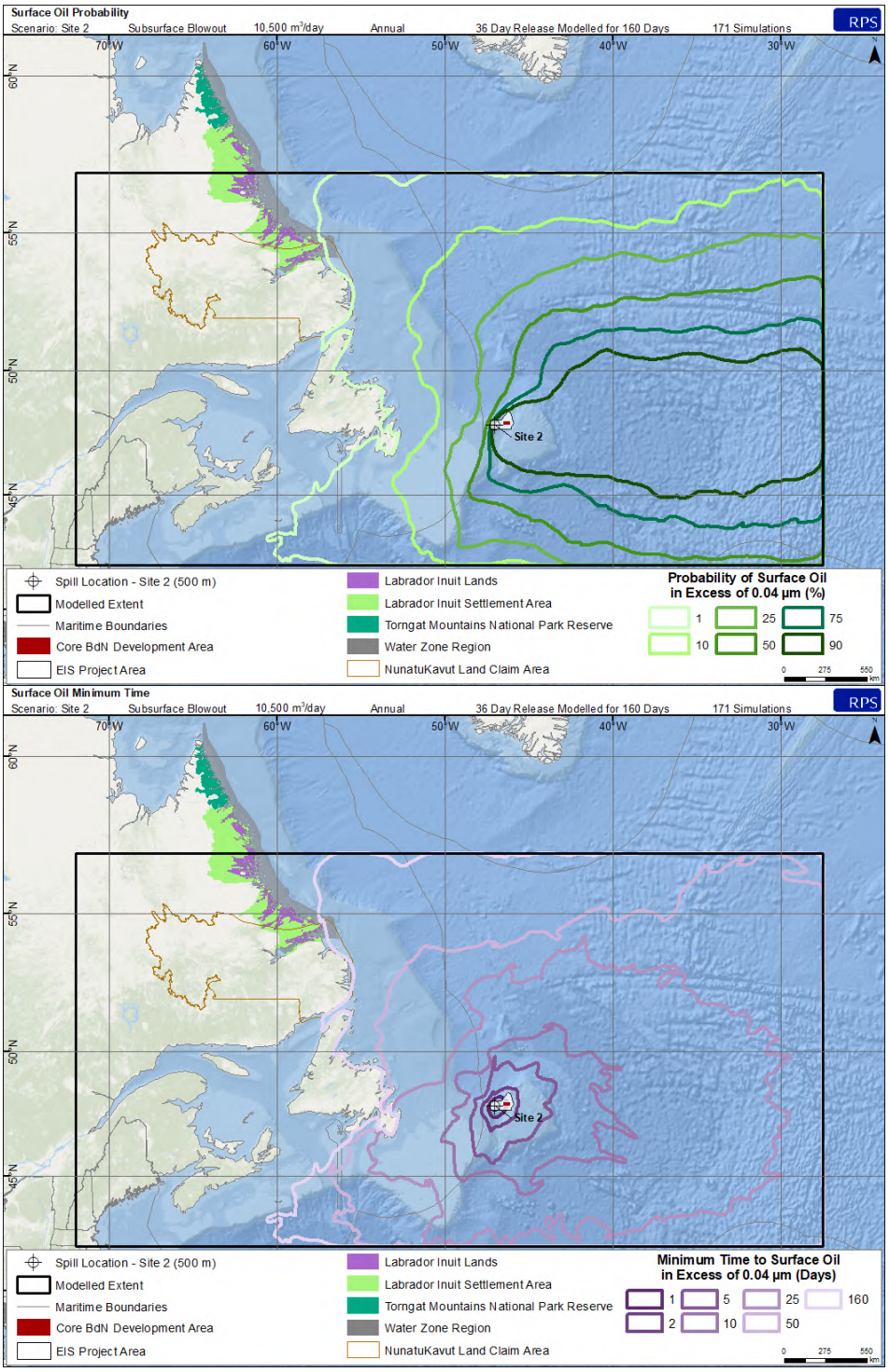

Figure 4-19. Annual probability of average surface oil thickness > 0.04 µm (top) and minimum time to threshold exceedance (bottom) resulting from a 36-day subsurface blowout at Site 2.

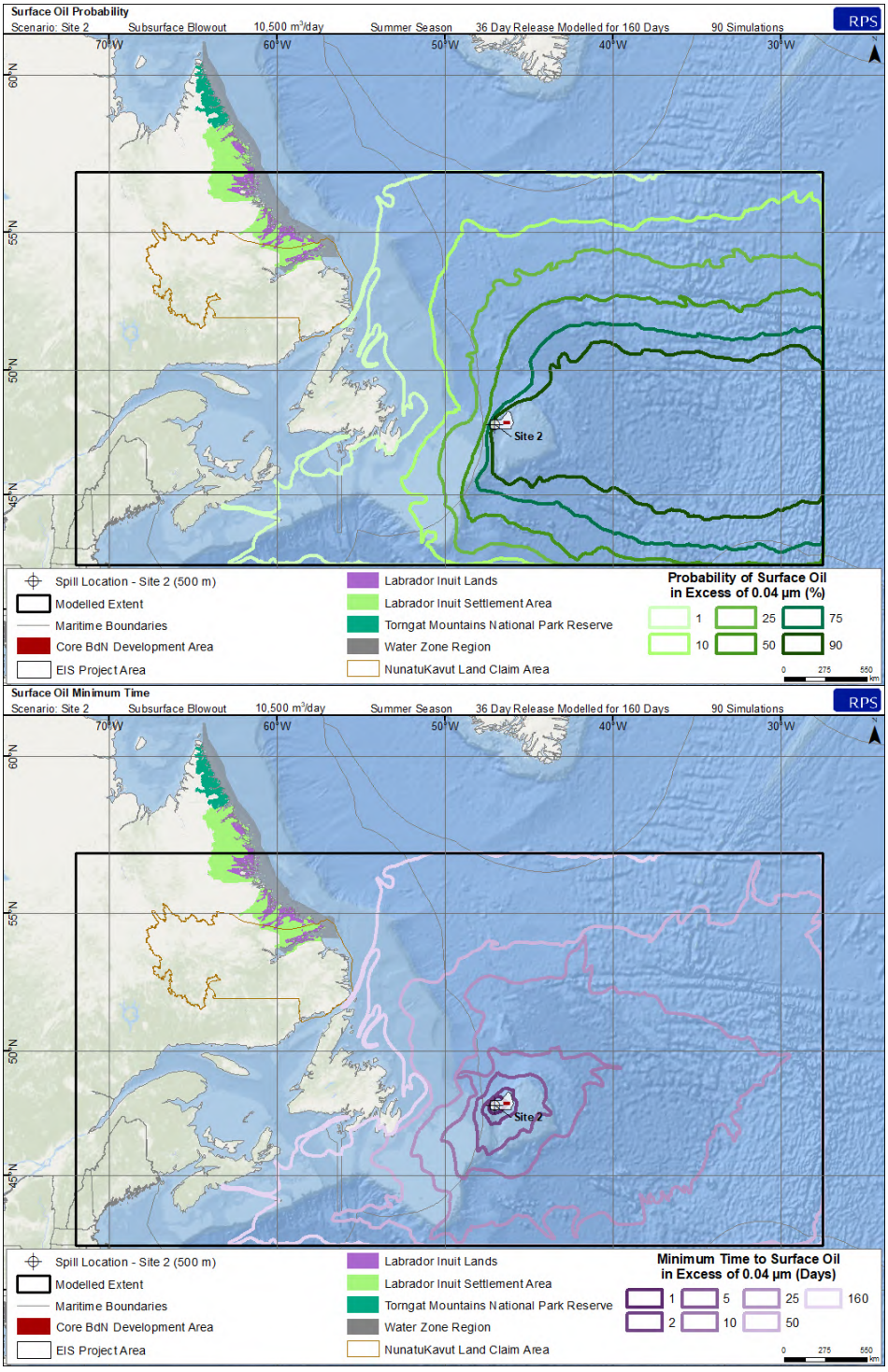

Figure 4-20. Summer probability of average surface oil thickness > 0.04 µm (top) and minimum time to threshold exceedance (bottom) resulting from a 36-day subsurface blowout at Site 2.

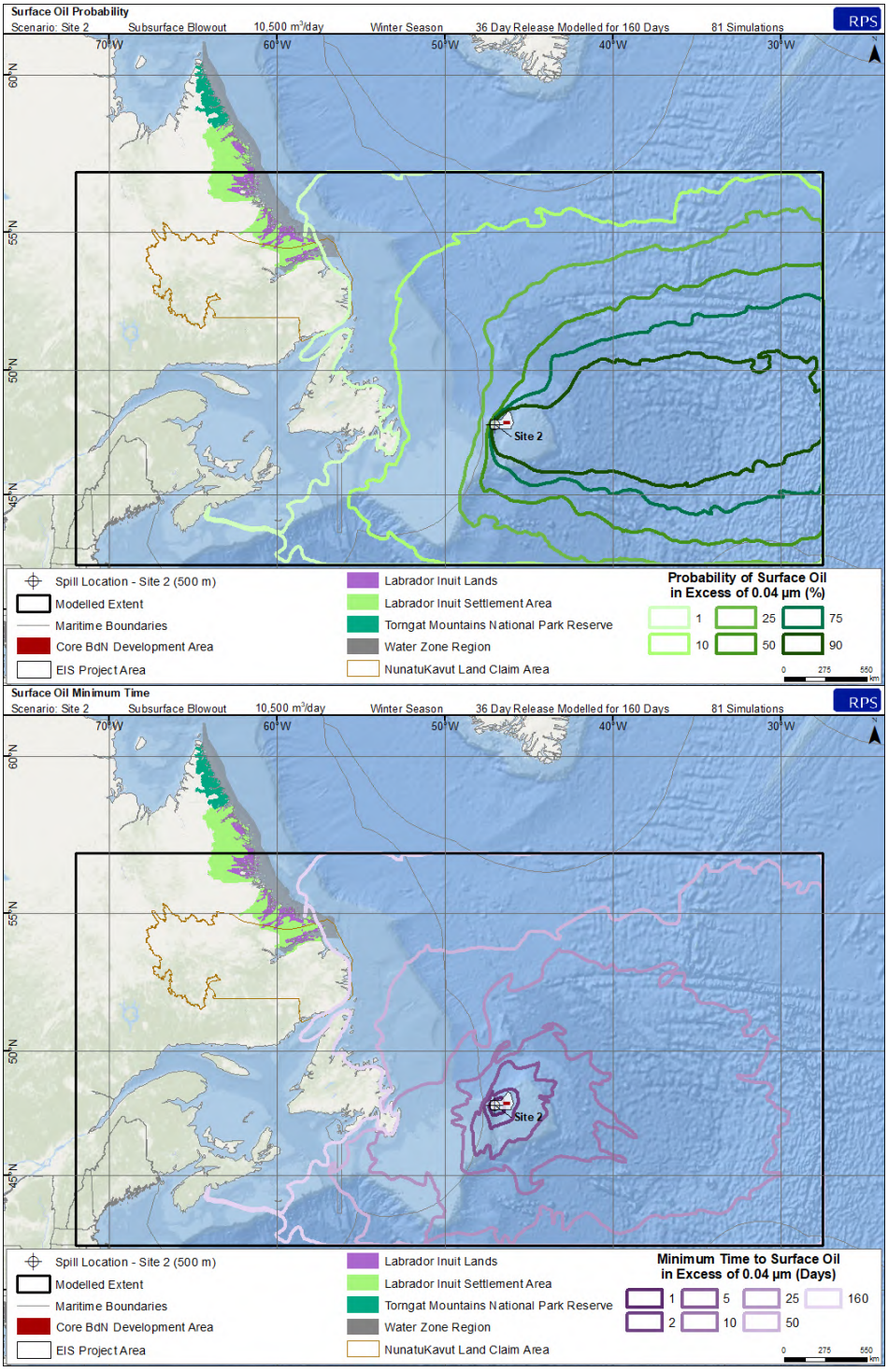

Figure 4-21. Winter probability of average surface oil thickness > 0.04 µm (top) and minimum time to threshold exceedance (bottom) resulting from a 36-day subsurface blowout at Site 2.

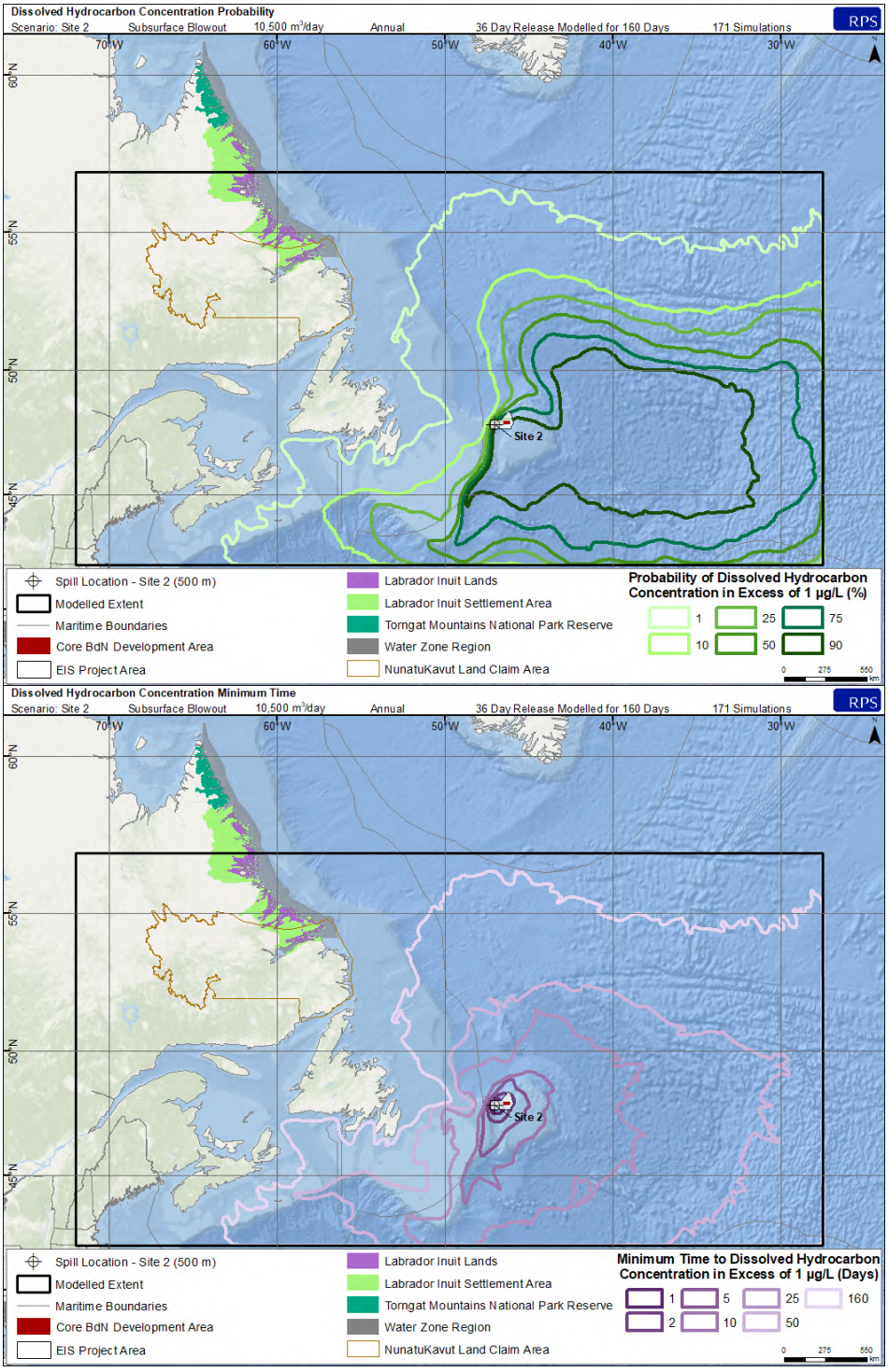

Figure 4-22. Annual probability of dissolved hydrocarbon concentrations > 1 µg/L at some depth in the water column (top) and minimum time to threshold exceedance (bottom) resulting from a 36-day subsurface blowout at Site 2.

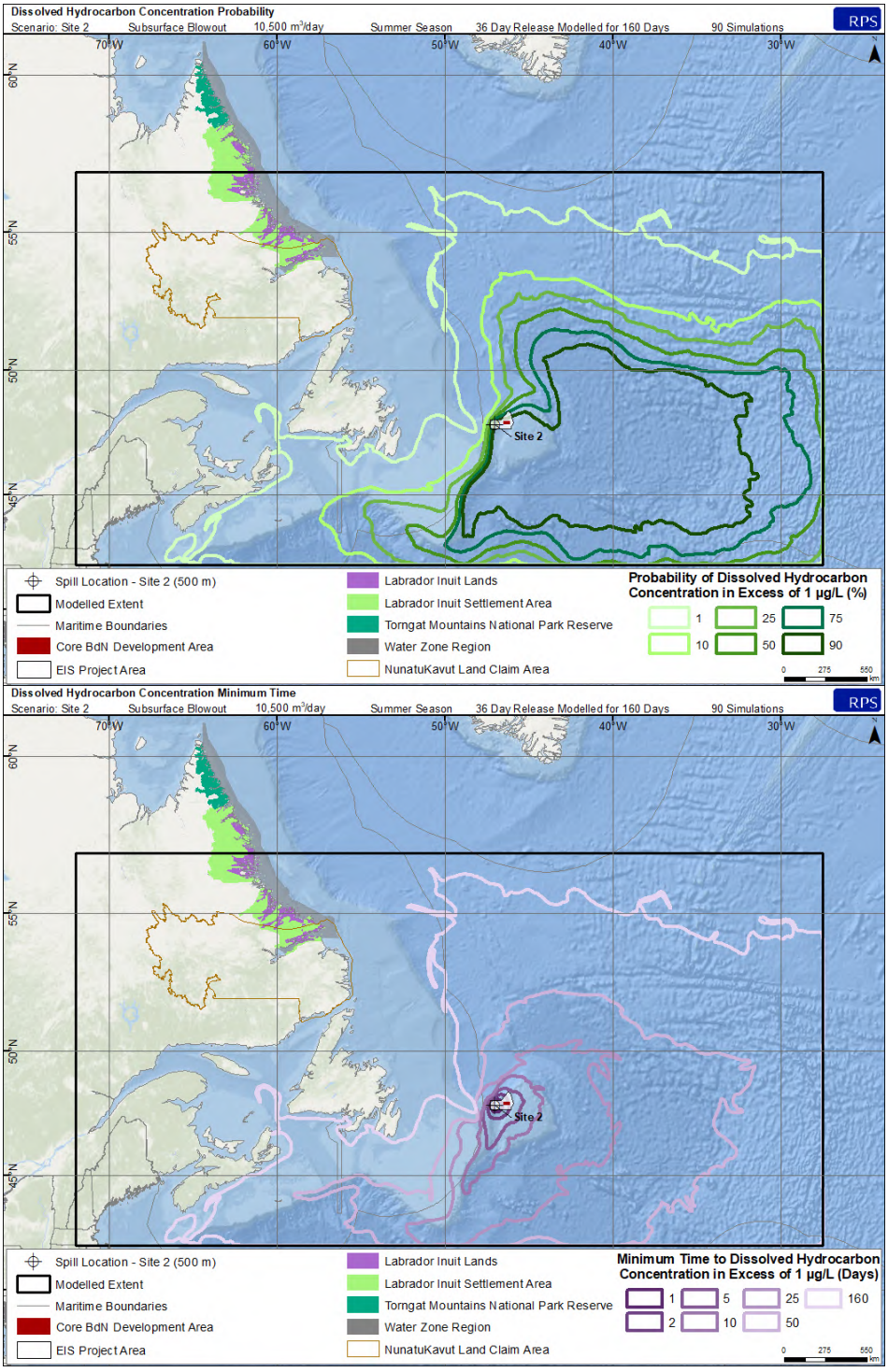

Figure 4-23. Summer probability of dissolved hydrocarbon concentrations > 1 µg/L at some depth in the water column (top) and minimum time to threshold exceedance (bottom) resulting from a 36-day subsurface blowout at Site 2.

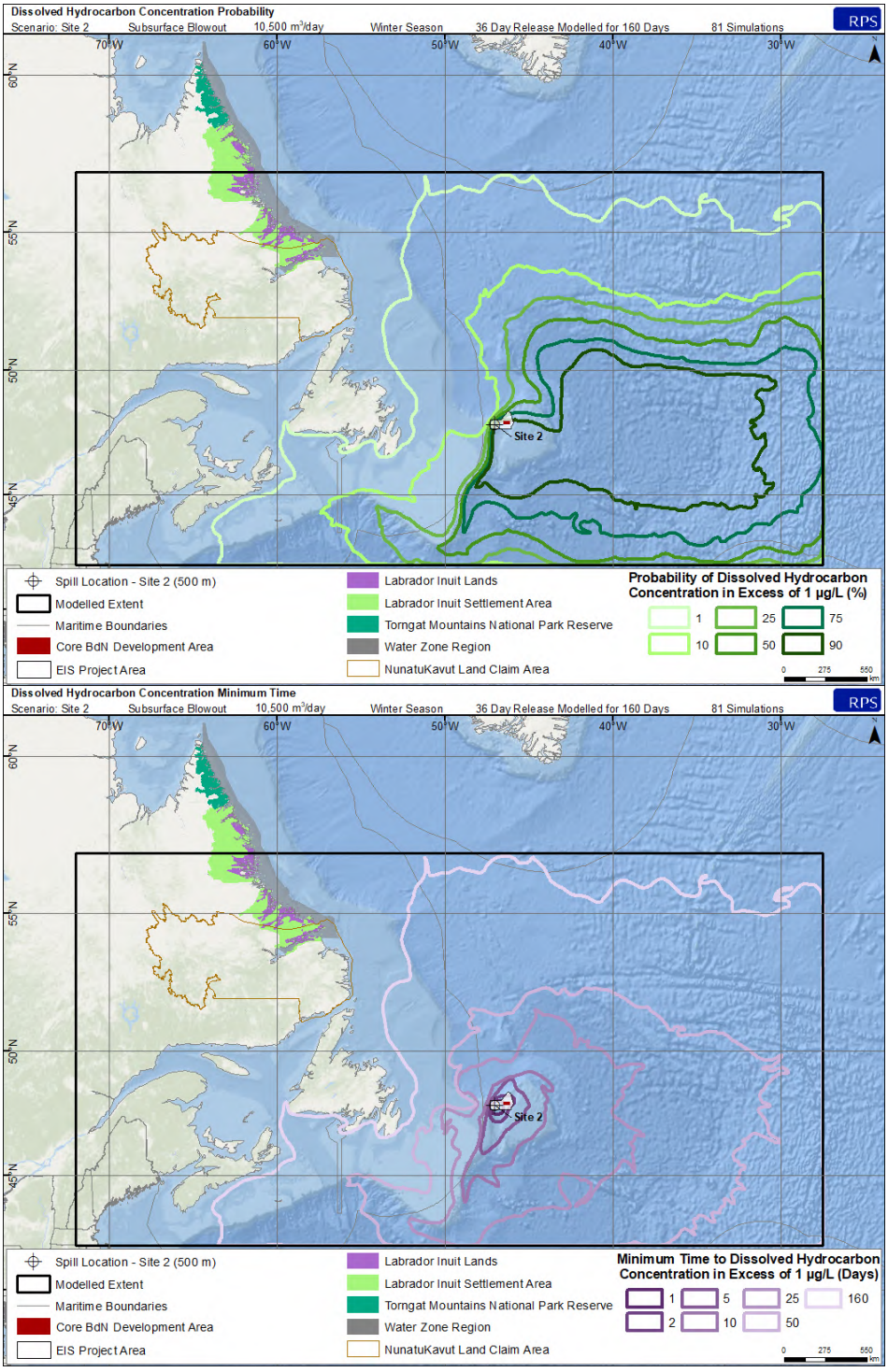

Figure 4-24. Winter probability of dissolved hydrocarbon concentrations > 1 µg/L at some depth in the water column (top) and minimum time to threshold exceedance (bottom) resulting from a 36-day subsurface blowout at Site 2.

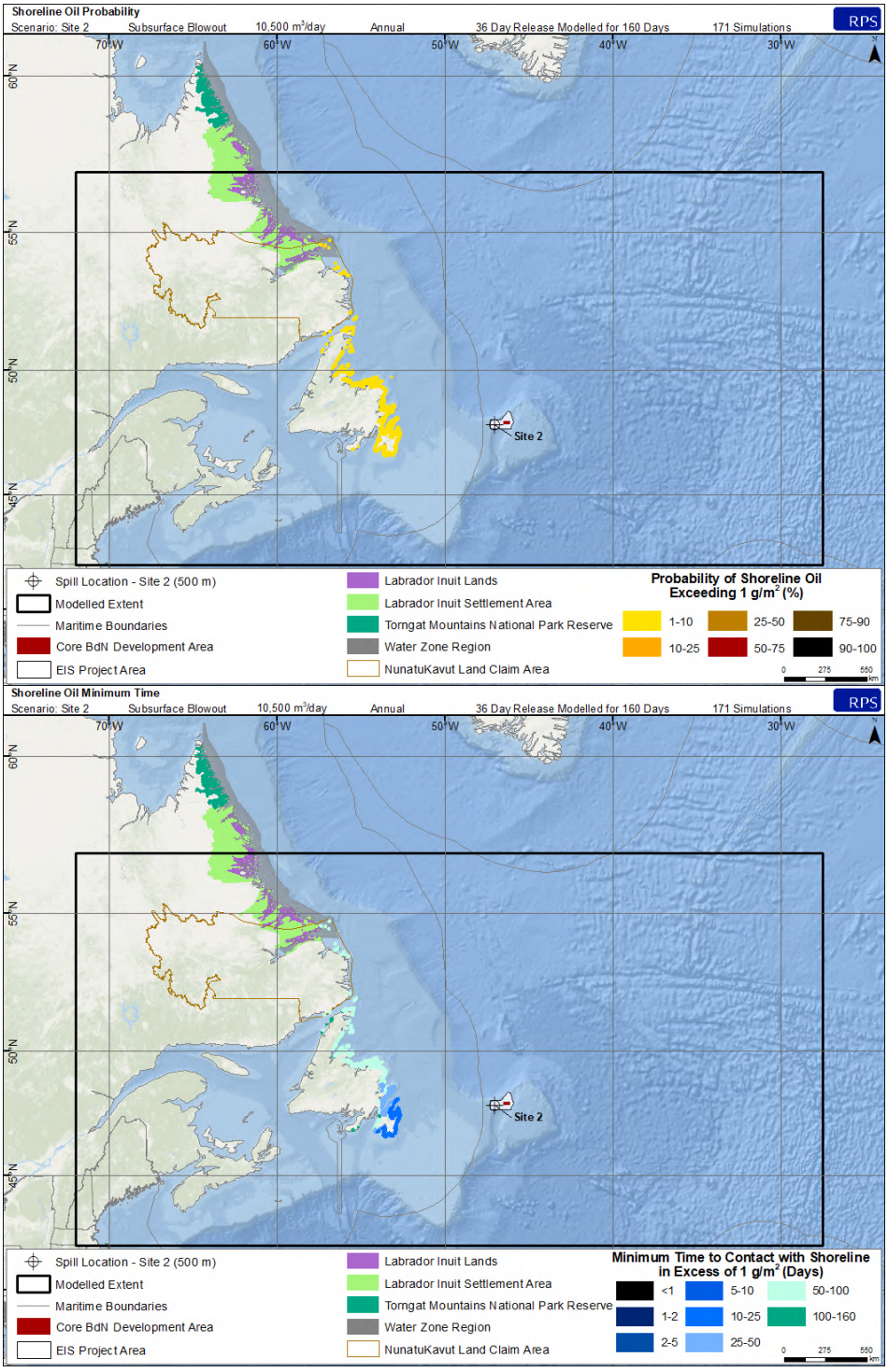

Figure 4-25. Annual probability of shoreline contact > 1 g/m² (top) and minimum time to threshold exceedance (bottom) resulting from a 36-day subsurface blowout at Site 2.

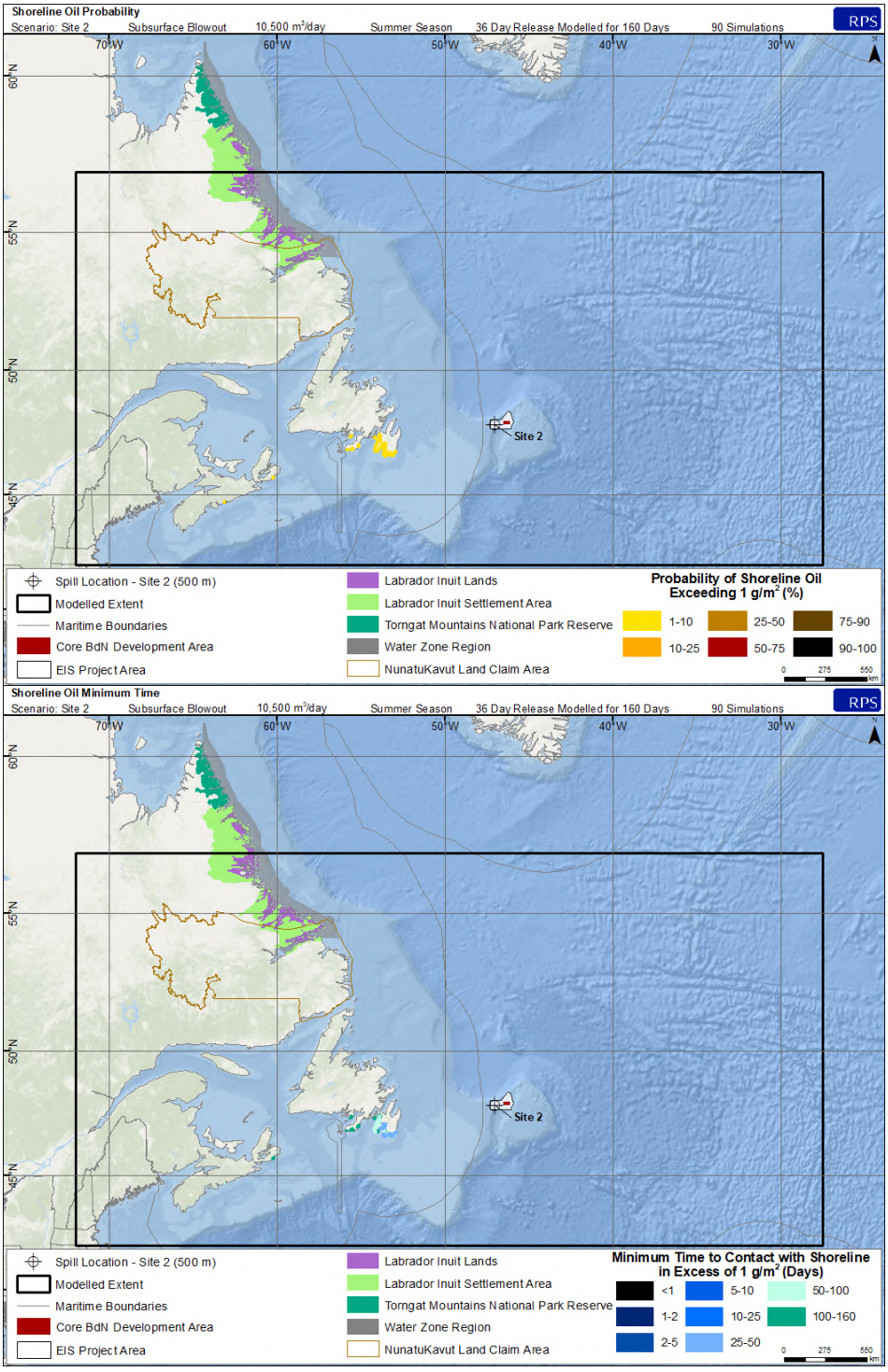

Figure 4-26. Summer probability of shoreline contact > 1 g/m² (top) and minimum time to threshold exceedance (bottom) resulting from a 36-day subsurface blowout at Site 2.

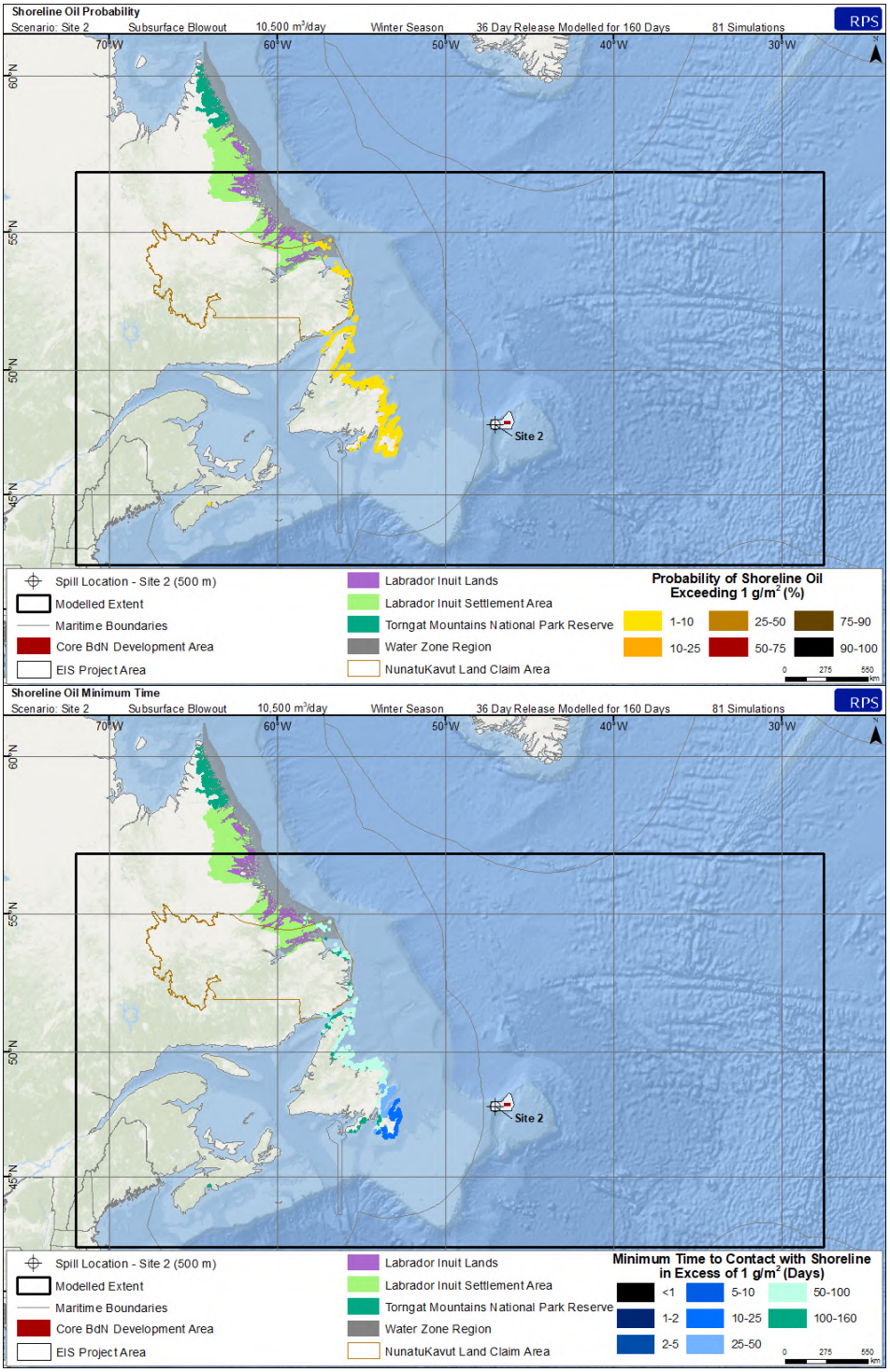

Figure 4-27. Winter probability of shoreline contact > 1 g/m² (top) and minimum time to threshold exceedance (bottom) resulting from a 36-day subsurface blowout at Site 2.

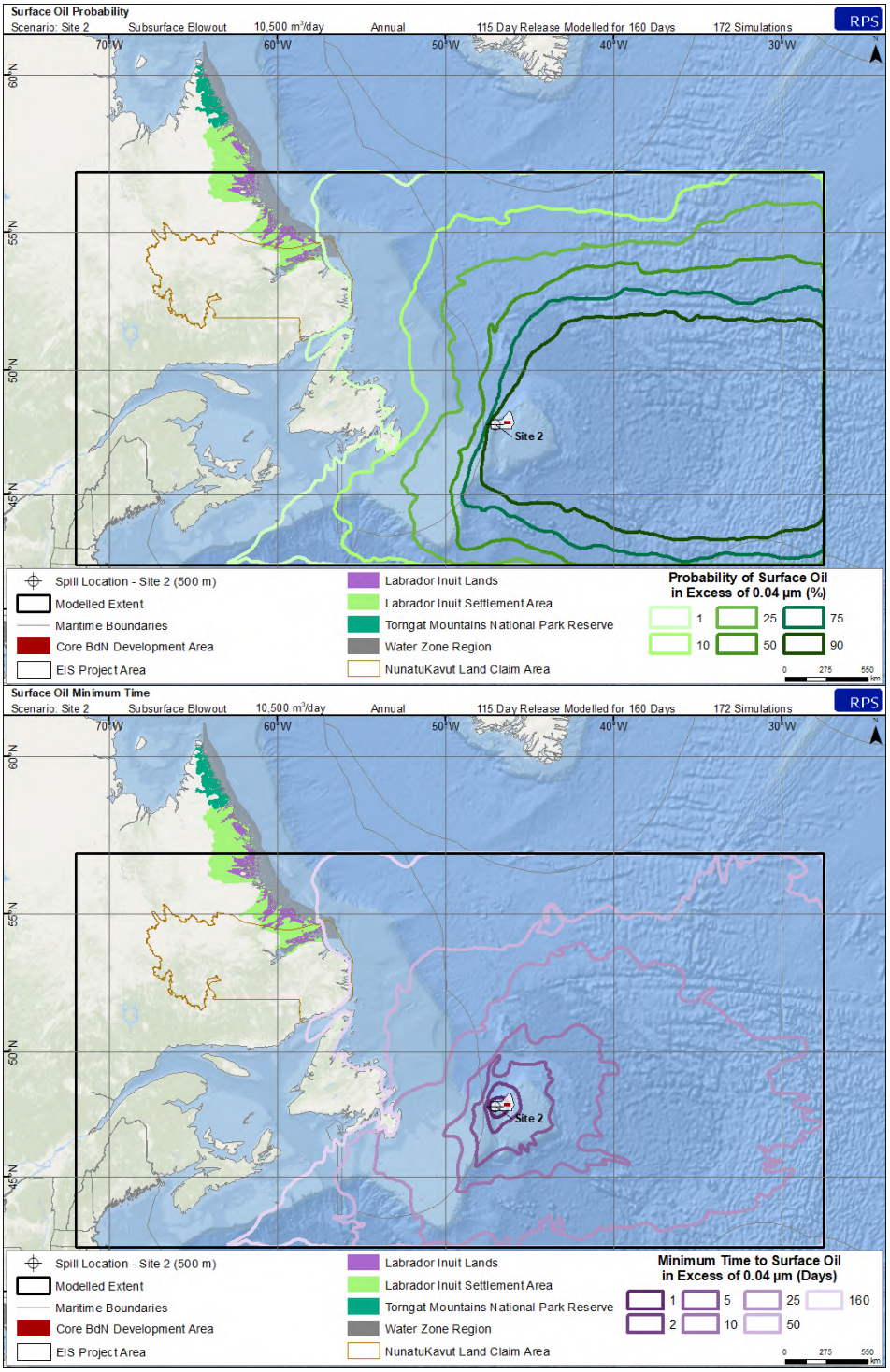

Figure 4-28. Annual probability of average surface oil thickness > 0.04 µm (top) and minimum time to threshold exceedance (bottom) resulting from a 115-day subsurface blowout at Site 2.

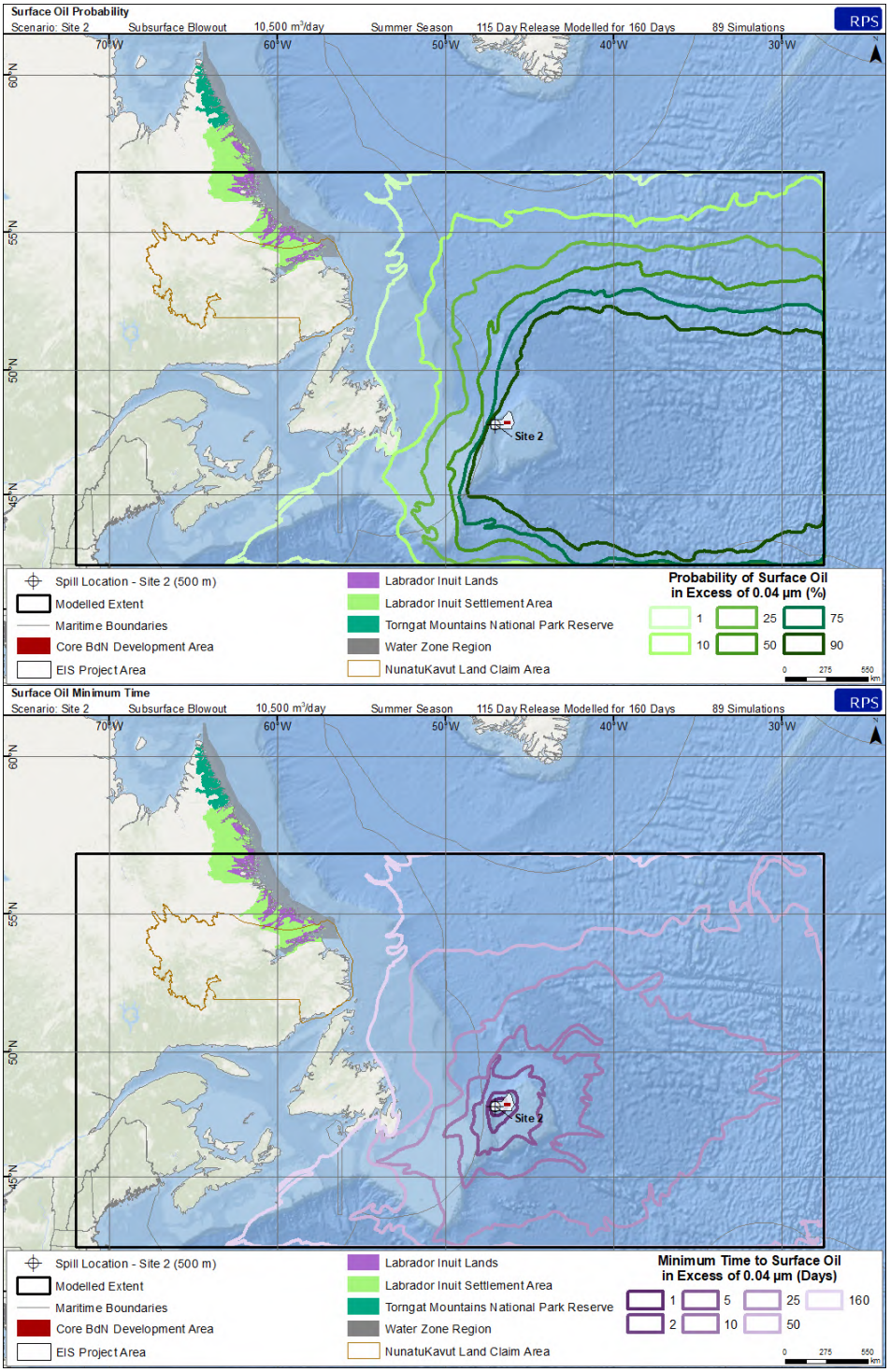

Figure 4-29. Summer probability of average surface oil thickness > 0.04 µm (top) and minimum time to threshold exceedance (bottom) resulting from a 115-day subsurface blowout at Site 2.

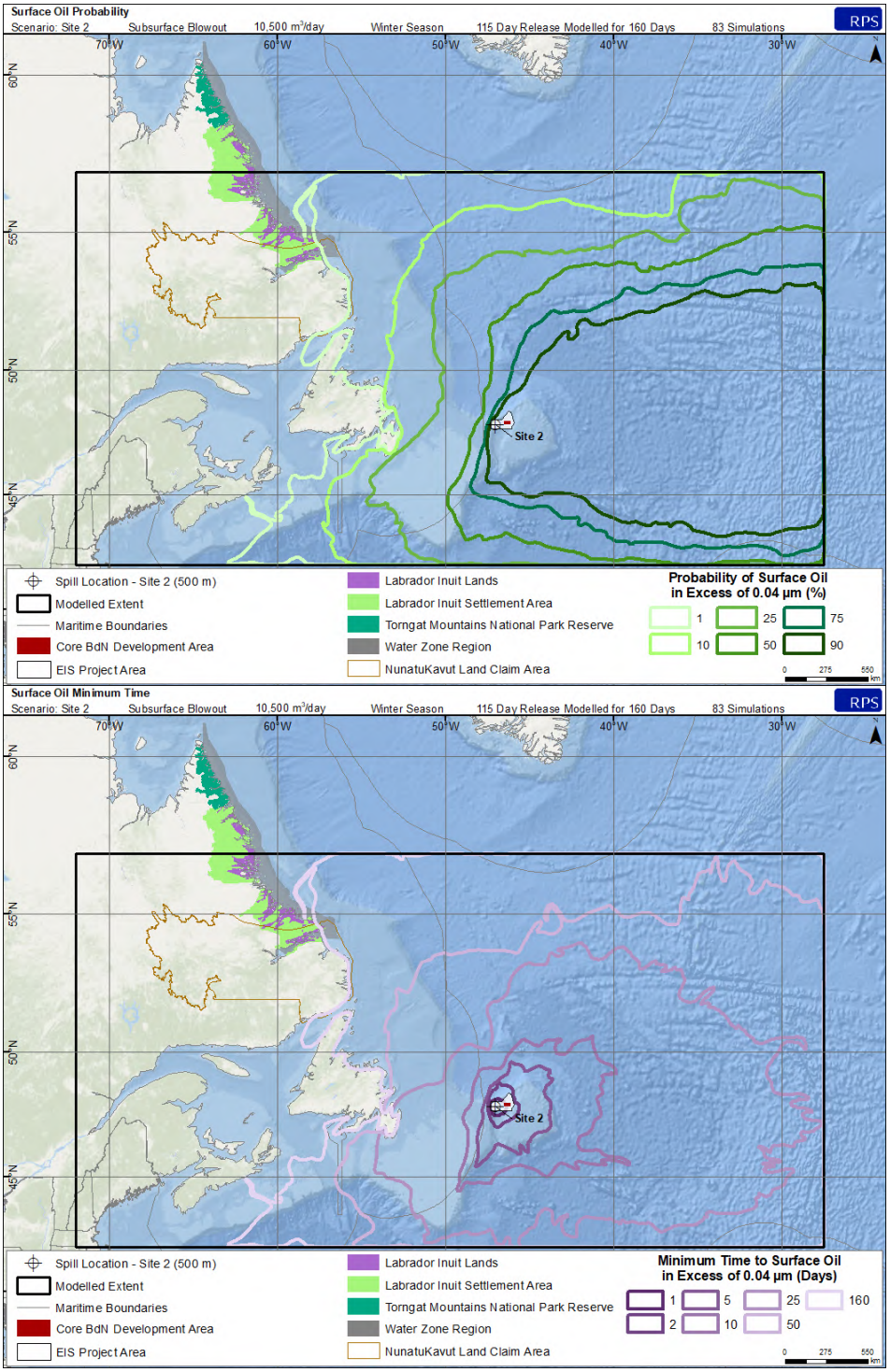

Figure 4-30. Winter probability of average surface oil thickness > 0.04 µm (top) and minimum time to threshold exceedance (bottom) resulting from a 115-day subsurface blowout at Site 2.

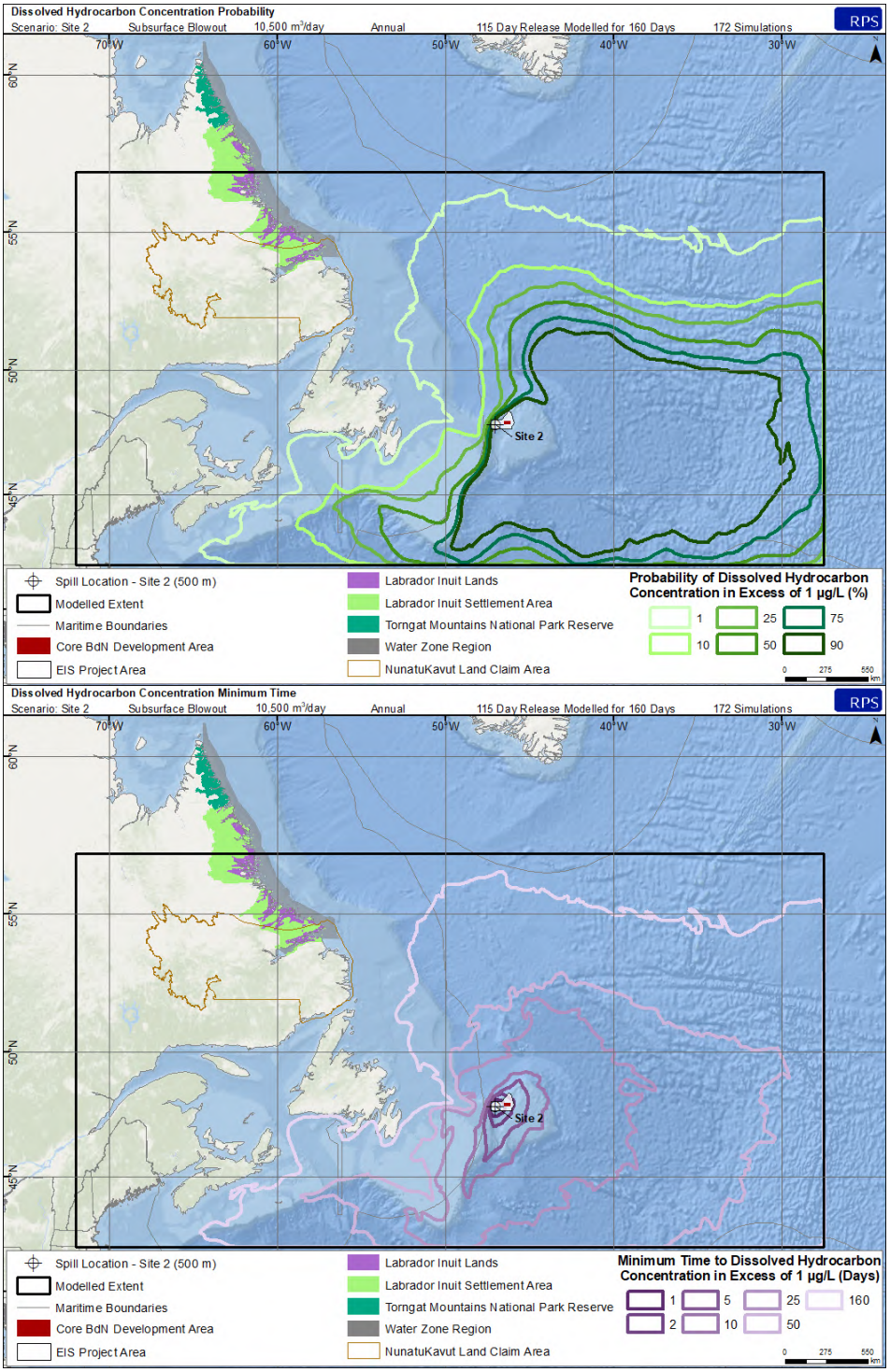

Figure 4-31. Annual probability of dissolved hydrocarbon concentrations > 1 µg/L at some depth in the water column (top) and minimum time to threshold exceedance (bottom) resulting from a 115-day subsurface blowout at Site 2.

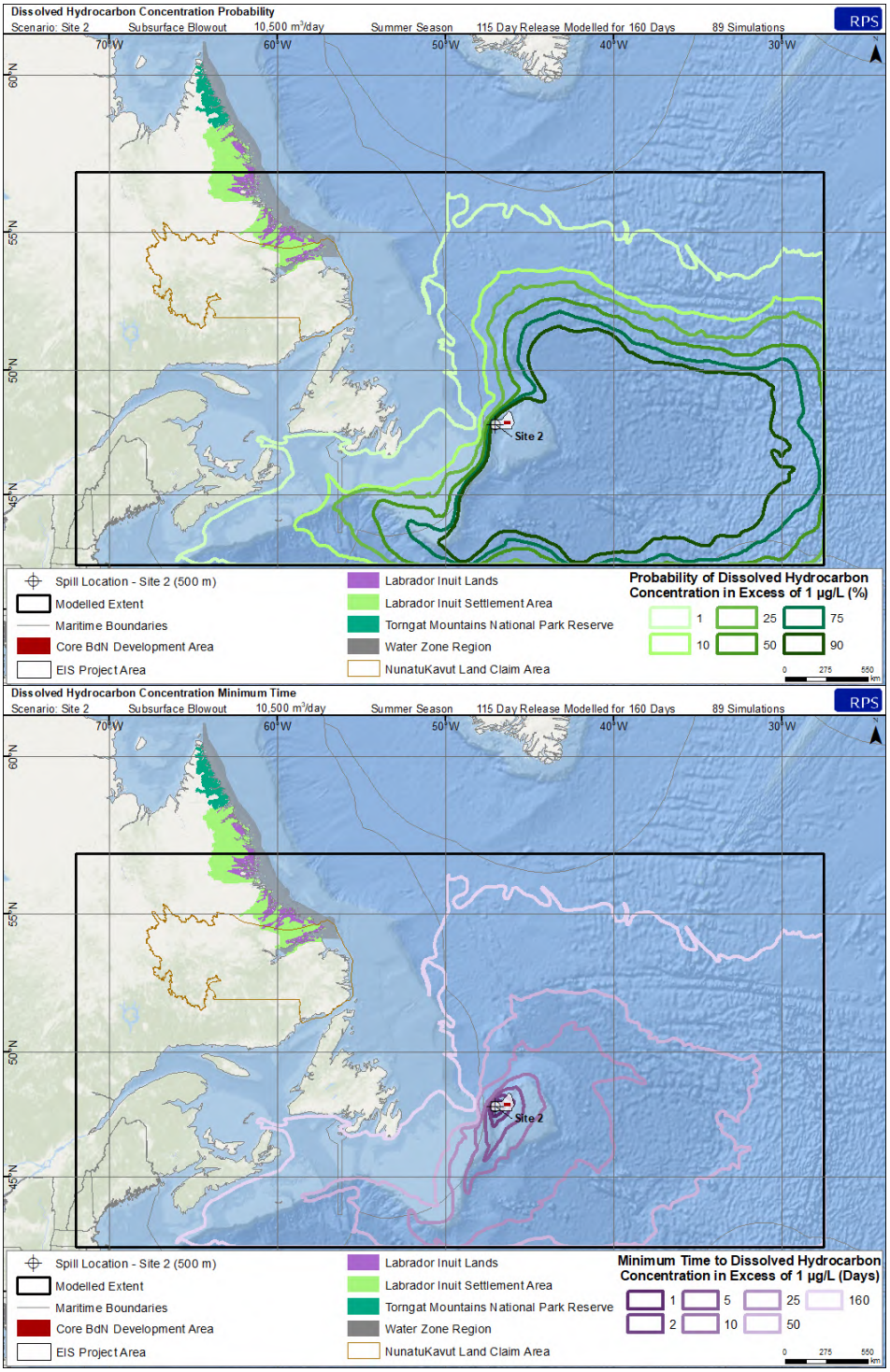

Figure 4-32. Summer probability of dissolved hydrocarbon concentrations > 1 µg/L at some depth in the water column (top) and minimum time to threshold exceedance (bottom) resulting from a 115-day subsurface blowout at Site 2.

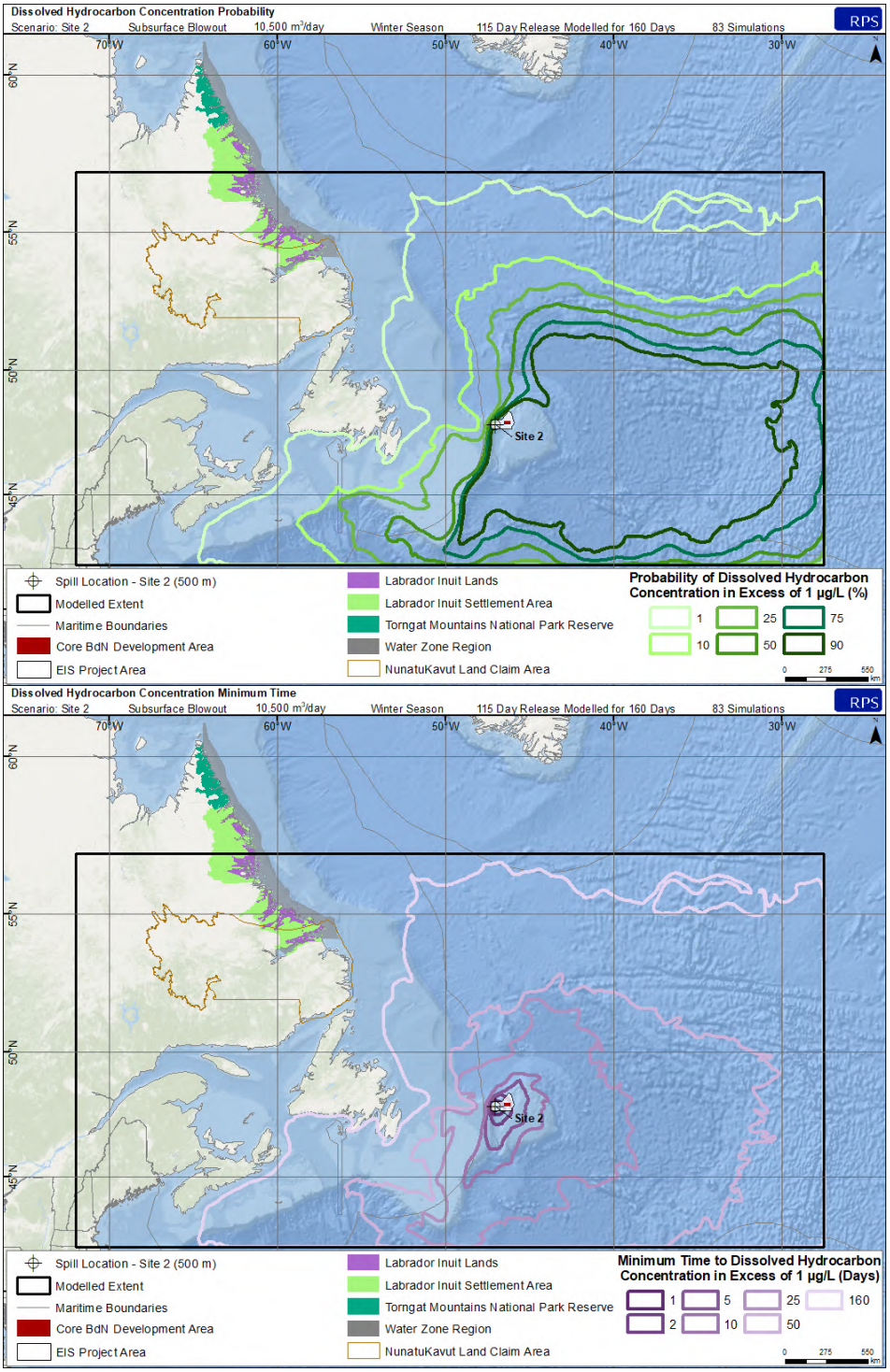

Figure 4-33. Winter probability of dissolved hydrocarbon concentrations > 1 µg/L at some depth in the water column (top) and minimum time to threshold exceedance (bottom) resulting from a 115-day subsurface blowout at Site 2.

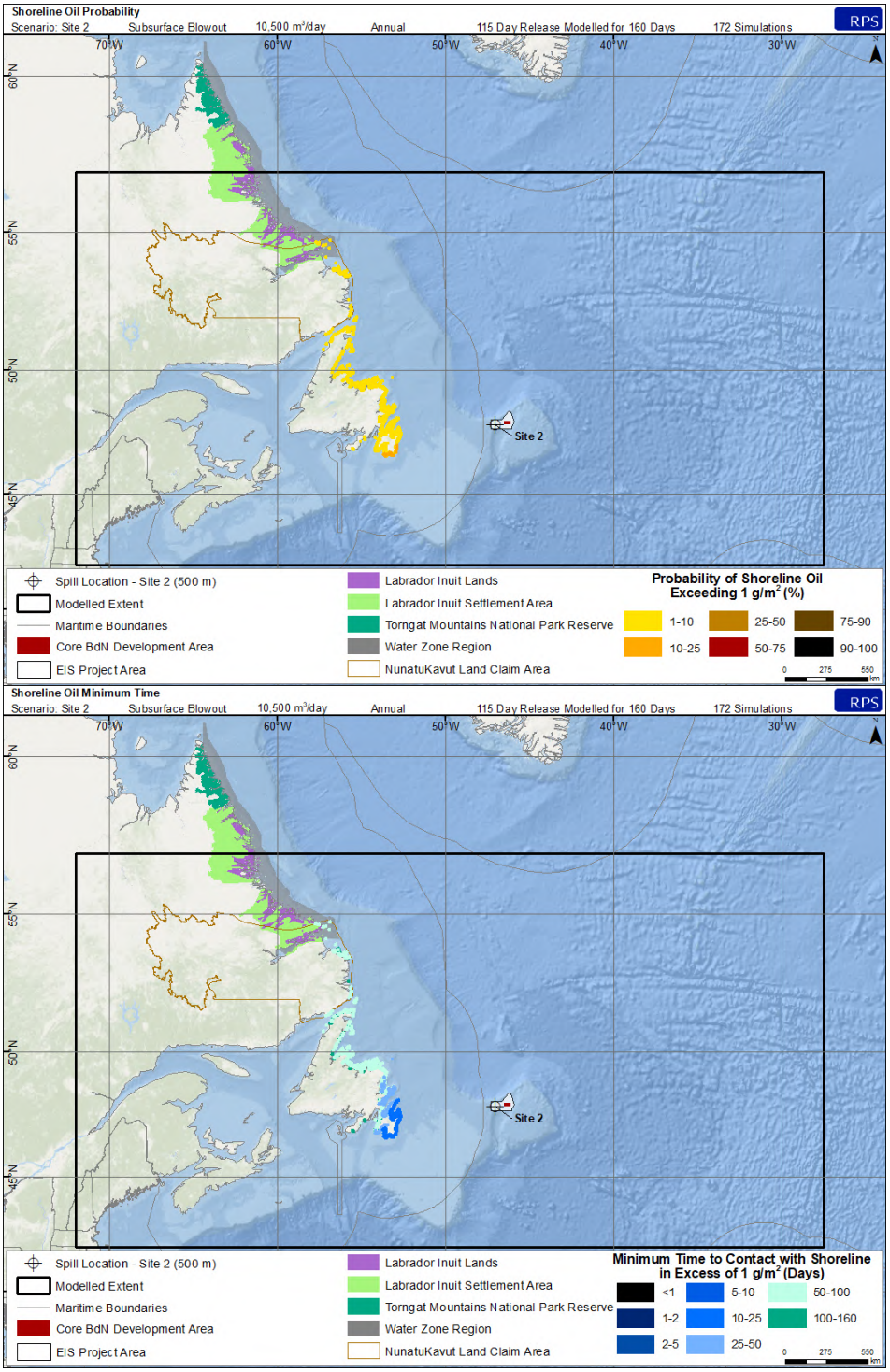

Figure 4-34. Annual probability of shoreline contact > 1 g/m² (top) and minimum time to threshold exceedance (bottom) resulting from a 115-day subsurface blowout at the Site 2 site.

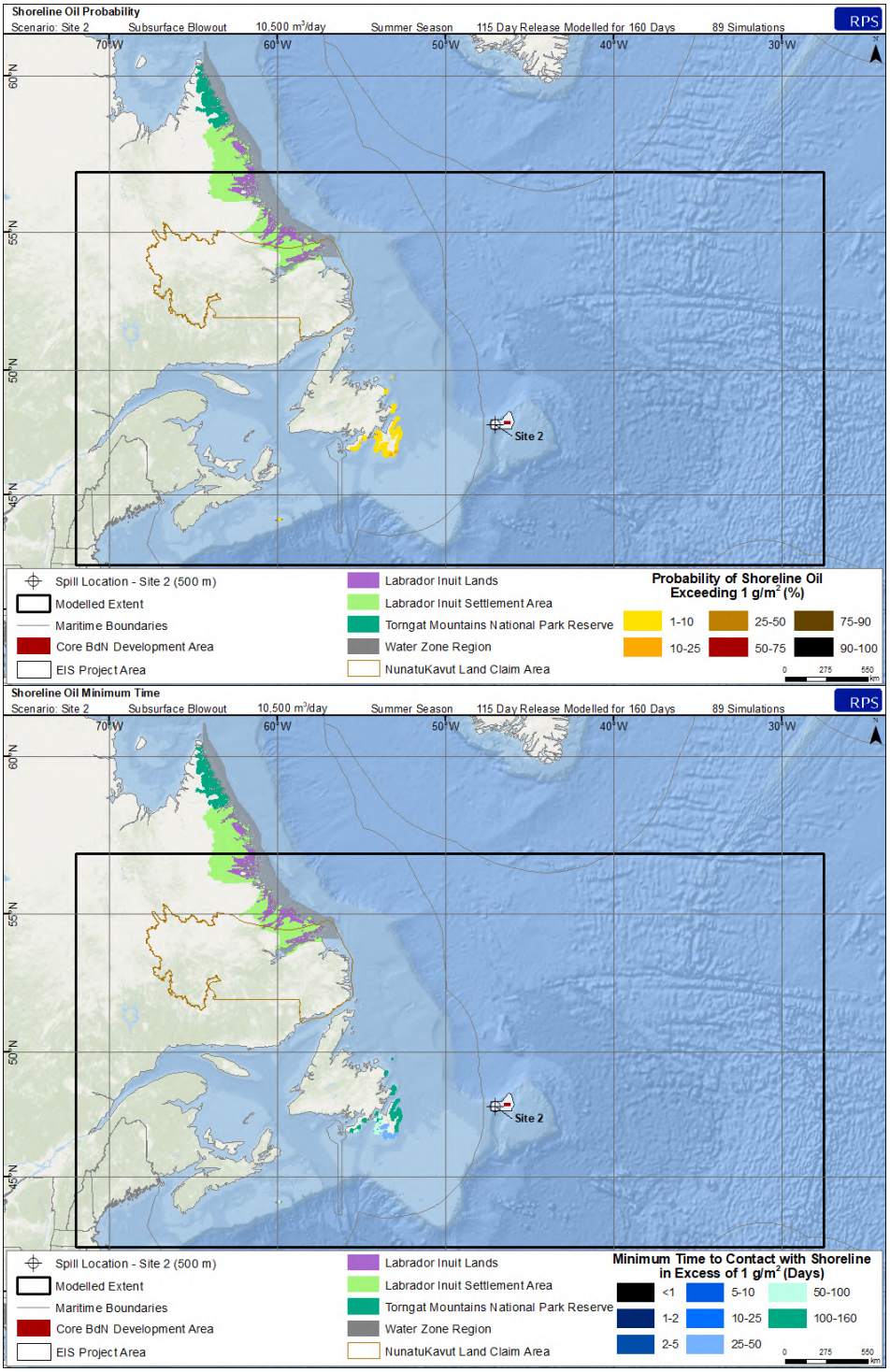

Figure 4-35. Summer probability of shoreline contact > 1 g/m² (top) and minimum time to threshold exceedance (bottom) resulting from a 115-day subsurface blowout at the Site 2 site.

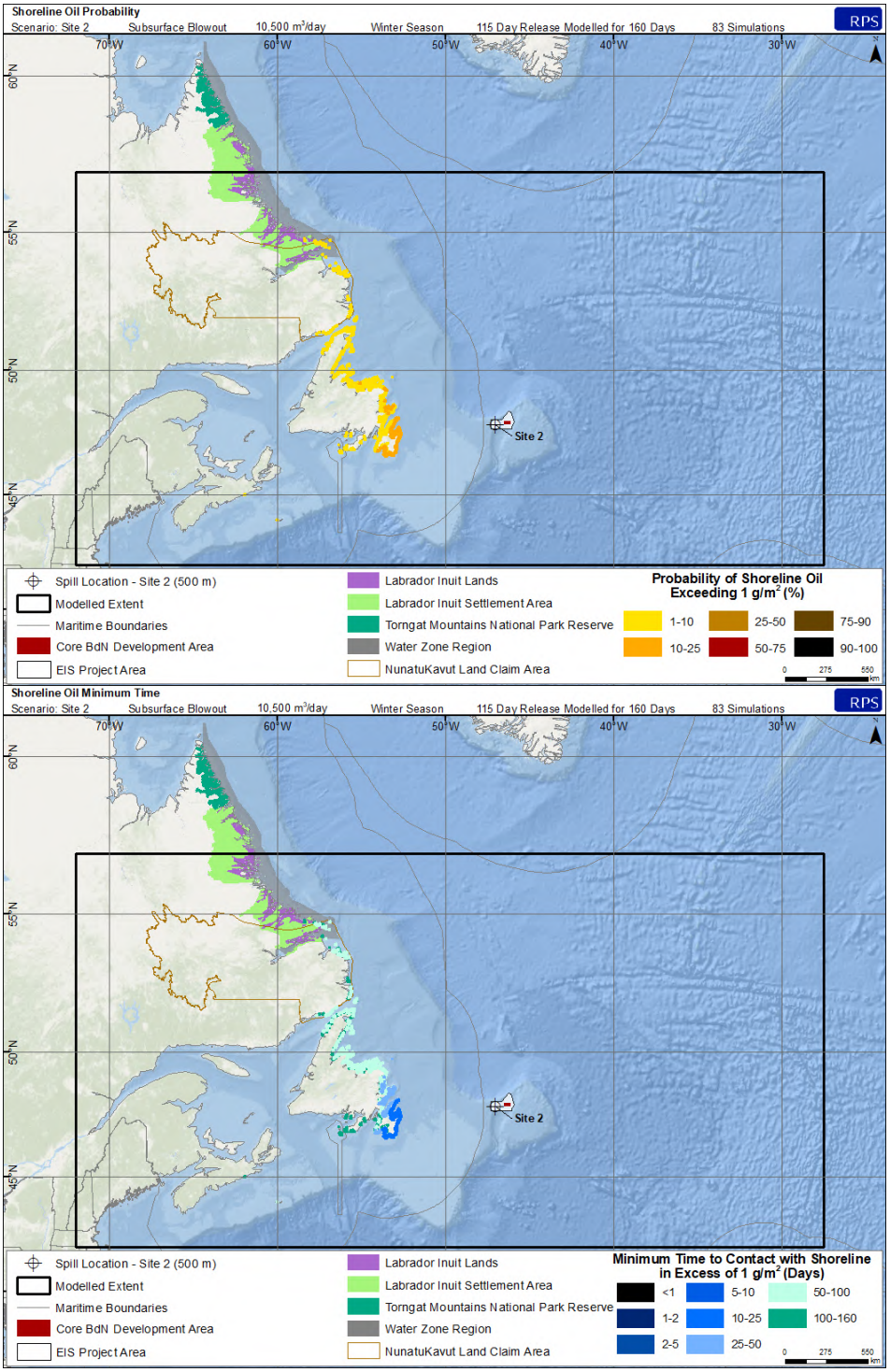

Figure 4-36. Winter probability of shoreline contact > 1 g/m² (top) and minimum time to threshold exceedance (bottom) resulting from a 115-day subsurface blowout at the Site 2 site.

4.1.3 Summary of Stochastic Results

A total of 171 (36-day release) and 172 (115-day release) individual model runs were simulated for the statistical analysis of the stochastic assessment at Site 1 and Site 2 representing subsurface blowouts in the waters offshore of Newfoundland. A 36-day release was modelled at Site 1 (1,134 m) and Site 2 (500 m) sites to represent capping stack response scenarios. Additionally, a 115-day release was modelled at each site to represent the longer duration required to respond to a blowout where a relief well must be drilled to shut-in the well. The model durations for each simulation were 160 days.

Summaries of the stochastic analyses of potential surface oil and water column exposure by dissolved hydrocarbons depict areas to the east of the release sites as having the highest potential likelihood (>90%) to exceed conservative socio-economic thresholds (Figure 4-1 through Figure 4-36). Lower probabilities of threshold exceedance are predicted to the north and south (10-25%), while generally <25% of releases have the potential to exceed thresholds to the west of the Project Area. Releases are predicted to result in oil in Canadian and International waters. In many cases, oil exposure above the identified threshold was predicted to extend beyond the extent of the model domain predominantly to the east and south. In these scenarios, the environmental forcing mechanisms (i.e., wind and currents) and the long time-frame modelled (160 days) allowed for the transport of oil at extremely conservative (low) thresholds outside of the model domain. The oil that was predicted to be transported out of the domain would have traveled hundreds of kilometers away from the hypothetical release location and typically would have done so on time scales greater than 25-50 days following the release. Based upon weathering rates, the oil that is predicted to be transported outside of the model domain would be highly weathered. At this point of weathering, the lighter and more toxic ends of the hydrocarbon would have evaporated and/or degraded which would reduce the toxicity of the remaining oil.

There were several identified differences in the distribution and spatial extent of predicted threshold exceedances between the modelled release scenarios at the two locations. The hypothetical releases at Site 1 occurred in a water depth that was deeper than that of Site 2 (1,134 m vs. 500 m). The shallower site (Site 2) had greater areas with >1% and 90% probability of surface oil exceeding 0.04 µm for both the short (36-day) and long (115-day) releases, when compared to the deeper site, Site 1 (Figure 4-1 to Figure 4-3; Figure 4-10 to Figure 4-12; Figure 4-19 to Figure 4-21; Figure 4-28 to Figure 4-30; Table 4-1). In general, no large differences in areas exceeding water column thresholds were predicted between the two sites (Figure 4-4 to Figure 4-6; Figure 4-13 to Figure 4-15; Figure 4-22 to Figure 4-24; Figure 4-31 to Figure 4-33; Table 4-1). The length of shoreline that was susceptible to oil making contact from a 36-day release was greater at Site 2 , compared to Site 1, while the length of shoreline susceptible to oil contact was generally greater at Site 1 for the 115-day release (Figure 4-7 to Figure 4-9; Figure 4-16 to Figure 4-18; Figure 4-25 to Figure 4-27; Figure 4-34 to Figure 4-36; Table 4-1).

Two release durations (36- and 115-day) were modelled to demonstrate the differences that may arise between scenarios investigating a capping stack implemented on day 36 versus the drilling of a relief well, with an anticipated completion and shut-in on day 115. The longer releases had slightly larger areas of >1% probability surface oil (Figure 4-1 to Figure 4-3; Figure 4-10 to Figure 4-12; Figure 4-19 to Figure 4-21; Figure 4-28 to Figure 4-30; Table 4-1), water column oil (Figure 4-4 to Figure 4-6; Figure 4-13 to Figure 4-15; Figure 4-22 to Figure 4-24; Figure 4-32 to Figure 4-34; Table 4-1), and shoreline contact with oil (Figure 4-7 to Figure 4-9; Figure 4-16 to Figure 4-18; Figure 4-25 to Figure 4-27; Figure 4-35 to Figure 4-36; Table 4-1) exceeding the identified thresholds, when compared to the shorter releases. However, the longer duration releases had much larger predicted areas of 90% probability of exceedance (Table 4-1). Due to the longer duration and therefore larger amount of oil being released, the 115-day release scenarios had a higher potential to exceed surface oil, water column oil, and shoreline oil thresholds. However, because both the 36-day and 115-day simulations were modelled for 160 days, all releases experienced the same environmental forcing (i.e. wind and currents). Because of this, large differences in the >1% probability contours were not predicted.

As stated above, the lengths of shoreline that were predicted to have shoreline contact were much longer at Site 2 for the 36-day releases, and longer at Site 1 for 115-day releases. Based upon 171 or 172 individual trajectories, it was predicted that as much as 3,933 km (Site 1) and 3,635 km (Site 2) of shoreline may be susceptible to oil making contact following a release (Table 4-1). Most of the shoreline contact was predicted to occur on the southern shore of Newfoundland (10-25% probability), and as far north as Labrador (1-10% probability) (Figure 4-7 to Figure 4-9; Figure 4-16 to Figure 4-18; Figure 4-25 to Figure 4-27; Figure 4-34 to Figure 4-36). As the southern shores of Newfoundland are closer to the release locations, they experience a higher probability of oil making contact. The probability of oil making contact with the shoreline was less than 22-25% for all scenarios, with the longest lengths of susceptible shoreline predicted for the 115-day winter release scenarios (Table 4-2). For each modelled scenario, oil has the potential to reach shore in as little as 13-15 days for winter scenarios and 31-35 days for summer scenarios (Table 4-2). Predicted contact with shoreline is extremely similar for Sites 1 and 2 due to the close proximity with one another. Therefore, the oil that was predicted to make contact with shorelines was expected to be weathered, as minimum time estimates ranged from weeks to over a month (Table 4-2).

Two seasons (summer and winter) were investigated to determine differences caused by seasonal variations in met-ocean conditions. Overall, summer scenarios had smaller predicted extents for both surface and water column oil (>1% probability), when compared to the winter scenarios. Therefore, the areas of 90% probability were greater in the summer scenarios, as oil was contained within a smaller region (Figure 4-1 to Figure 4-6; Figure 4-10 to Figure 4-15; Figure 4-19 to Figure 4-24; Figure 4-28 to

Figure 4-33; Table 4-1). Due to the larger predicted extent in winter scenarios, more shoreline area was susceptible to stranding oil when compared to summer scenarios (Figure 4-7 to Figure 4-9; Figure 4-16 to Figure 4-18; Figure 4-25 to Figure 4-27; Figure 4-34 to Figure 4-36).

As stated previously, stochastic figures do not imply that the entire contoured area would be covered with oil in the event of a single release, nor do they provide any information on the quantity of oil in each area. The large threshold exceedance footprints in annual results are not the expected exposure from any single release of oil, but rather areas where there is >1% probability that exposure above the thresholds was predicted to occur, based on the combination of either 171 or 172 (annual), 90 or 89 (summer), or 81 or 83 (winter) individual releases analyzed together.

Table 4-1. Summary of predicted areas of socio-economic threshold exceedance (km^2) for surface and water column, and lengths (km) of shoreline predicted to potentially be affected. Areas are displayed by season (annual, winter, and summer), by the size of the regions within specific probability bins in the modelled domain.

Stochastic Scenario Parameters				Areas Exceeding Threshold (km^2)		
Component and Threshold	**Scenario**	**Site**	**Probability Contour or Bin**	**Annual Results**	**Winter (ice cover)**	**Summer (ice-free)**
Surface Oil > 0.04 µm, on average	36-day release	Site 1 (10,500 m^3/d)	1%	3,356,000	3,392,000	3,217,000
			10%	2,680,000	2,881,000	2,505,000
			90%	621,700	526,900	775,200
	115-day release	Site 1 (10,500 m^3/d)	1%	3,434,000	3,565,000	3,204,000
			10%	2,883,000	3,029,000	2,695,000
			90%	1,143,000	1,133,000	1,324,000
	36-day release	Site 2 (10,500 m^3/d)	1%	3,439,000	3,475,000	3,332,000
			10%	2,653,000	2,829,000	2,536,000
			90%	747,500	635,000	905,500
	115-day release	Site 2 (10,500 m^3/d)	1%	3,474,000	3,535,000	3,312,000
			10%	2,884,000	2,998,000	2,681,000
			90%	1,300,000	1,289,000	1,436,000
Water Column Dissolved Hydrocarbons > 1 µg/L at some depth within the water column	36-day release	Site 1 (10,500 m^3/d)	1%	2,929,000	3,219,000	2,814,000
			10%	2,012,000	2,050,000	1,985,000
			90%	517,500	317,500	774,100
	115-day release	Site 1 (10,500 m^3/d)	1%	2,894,000	3,130,000	2,763,000
			10%	2,159,000	2,279,000	2,089,000
			90%	943,200	897,300	1,103,000
	36-day release	Site 2 (10,500 m^3/d)	1%	2,881,000	3,134,000	2,819,000
			10%	2,087,000	2,143,000	2,053,000
			90%	657,800	639,000	782,700
	115-day release	Site 2 (10,500 m^3/d)	1%	2,922,000	3,119,000	2,793,000
			10%	2,182,000	2,252,000	2,115,000
			90%	1,065,000	1,044,000	1,112,000
				Lengths Exceeding Threshold (km)		
Shoreline Contact with Oil > 1 g/m^2, on average	36-day release	Site 1 (10,500 m^3/d)	1 - 5%	1,282	1,322	356
			5 - 15%	3	169	-
			15 - 25%	-	-	-
	115-day release	Site 1 (10,500 m^3/d)	1 - 5%	3,933	2,451	635
			5 - 15%	804	3,117	71
			15 - 25%	-	163	-
	36-day release	Site 2 (10,500 m^3/d)	1 - 5%	3,469	3,635	405
			5 - 15%	46	859	21
			15 - 25%	-	-	-
	115-day release	Site 2 (10,500 m^3/d)	1 - 5%	3,206	2,169	764
			5 - 15%	1,043	2,933	114
			15 - 25%	6	156	-

Table 4-2. Shoreline contact probabilities and minimum time for oil exposure exceeding 1 g/m^2.

Scenario	Release Site	Scenario Timeframe	Average Probability of Shoreline Oil Contact (%)	Maximum Probability of Shoreline Oil Contact (%)	Minimum Time to Shore (days)	Maximum Time to Shore (days)
36-day release	Site 1 (10,500 m^3/d)	Annual	2	5	13	121
		Winter	4	11	13	138
		Summer	2	4	34	143
115-day release		Annual	4	12	15	147
		Winter	6	22	15	160
		Summer	2	8	31	160
36-day release	Site 2 (10,500 m^3/d)	Annual	2	8	13	121
		Winter	4	11	13	138
		Summer	2	8	34	143
115-day release		Annual	4	17	14	150
		Winter	7	25	14	159
		Summer	2	8	31	160

4.2 Deterministic Analysis Results

Individual trajectories of interest were selected from the stochastic ensemble of results for the deterministic analysis. The deterministic trajectory and fate simulations provided an estimate of the transport of oil through the environment as well as its physical and chemical behavior for the specific set of modelled environmental conditions. Representative 95th percentile trajectories for surface oil exposure, water column concentration of total hydrocarbons, and contact with shoreline were identified from the stochastic scenarios for each site modelled and release duration (36 vs. 115 days). This resulted in deterministic scenarios for surface oil exposure, water column concentration, and shoreline contact for each site and release duration, resulting in twelve individual trajectories associated with subsurface blowouts (Table 2-5). Four additional batch spills were modelled associated with different types of accidents/malfunctions. In addition, several shorter duration and smaller volume releases were modelled to be representative of spills that could occur from different sources during production activities. Surface releases were modelled from the floating production storage and offloading unit (FPSO), shuttle tanker releases during offloading, and bunkering operations (i.e., transfer from a vessel). An additional seabed batch spill was modelled to be representative of a loss in a production flowline.

The following sections contain figures corresponding to each identified representative case and tables summarizing the areas exceeding specified thresholds. During modelling, components of oil were tracked as entrained droplets of whole oil, dissolved hydrocarbon constituents, floating surface oil, and stranded oil on shorelines. The figures provided in the subsequent sections (Sections 4.2.1 through 4.2.4) depict the cumulative footprint of all oil predicted to be within a region over the entire modelled duration. Therefore, the depicted footprints are much larger than the amount of oil that would be present in a region at any given time following the release of oil. This concept is illustrated in Figure 4-37, which portrays predicted surface oil thickness at five specific time steps or “snapshots” in time (days 2, 10, 50, 100, and 160) for the 95th percentile surface oil thickness case at Site 1. Note the patchy and discontinuous nature of the predicted footprint as the released oil was predicted to spread and thin over time. Figure 4-38 portrays the cumulative footprint for the exact same simulation. The area covered is much larger, depicting the maximum surface oil thickness that was predicted to occur at each location over the entire modelled time period. The remaining figures in this report will depict cumulative footprints as opposed to “snapshots” at given time steps to provide conservative estimates of potentially affected areas.

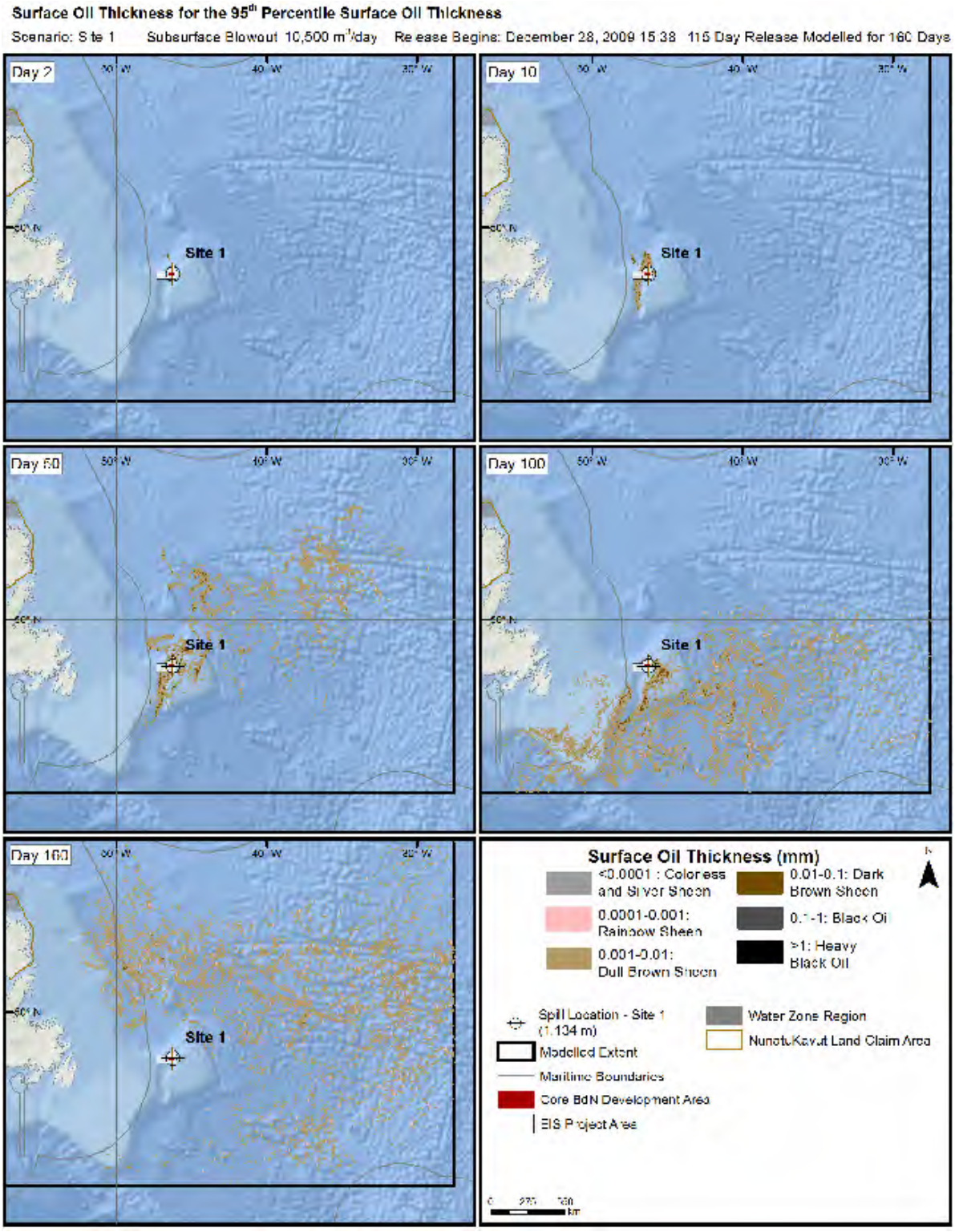

Figure 4-37. Predicted surface oil thickness for the 95th percentile surface oil exposure case for Site 1 at days 2, 10, 50, 100, and 160.

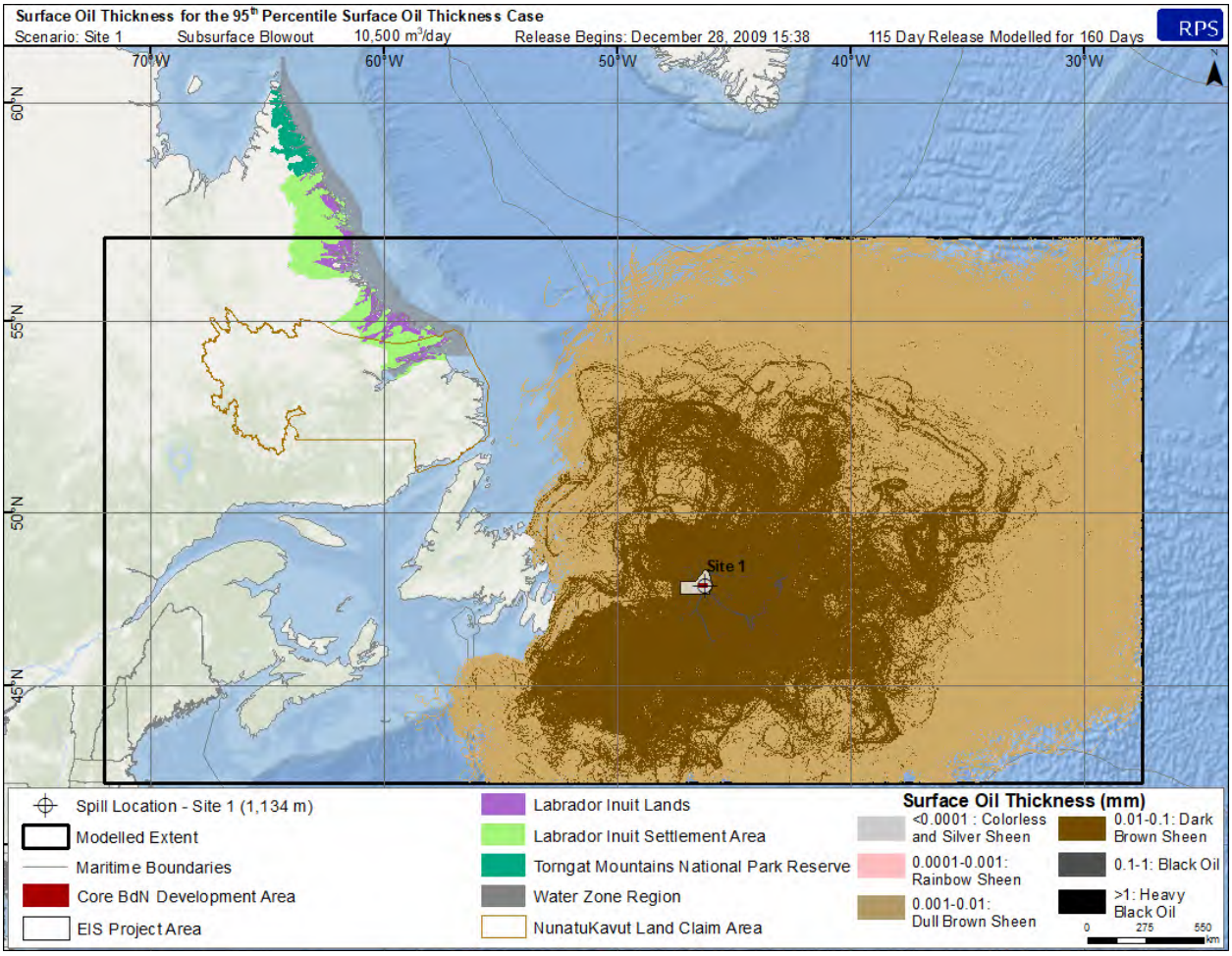

Figure 4-38. Maximum cumulative surface oil thickness for the 95th percentile surface oil exposure case for Site 1. Note that the information contained in this figure is the same scenario that was presented in Figure 4-37.

The types of figures that were used to summarize modelling results are provided, along with brief descriptions of the information that they portray. Note that the thicknesses and concentrations were calculated on a grid with a resolution (i.e., grid cell size) of 1,800 m by 2,500 m, which is equivalent to 0.02 degrees by 0.02 degrees. For concentration grids, vertical binning included 20 m increments.

1. **Mass Balance Plots**: Illustrate the predicted weathering and fate of oil for a specific run over the entire model duration as a fraction of the oil released up to that point. Components of the oil tracked over time include the amount of oil on the sea surface, the total entrained hydrocarbons in the water column, the amount of oil in contact with the shore, the oil evaporated into the atmosphere, and the degraded oil (accounts for both photo-oxidation and biodegradation).

2. **Surface Oil Thickness Maps**: Depict the predicted footprint of maximum floating surface oil and the associated oil thicknesses (mm) over all modelled time steps for an individual release simulation. The minimum thickness of surface oil > 0.04 µm is displayed (cumulative over all modelled time steps). Note that floating oil mass is calculated as an average over grid cells, thus in reality, the oil would be patchy and discontinuous and could be thinner or thicker within particular areas of a single grid cell.
3. **Water Column Dissolved Hydrocarbon Concentration Maps**: Depict the predicted footprint of the vertical maximum water column concentration of dissolved hydrocarbons over all modelled time steps for an individual release simulation. Dissolved hydrocarbons are the constituents of the oil with the greatest potential to affect water column biota. Only concentrations above 1 µg/L for the representative cases are displayed (see Table 2-2). For the small volume batch spills, the volumes released were insufficient to produce dissolved hydrocarbon footprints at the gridded resolution used (the dissolved hydrocarbons comprise roughly 1% of total hydrocarbons released). Therefore, total hydrocarbon concentrations in the water column are displayed instead of the dissolved hydrocarbons.
4. **Water Column Total Hydrocarbon Concentration Maps**: Depict the predicted footprint of the vertical maximum water column concentration of total hydrocarbons over all modelled time steps for an individual release simulation. Only concentrations above 1 µg/L for the representative cases are displayed (see Table 2-2).
5. **Shoreline and Sediment Total Hydrocarbon Concentration Maps**: Depict the predicted total mass of oil (per unit area as g/m^2) making contact with the shoreline and sediments. For the smaller volume batch spills, the volumes released were insufficient to produce total hydrocarbon concentrations on the shore or sediment. Therefore, these maps are not provided for the batch spills.

4.2.1 Surface Oil Exposure Cases

Results for the identified 95th percentile scenarios for floating surface oil exposure for the releases at Site 1 and Site 2 are provided in the figures below. Note that the modelled release dates for each scenario differed. The simulation for the 36-day release at Site 1 spanned February to July 2010, while the 115-day release spanned December 2009 to June 2010. At Site 2, the simulation for the 36-day release spanned November 2009 to May 2010 and mid-January through June 2010 for the 115-day release (Table 2-5). For both sites, the released oil was predicted to rise rapidly to the surface where it spread, being transported by surface winds and currents creating discontinuous patchy surface slicks (Figure 4-39 and Figure 4-40; Figure 4-44 and Figure 4-45).

In each of the modelled scenarios, surface oil was predicted to be thickest closest to the release location, with maximum thicknesses corresponding to a visual appearance of black oil within a few kilometers of the release location. The majority of the footprints were predicted to have a maximum thickness closer in appearance to dark brown and dull brown sheens. The 36-day releases at Site 1 and Site 2 resulted in smaller footprints which tended to cover regions to the south and east of the release sites, while the 115-day releases were predicted to result in much larger surface oil footprints that included regions to the north in addition to the areas to the south and east of the release sites.

The combined effects of a subsurface release and the entrainment of surface oil into the water column from wind induced surface breaking waves were predicted to result in concentrations of dissolved and total hydrocarbons in the water column that exceeded the identified thresholds (Figure 4-41 and Figure 4-42; Figure 4-46 and Figure 4-47). Due to the larger release volume, the 115-day releases at both Site 1 and Site 2 were predicted to result in larger footprints of dissolved hydrocarbon and total hydrocarbon concentrations (THC), when compared to the 36-day releases. The majority of these modelled 95th percentile surface oil cases resulted in a small portion of the released oil mass (0.07%) predicted to contact portions of eastern Newfoundland and the Avalon Peninsula with concentrations exceeding the 100 g/m^2 biological threshold (with the exception of the 36-day release at Site 1, which was not predicted to contact shore). At these locations patchy and discontinuous oil was predicted to make contact with shorelines at values in excess of 500 g/m^2.

At the end of the 160-day simulations (36-day and 115-day releases at Sites 1 and 2), results were quite similar with minor differences in the predicted mass balance. At Site 1, 3-13% of the oil was predicted to remain on the water surface, approximately 46-48% evaporated into the atmosphere, 1-2% remained entrained within the water column, ≤0.1% adhered to suspended sediment, 33-34% degraded, <1% made contact with the shore (115 day release only), and 6-15% was transported outside of the model domain (Figure 4-39 and Table 4-4). At Site 2, 5-11% of the oil was predicted to remain on the water surface, approximately 46-48% evaporated into the atmosphere, 1-2% remained entrained within the water column, ≤0.1% adhered to suspended sediment, 32-35% degraded, <1% made contact with the shore, and 10-11% was transported outside of the model domain (Figure 4-44 and Table 4-4).

4.2.1.1 Site 1 Subsurface Releases

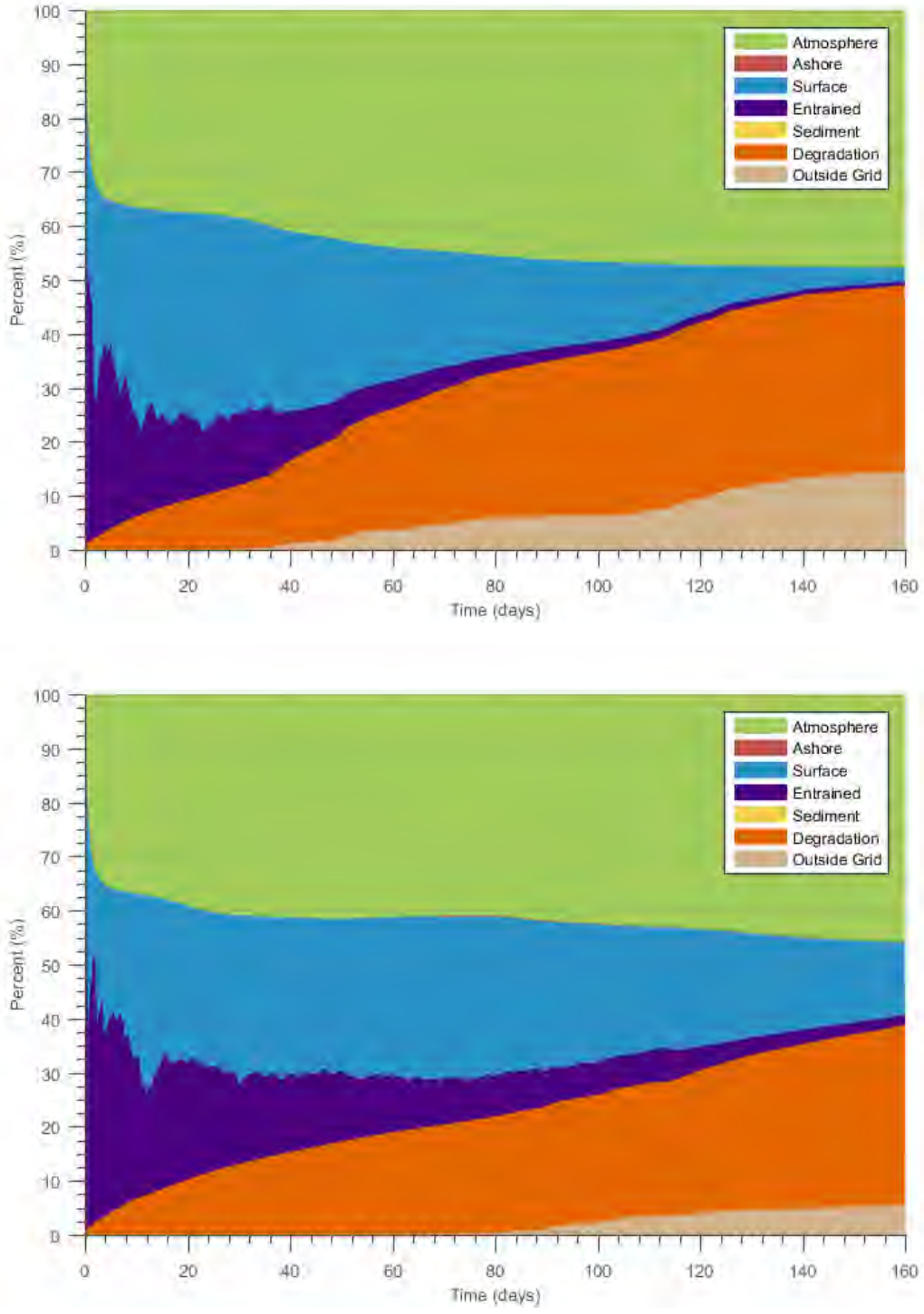

Figure 4-39. Mass balance plots for the 95th percentile surface oil thickness cases at Site 1 for the 36-day (top) and the 115-day release (bottom).

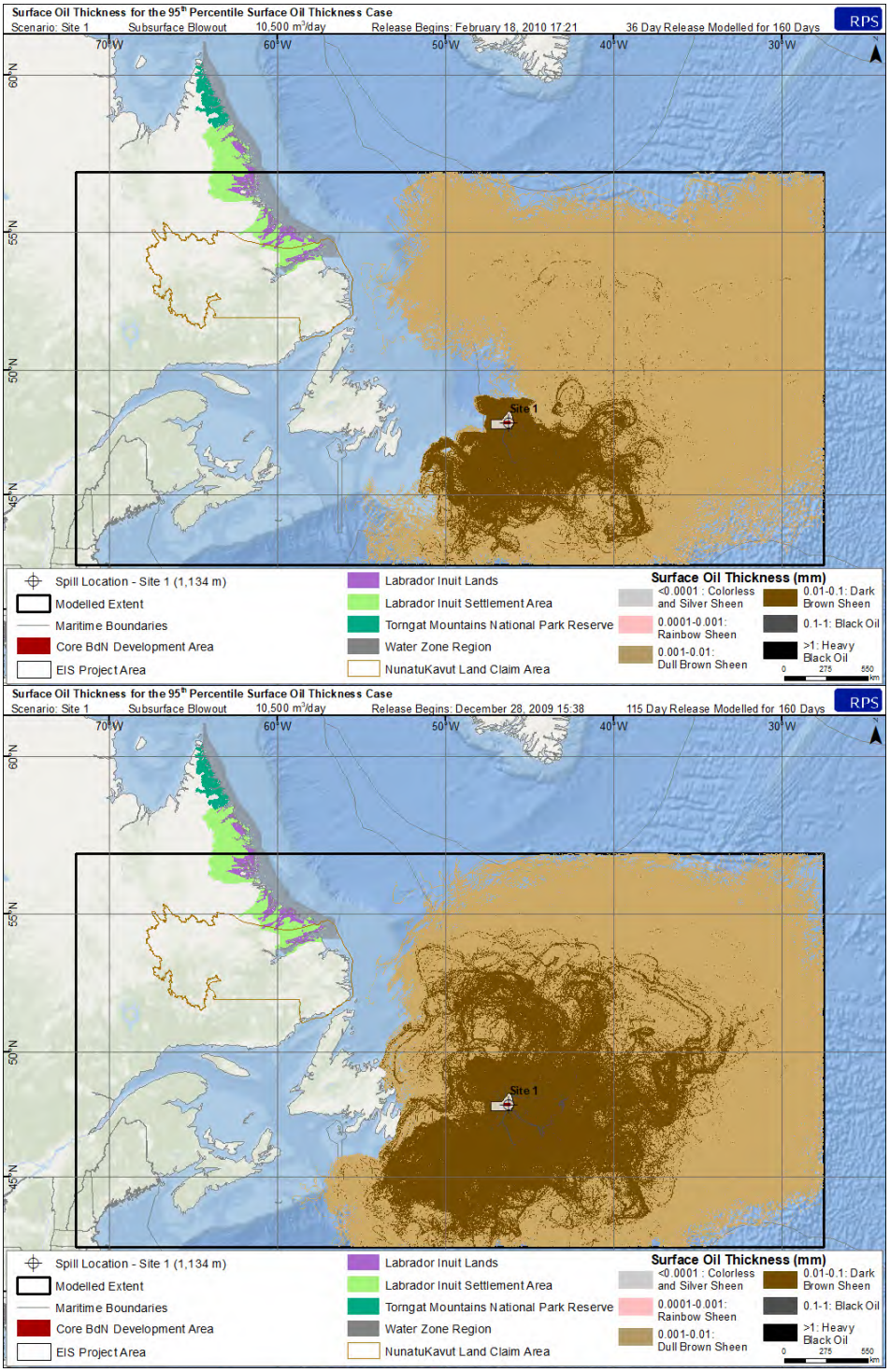

Figure 4-40. Surface oil thickness for the 95th percentile surface oil thickness case at Site 1 for the 36-day (top) and the 115-day release (bottom).

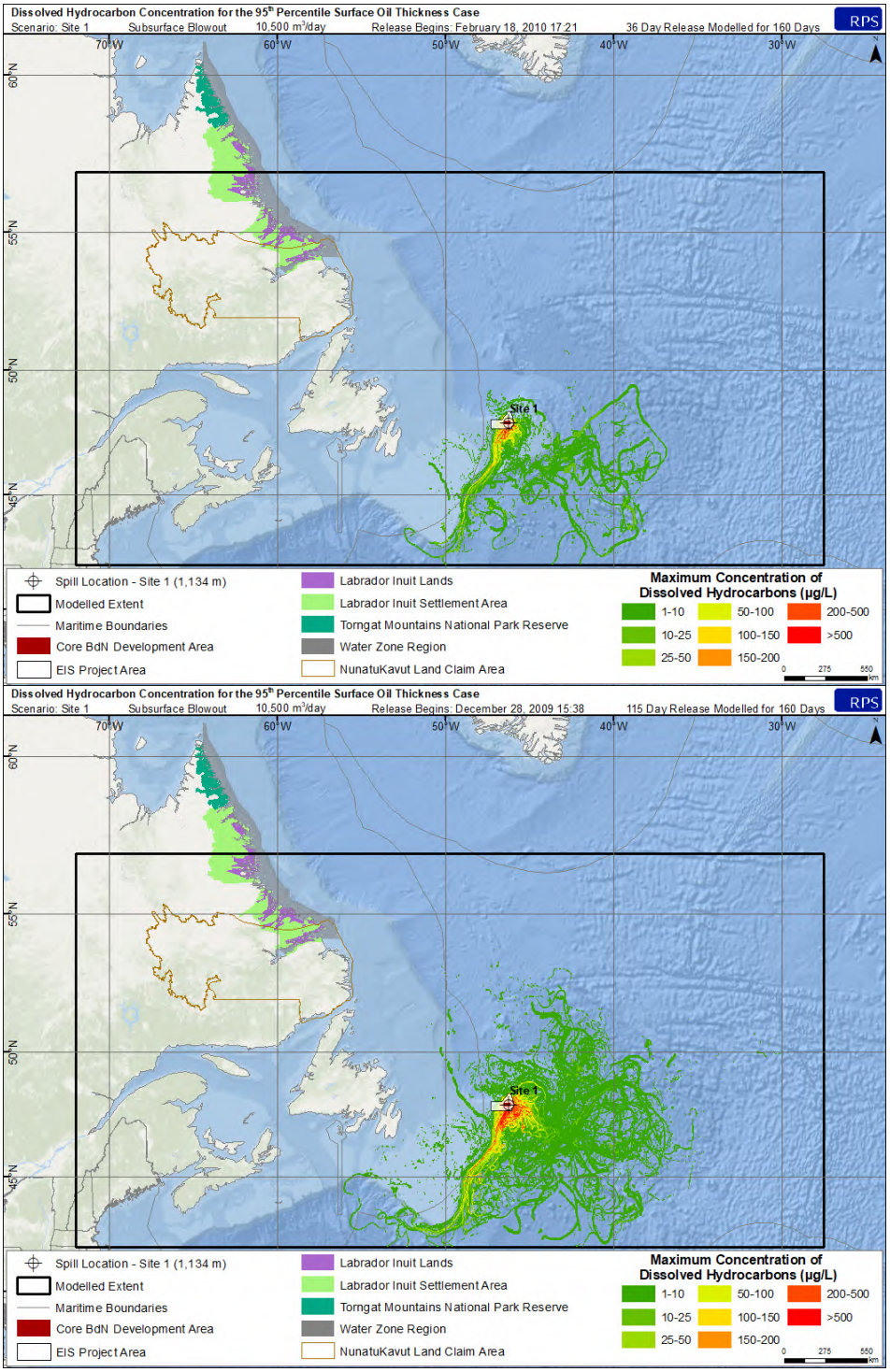

Figure 4-41. Maximum dissolved hydrocarbon concentration at any depth in the water column for the 95th percentile surface oil thickness case for Site 1 for the 36-day (top) and the 115-day release (bottom).

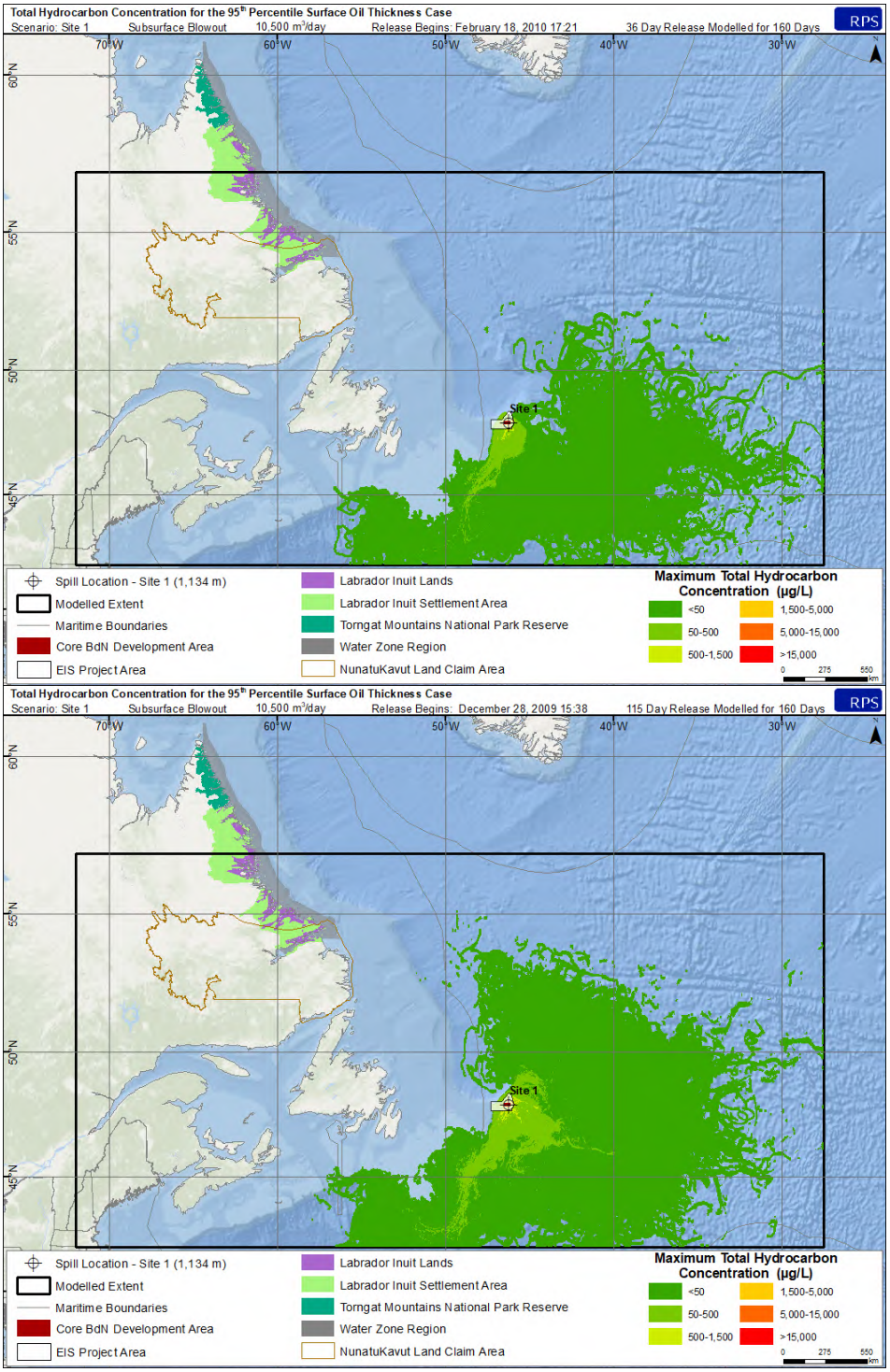

Figure 4-42. Maximum total hydrocarbon concentration (THC) at any depth in the water column for the 95th percentile surface oil thickness case for Site 1 for the 36-day (top) and the 115-day release (bottom).

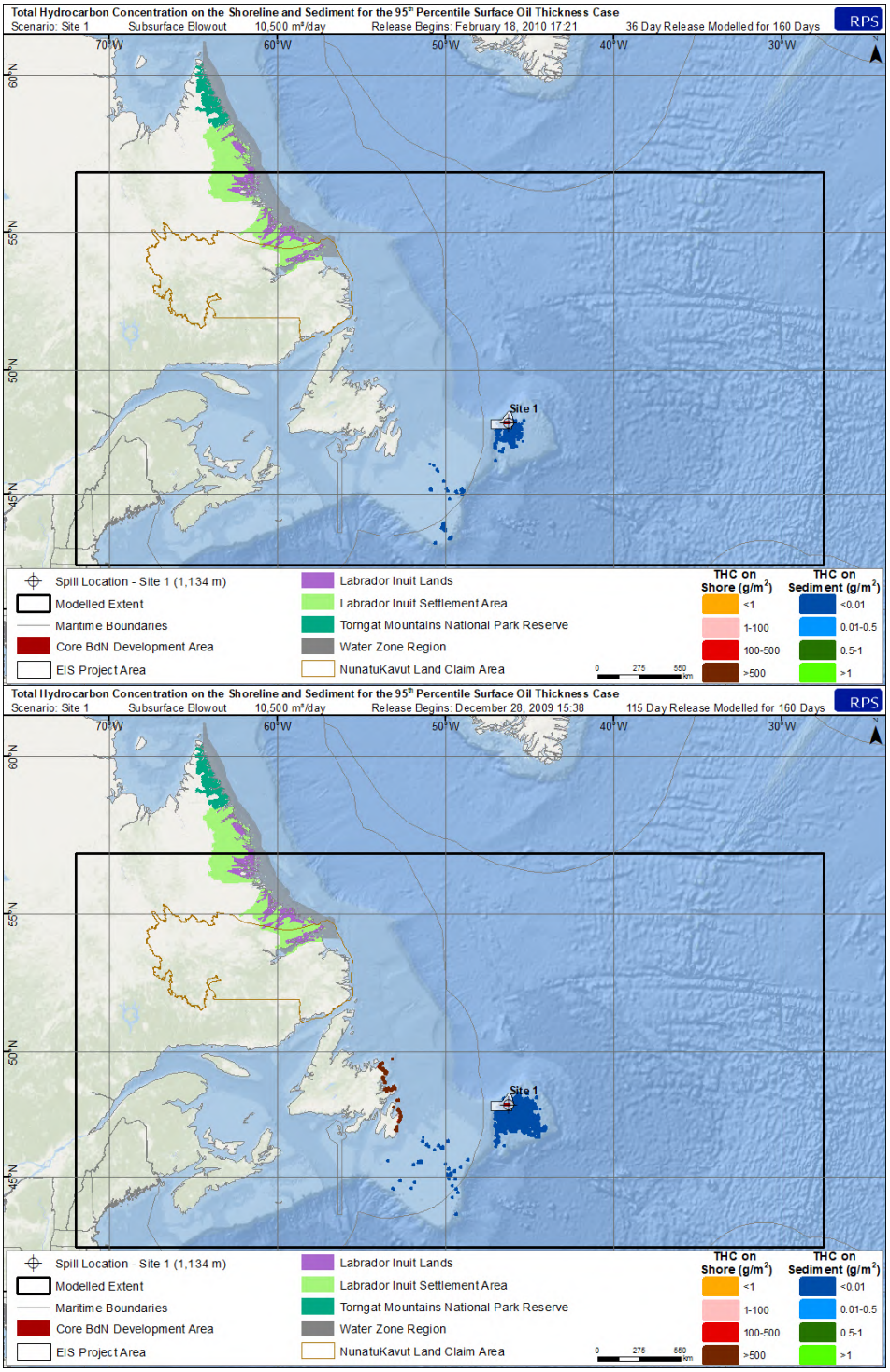

Figure 4-43. Total hydrocarbon concentration (THC) on the shore and sediment for the 95th percentile surface oil thickness case for Site 1 for the 36-day (top) and the 115-day release (bottom).

4.2.1.2 Site 2 Subsurface Releases

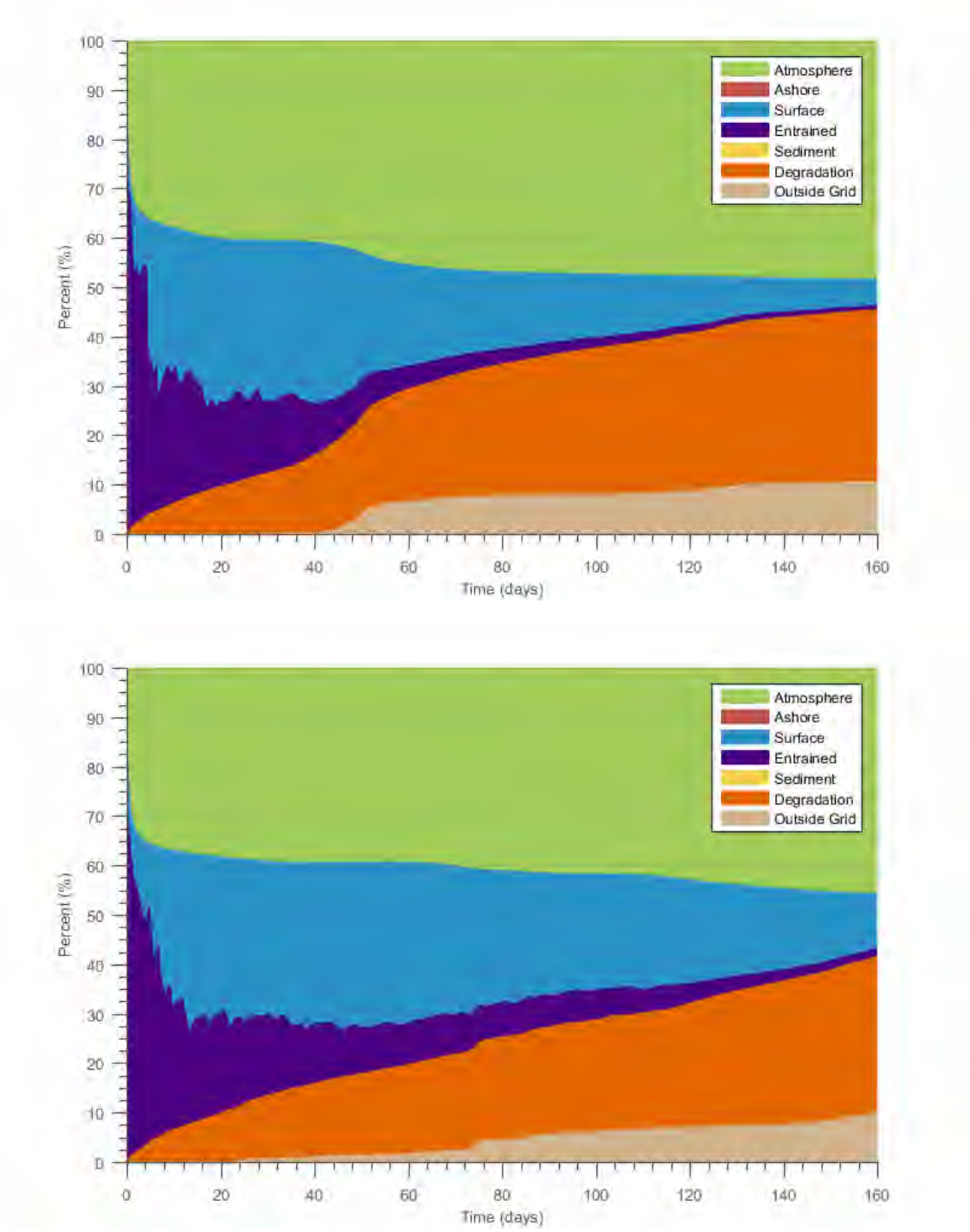

Figure 4-44. Mass balance plots for the 95th percentile surface oil thickness cases at Site 2 for the 36-day (top) and the 115-day release (bottom).

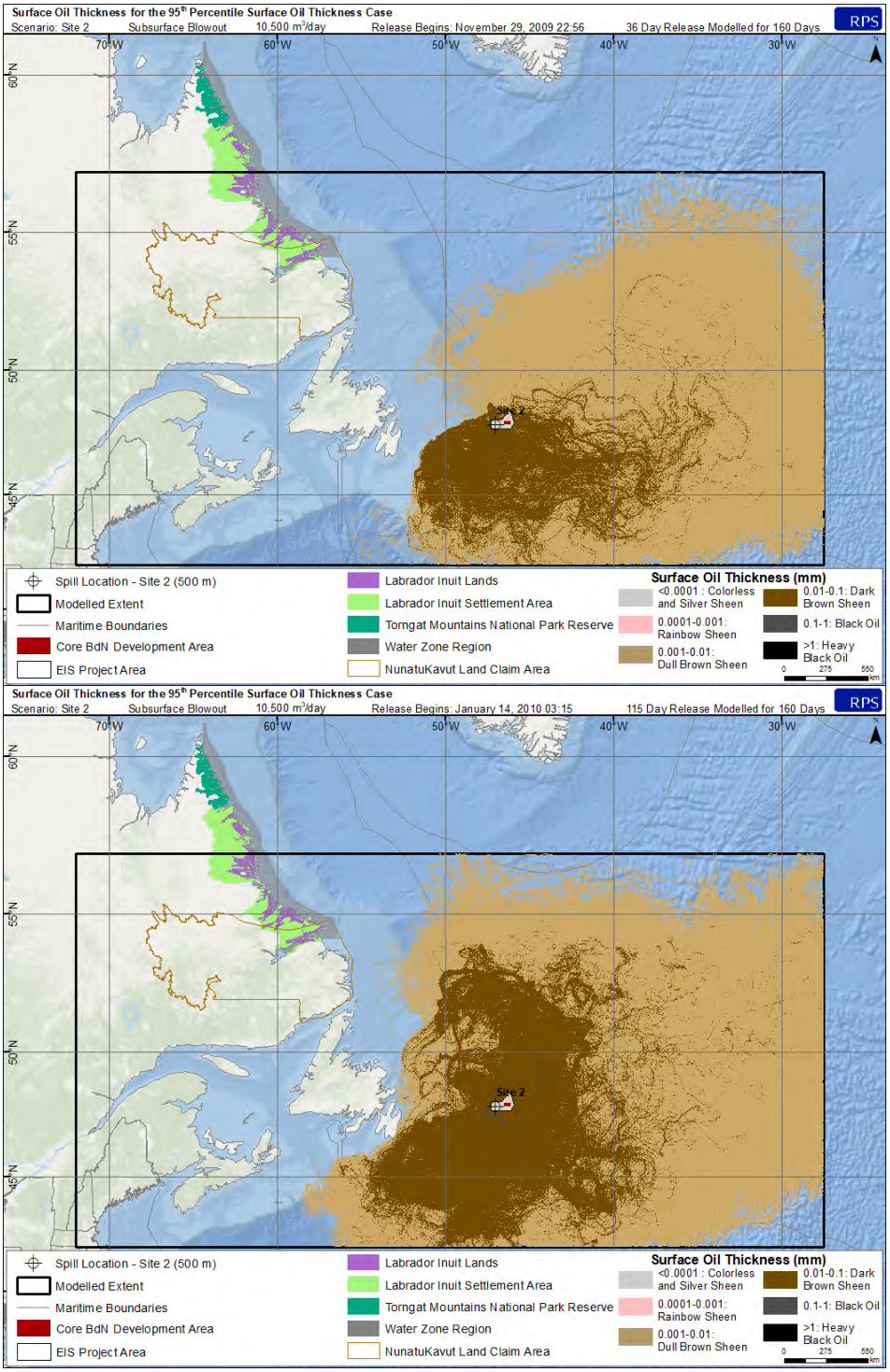

Figure 4-45. Surface oil thickness for the 95th percentile surface oil thickness case at Site 2 for the 36-day (top) and the 115-day release (bottom).

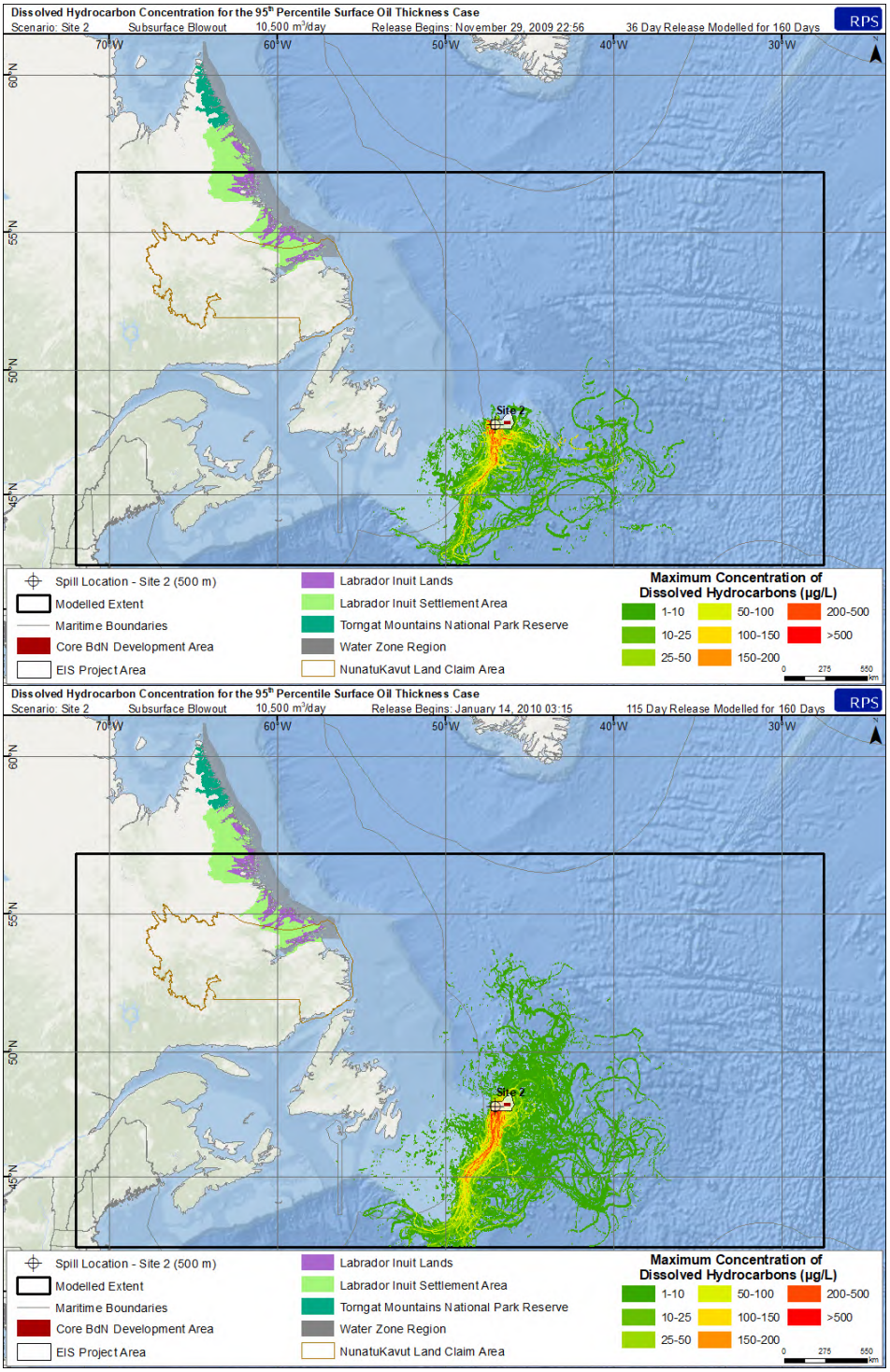

Figure 4-46. Maximum dissolved hydrocarbon concentration at any depth in the water column for the 95th percentile surface oil thickness case for Site 2 for the 36-day (top) and the 115-day release (bottom).

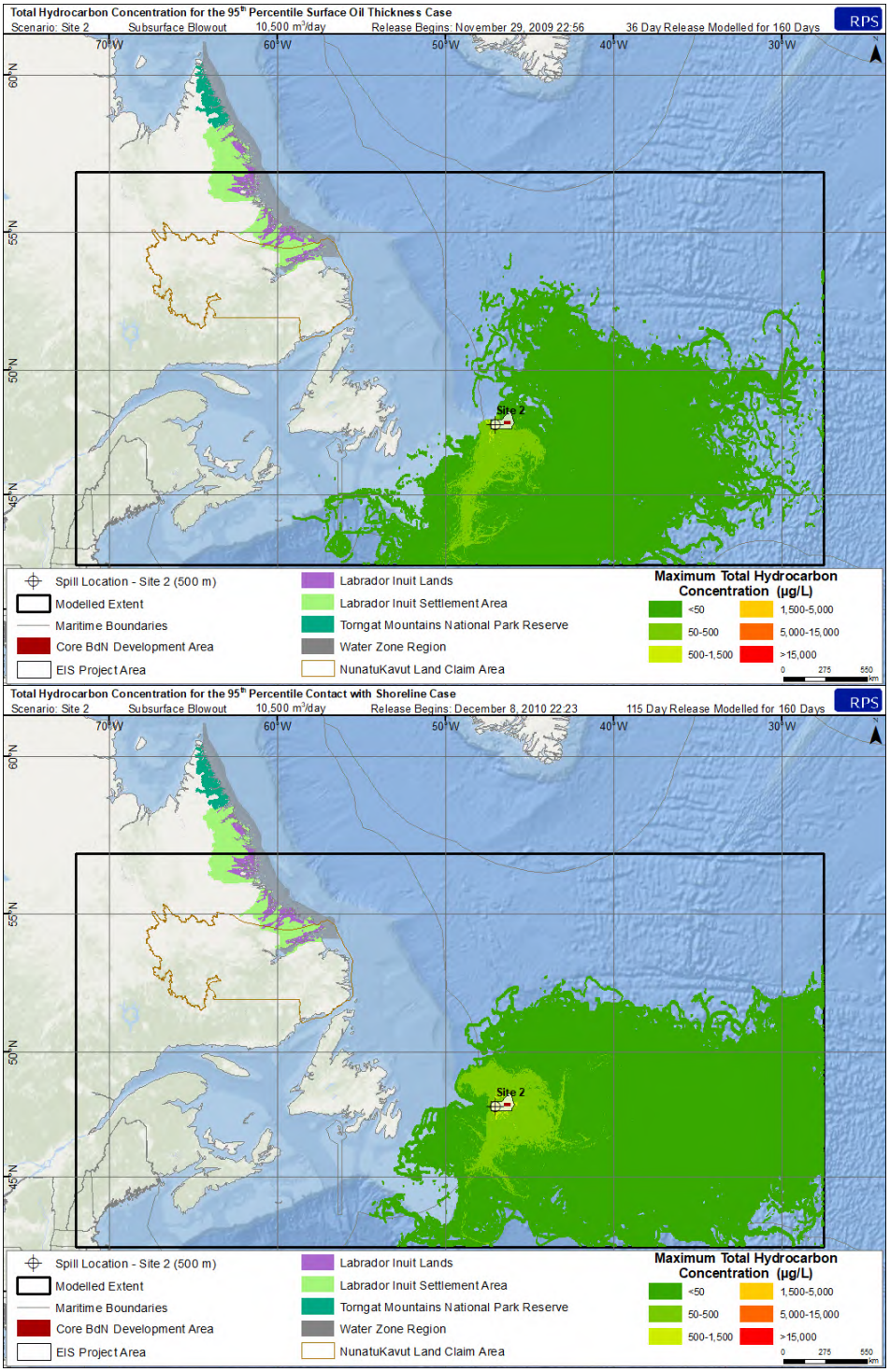

Figure 4-47. Maximum total hydrocarbon concentration (THC) at any depth in the water column for the 95th percentile surface oil thickness case for Site 2 for the 36-day (top) and the 115-day release (bottom).

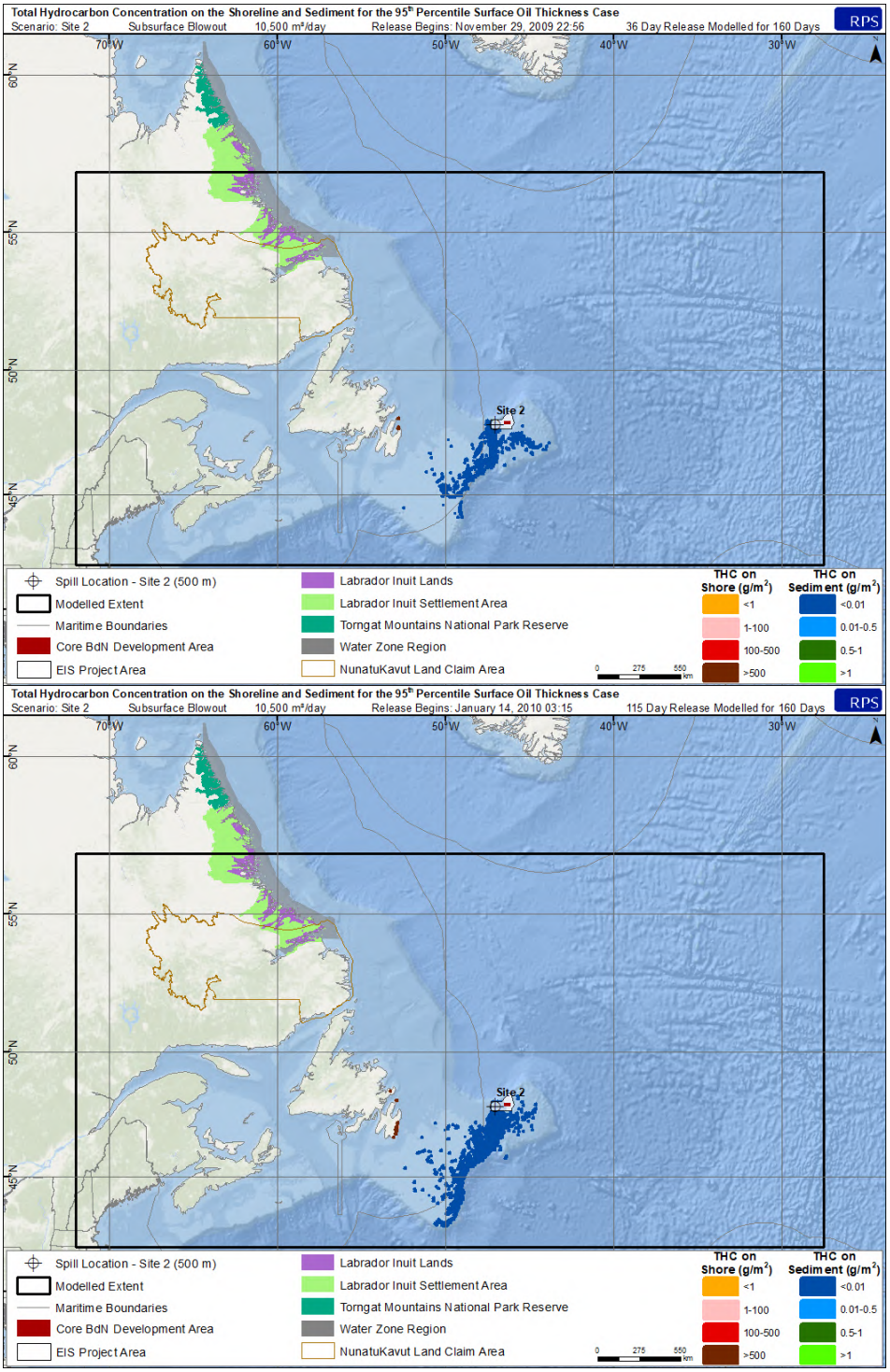

Figure 4-48. Total hydrocarbon concentration (THC) on the shore and sediment for the 95th percentile surface oil thickness case for Site 2 for the 36-day (top) and the 115-day release (bottom).

4.2.2 Water Column Exposure Cases

Results for the identified 95th percentile water column exposure cases for the releases at Site 1 and Site 2 are shown below. As previously noted, the modelled release dates for each scenario differed from one another and from the surface cases. At Site 1, the simulation for the 36-day release spanned November 2010 to mid-April 2011, while the 115-day release spanned from late-May to November 2008. At Site 2, the simulation for the 36-day release spanned late-April to October 2012 and September 2010 to mid-February 2011 for the 115-day release (Table 2-5).

To reiterate, the combined effects of a subsurface release and the entrainment of surface oil from wind-induced surface breaking waves into the water column were predicted to result in both dissolved and total hydrocarbon concentrations in the water column that exceeded the identified thresholds of interest (Figure 4-51 and Figure 4-52; Figure 4-56 and Figure 4-57). Concentrations of dissolved and total hydrocarbons were predicted to be highest around the release site. Concentrations dissipated as the oil was transported away from the release location as mixing within the water column dispersed oil and evaporation from the water surface, volatilization from the water column, and degradation reduced the total amount of hydrocarbons present. As total hydrocarbons represent the dissolved phase (i.e., soluble fraction making up <1% of the whole oil) plus the particulate phase (i.e., whole oil droplets) within the water column, THC has a much larger footprint than the predicted dissolved phase. For each site, the 115-day release was predicted to result in a larger overall cumulative footprint, as well as a larger footprint of the higher concentrations. The footprints of these predicted concentration exceedances are very similar to the surface oil trajectories, with the largest portion of the oil predicted to be transported towards the east (Figure 4-51 and Figure 4-52; Figure 4-56 and Figure 4-57). While the highest concentrations of THC are predicted near the release site at the trap height (see Section 3.7), the majority of the predicted THC concentrations within the cumulative footprint are within tens of meters of the surface. This is due to the majority of the predicted THC being the result of entrained oil from wind-induced surface breaking waves. Elevated concentrations of soluble hydrocarbons within the water column at the trap height may extend for several kilometers, however natural dispersion and degradation would reduce the predicted in-water concentrations rapidly as the distance from the release location increased.

There was no shoreline contact from oil released for the 95th percentile water column exposure cases for the 115-day release at Site 1 (Figure 4-53 and Table 4-3). This is explained by the fact that each scenario is initialized on a different day and results are driven by the specific hydrodynamic and environmental conditions at the time of the release. There were certainly main runs that did result in shoreline contact form oil, however, the 95th percentile water column exposure case for the 115-day release at Site 1 did not and was selected for water column criteria, not shoreline length potentially

affected. However, the 36-day release at Site 1 and both releases at Site 2 were predicted to make contact with the eastern shoreline of Newfoundland, including the Avalon Peninsula and some portions of southern Labrador, spanning over 3,000 km of coastline above the 1 g/m^2 threshold (Figure 4-53 and Figure 4-58; Table 4-3). Note that the predicted shoreline contact from these 95th percentile water column scenarios actually corresponded with the maximum (100th percentile or modelled "worst case") shoreline oil scenarios. Therefore, the 95th percentile shoreline exposure cases will have smaller volumes of oil predicted to reach shorter lengths of shorelines.

At the end of the 160-day simulations at Site 1, 1-2% of the oil was predicted to remain on the water surface, approximately 47-51% evaporated into the atmosphere, 1-3% remained entrained within the water column, ≤0.1% adhered to suspended sediment, 29-37% degraded, <2% made contact with the shore, and 13-15% was transported outside of the model domain (Figure 4-49 and Table 4-4). At the end of the 160-day simulations at Site 2, <1-8% of the oil was predicted to remain on the water surface, approximately 47-50% evaporated into the atmosphere, 1-3% remained entrained within the water column, ≤0.1% adhered to suspended sediment, 33-34% degraded, <1% made contact with the shore, and 9-15% was transported outside of the model domain (Figure 4-54 and Table 4-4).

4.2.2.1 Site 1 Subsurface Releases

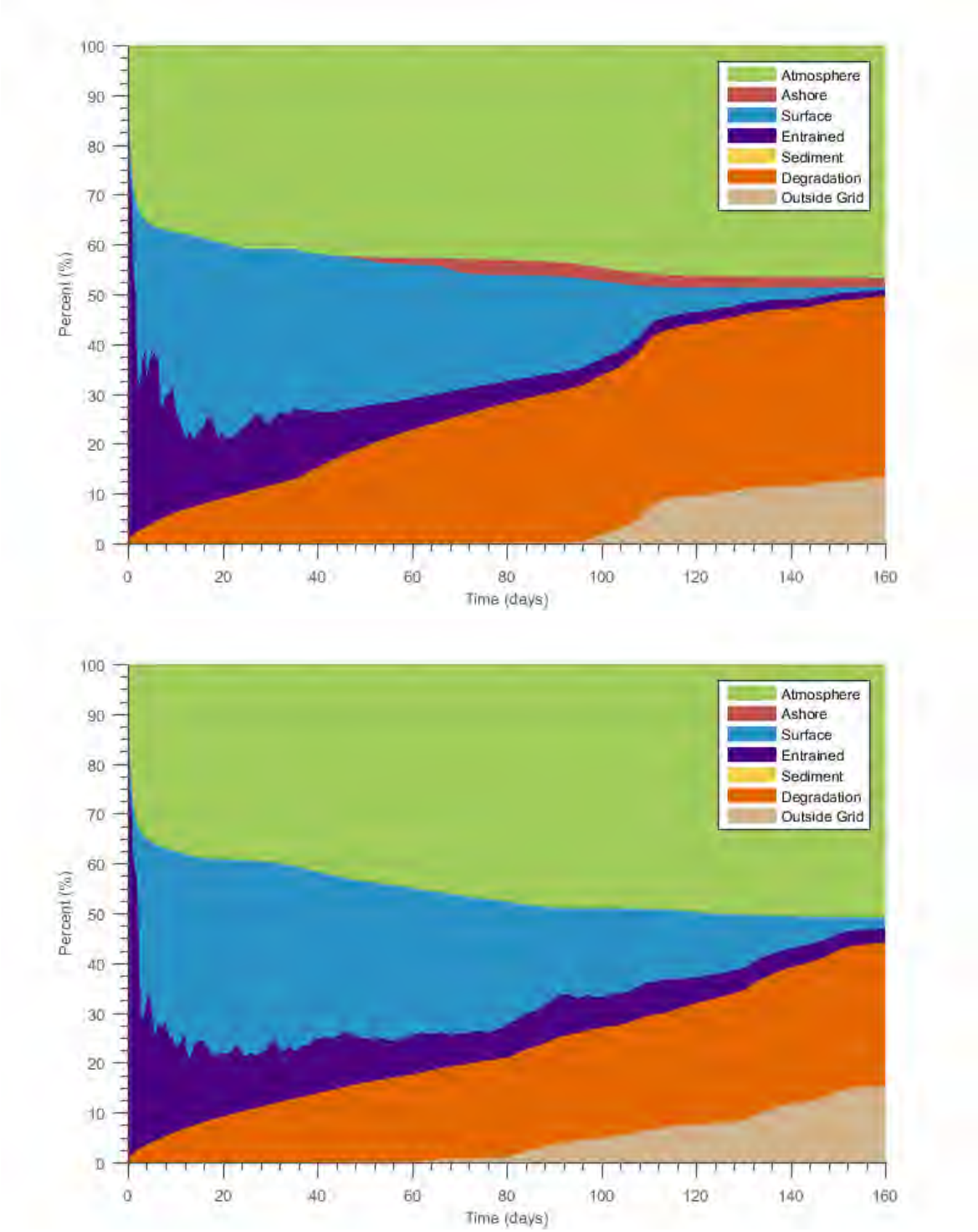

Figure 4-49. Mass balance plots of the 95th percentile water column case for Site 1 for the 36-day (top) and the 115-day release (bottom).

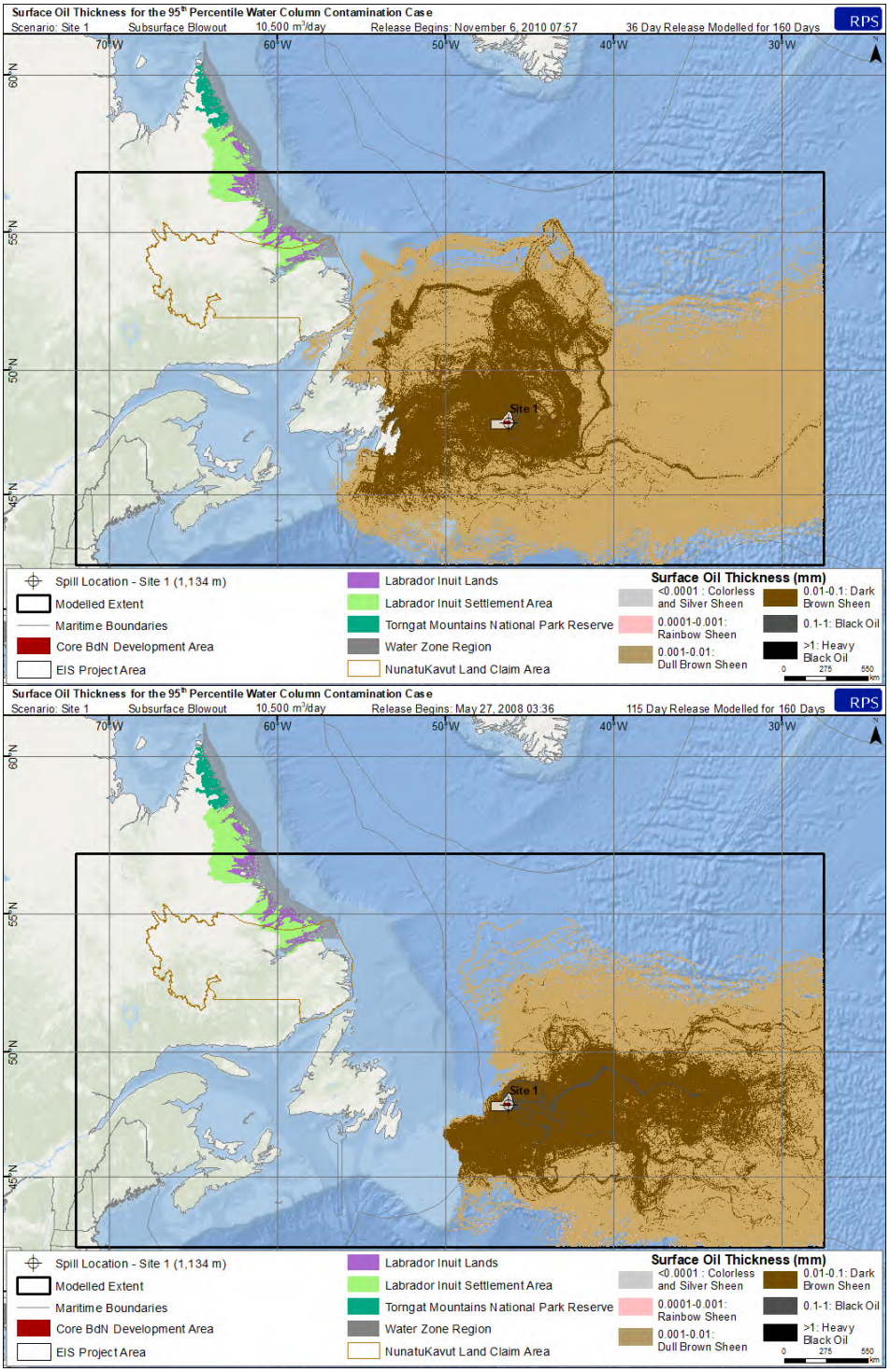

Figure 4-50. Surface oil thickness for the 95th percentile water column case resulting from a subsurface blowout at Site 1 for the 36-day (top) and the 115-day release (bottom).

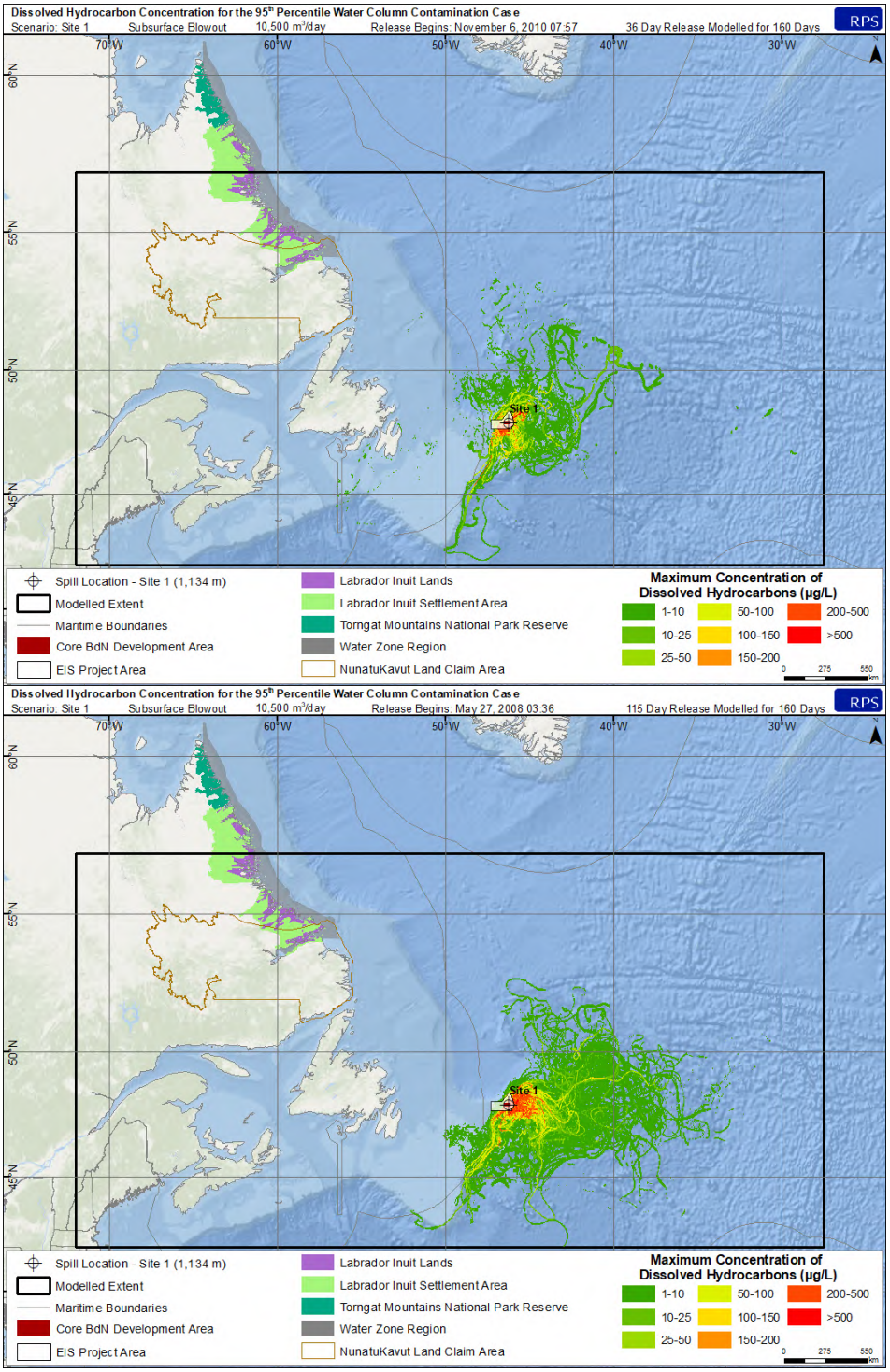

Figure 4-51. Maximum dissolved hydrocarbons at any depth in the water column for the 95th percentile water column case from a subsurface blowout at Site 1 for the 36-day (top) and the 115-day release (bottom).

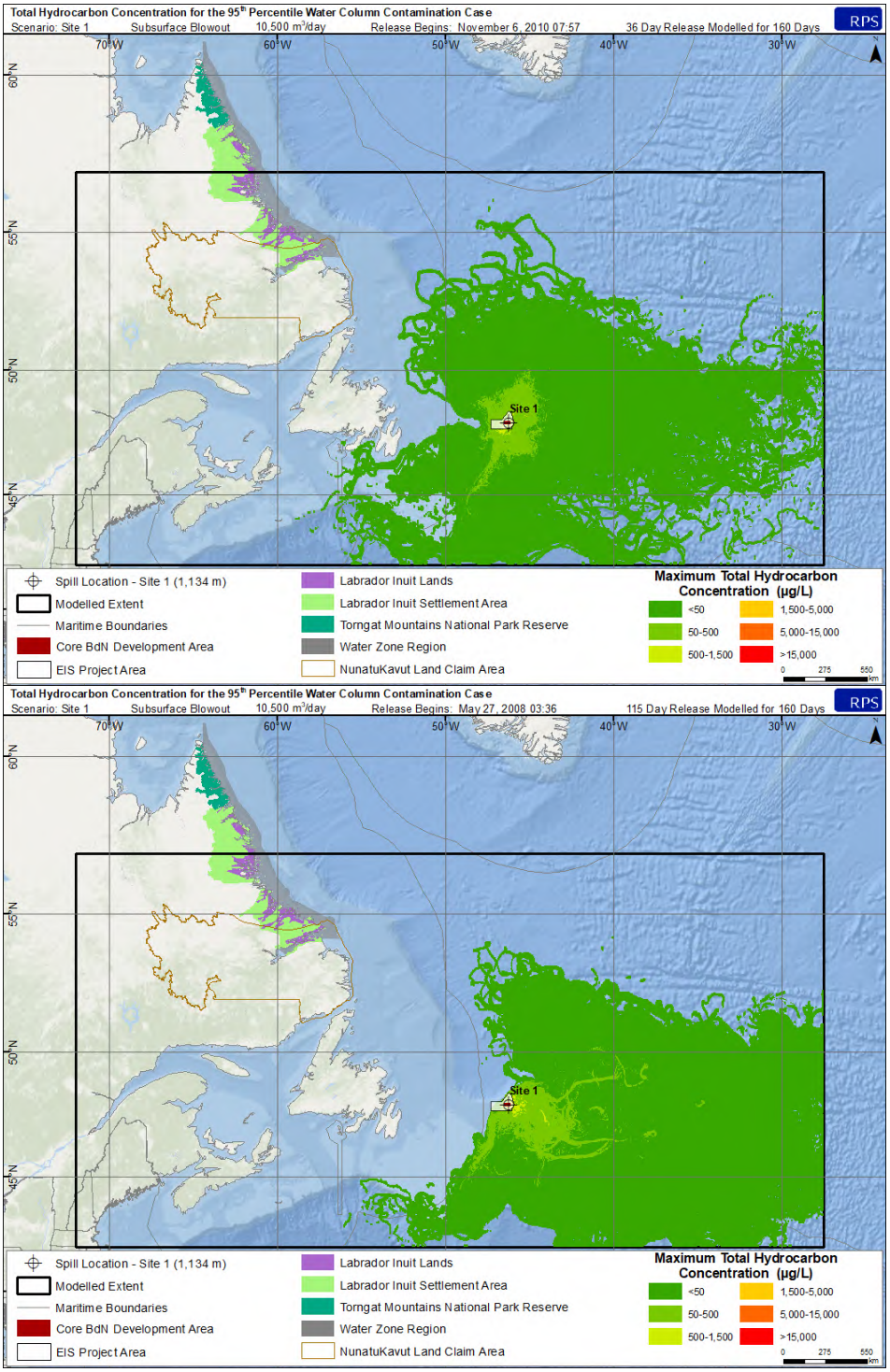

Figure 4-52. Maximum total hydrocarbon concentration (THC) at any depth in the water column for the 95th percentile water column case from a subsurface blowout at Site 1 for the 36-day (top) and the 115-day release (bottom).

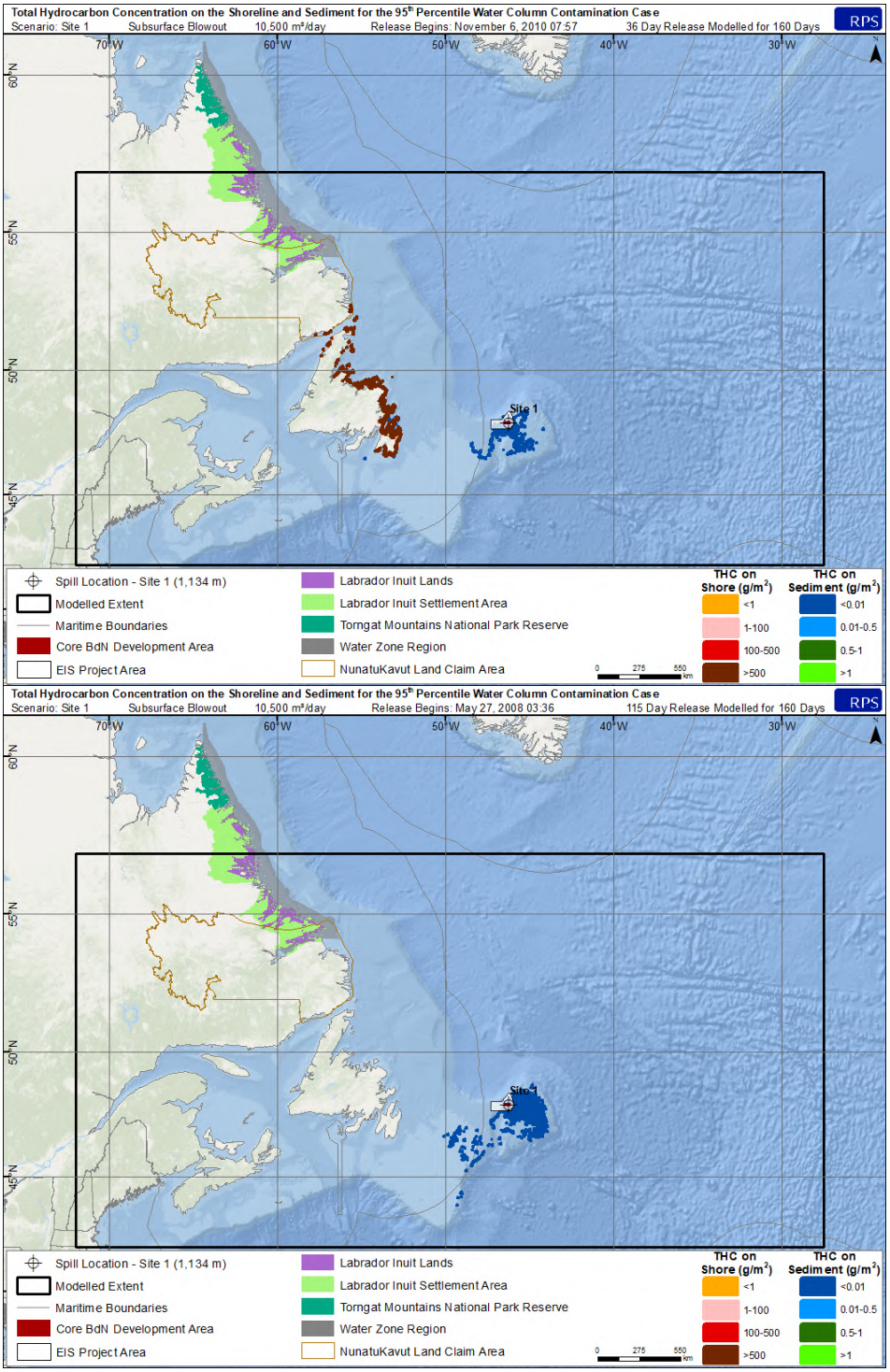

Figure 4-53. Total hydrocarbon concentration (THC) on the shore and sediment for the 95th percentile water column case from a subsurface blowout at Site 1 for the 36-day (top) and the 115-day release (bottom).

4.2.2.2 Site 2 Subsurface Releases

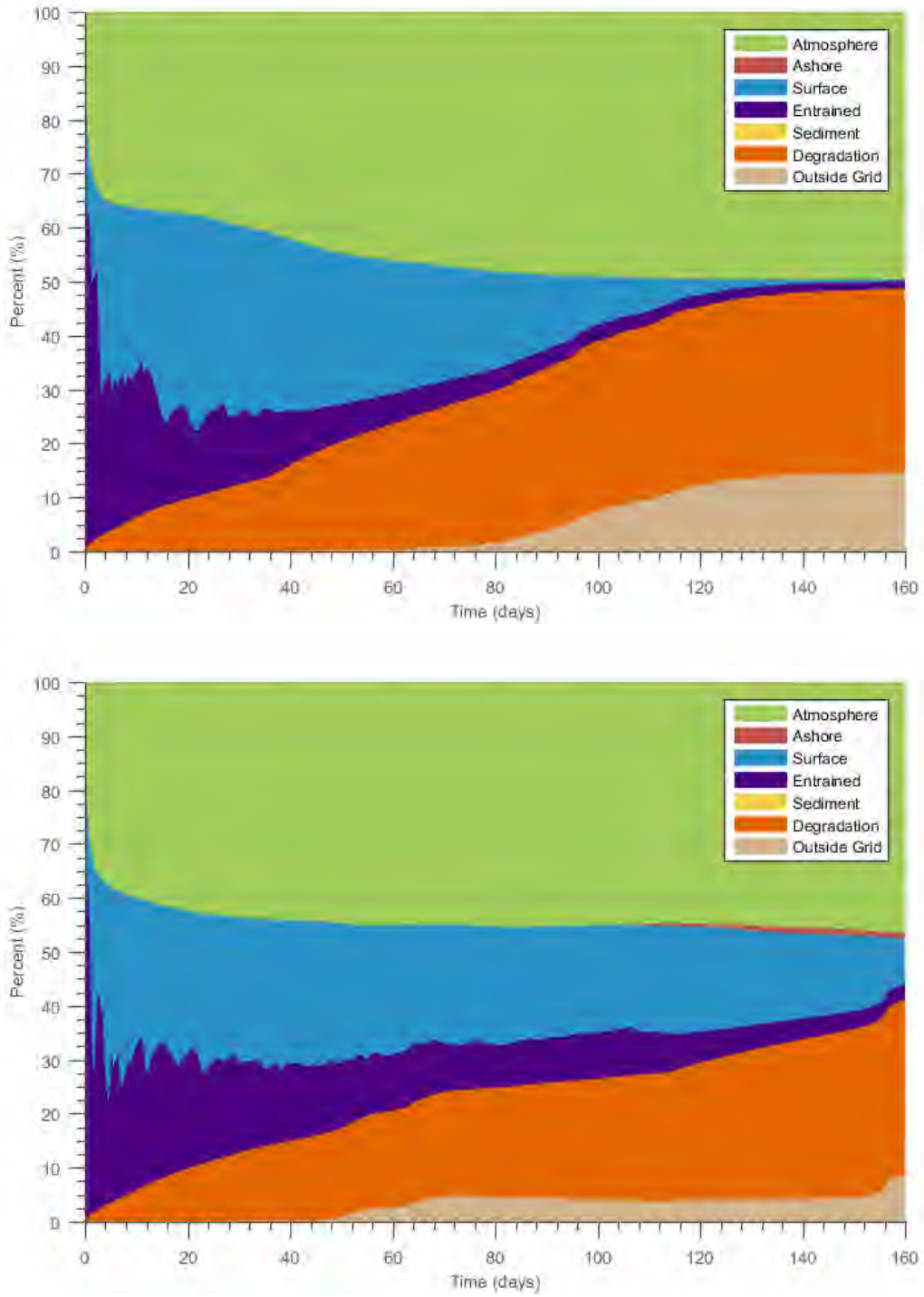

Figure 4-54. Mass balance plots of the 95th percentile water column case for Site 2 for the 36-day (top) and the 115-day release (bottom).

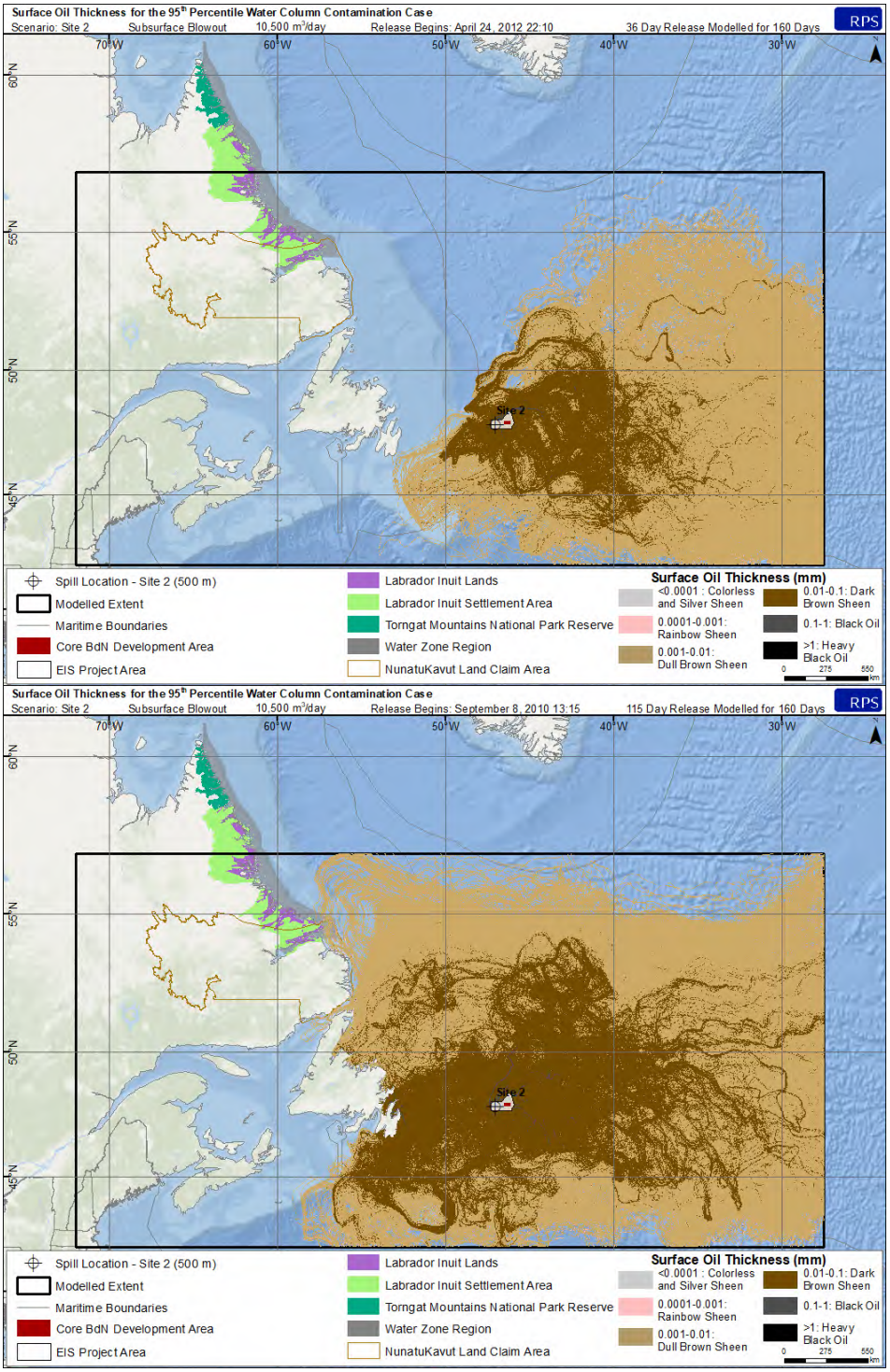

Figure 4-55. Surface oil thickness for the 95th percentile water column case resulting from a subsurface blowout at the Site 2 for the 36-day (top) and the 115-day release (bottom).

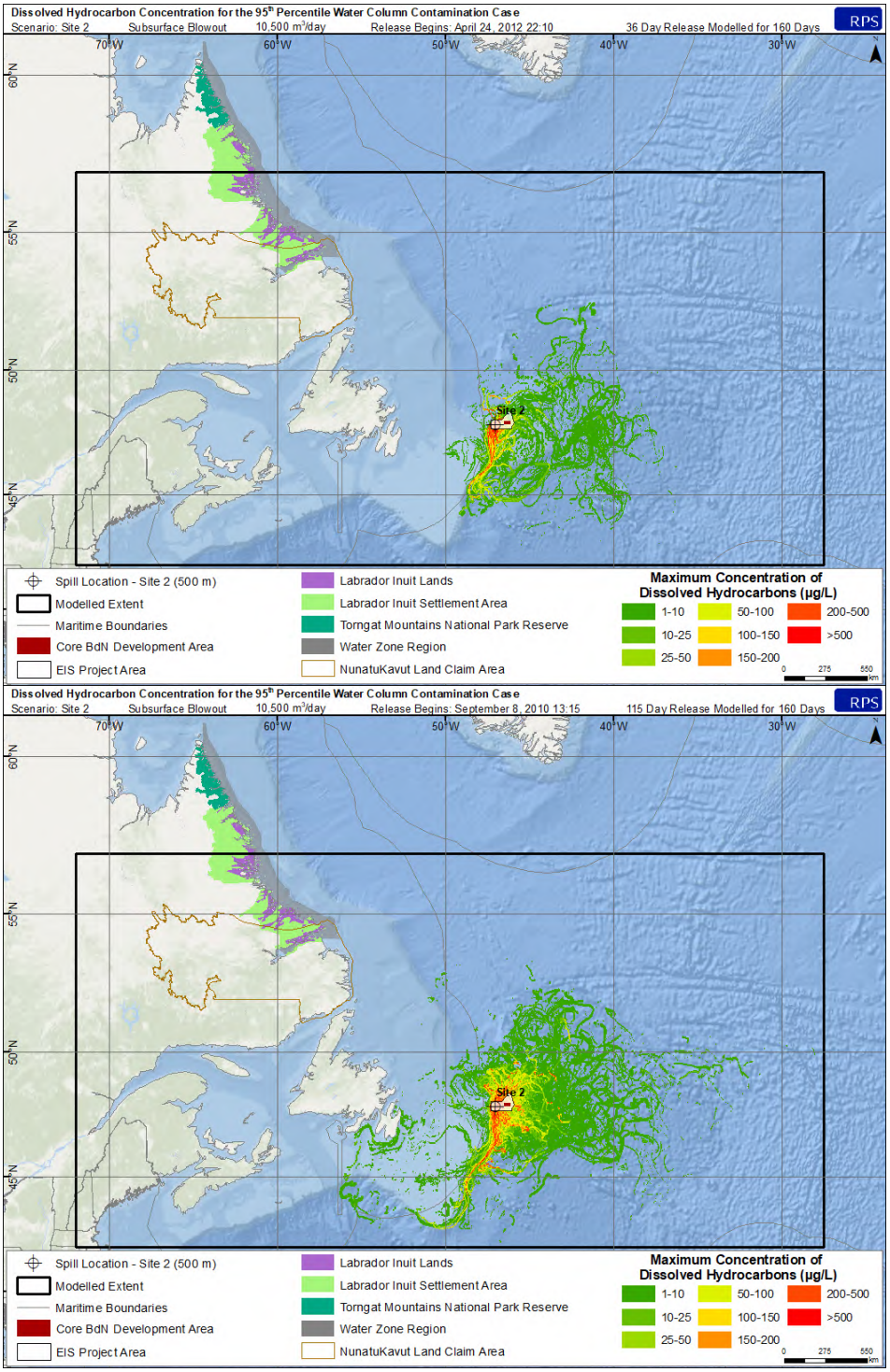

Figure 4-56. Maximum dissolved hydrocarbons at any depth in the water column for the 95th percentile water column case from a subsurface blowout at the Site 2 for the 36-day (top) and the 115-day release (bottom).

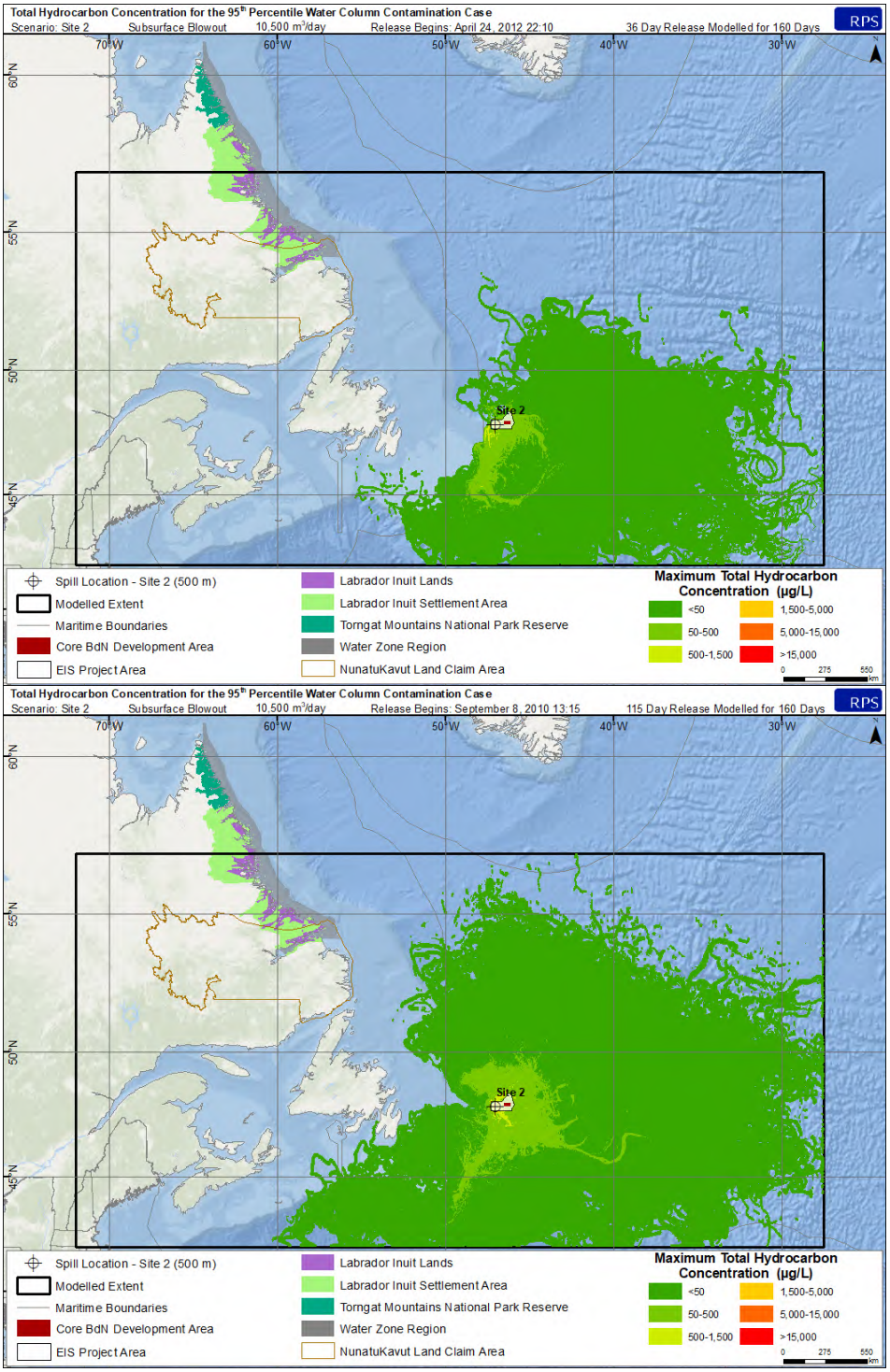

Figure 4-57. Maximum total hydrocarbon concentration (THC) at any depth in the water column for the 95th percentile water column case from a subsurface blowout at the Site 2 for the 36-day (top) and the 115-day release (bottom).

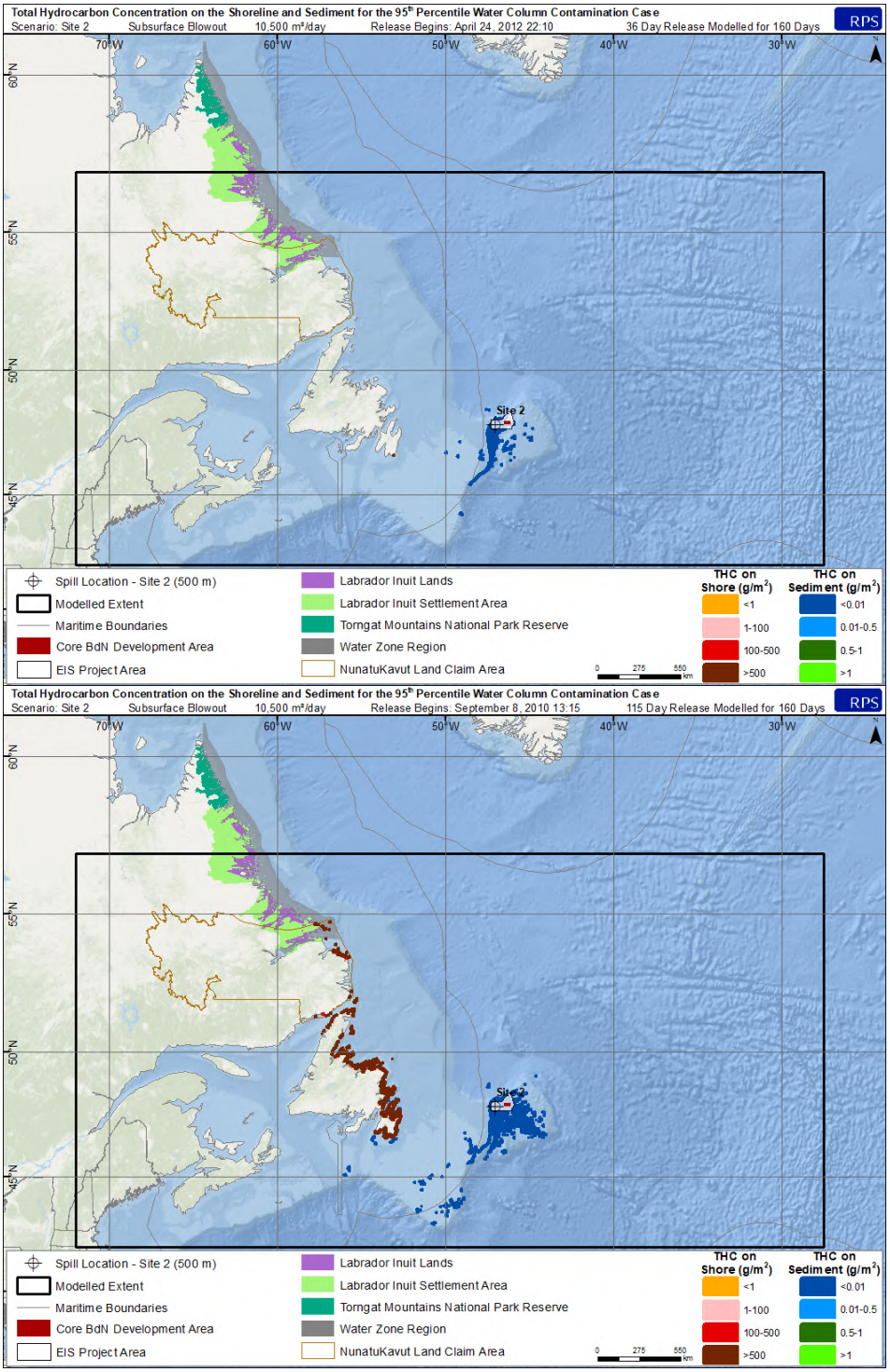

Figure 4-58. Total hydrocarbon concentration (THC) on the shore and sediment for the 95th percentile water column case from a subsurface blowout at the Site 2 for the 36-day (top) and the 115-day release (bottom).

4.2.3 Shoreline Exposure Case

Results for the identified 95th percentile shoreline exposure cases for the releases at Site 1 and Site 2 are shown below. The maximum probability of shoreline oil (Table 4-2) exposure ranged between 4 and 22% at Site 1 and 8 and 25% at Site 2. The majority of the predicted oil contact with shorelines occurred on the Avalon Peninsula and south coast of Newfoundland near St. Lawrence (Figure 4-63 and Figure 4-68). However, only a very small portion of the cumulative trajectory was predicted to move in this direction, with <1% of the total release volume predicted to make contact with the shoreline (Figure 4-59; Table 4-4). The selected 95th percentile shoreline exposure cases for the 115-day releases at Site 1 and Site 2 occurred on the same date and spanned from December 2010 to mid-May 2011. The simulation for the 36-day release at Site 1 spanned from late-February to August 2006 and at Site 2 spanned April to mid-September 2008. Contact with the shoreline from the 36-day releases was predicted to occur 45-92 days into the simulation and would likely contain highly weathered oil (i.e. lighter ends would have evaporated, dissolved, and degraded thereby reducing the toxicity of the residual oil). However, shoreline contact from the representative 115-day releases was predicted to occur between 14-15 days and would therefore be expected to contain fresher oil (than the 45-92 day old oil), although it would still be highly weathered (Figure 4-59 and Figure 4-64).

The stranding of oil on shorelines was unlikely for the majority of the release volume due to a combination of the forcing parameters transporting surface and entrained oil generally to the east away from shorelines. In particular, the predominately westerly winds (Figure 3-4) tend to transport oil offshore. The surface currents are variable (Figure 3-7 and Figure 3-8) and do not continuously transport oil in any one specific direction for significant periods of time. In addition, the release sites are located approximately 450 km offshore. Therefore, there would be a large amount of time required to pass before any oil made its way to shore, at which point evaporation and degradation would have likely heavily weathered the oil.

In the case of all four 95th percentile shoreline exposure cases, the combination of wind and current conditions resulted in a very small portion of the release contacting the shoreline. However, the total hydrocarbon concentration on shore was predicted to exceed 500 g/m^2, which was above the socio-economic (1 g/m^2) and ecological (100 g/m^2) thresholds, for approximately 138-792 km depending on the site and duration modelled in the shoreline exposure scenarios (Figure 4-63 and Figure 4-68; Table 4-3).

At the end of the 160-day simulations at Site 1, 1-2% of the oil was predicted to remain on the water surface, approximately 46-47% evaporated into the atmosphere, 1-2% remained entrained within the water column, ≤0.1% adhered to suspended sediment, 27-33% degraded, <0.04% made contact with the

shore, and up to 23% was transported outside of the model domain (Figure 4-59 and Table 4-4). At the end of the 160-day simulations at Site 2, <1-2% of the oil was predicted to remain on the water surface, approximately 46-50% evaporated into the atmosphere, 1-2% remained entrained within the water column, ≤0.1% adhered to suspended sediment, 28-35% degraded, <0.1% made contact with the shore, and 14-22% was transported outside of the model domain (Figure 4-64 and Table 4-4).

4.2.3.1 Site 1 Subsurface Releases

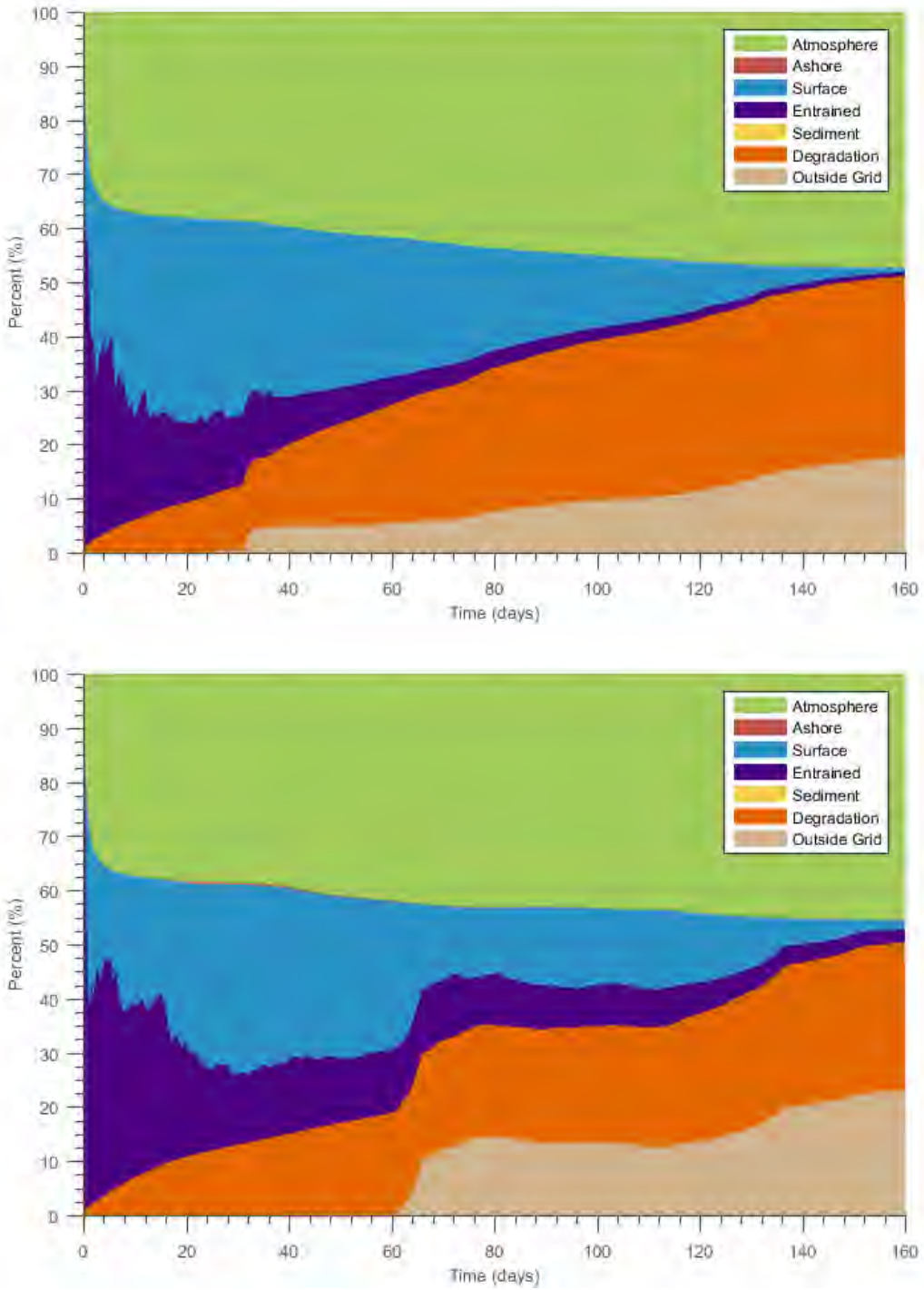

Figure 4-59. Mass balance plot of the 95th percentile contact with shoreline case for Site 1 for the 36-day (top) and the 115-day release (bottom).

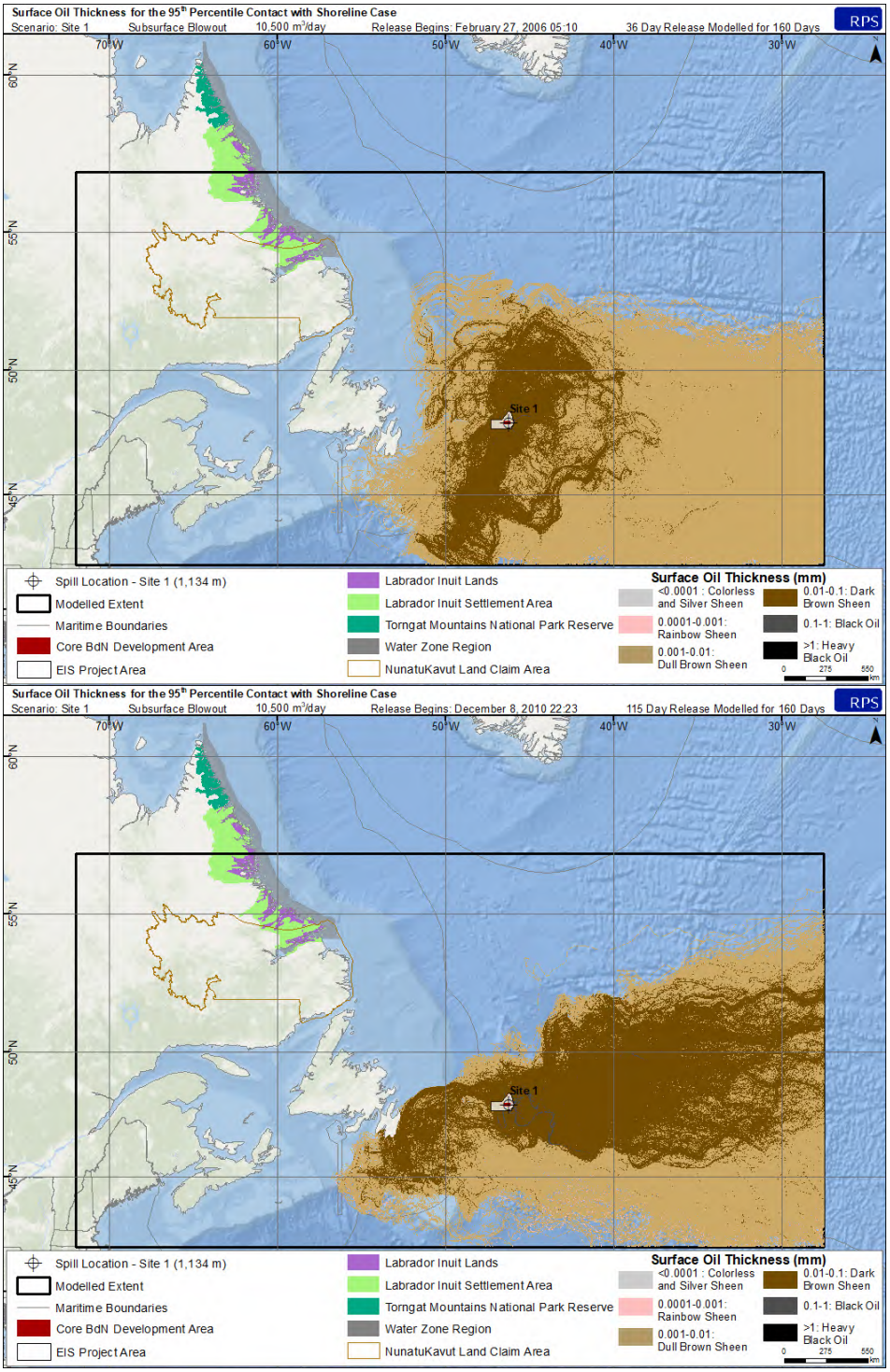

Figure 4-60. Surface oil thickness for the 95th percentile contact with shoreline case for Site 1 for the 36-day (top) and the 115-day release (bottom).

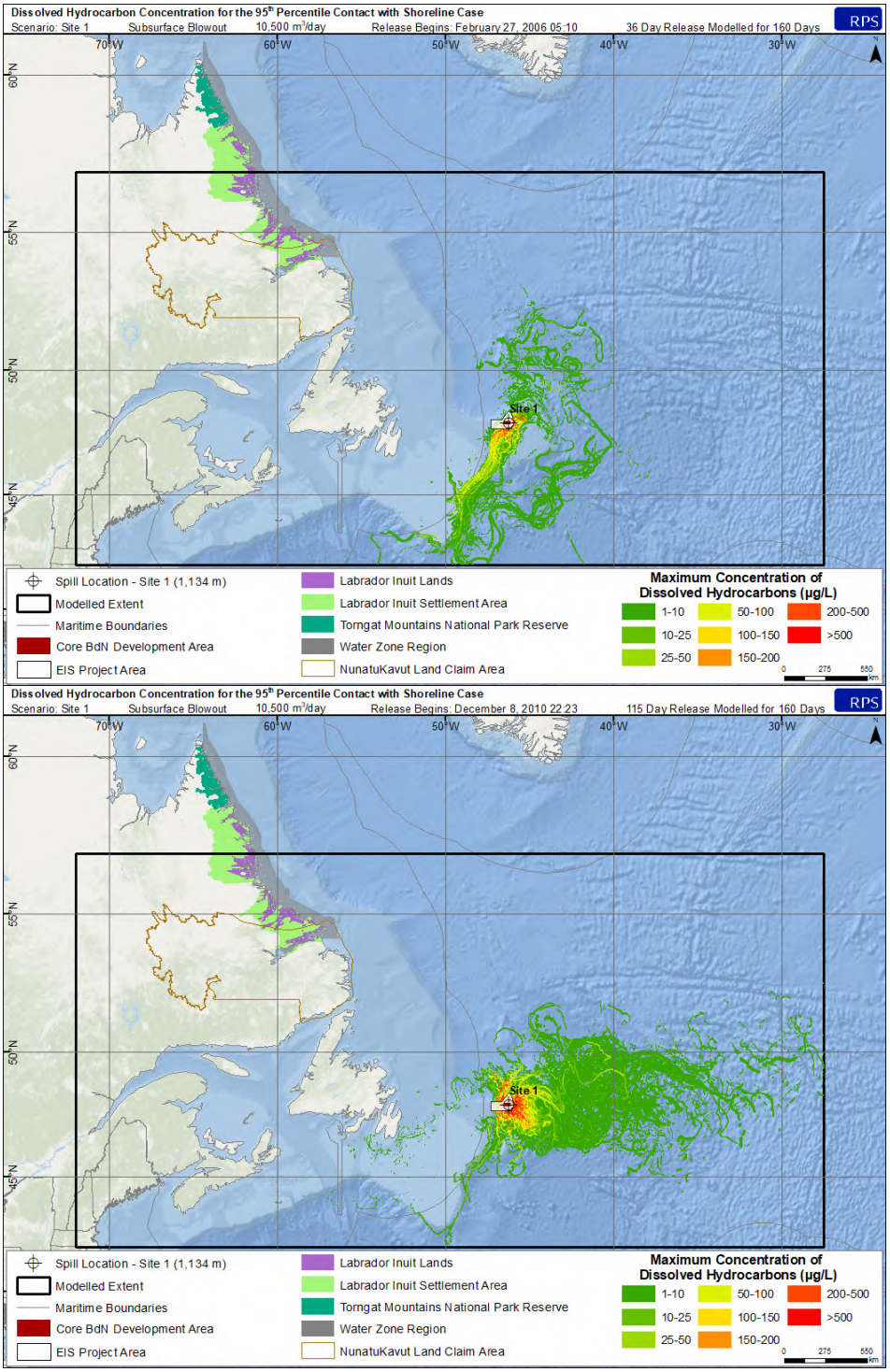

Figure 4-61. Maximum dissolved hydrocarbons at any depth in the water column for the 95th percentile contact with shoreline case for Site 1 for the 36-day (top) and the 115-day release (bottom).

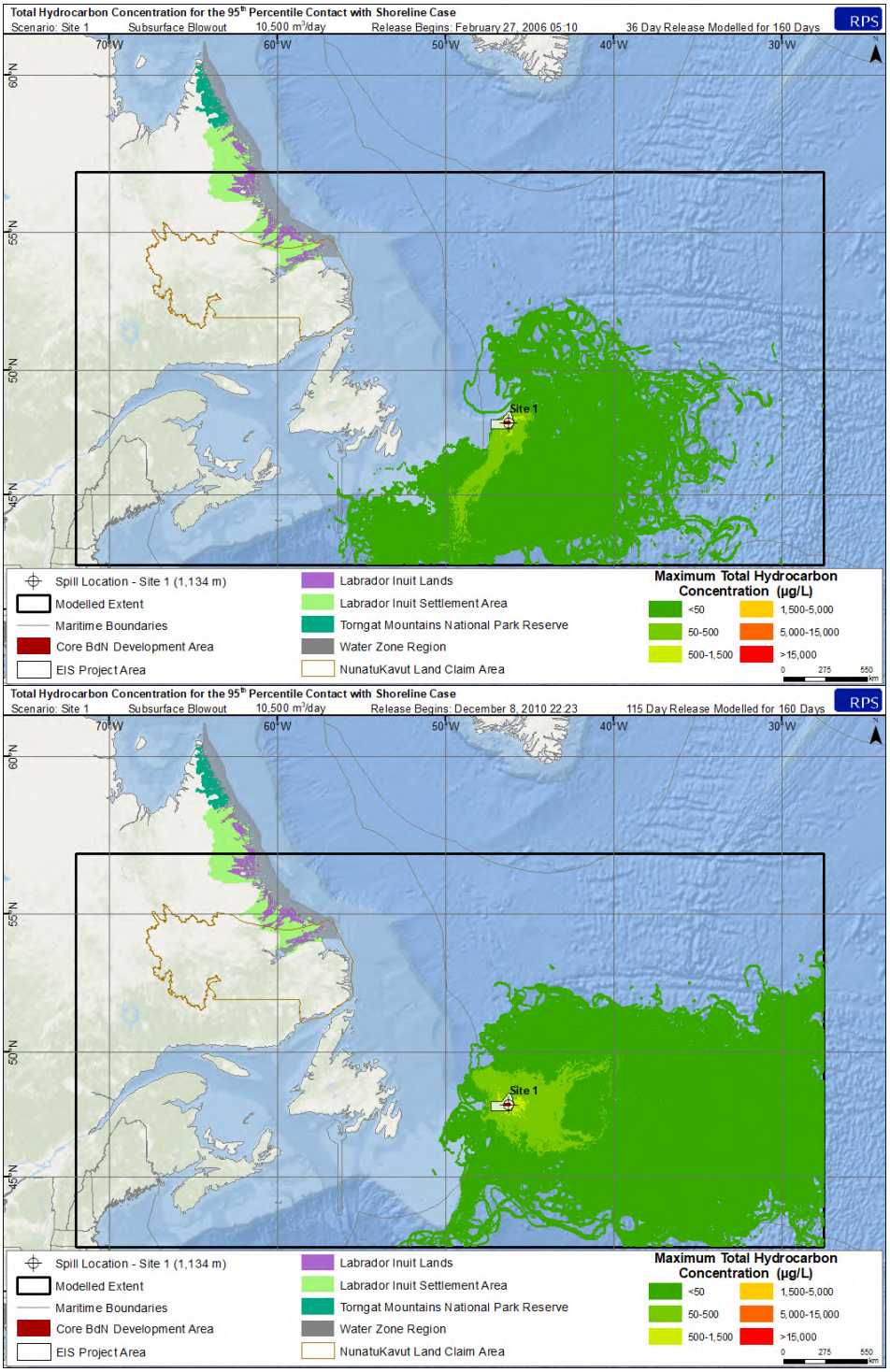

Figure 4-62. Maximum total hydrocarbon concentration (THC) at any depth in the water column for the 95th percentile contact with shoreline case from a subsurface blowout at Site 1 site for the 36-day (top) and the 115-day release (bottom).

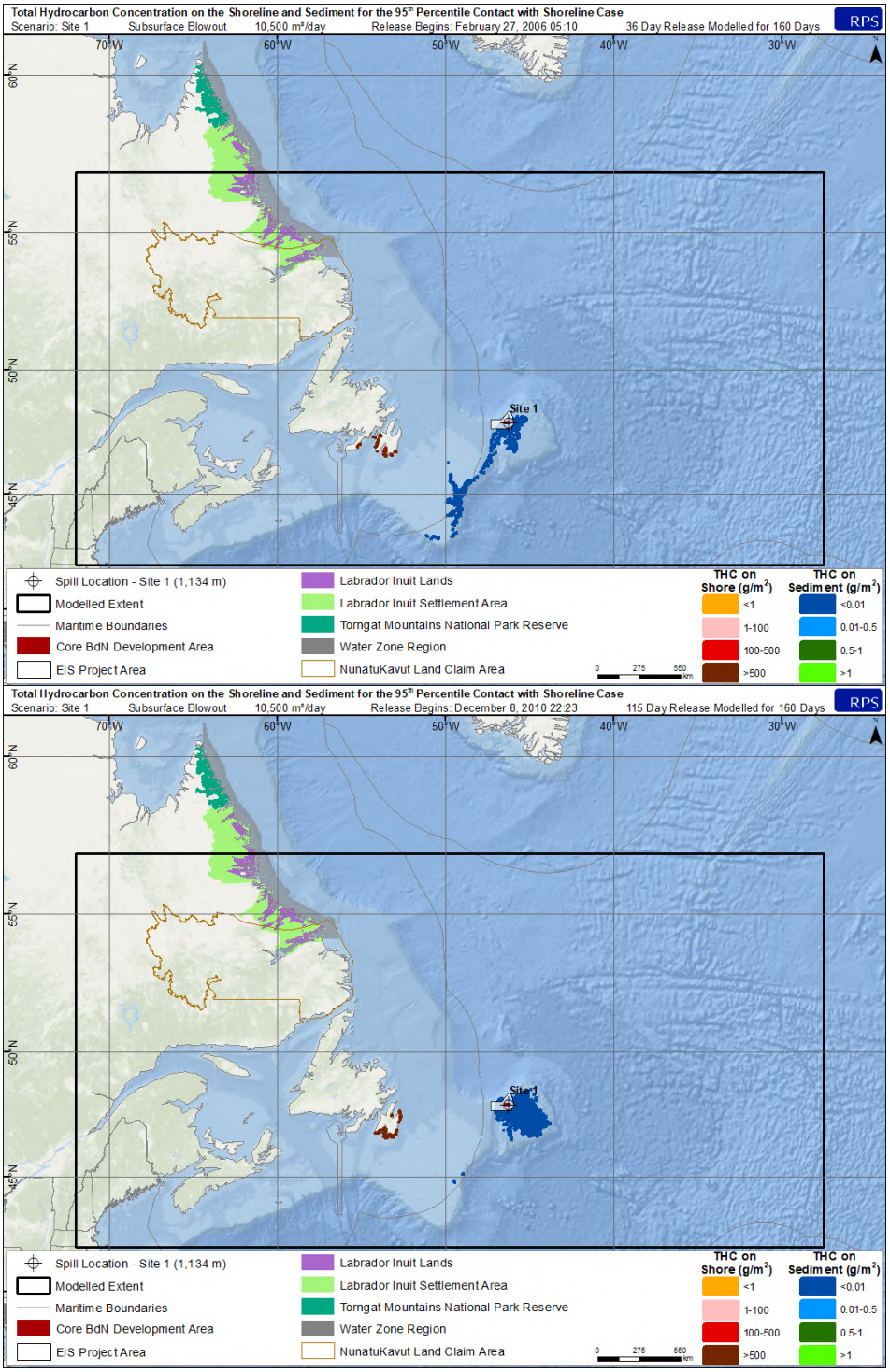

Figure 4-63. Total hydrocarbon concentration (THC) on the shore and sediment for the 95th percentile contact with shoreline case from a subsurface blowout at Site 1 site for the 36-day (top) and the 115-day release (bottom).

4.2.3.2 Site 2 Subsurface Releases

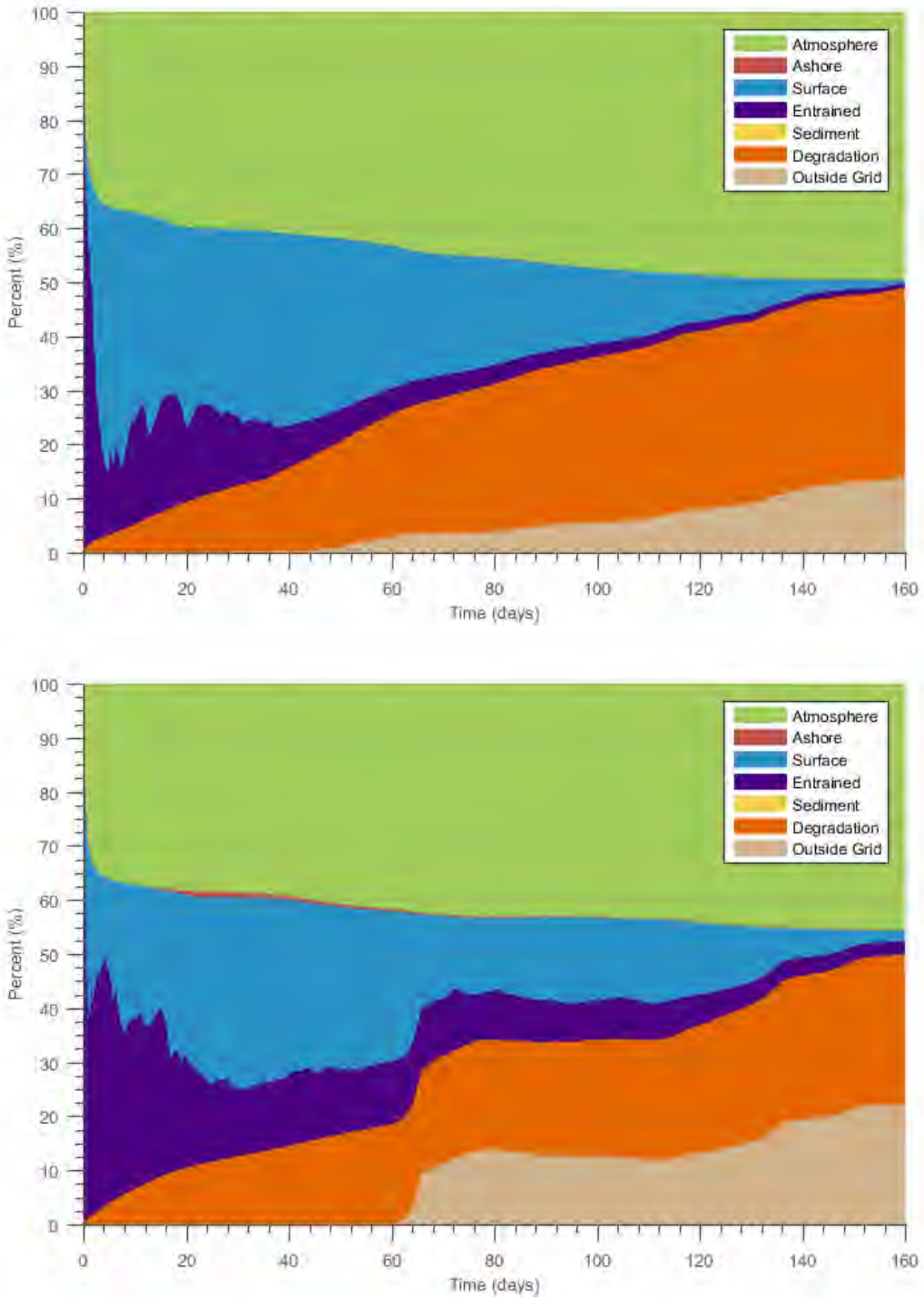

Figure 4-64. Mass balance plot of the 95th percentile contact with shoreline case for Site 2 for the 36-day (top) and the 115-day release (bottom).

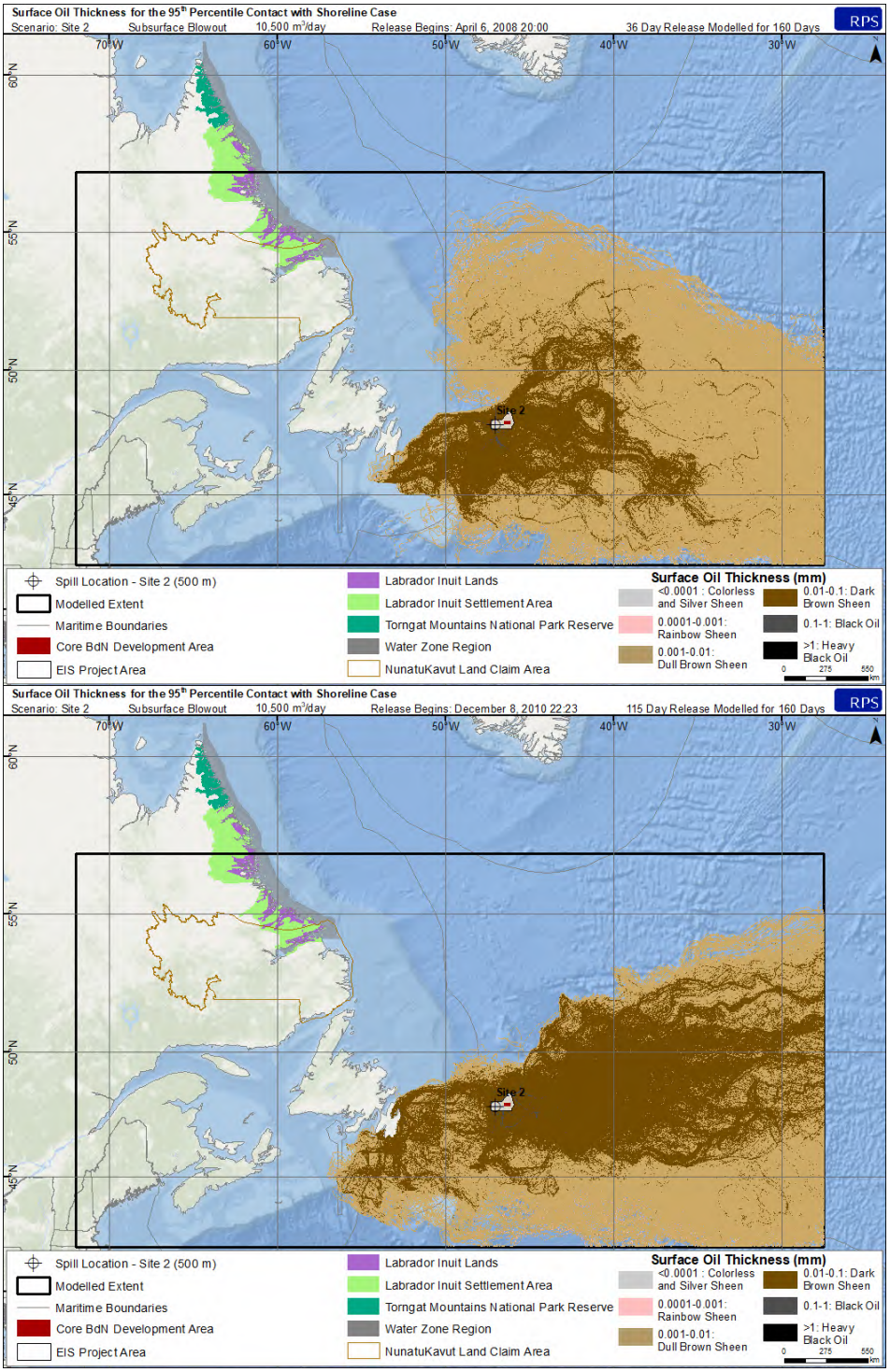

Figure 4-65. Surface oil thickness for the 95^{h} percentile contact with shoreline case for Site 2 for the 36-day (top) and the 115-day release (bottom).

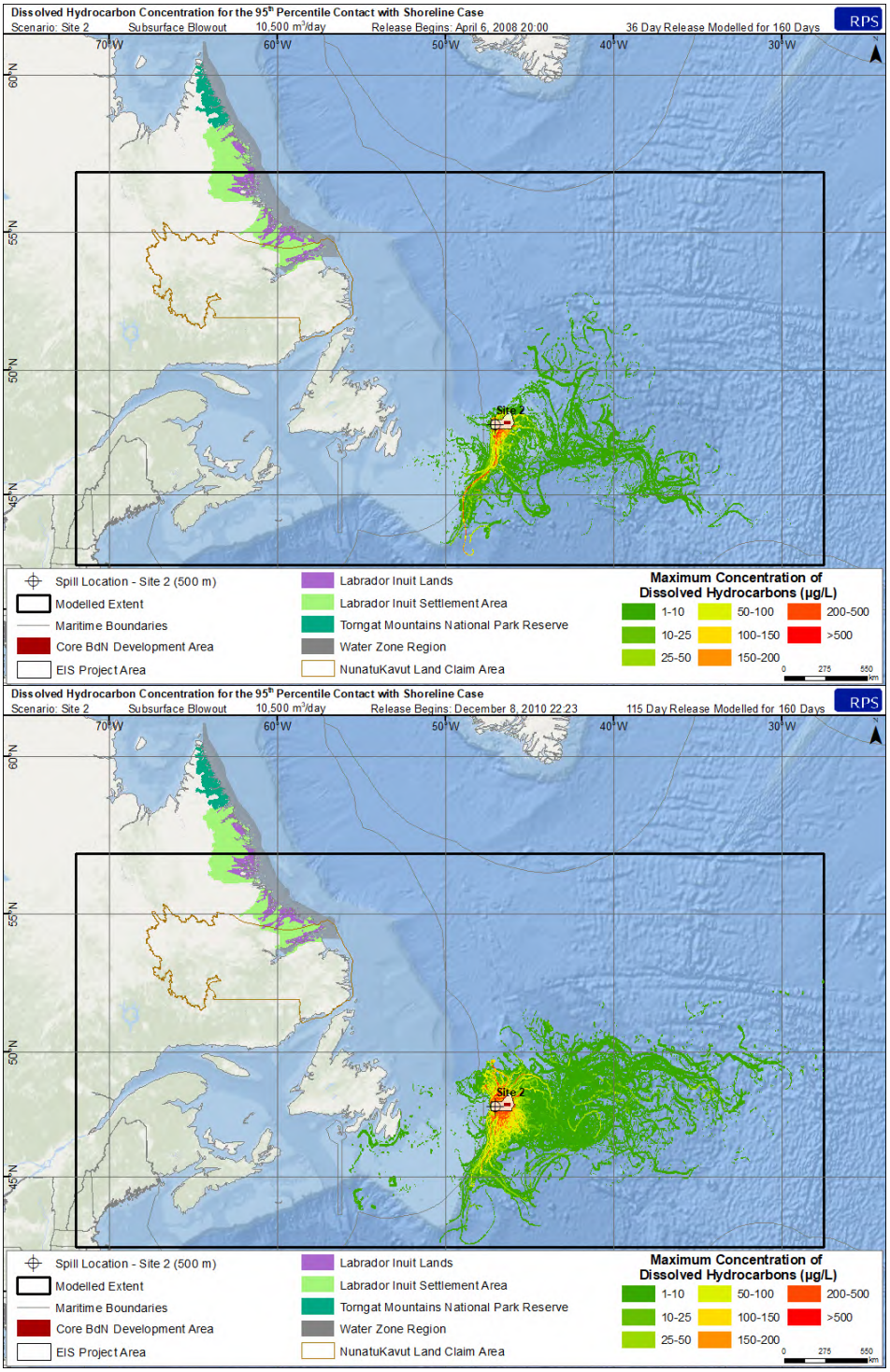

Figure 4-66. Maximum dissolved hydrocarbons at any depth in the water column for the 95th percentile contact with shoreline case for Site 2 for the 36-day (top) and the 115-day release (bottom).

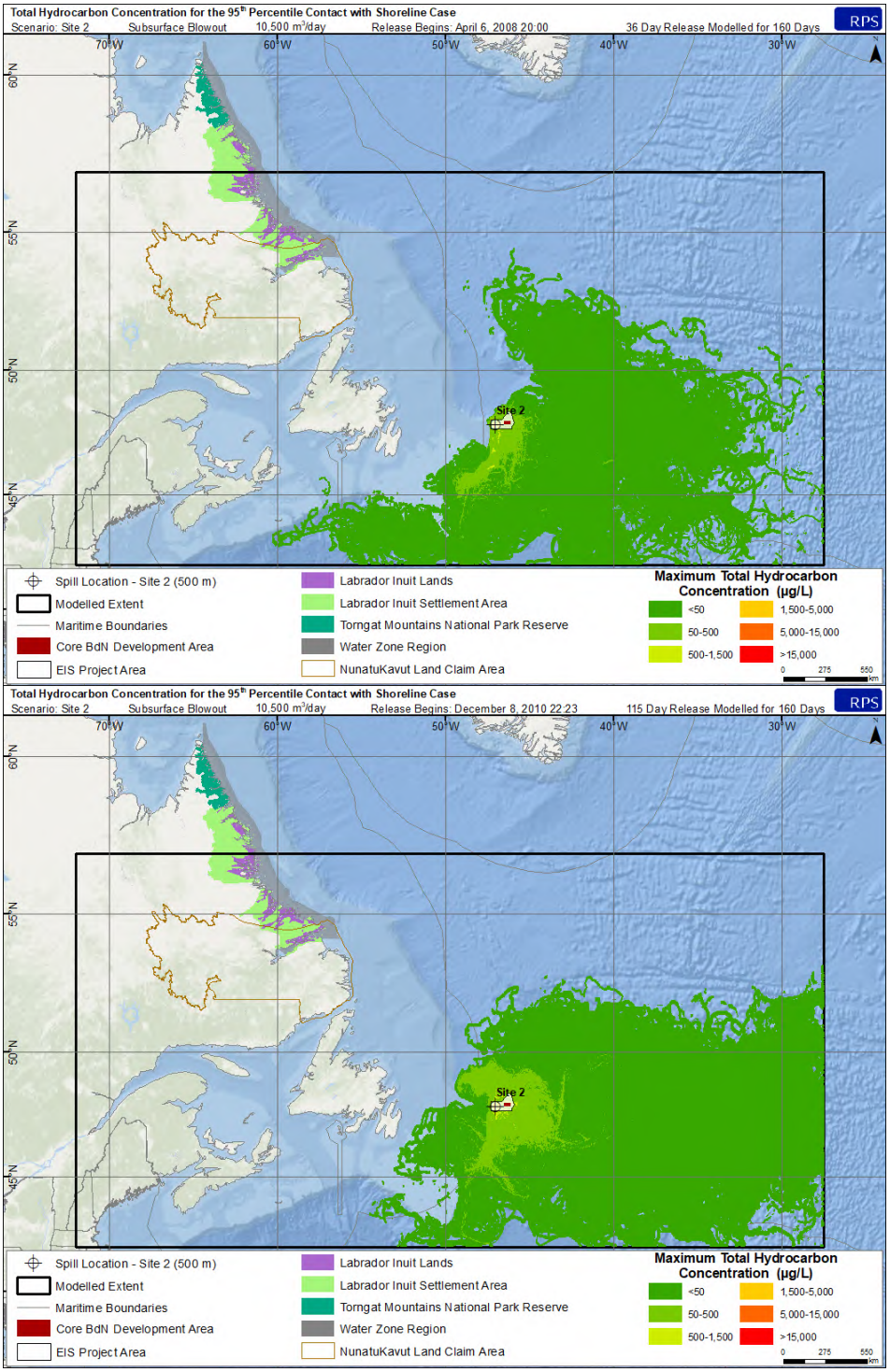

Figure 4-67. Maximum total hydrocarbon concentration (THC) at any depth in the water column for the 95th percentile contact with shoreline case from a subsurface blowout at the Site 2 site for the 36-day (top) and the 115-day release (bottom).

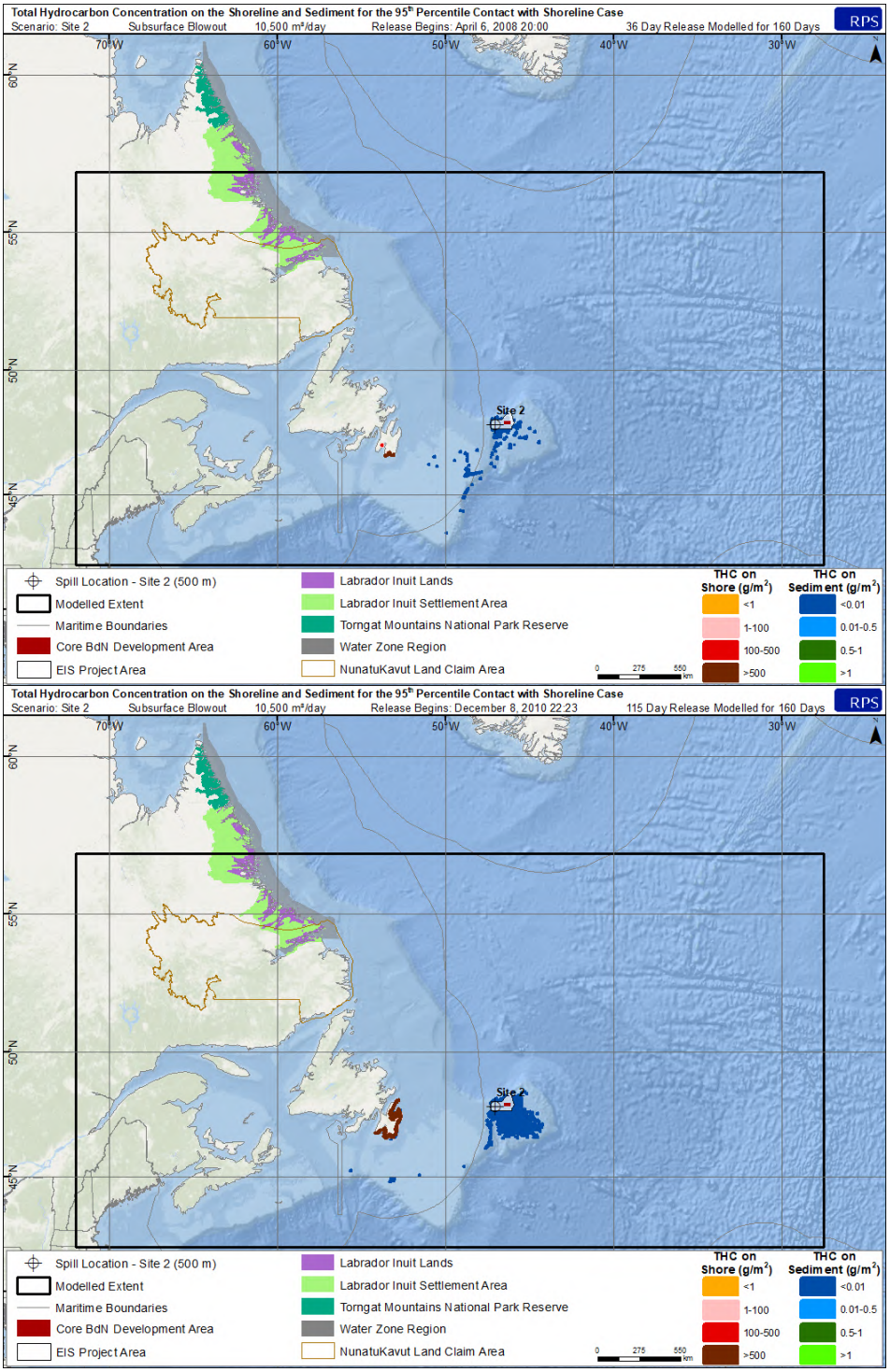

Figure 4-68. Total hydrocarbon concentration (THC) on the shore and sediment for the 95th percentile contact with shoreline case from a subsurface blowout at the Site 2 site for the 36-day (top) and the 115-day release (bottom).

4.2.4 Batch Spills

Results for the batch spill scenarios are provided in the figures below. Four shorter duration (30 day) and smaller volume releases were modelled to be representative of spills that could occur from different sources (Table 2-5). Releases from the FPSO were investigated as surface releases of BdN totaling 8,300 m^3 over a two-day period. The shuttle tanker was modelled as a surface release during offloading totaling 1,000 m^3 over a one-hour period. Additional surface releases from bunkering operations (i.e., transfer from a vessel) were modelled as 6 m^3 of marine diesel. An additional seabed batch spill was modelled to be representative of a loss of hydrocarbons in a production flowline with 500 m^3 of BdN crude being released over one day.

The scenarios were selected to occur during the calmest wind-speed period during the summer/ice-free conditions, which would result in the largest amount of oil on the water surface (i.e., the "worst-case" scenario). The selected date was June 4, 2009 (Table 2-5).

Due to the small release volume and the size of the concentration gridding (1,800 m by 2,500 m), predicted concentrations of dissolved hydrocarbons were not expected for the batch spills and thus figures have not been presented below. In their place, total hydrocarbon concentrations are presented. The predicted THC concentrations extended roughly 100 - 350 km from the release location. Surface oil was predicted to spread rapidly with maximum thicknesses corresponding with a visual appearance of a dull brown sheen for the BdN releases and a colorless or silver sheen for the marine diesel. None of the modelled batch spills were predicted to result in any oil contacting shorelines.

At the end of the 30-day BdN surface batch spill simulations (8,300 m^3 and 1,000 m^3) , 29% of the released volume was predicted to remain floating on the water surface, 37-39% evaporated into the atmosphere, 10-11% remained entrained in the water column, 0.01% adhered to suspended sediment, 0% contacted the shore, and 22-24% degraded (Figure 4-69 and Table 4-4). At the end of the marine diesel surface batch spill, it was predicted that <1% remained at the water surface, 58% evaporated, 12% was entrained in the water column, and 30% degraded (Figure 4-70 and Table 4-4). However, at the end of the 30-day simulation of the seafloor batch spill of BdN at Site 1, 32% was predicted to remain on the water surface, while 42% evaporated, 6% entrained, 0% in sediments, and 20% degraded (Figure 4-71 and Table 4-4).

4.2.4.1 Proposed FPSO Site & Site 1 Batch Releases

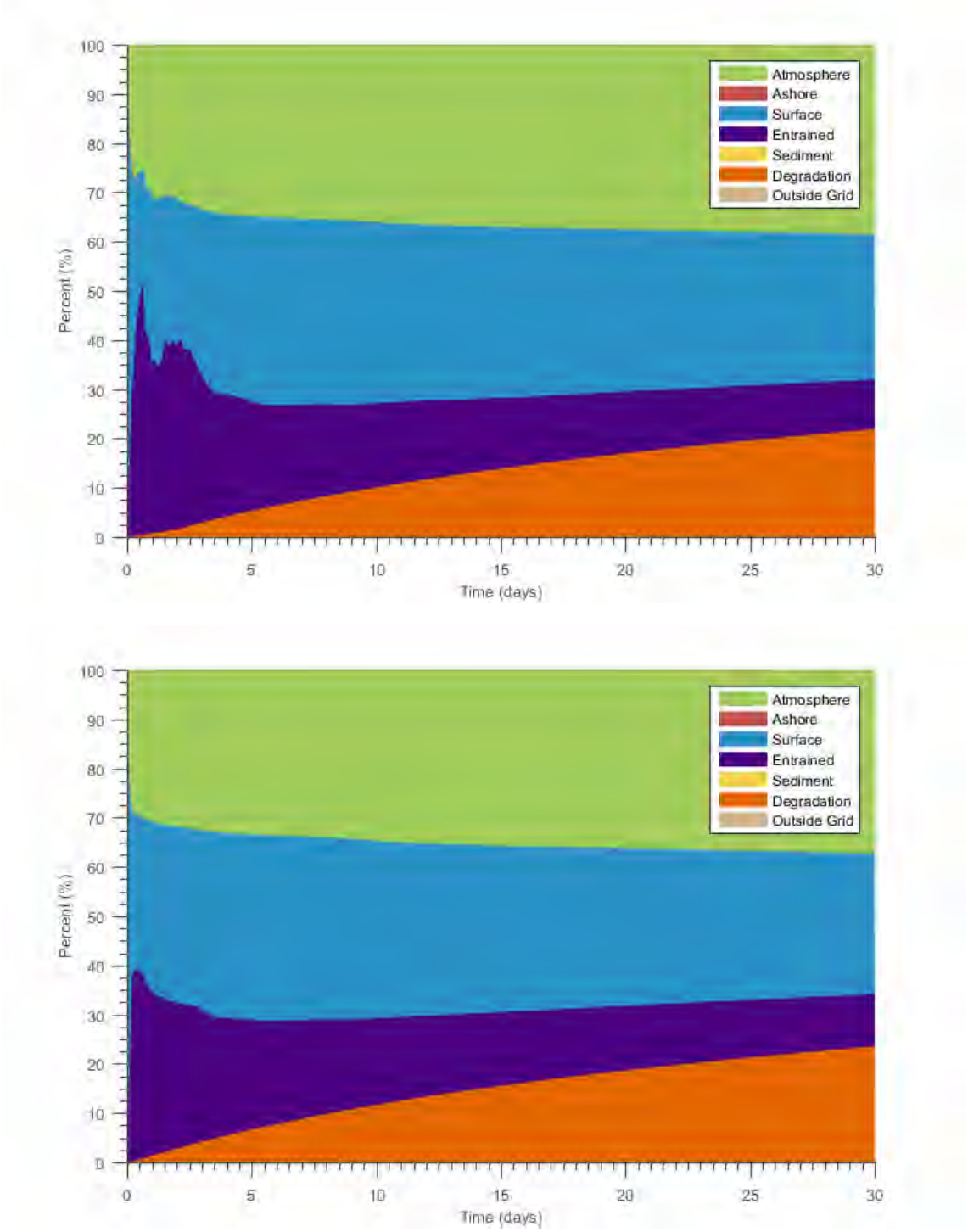

Figure 4-69. Mass balance plots of the BdN surface batch spills of 8,300 m^3 and 1,000 m^3 at the proposed FPSO site.

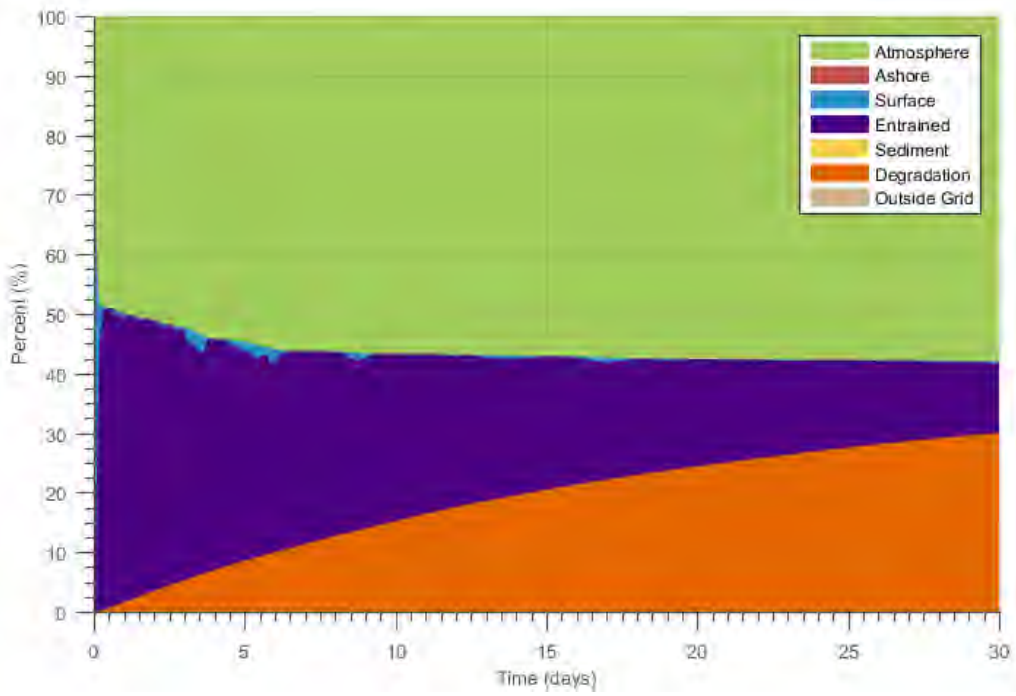

Figure 4-70. Mass balance plot of the Marine Diesel batch spill of 6 m^3 at the proposed FPSO site.

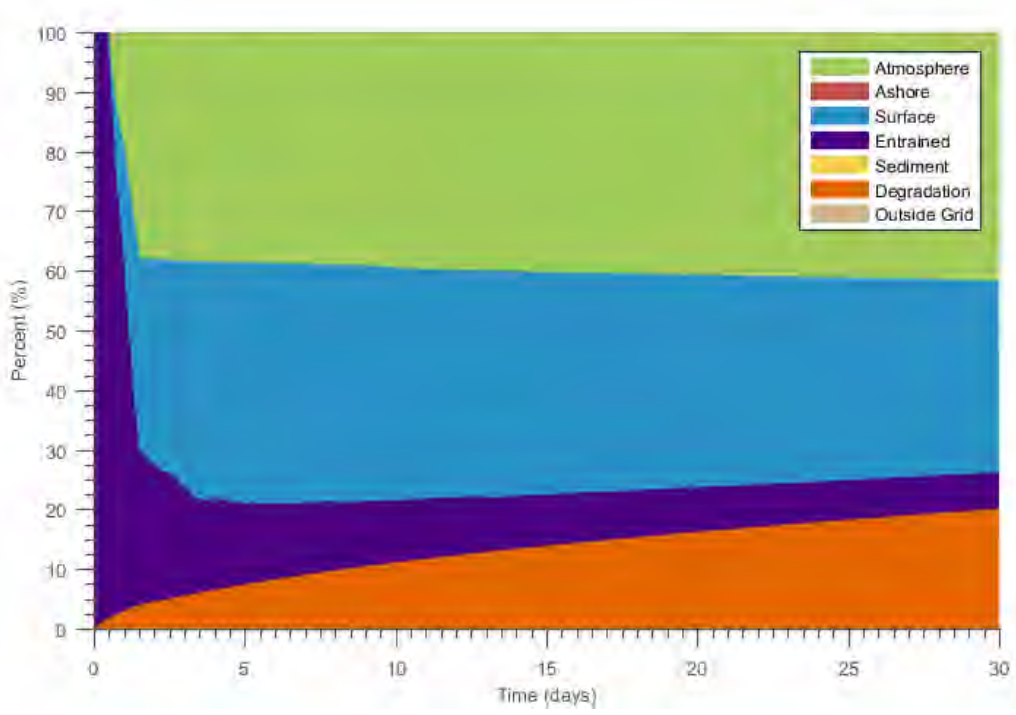

Figure 4-71. Mass balance plots of the BdN subsurface batch spill of 500 m^3 at Site 1.

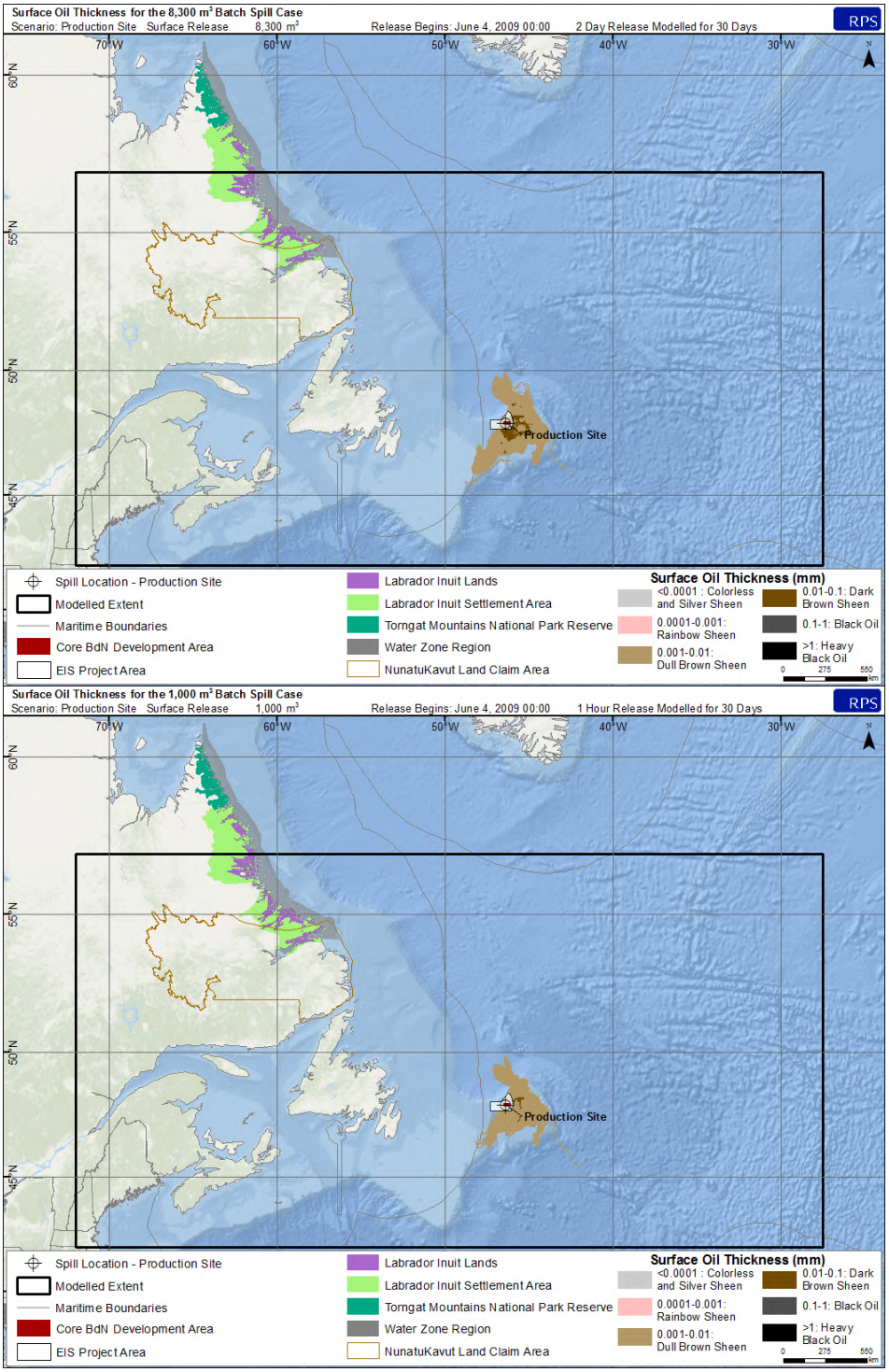

Figure 4-72. Surface oil thickness for the proposed FPSO site BdN surface batch spills of 8,300 m^3 (top) and 1,000 m^3 (bottom). The minimum thickness of surface oil > 0.04 µm is displayed (cumulative over all modelled time steps).

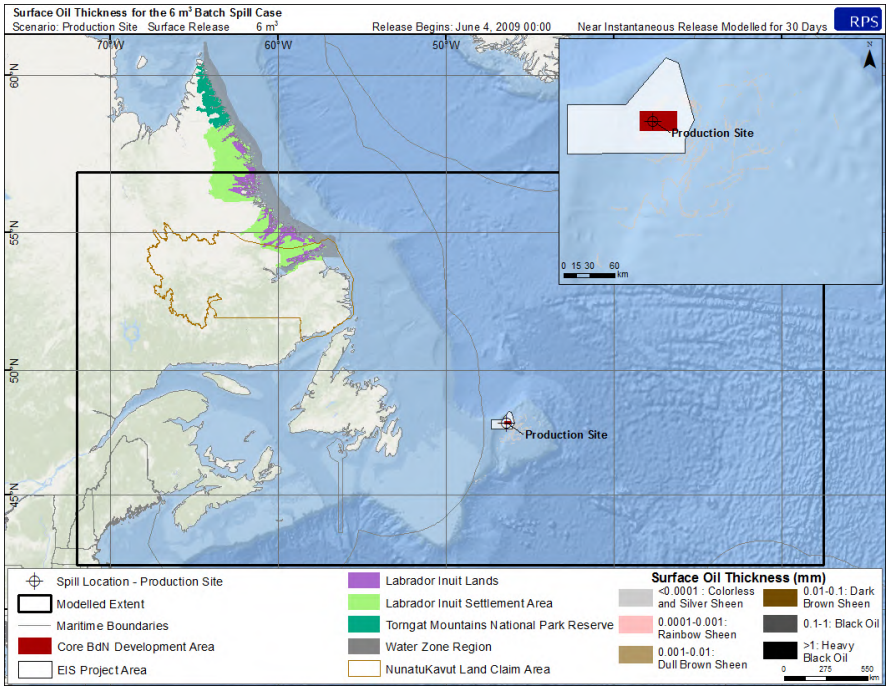

Figure 4-73. Surface oil thickness for the proposed FPSO site Marine Diesel surface batch spill of 6 m^3. The minimum thickness of surface oil > 0.04 µm is displayed (cumulative over all modelled time steps).

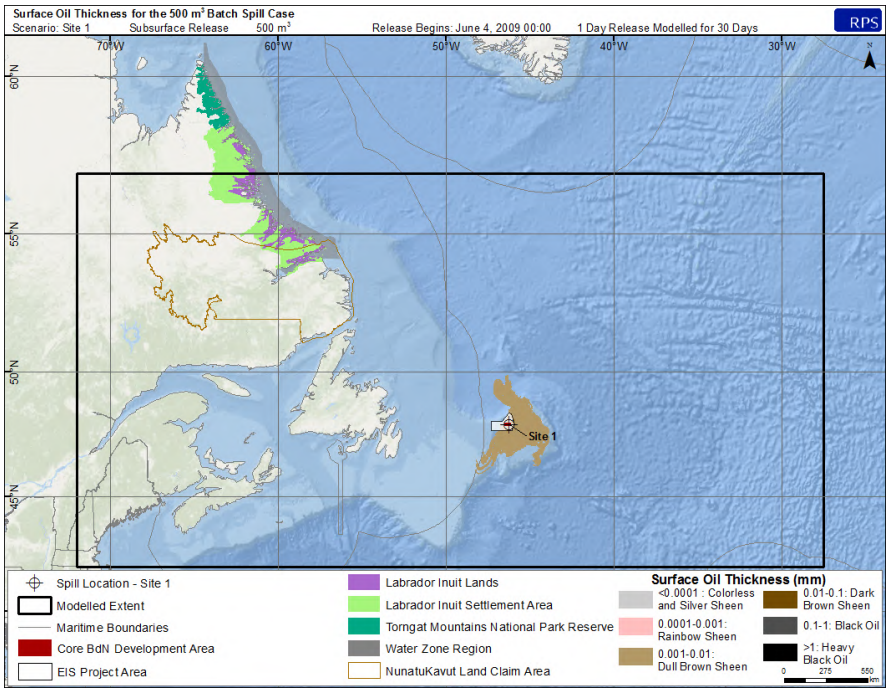

Figure 4-74. Surface oil thickness for Site 1 BdN seabed batch spill of 500 m^3. The minimum thickness of surface oil > 0.04 µm is displayed (cumulative over all modelled time steps).

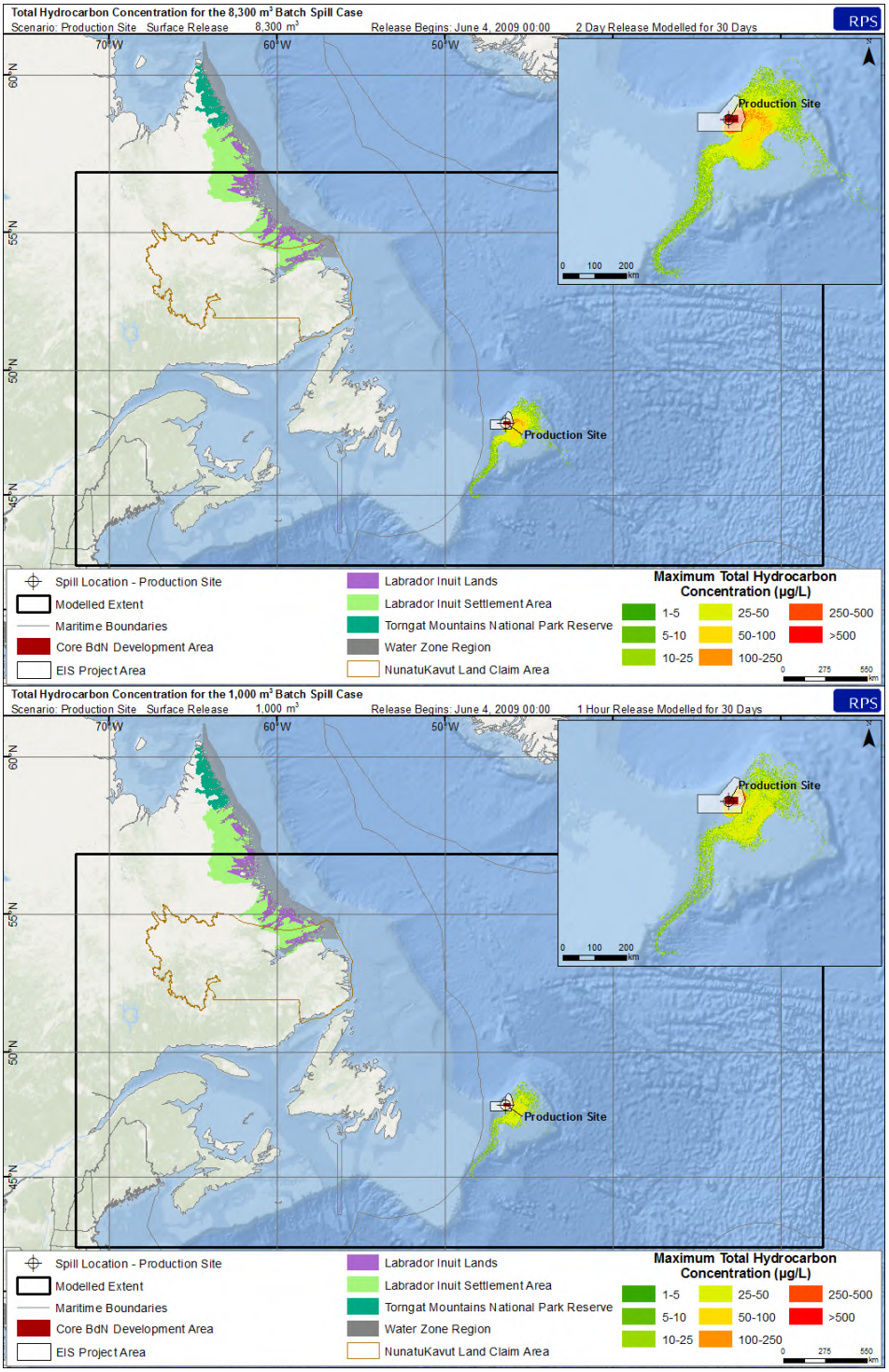

Figure 4-75. Maximum total hydrocarbon concentration (THC) at any depth in the water column for the proposed FPSO site BdN surface batch spills of 8,300 m³ (top) and 1,000 m³ (bottom). The minimum threshold of THC > 1 µg/L is displayed (cumulative over all modelled time steps).

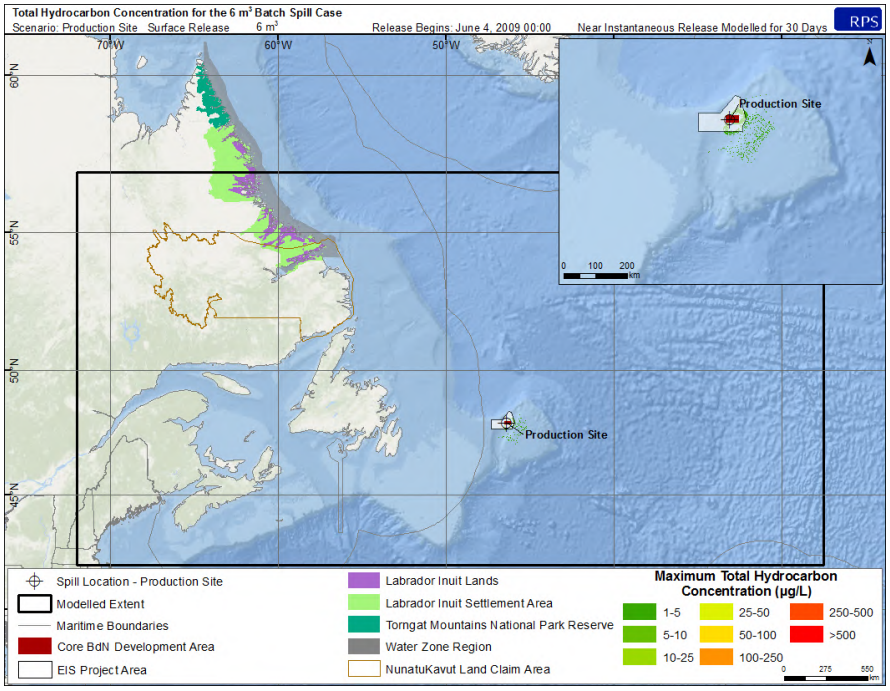

Figure 4-76. Maximum total hydrocarbon concentration (THC) at any depth in the water column for the proposed FPSO site marine diesel surface batch spill of 6 m³. The minimum threshold of THC > 1 µg/L is displayed (cumulative over all modelled time steps).

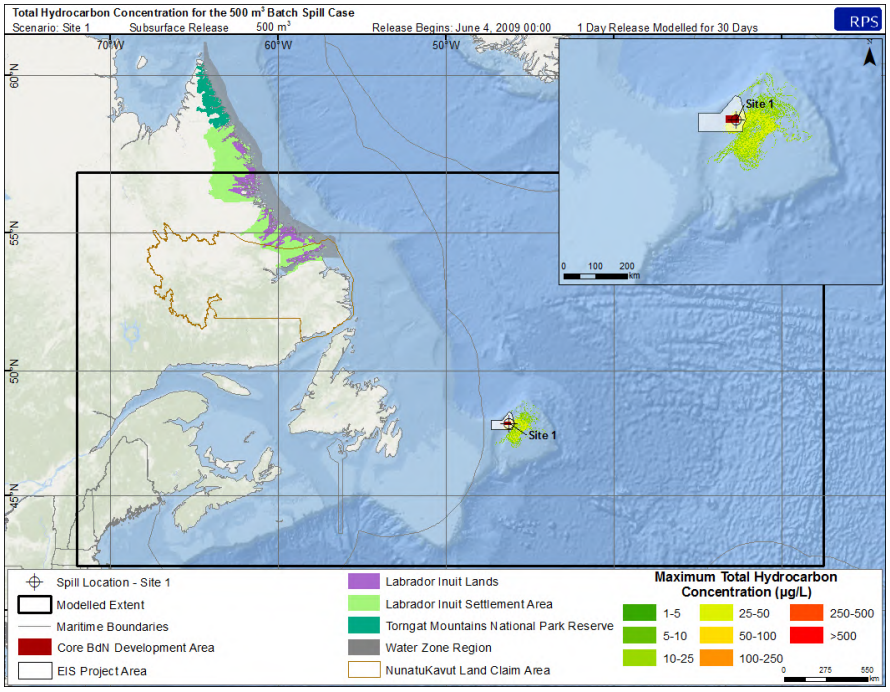

Figure 4-77. Maximum total hydrocarbon concentration (THC) at any depth in the water column for Site 1 BdN seabed batch spill of 500 m³. The minimum threshold of THC > 1 µg/L is displayed (cumulative over all modelled time steps).

4.2.5 Summary of Deterministic Results

4.2.5.1 Representative Cases: Surface, Water Column, and Shoreline Oil

For most representative deterministic scenarios for subsurface releases, the amount of oil remaining on the surface or on sediments at the end of the simulation was less than five percent (Table 4-4). This is due to the highly volatile nature and larger fraction of lower molecular weight compounds of the BdN leading to large percentages evaporated (45-51%) and degraded (27-36%). Entrainment into the water column was predicted to range between <1% and 3% at the end of the 160-day model run. Shoreline contact was relatively minimal (with respect to total release volume) for these simulations, where even the 95th percentile shoreline contact case was predicted to have less than 0.1% of the released oil reaching shorelines (the 95th percentile water column case, which was the 100th percentile shoreline case had 1.78%). In all simulations, portions of the oil traveled outside the model grid after 160 days, with a maximum of 23% leaving the model domain (Table 4-4).

The 95th percentile representative surface oil exposure, water column exposure, and shoreline contact cases were identified for both Site 1 and Site 2 sites. Most of the surface oil in all cases were predicted to have an average thickness within the range of 0.001 – 0. 1 mm (1 – 100 µm), which would result in a visual appearance that would be discontinuous, patchy dull brown sheens to dark brown sheens. Thickest oil was predicted to be located within 10 km of the release site (0.1 - 1 mm; black oil), with thinner 0.0001 - 0.001 mm (rainbow sheen) oil making up the outer fringes of the release. Note that floating oil mass is calculated as an average over grid cells, thus in reality, the oil would be patchy and could be thinner or thicker within particular areas of each grid cell. The area of surface oil exposure for the 36-day and 115-day 95th percentile cases at Site 1 (2,589,000 km^2 and 2,970,000 km^2; Table 4-3) is larger than that of the 95th percentile cases at Site 2 (2,316,000 km^2 and 2,891,000 km^2; Table 4-3). This is likely due to a combination of the release location, depth of release, and the variable date range modelled between individual simulations.

In all cases, nearly all of the surface oil was predicted to either become entrained, evaporated, degraded, or be transported outside of the grid by the end of the 160-day simulation (Figure 4-39, Figure 4-44, Figure 4-49, Figure 4-54, Figure 4-59, Figure 4-64, and Table 4-4). The 95th percentile case represents what could be expected from a “credible worst case” unmitigated blowout, where the environmental conditions would be such to maximize potential exposure. Note that all scenarios assume a completely unmitigated release, which is an unlikely situation, as emergency response measures would be employed in the event of a spill. For surface oil, each 95th percentile case at both Site 1 and Site 2 occurred during the winter season (defined as ice for more than half the days of the model run;

Table 2-5). The higher winds during this time period likely transported the oil further in these winter runs, resulting in a larger surface oil footprint and therefore selection as the 95th percentile case.

The maximum subsurface water volumes exposed to THC concentrations for the 95th percentile water column cases were predicted to range between 73,500 km^3 and 120,000 km^3 (Table 4-3). A region of >500 µg/L dissolved hydrocarbons was predicted to spread primarily east of the release site in the 95th percentile cases at Site 1 and primarily south at the Site 2 site. Entrained oil concentrations in surface waters were predicted to vary considerably from day to day, as would be expected due to their dependence on variable wind and wave conditions which would entrain surface oil into the water column as whole oil droplets that would eventually resurface under quiescent conditions. The amount of entrained oil stopped increasing after the blowout was modelled to cease at the representative 36 or 115 days. For the water column simulations at Site 1, the identified 95th percentile worst-case 36-day release occurred during winter, while the 115-day release occurred in the summer. However, at Site 2, the identified 95th percentile worst-case 36-day release occurred during summer and the 115-day release occurred in the winter (Table 2-5).

Because the Site 2 site was closer to shore and at a shallower depth, the site was more likely to results in oil contacting the shoreline. In each of the 95th percentile shoreline exposure cases, the combination of wind and current conditions resulted in a portion (<0.1%) of the oil making contact with the shoreline. Although this is a small fraction of the total volume of oil released, the THC on shorelines was predicted to exceed 500 g/m^2. The 95th percentile cases for shoreline contact at Site 1 occurred during the winter. At Site 2, the 36-day release occurred during summer, while the 115-day release occurred during winter (Table 2-5).

4.2.5.2 Batch Spills

To simulate accidental smaller scale discharges, near-instantaneous (ranging from 2-minute to 2-day release durations) batch spills of BdN and marine diesel were modelled. One 500 m^3 release simulating an accidental discharge of BdN crude from a production flowline was modelled at Site 1 and three additional batch spills ranging in volume from 6 m^3 to 8,300 m^3 were modelled at the proposed FPSO location (Table 2-5). All batch spills were modelled for thirty days. The marine diesel used in the bunkering batch spill is a standard diesel that had a low viscosity and a high aromatic content that was expected to evaporate quickly during the summertime releases, while the other batch spills were modelled using BdN crude oil.

At the proposed FPSO site, the larger 8,300 m^3 and 1,000 m^3 surface batch spills of BdN crude were both predicted to result in a cumulative area of surface oil >0.04 µm that extended roughly 200 - 300 km to the east from the release location covering a region of approximately 59,670 km^2 and 34,140 km^2,

respectively (Figure 4-72 and Table 4-3). Furthermore, both of these batch spills resulted in dull brown sheens (0.001 to 0.01 mm) in a region that was predicted to extend roughly 375 km to the southeast from the release site, with regions of thicker dark brown sheens (0.01 – 0.1 mm) of oil found within 100 km or less of the release location (Figure 4-72). The smaller 6 m^3 surface batch spill of marine diesel was predicted to result in a patchy distribution of colorless or silver sheen of oil < 0.0001 mm (0.1 µm), where the area of oil >0.04 µm was 84 km^2 (Figure 4-73 and Table 4-3). Finally, the seabed release of 500 m^3 of BdN from Site 1 was predicted to result in a primarily dull brown sheen (0.001 to 0.01 mm) that extended approximately 300 km to the southwest from the release location, where the region exceeding >0.04 µm was 32,670 km^2 (Figure 4-74 and Table 4-3). Overall, the distances covered by these surface oil trajectories were the result of strong surface winds in the area. Oil was not predicted to reach any shorelines from the modelled batch spills.

Predicted maximum in-water THC concentrations varied between model simulations, with the 8,300 m^3 release resulting in the largest overall volume (1,564 km^3) exceeding 1 µg/L (Table 4-3). The areas where concentrations were predicted to exceed 500 µg/L were in the immediate vicinity of the release site for both the 8,300 and 1,000 m^3 surface batch spills of BdN (Figure 4-75). The marine diesel batch spill of 6 m^3 resulted in the smallest volume of water (98 km^3) exposed to THC concentrations exceeding 1 µg/L, where concentrations were generally less than 5 µg/L in an area within 200 km of the release site (Figure 4-76 and Table 4-3). The seabed batch spill of BdN at Site 1 was predicted to result in concentrations up to 100 µg/L within 250 km from the release site (Figure 4-77). Note that for the batch spill cases, the water column concentration was measured as THC, not as dissolved hydrocarbons as in the other deterministic and stochastic scenarios. The reasons behind this were twofold including: 1) the concentration gridding resolution and the 2) small release volumes. Therefore, the areas of predicted concentrations of dissolved hydrocarbons in the water column (which comprise <1% of THC) above the identified threshold were generally too small to present in figures.

Table 4-3. Representative deterministic cases and associated areas, lengths, and volumes exceeding specified thresholds for 95th percentile surface, water column, and shoreline contact trajectories at Site 1 and Site 2 sites and batch spills.

Scenario Name	Site	Released Volume	Approximate Surface Area exceeding thickness thresholds (km²)		Approximate Shore Length exceeding mass per unit area thresholds (km)		Approximate Subsurface Volume exceeding THC threshold (km³)
			Socio-economic (0.04 µm)	Ecologic (10 µm)	Socio-economic (1 g/m²)	Ecologic (100 g/m²)	Socio-economic* (1 µg/L)
Subsurface Blowout Releases							
95th percentile surface oil exposure case- 36 d	Site 1	378,000 m³ (10,500 m³/d)	2,589,000	451,000	-	-	59,850
95th percentile water column case- 36 d†			2,404,000	595,700	3,234	3,123	90,350
95th percentile shoreline contact case- 36 d			2,132,000	498,000	141	138	58,500
95th percentile surface oil exposure case- 115 d		1,207,500 m³ (10,500 m³/d)	2,970,000	1,094,000	316	313	76,850
95th percentile water column case- 115 d			1,797,000	660,900	-	-	86,850
95th percentile shoreline contact case- 115 d			2,012,000	928,700	344	325	82,600
95th percentile surface oil exposure case- 36 d	Site 2	378,000 m³ (10,500 m³/d)	2,316,000	517,000	15	15	73,850
95th percentile water column case- 36 d			2,058,000	495,200	3	3	73,500
95th percentile shoreline contact case- 36 d			2,150,000	545,300	77	71	74,750
95th percentile surface oil exposure case- 115 d		1,207,500 m³ (10,500 m³/d)	2,891,000	988,100	64	61	83,300
95th percentile water column case- 115 d†			3,105,000	1,200,000	3,636	3,501	120,000
95th percentile shoreline contact case- 115 d			2,131,000	984,400	850	792	88,800
Surface/Subsurface Batch Spills							
Surface BdN Batch Spill of 8,300 m³	Prod. Site	8,300 m³	59,670	2,698	-	-	1,564
Surface BdN Batch Spill of 1,000 m³		1,000 m³	34,140	452	-	-	1,023
Surface Marine Diesel Batch Spill of 6 m³		6 m³	84	<1	-	-	98
Seafloor BdN Batch Spill of 500 m³	Site 1	500 m³	32,670	12	-	-	546

*There is only 1 category threshold (socio-economic) for THC –calculated by multiplying the area times the depth of the grid cell.

† Note that the predicted shoreline oil from these 95th percentile water column scenarios actually corresponded with the maximum (100th percentile or modelled "worst case") shoreline oil scenarios. Therefore, the 95th percentile shoreline exposure cases will have smaller volumes of oil predicted to reach shorter lengths of shorelines.

Table 4-4. Summary of the mass balance information for all representative scenarios. All values represent a percentage of the total amount of released oil at the end of the 160-day (95th percentile) or 30-day (batch spill) scenarios.

Summary of Mass Balance Information at the End of the Simulation (Percentage of Released Oil)								
Scenario Name	**Site**	**Surface (%)**	**Evaporated (%)**	**Water Column (%)**	**Sediment (%)**	**Ashore (%)**	**Degraded (%)**	**Outside Grid (%)**
Subsurface Blowout Releases								
95th percentile surface oil exposure case- 36 d	Site 1	2.60	47.75	0.66	<0.01	0.00	34.43	14.56
95th percentile water column case- 36 d		0.55	46.75	1.24	0.01	1.78	36.38	13.29
95th percentile shoreline contact case- 36 d		0.76	47.30	0.74	0.01	0.03	33.47	17.68
95th percentile surface oil exposure case- 115 d		13.31	45.95	1.81	0.01	0.07	33.26	5.60
95th percentile water column case- 115 d		2.22	50.84	2.79	0.01	0.00	28.93	15.22
95th percentile shoreline contact case- 115 d		1.75	45.49	2.33	0.01	0.04	27.47	22.92
95th percentile surface oil exposure case- 36 d	Site 2	5.37	48.26	0.82	0.01	0.00	34.84	10.70
95th percentile water column case- 36 d		0.27	49.65	1.31	0.01	<0.01	34.15	14.61
95th percentile shoreline contact case- 36 d		0.71	49.57	0.82	0.01	0.03	34.84	14.03
95th percentile surface oil exposure case- 115 d		10.94	45.61	1.58	0.01	0.01	31.63	10.22
95th percentile water column case- 115 d		8.40	46.57	2.75	0.01	0.96	32.50	8.80
95th percentile shoreline contact case- 115 d		2.07	45.57	2.28	0.01	0.10	27.80	22.17
Surface/Subsurface Batch Spills								
Surface BdN Batch Spill of 8,300 m^3	Prod. Site	29.39	38.62	10.10	0.01	0.00	21.88	0.00
Surface BdN Batch Spill of 1,000 m^3		28.51	37.33	10.60	0.01	0.00	23.56	0.00
Surface Marine Diesel Batch Spill of 6 m^3		0.35	57.95	11.65	0.00	0.00	30.04	0.00
Seafloor BdN Batch Spill of 500 m^3	Site 1	32.12	41.66	6.13	0.01	0.00	20.08	0.00

4.3 Mitigation Model Results

To analyze the potential effectiveness of response options on a release of crude oil, results from the unmitigated 95th percentile surface oil cases for the 36-day releases at Site 1 and Site 2 (Section 4.2.1) were compared to an identical release scenario that included various realistic response options. This release scenario was selected as it represented an uncontrolled subsurface blowout for the first 36 days with dispersant use (subsurface, aerial, and vessel applications) in the early phases of the release (i.e. within days). A dispersant-only mitigated scenario for 115 days (i.e. assume no cap-and-contain possible nearly four months) was not modelled, as Equinor has noted that this containment method is likely and anticipated within 36-days.

For both release sites, oil in the unmitigated release scenarios was predicted to rise rapidly to the surface where it spread due to surface winds and currents. In the mitigation scenarios, SSDI began on Day 5, and as such, entrained oil was predicted to increase substantially. SSDI was predicted to reduce the droplet size distribution of the released oil, which slowed the rise rate of a portion of the oil and allowed for another portion to remain entrained within the water column. The end result of the SSDI was a larger fraction of the released oil remaining within the water column, where it naturally dispersed more completely, with a higher potential for degradation within the water column. For the fraction of oil that did surface, additional treatment from aerial dispersant and vessel dispersant to the water surface aided in the entrainment of surface oil into the water column. This entrainment was made easier by the effectiveness of the dispersant to reduce the viscosity of the oil. A reduction in viscosity requires less energy for surface breaking waves to entrain and disperse surface floating oil as small droplets within the water column where dispersion and degradation may therefore be enhanced.

As would be expected, the thickness of surface oil and the size of the footprint were greatly reduced in the mitigation scenarios (Figure 4-80 and Figure 4-81). Concentrations of dissolved and total hydrocarbons were elevated within approximately 10 km of the release location for the mitigation scenarios, due to the enhanced dispersion and resulting dissolution, when compared to the unmitigated cases (Figure 4-82 through Figure 4-85). However, with the reduction in surface floating oil and less extensive transport, the concentration and size of the cumulative footprint were smaller for the dispersant mitigated cases, when compared to the unmitigated case. Even with the enhanced amount of hydrocarbons in the water column, there was a reduction in the predicted spatial extent for sediment oiling with a trend towards more localized and continuous sediment oiling. The THC concentrations within sediments in the dispersant mitigated scenarios was predicted to be <0.01 g/^{2}, as it was for the unmitigated scenarios (Figure 4-86 and Figure 4-87).

At the end of the simulations at Site 1, the predicted percent of the oil remaining on the water surface was slightly less (3 vs. 2%) with nearly half as much of the released oil evaporated to the atmosphere (48 vs. 25%). While the percent of oil that was predicted to remain entrained in the water column at the end of the 160-day simulation was nearly identical (<1%), the predicted percentage of oil degraded was much higher (34 vs. 57%) (Figure 4-78 and Table 4-5). The same trends were predicted for the releases at Site 2, where the floating surface oil at the end of the simulation was slightly less (5 vs. 4%), the percent evaporated was significantly less (48 vs. 28%), entrained oil was nearly the same (<1%), and the percent of oil degraded was much higher (35 vs. 53%) (Figure 4-79 and Table 4-5). As noted in Section 3.8.1, effective dispersant use is expected to increase the overall amount of oil biodegraded within the water column, which is what was predicted within these mitigation cases.

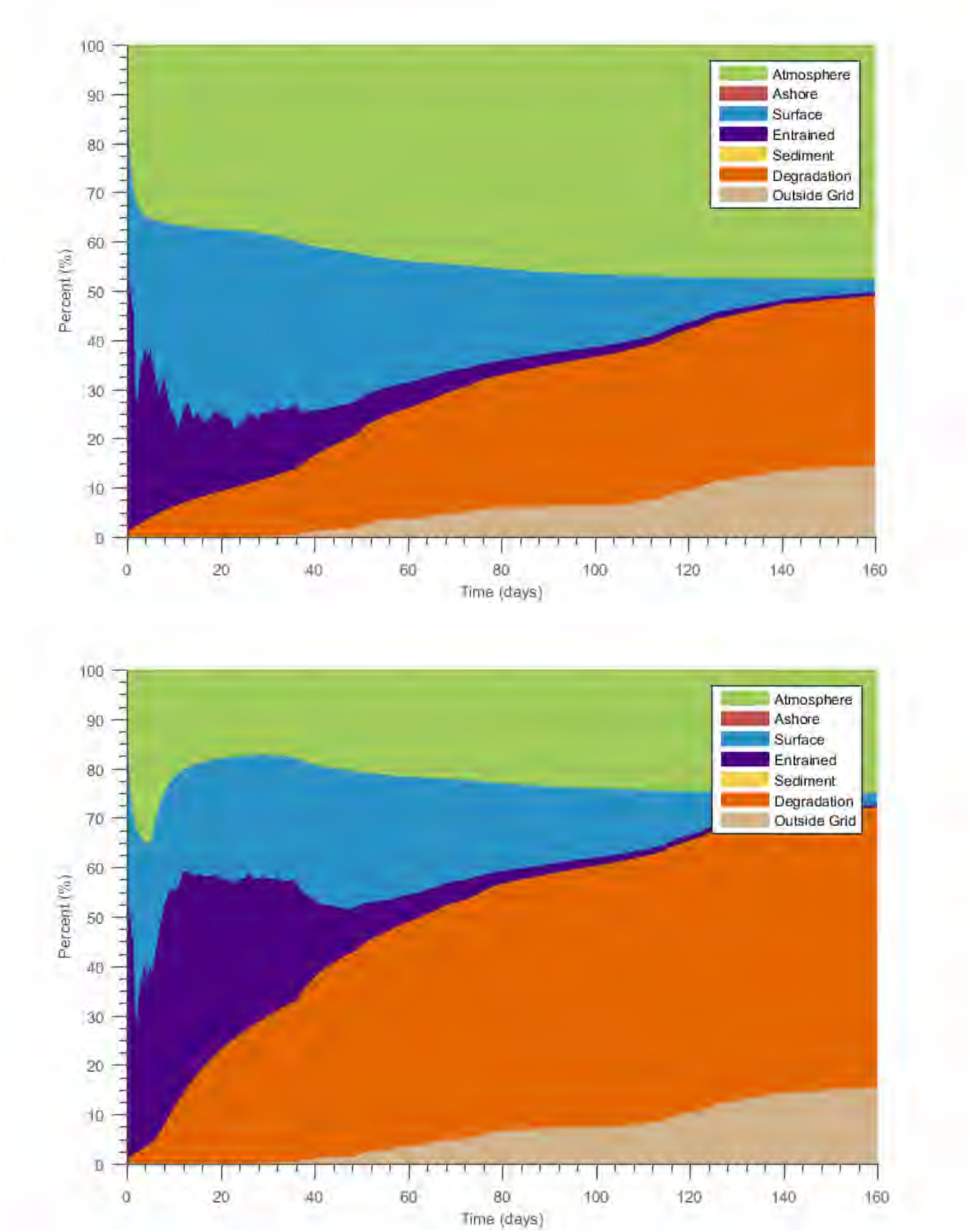

Figure 4-78. Mass balance predictions of the 95th percentile average surface oil thickness case for the unmitigated 36-day blowout at Site 1 (top) and the same mitigated scenario with response options (bottom).

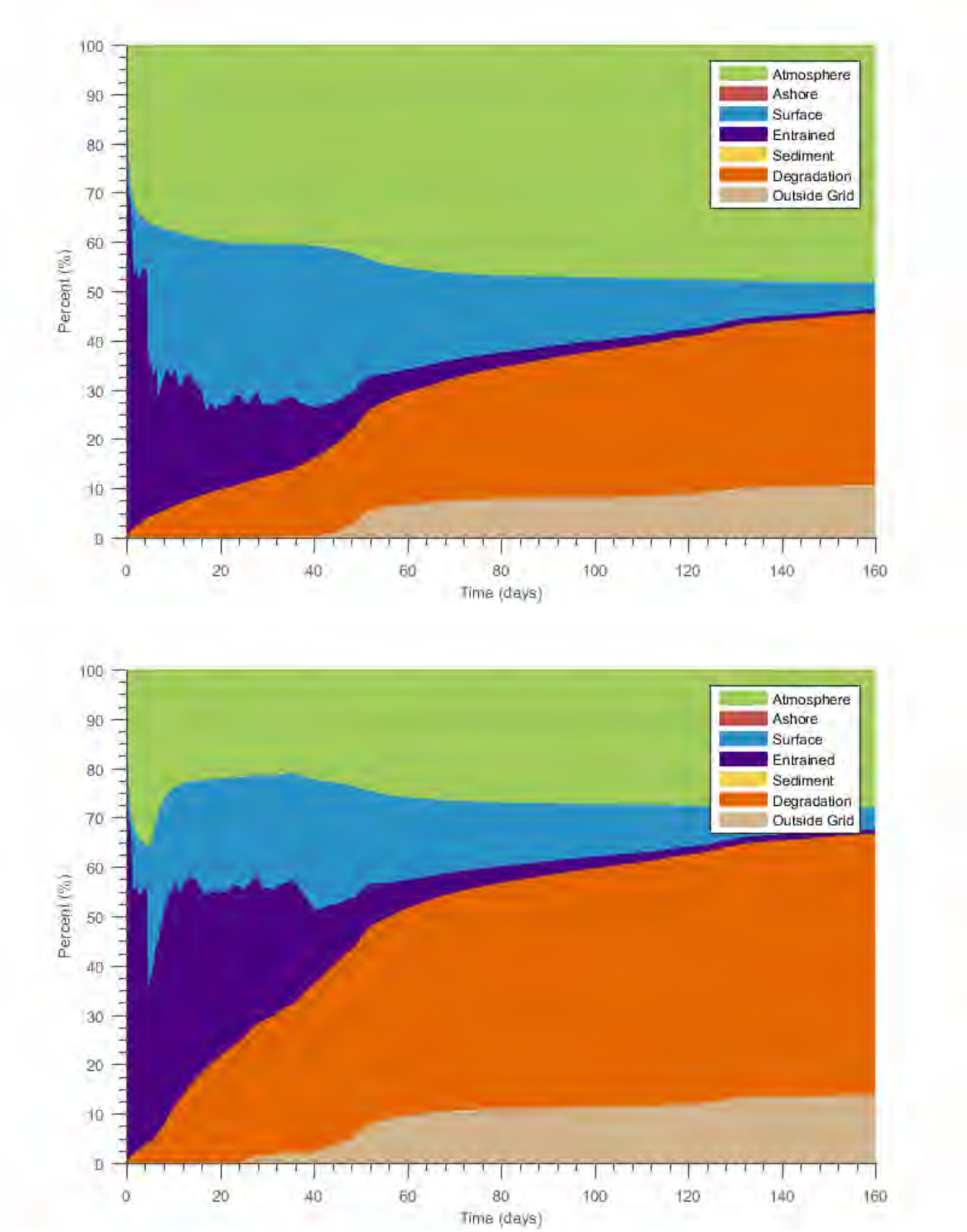

Figure 4-79. Mass balance predictions of the 95th percentile average surface oil thickness case for the unmitigated 36-day blowout at Site 2 (top) and the same mitigated scenario with response options (bottom).

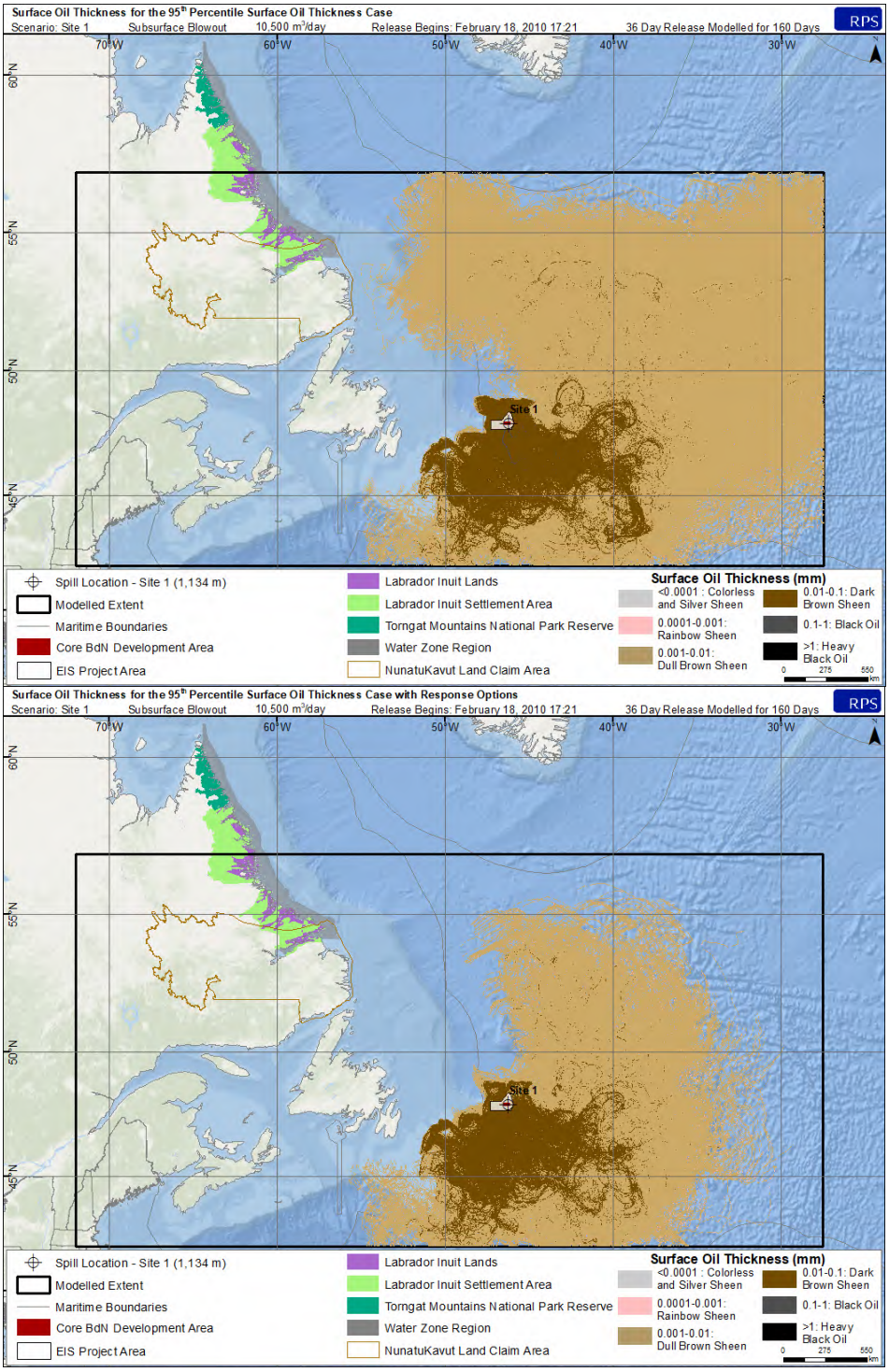

Figure 4-80. Cumulative maximum surface oil thickness for the 95th percentile average surface oil thickness case for the unmitigated 36-day blowout at Site 1 (top) and the same mitigated scenario with response options (bottom).

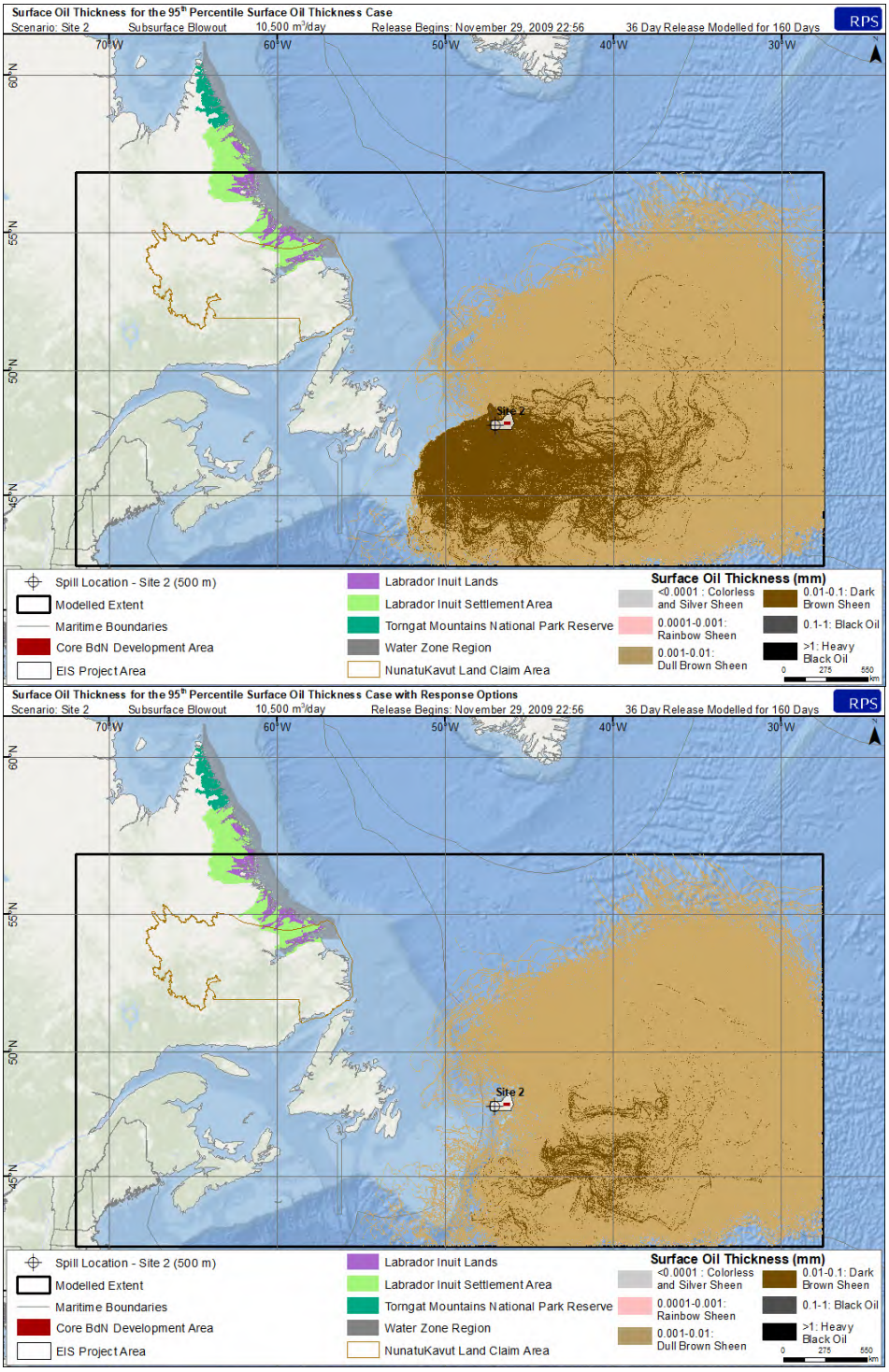

Figure 4-81. Cumulative maximum surface oil thickness for the 95th percentile average surface oil thickness case for the unmitigated 36-day blowout at Site 2 (top) and the same mitigated scenario with response options (bottom).

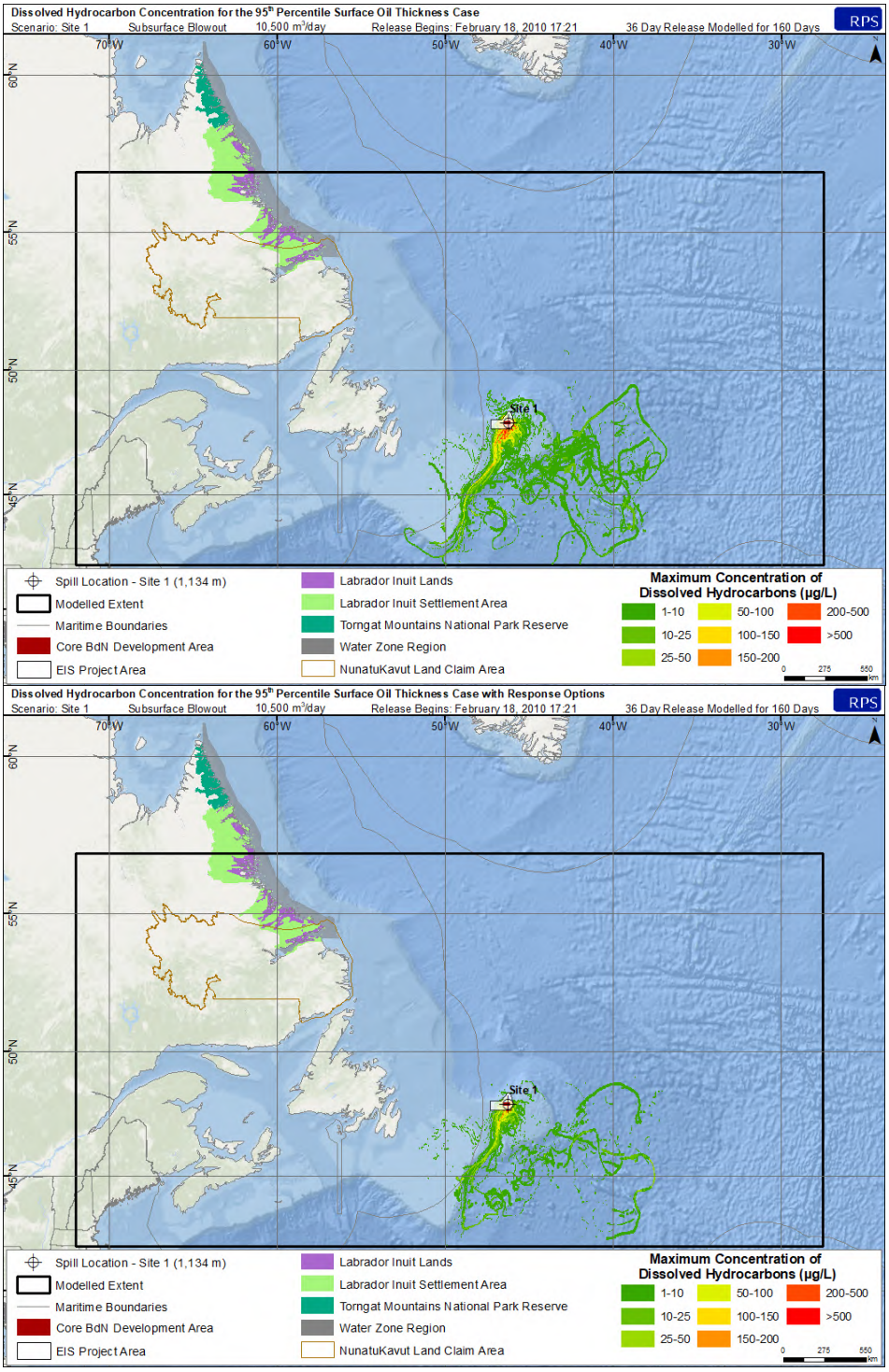

Figure 4-82. Maximum dissolved hydrocarbon concentration at any depth in the water column for the 95th percentile average surface oil thickness case for the unmitigated 36-day blowout at Site 1 (top) and the same mitigated scenario with response options (bottom).

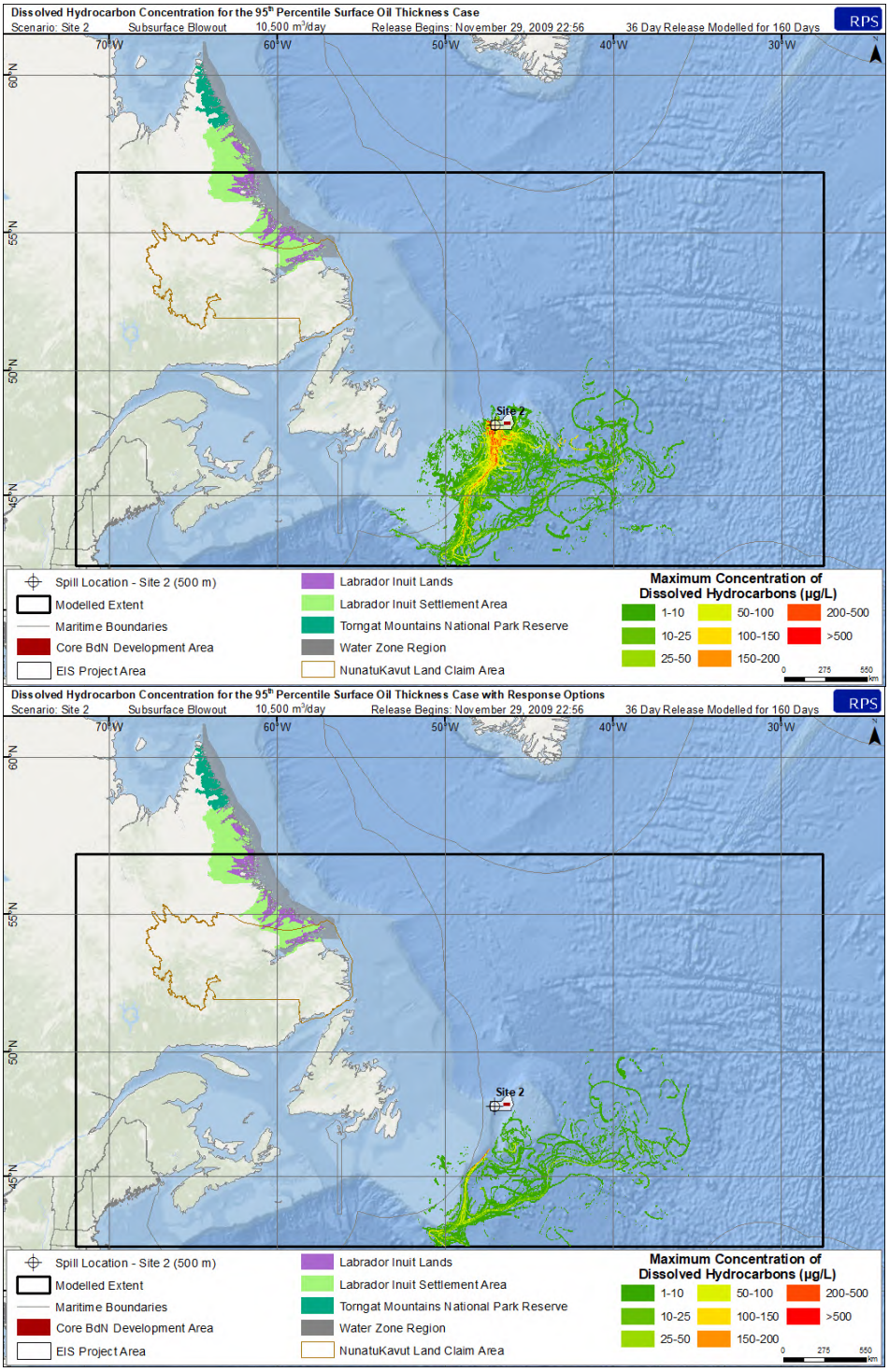

Figure 4-83. Maximum dissolved hydrocarbon concentration at any depth in the water column for the 95th percentile average surface oil thickness case for the unmitigated 36-day blowout at Site 2 (top) and the same mitigated scenario with response options (bottom).

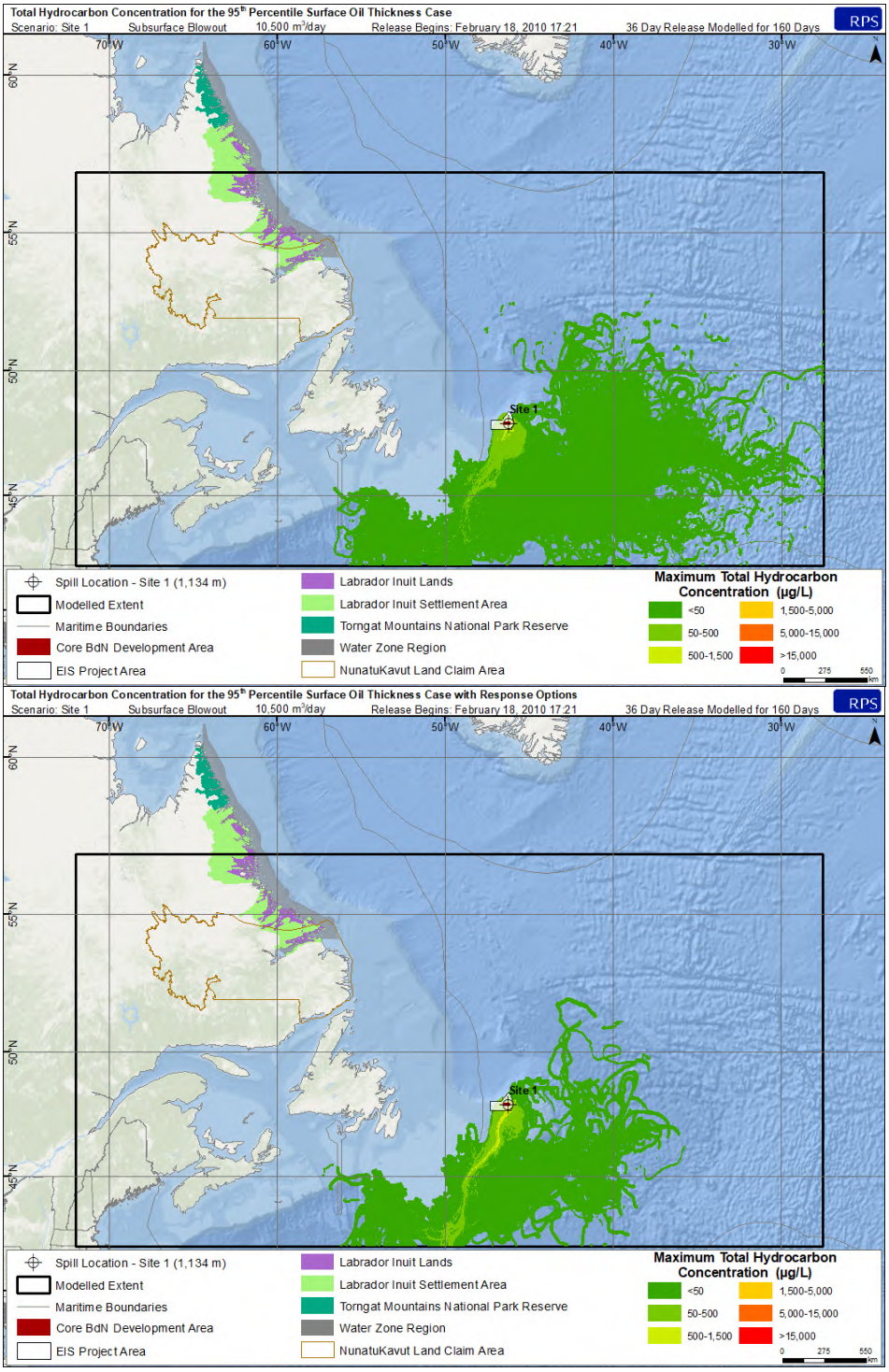

Figure 4-84. Maximum total hydrocarbon concentration (THC) at any depth in the water column for the 95th percentile average surface oil thickness case for the unmitigated 36-day blowout at Site 1 (top) and the same mitigated scenario with response options (bottom).

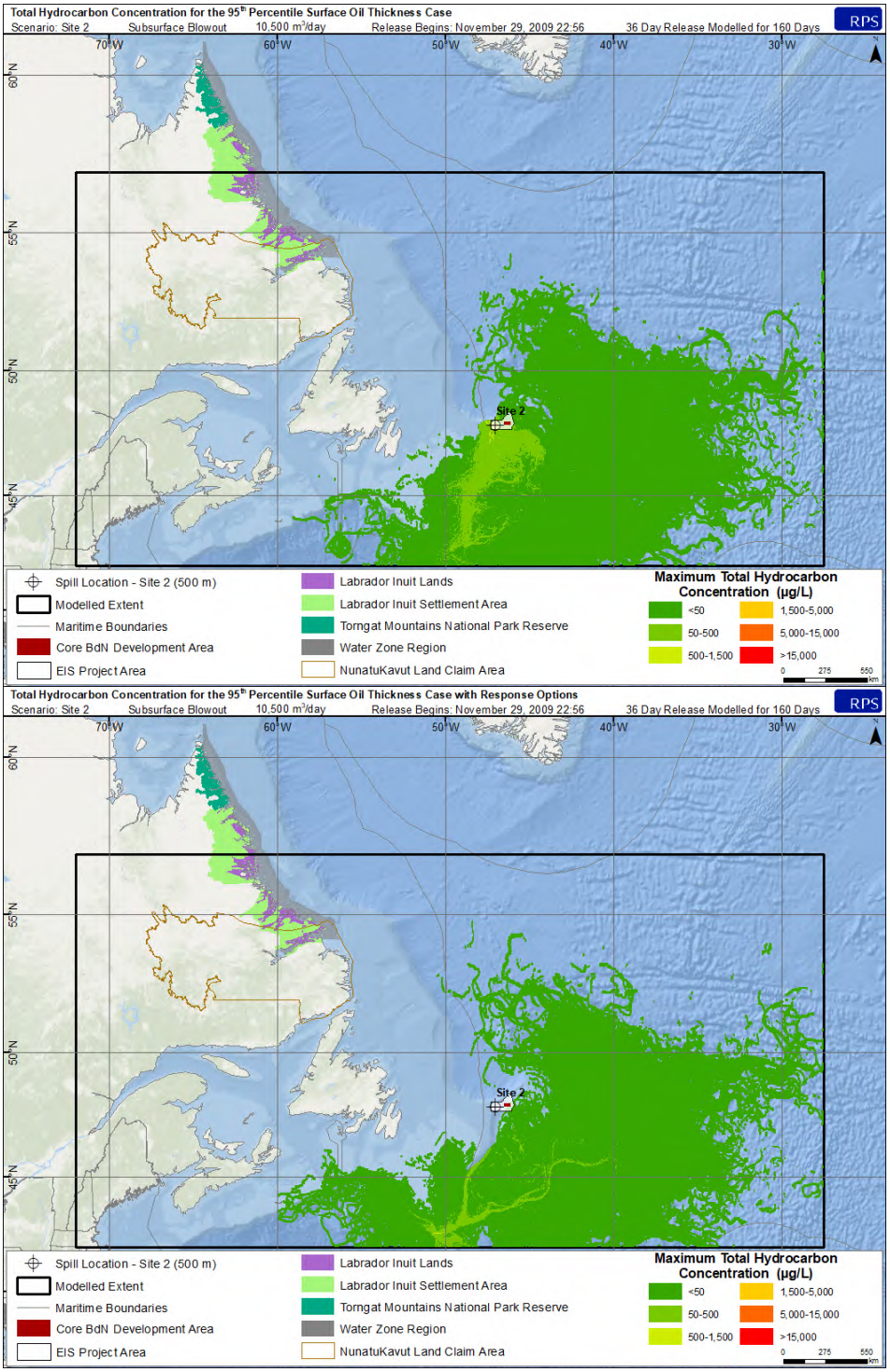

Figure 4-85. Maximum total hydrocarbon concentration (THC) at any depth in the water column for the 95th percentile average surface oil thickness case for the unmitigated 36-day blowout at Site 2 (top) and the same mitigated scenario with response options (bottom).

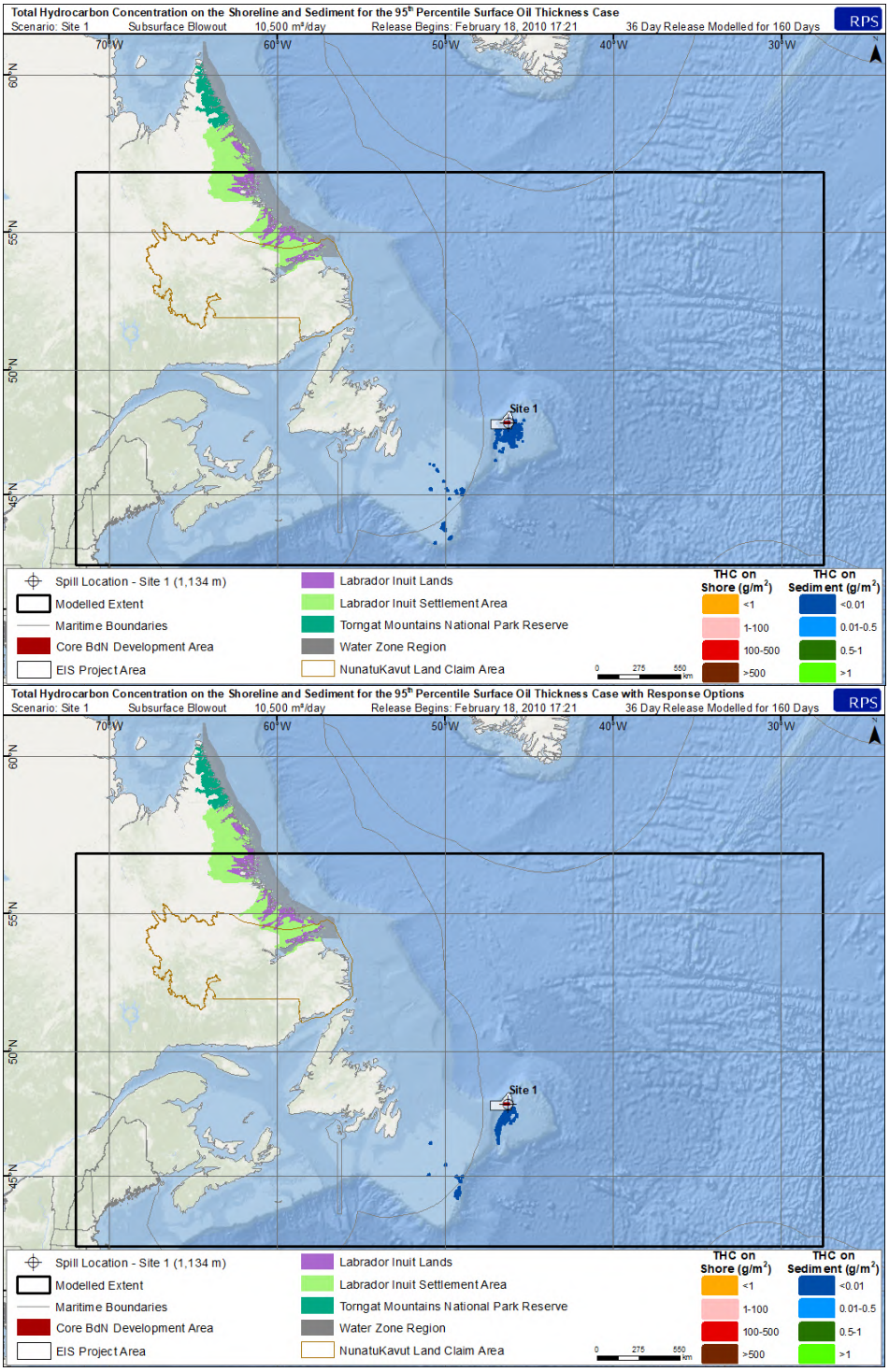

Figure 4-86. Total hydrocarbon concentration (THC) on the shore and sediment for the 95th percentile average surface oil thickness case for the unmitigated 36-day blowout at Site 1 (top) and the same mitigated scenario with response options (bottom).

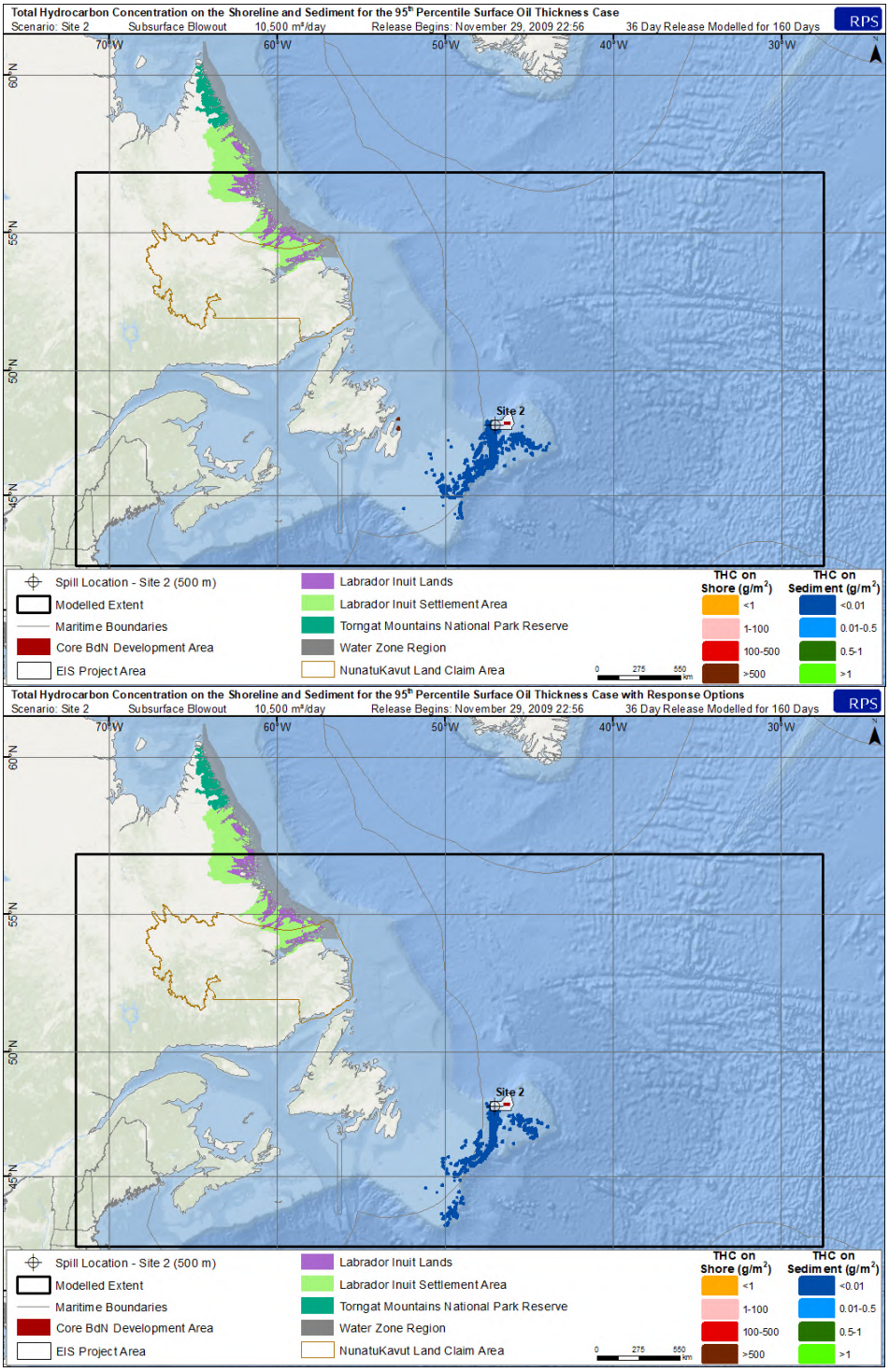

Figure 4-87. Total hydrocarbon concentration (THC) on the shore and sediment for the 95th percentile average surface oil thickness case for the unmitigated 36-day blowout at Site 2 (top) and the same mitigated scenario with response options (bottom).

4.3.1 Mitigation Response Summary & Conclusions

To analyze the potential effectiveness of response options on a release of crude oil, results of the unmitigated release modelling conducted for the 95th percentile surface oil cases for the 36-day release (Section 4.2.1) were compared to the identical scenario with dispersant response options added. A summary of the mass balance information for each unmitigated/mitigated pair for releases at both sites are presented in Table 4-5. Of note, evaporation was greatly reduced, and degradation enhanced in the mitigation scenarios. Several thresholds of concern were investigated to compare the exposure of water surface areas to surface oiling (Table 4-6). The predicted exposure of areas of threshold exceedances were compared between the unmitigated scenarios and the modelled response options to determine the predicted effects that response options would have on the ultimate trajectory and fate of released oil. Results are provided as the cumulative footprint of potentially-affected area that would exceed each threshold over the entire course of each 160-day model run.

Table 4-5. Summary of the mass balance information for all representative scenarios. All values represent a percentage of the total amount of released oil.

Summary of Mass Balance Information at the End of the Simulation (Percentage of Released Oil)									
Scenario Information			Surface (%)	Evaporated (%)	Water Column (%)	Sediment (%)	Ashore (%)	Degraded (%)	Outside Grid (%)
Site	Scenario	Product							
Site 1	Unmitigated	BdN	2.60	47.75	0.66	0.00	0.00	34.43	14.56
	Mitigated		2.32	25.03	0.52	0.01	0.00	56.75	15.32
Site 2	Unmitigated	BdN	5.37	48.26	0.82	0.01	0.00	34.84	10.70
	Mitigated		4.02	28.03	0.91	0.01	0.00	52.91	13.84

Table 4-6. Summary of the surface areas above indicated thresholds for the unmitigated and mitigated scenarios.

Scenario Information			Approximate Surface Area exceeding thickness thresholds (km²)	
Site	Scenario	Product	Socio-economic (0.04 µm)	Ecologic (10 µm)
Site 1	Unmitigated	BdN	2,589,000	451,000
	Mitigated		1,602,000	372,500
Site 2	Unmitigated	BdN	2,316,000	517,000
	Mitigated		2,131,000	127,200

For both the modelled releases at Site 1 and Site 2, response actions greatly reduced the surface area predicted by the identified thresholds for surface exposure (Table 4-6). As SSDI began on Day 5, the released oil was predicted to break into smaller droplets with slower rise velocity and higher potential for dissolution and degradation, with a fraction of oil (smallest droplets) predicted to become permanently entrained. Surface application of dispersants was predicted to break up oil slicks on the water surface and reduce the surface oil footprints, when compared to the unmitigated scenarios (Table 4-6). As expected, the unmitigated release scenarios were predicted to result in the largest footprints of surface oil and with the potential for thicker oil (Table 4-6).

Should response effectiveness or timing be improved, progressively smaller regions of surface oil exposure would be predicted to be affected. The addition of response options was predicted to both decrease the amount of oil on the surface and increase the amount of oil entrained in the water column, which led to higher quantities of oil predicted to degrade within the water column.

5 Discussion and Conclusions

Generally, most surface oil from the hypothetical release locations was predicted to move eastward due to the prevailing westerly winds. Winds and currents in the Project Area are similar throughout the year, with most notable differences in wind intensity. The increased winds during winter conditions have the potential to enhance surface breaking waves and result in more predicted entrainment of oil, which lowers the likelihood that oil will remain on the surface for extended periods of time. Stochastic results indicate that the probability for oil contacting shoreline reached a maximum 25% but was generally 5-12%. Shoreline contact was more likely to occur during winter months due to the wind speed and direction during this period of time. Based on the results of the stochastic analysis of hundreds of model scenarios and depending on the time of year and environmental conditions, areas susceptible to shoreline oiling included the southern shores of Labrador to the entire east coast of Newfoundland, the Avalon Peninsula, and in some instances Sable Island and the northeastern shores of Nova Scotia.

Mitigation (i.e., SSDI, aerial surface dispersant application, and vessel surface dispersant application) modelling performed on the 95th percentile surface oil exposure cases for the 36-day release predicted that the SSDI would likely be effective in breaking up the released oil into smaller droplets, slowing the rise velocity of oil in the water column, and permanently entraining some of the oil droplets, enhancing dispersion and allowing for additional biodegradation when compared to the unmitigated cases.

The releases modelled in this study may be considered representative of other potential releases in the Project Area. The depth of release of Site 1 and Site 2 sites (1,134 and 500 m, respectively) are within the range of water depths present within the Project Area (350 m to 1,200 m).

The hypothetical releases modelled in this study are not intended to predict a specific future event, but rather are intended to be used as a tool in environmental assessments and spill contingency planning. The results presented in this document demonstrate that there are a range of potential trajectories and fates that could result if a release of crude oil, a batch spill of crude oil, or a batch spill of marine diesel were to occur at any point throughout the year. The specific trajectories and fates vary greatly for each release based upon the environmental conditions occurring at the time of the release. While each oil release is unique, and uncertainties exist, the results of this modelling study suggest that, if oil were to be released in the Project Area, it has a high likelihood of moving away from shore to the east with less likelihood of shoreline oil exposure.

6 References

Albers, P.H. and R.C. Szaro, 1978. Effects of No. 2 Fuel Oil on Common Eider Eggs. Marine Pollution Bulletin 9: 138-139.

Albers, P.H., 1980. Transfer of Crude Oil from Contaminated Water to Bird Eggs. Environmental Research 22(2): 307-314.

Anderson, J.W., S.L. Kiesser, R.M. Bean, R.M., R.G. Riley, and B.L. Thomas, 1981. Toxicity of chemically dispersed oil to shrimp exposed to constant and decreasing concentrations in a flowing system, Proceedings 1981 Oil Spill Conference, American Petroleum Institute, Washington, D.C., API Publication No. 4334, p. 69-75.

Anderson, J.W., 1985. Toxicity of dispersed and undispersed Prudhoe Bay crude oil fractions to shrimp, fish, and their larvae. American Petroleum Institute Publication No. 4441, Washington, D.C., USA, August 1985, 52p.

Anderson, J.W., R.G. Riley, S.L. Kiesser, and J. Gurtisen, 1987. Toxicity of dispersed and undispersed Prudhoe Bay crude oil fractions to shrimp and fish. In Proceedings 1987 Oil Spill Conference (Prevention, Behavior, Control, Cleanup), Tenth Biennial, American Petroleum Institute, Washington, D.C., pp.235-240.

Atlas, R. and Bragg, J. 2009. Bioremediation of marine oil spills: when and when not – the Exxon Valdez experience. Microbial Biotechnology 2(2):213-221.

Bælum, J., Borglin, S., Chakraborty, R., Fortney, J.L., Lamendella, R., Mason, O.U., Auer, M., Zemla, M., Bill, M., Conrad, M.E., Malfatti, S.A., Tringe, S.G., Holman, H.-Y., Hazen1, T.C., Jansson, J.K., 2012. Deep-sea bacteria enriched by oil and dispersant from the Deepwater Horizon spill. Environ. Microbiol. 14, 2405– 2416.

Bleck, R., 1998: Ocean modeling in isopycnic coordinates. Chapter 18 in Ocean Modeling and Parameterization, E. P. Chassignet and J. Verron, Eds., NATO Science Series C: Mathematical and Physical Sciences, Vol. 516, Kluwer Academic Publishers, 4223-448.

Bleck, R. 2002. An oceanic general circulation model framed in hybrid isopycnic-cartesian coordinates. Ocean Modeling, 4, 55-88.

Blum, D.J. and R.E. Speece, 1990. Determining chemical toxicity to aquatic species, Environmental Science and Technology. 24: 284-293.

Bonn Agreement. 2009. Bonn Agreement Aerial Operations Handbook, 2009. London, UK. Available: http://www.bonnagreement.org/site/assets/files/1081/ba-aoh revision 2 april 2012-1.pdf, Accessed 4 June 2015.

Bonn Agreement, 2011. Bonn Agreement Oil Appearance Code Photo Atlas. Available: http://www.bonnagreement.org/site/assets/files/1081/photo_atlas_version_20112306-1.pdf. Accessed: April 2017.

Bradbury, S., R. Carlson, and T. Henry, 1989. Polar narcosis in aquatic organisms. Aquatic Toxicology and Hazard Assessment 12: 59-73.

Brakstad, O.G., Daling, P.S., Faksness, L.-G., Almås, I.K., Vang, S.-H., Syslak, S., Leirvik, F., 2014. Depletion and biodegradation of the Macondo 252 oil in dispersions and emulsions generated in an oil-on-seawater mesocosm flume basin. Mar. Poll. Bull. 84, 125–134.

Brakstad, O.G., Nordtug, T., Throne-Holst, M., 2015. Biodegradation of dispersed Macondo oil in seawater at low temperature and different oil droplet sizes. Mar. Poll. Bull. 93:144-152.

Canada-Newfoundland and Labrador Offshore Petroleum Board (C-NLOPB). 2014. Eastern Newfoundland Strategic Environmental Assessment. Final Report. Prepared by AMEC Environment & Infrastructure, AMEC TF 1382502. Available: http://www.cnlopb.ca/pdfs/enlsea/ch1-3.pdf?lbisphpreq=1. Accessed: March 2017.

Chassignet, E. P., L. T. Smith, R. Bleck, and F. O. Bryan, 1996: A model comparison: numerical simulations of the North and Equatorial Atlantic oceanic circulation in depth and isopycnic coordinates. J. Phys. Oceanogr., 26, 1849-1867.

Chassignet, E.P., Z.D. Garraffo, 2001. Viscosity parameteriation and gulf stream separation. In: Hawaii U., Muller P., Henderson, D. (Eds.). String to Mixing in Stratified Ocean, Proceedings of Aha Huliko'a Hawaiian Winter Workshop, pp. 27-41.

Clark, R.B., 1984. Impact of Oil Pollution on Seabirds. Environmental Pollution (Series A) 33: 1-22.

Conkright, M.E., J.I. Antonov, O. Baranova, T.P. Boyer, H.E. Garcia, R. Gelfeld, D. Johnson, R.A. Locarnini, P.P. Murphy, T.D. O'Brien, I. Smolyar, and C. Stephens. 2002. World Ocean Database 2001, Volume 1: Introduction. Sydney Levitus (ed.). NOAA Atlas NESDIS 42, U.S. Government Printing Office, Washington, D.C., 167 pp.

Cooper, M. and K.A. Haines, 1996.Altimetric assimilation with water property conservation. Journal of Geophysical Research, vol. 24, pp. 1059-1077.

Cummings, J.A. 2005. Operational multivariate ocean data assimilation. Quarterly Journal of the Royal Meteorological Society. Part C, 133(613), 3583-3604.

Deepwater Horizon Natural Resource Damage Assessment Trustee Council (DWH NRDA Trustees). 2016. The Deepwater Horizon Oil Spill Final Programmatic Damage Assessment and Restoration Plan and Final Programmatic Environmental Impact Statement. National Oceanic and Atmospheric Administration, Office of Response and Restoration. [http://www.gulfspillrestoration.noaa.gov/restoration-planning/gulf-plan/].

Di Toro, D.M. and J.A. McGrath, 2000. Technical basis for narcotic chemicals and polycyclic aromatic hydrocarbon criteria. II. Mixtures and sediments. Environmental Toxicology and Chemistry 19(8): 1971-1982.

Di Toro, D.M., J.A. McGrath, and D.J. Hansen, 2000. Technical basis for narcotic chemicals and polycyclic aromatic hydrocarbon criteria. I. Water and tissue. Environmental Toxicology and Chemistry 19(8): 1951-1970.

Engelhardt, F.R., 1983. Petroleum Effects on Marine Mammals. Aquatic Toxicology 4: 199-217.

Environment and Climate Change Canada (ECCC). 2017. Canadian Ice Service. Available: https://www.ec.gc.ca/glaces-ice/. Accessed: March 2017.

Environmental Science and Technology Center (ESTC), 2001. Release Technology Database, Oil Technology Database. Available:http://www.etc-cte.ec.gc.ca/databases/OilProperties/oil_prop_e.html. Accessed: 2016.

French, D.P. and F.W. French III, 1989. The biological component of the CERCLA Type A damage Assessment Model system. Oil and Chemical Pollution 5:125 163.

French, D.P., 1991. Estimation of exposure and resulting mortality of aquatic biota following spills of toxic substances using a numerical model, Aquatic Toxicology and Risk Assessment: Fourteenth Volume, ASTM STP 1124, (M.A. Mayes and M.G. Barron, Eds.) American Society for Testing and Materials, Philadelphia, pp. 35 47.

French, D., M. Reed, K. Jayko, S. Feng, H. Rines, S. Pavignano, T. Isaji, S. Puckett, A. Keller, F.W. French III, D. Gifford, J. McCue, G. Brown, E. MacDonald, J. Quirk, S. Natzke, R. Bishop, M. Welsh, M. Phillips, and B.S. Ingram, 1996. Final Report, The CERCLA Type A Natural Resource Damage Assessment Model for Coastal and Marine Environments (NRDAM/CME), Technical Documentation, Vol. I - V., Office of Environmental Policy and Compliance, U.S. Department of the Interior, Washington, DC, Contract No. 14-0001-91-C-11.

French McCay, D, 2001. Development and Application of an Oil Toxicity and Exposure Model, OilToxEx. Final Report to NOAA Damage Assessment Center, Silver Spring, MD, January 2001, 50p plus appendices.

French McCay, D.P., 2002. Development and Application of an Oil Toxicity and Exposure Model, OilToxEx. Environmental Toxicology and Chemistry 21(10): 2080-2094.

French McCay, D.P., 2003. Development and Application of Damage Assessment Modeling: Example Assessment for the North Cape Oil Spill. Marine Pollution Bulletin, Volume 47, Issues 9-12, September-December 2003, pp. 341-359.

French McCay, D.P., 2004. Oil release impact modelling: Development and validation. Environmental Toxicology and Chemistry 23(10): 2441-2456.

French McCay, D.P. and J.J. Rowe. 2004. Evaluation of Bird Impacts in Historical Oil Release Cases Using the SIMAP Oil Release Model. Proceedings of the Twenty-seventh Arctic and Marine Oil Spill Program (AMOP) Technical Seminar. Emergencies Science Division, Environment Canada, Ottawa, ON, Canada. pp. 421-452.

French McCay, D.P, 2009. State-of-the-Art and Research Needs for Oil Release Impact Assessment Modelling. In Proceedings of the 32nd AMOP Technical Seminar on Environmental Contamination and Response, Emergencies Science Division, Environment Canada, Ottawa, ON, Canada, pp. 601-653.

French McCay, D., Reich, D., Rowe, J., Schroeder, M., and E. Graham. 2011. Oil Spill Modeling Input to the Offshore Environmental Cost Model (OECM) for US-BOEMRE's Spill Risk and Cost Evaluations. In Proceedings of the 34th AMOP Technical Seminar on Environmental

Contamination and Response, Emergencies Science Division, Environment Canada, Ottawa, ON, Canada.

French McCay, D., Reich, D., Michel, J., Etkin, D., Symons, L., Helton, D., and J. Wagner. 2012. Oil Spill Consequence Analyses of Potentially-Polluting Shipwrecks. In Proceedings of the 34th AMOP Technical Seminar on Environmental Contamination and Response, Emergencies Science Division, Environment Canada, Ottawa, ON, Canada.

French McCay DP, Jayko K, Li Z, Horn M, Kim Y. 2015. Technical Reports for Deepwater Horizon Water Column Injury Assessment–WC_TR14: Modeling Oil Fate and Exposure Concentrations in the Deepwater Plume and Cone of Rising Oil Resulting from the DWHOS. DWH NRDA Water Column Technical Working Group Report. Prepared for National Oceanic and Atmospheric Administration by RPS ASA, South Kingstown, RI. Administrative Record no. DWH-AR0285776.pdf. Available online: https://www.doi.gov/deepwaterhorizon/adminrecord

French McCay, D. 2016. Potential Effects Thresholds for Oil Spill Risk Assessments. In: Proceedings of the 39th AMOP Technical Seminar on Environmental Contamination and Response, Emergencies Science Division, Environment Canada, Ottawa, ON, Canada. p. 285-303.

French-McCay, D., D. Crowley, J. Rowe, M. Bock, H. Robinson, R. Wenning, A. H. Walker, J. Joeckel, and T. Parkerton. 2018a. Comparative Risk Assessment of Spill Response Options for a Deepwater Oil Well Blowout: Part I. Oil Spill Modeling. Mar. Pollut. Bull. https://doi.org/10.1016/j.marpolbul.2018.05.042.

French McCay, Jayko, D.K., Li, Z., Horn, M., Isaji, T. and Spaulding, M. 2018b (in press). Volume II: Appendix II - Oil Transport and Fates Model Technical Manual. In: Galagan, C.W., D. French-McCay, J. Rowe, and L. McStay, editors. Simulation Modeling of Ocean Circulation and Oil Spills in the Gulf of Mexico. Prepared by RPS ASA for the US Department of the Interior, Bureau of Ocean Energy Management, Gulf of Mexico OCS Region, New Orleans, LA. OCS Study BOEM 20xx-xxx; xxx p.

French McCay, D., Horn, M., Li, Z., Crowley, D., Spaulding, M., Mendelsohn, D., Jayko, K., Kim, Y., Isaji, T., Fontenault, J., Shmookler, R. and Rowe, J. 2018c (in press). Volume III: Data Collection, Analysis and Model Validation. In: Galagan, C.W., D. French-McCay, J. Rowe, and L. McStay, editors. Simulation Modeling of Ocean Circulation and Oil Spills in the Gulf of Mexico. Prepared by RPS ASA for the US Department of the Interior, Bureau of Ocean Energy Management, Gulf of Mexico OCS Region, New Orleans, LA. OCS Study BOEM 20xx-xxx; xxx p.

General Bathymetric Chart of the Oceans (GEBCO). 2003. Centenary Edition of the GEBCO Digital Atlas, published on behalf of the Intergovernmental Oceanographic Commission (IOC) and the International Hydrographic Organization (IHO) as part of the General Bathymetric Chart of the Oceans; British Oceanographic Data Centre (BODC), Liverpool.

Geraci, J.R. and D.J. St. Aubin, 1988. Synthesis of Effects of Oil on Marine Mammals, Report to U.S. Department of the Interior, Minerals Management Service, Atlantic OCS Region, OCS Study, MMS 88 0049, Battelle Memorial Institute, Ventura, CA, 292 p.

Greenlaw, M.E., A.G. Gromack, S.P. Basquill, D.S. MacKinnon, J.A. Lynds, R.B. Taylor, D.J. Utting, J.R. Hackett, J. Grant, D.L. Forbes, F. Savoie, D. Bérubé, K.J. Connor, S.C. Johnson, K.A. Coombs, and

R. Henry. 2013. A physiographic coastline classification of the Scotian Shelf bioregion and environs: the Nova Scotia coastline and the New Brunswick Fundy shore. Fisheries and Oceans Canada. Canadian Science Advisory Secretariat Research Document 2012/051. 43pp.

Halliwell, G. R., Jr., 1997.Simulation of decadal/interdecadal variability the North Atlantic driven by the anomalous wind field. Proceedings, Seventh Conference on Climate Variations, Long Beach, CA, 97-102.

Halliwell, G. R., Jr., 1998. Simulation of North Atlantic decadal/multi-decadal winter SST anomalies driven by basin-scale atmospheric circulation anomalies. Journal of Physical Oceanography, 28, 5-21.

Halliwell, G.R. 2002.HYCOM Overview. http://www.hycom.org. June 27, 2011.

Halliwell, G. R., Jr., R. Bleck, and E. Chassignet, 1998. Atlantic Ocean simulations performed using a new hybrid-coordinate ocean model. EOS, Fall 1998 AGU Meeting.

Halliwell, G .R, R. Bleck, E. P. Chassignet, and L.T. Smith, 2000: mixed layer model validation in Atlantic Ocean simulations using the Hybrid Coordinate Ocean Model (HYCOM). EOS, 80, OS304.

Han, G. and C.L. Tang, 1999. Velocity and transport of the Labrador Current determined from altimetric, hydrographic, and wind data. Journal of Geophysical Research: Oceans Banner. Volume 4, Issue C8, 15 August 1999. pp. 18047-18057.

Hazen, T. C., E. A. Dubinsky, T. Z. Desantis, G. L. Andersen, Y. M. Piceno, N. Singh, J. K. Jansson, A. Probst, S. E. Borglin, J. L. Fortney, W. T. Stringfellow, M. Bill, M. E. Conrad, L. M. Tom, K. L. Chavarria, T. R. Alusi, R. Lamendella, D. C. Joyner, C. Spier, J. Baelum, M. Auer, M. L. Zemla, R. Chakraborty, E. L. Sonnenthal, P. D'haeseleer, H. Y. N. Holman, S. Osman, Z. Lu, J. D. Van Nostrand, Y. Deng, J. Zhou and O. U. Mason. 2010. Deep-sea oil plume enriches indigenous oil-degrading bacteria. Science 330:204-208.

Hazen, T.C., Prince, R.C., Mahmoudi, N., 2016. Marine Oil Biodegradation, Environmental Science and Technology, 50, 5, pp. 2121-2129.

Hodson, P.V., D.G. Dixon, and K.L.E. Kaiser, 1988. Estimating the Acute Toxicity of Waterborne Chemicals in Trout from Measurements of Median Lethal Dose and the Octanol-Water Partition Coefficient. Journal of Environmental Toxicology and Chemistry 7:443-454.

Hoffman, D.J., 1978. Embryotoxic Effects of Crude Oil in Mallard Ducks and Chicks. Toxicology and Applied Pharmacology 46: 183-190.

Hu, D., 1996: On the Sensitivity of Thermocline Depth and Meridional Heat Transport to Vertical Diffusivity in OGCMs. J. Physical Oceanography, 26, 1480-1494.

Hurlburt, H.E., Hogan, P.J., 2000. Impact of 1/8 to 1/64 resolution on Gulf stream model-data comparisons in basin-scale Atlantic Ocean models. Dynamics of Atmospheres and Oceans, No. 32, pp. 283-329.

Incardona, J.P., M.G. Carls, L. Holland, T.L. Linbo, D.H. Baldwin, M.S. Myers, K.A. Peck, M. Tagal, S.D. Rice, and N.L. Scholz, 2015. Very low embryonic crude oil exposures cause lasting cardiac defects in salmon and herring. Scientific Reports 5

Intertek, 2016. Preliminary Laboratory Report for Statoil Petroleum AS. Analysis of water sample from L 76-z. Intertek West Lab AS, Tananger Norway. 23 February 2016.

Jenssen, B. M. and M. Ekker, 1991a. Dose Dependent Effects of Plumage-Oiling on Thermoregulation of Common Eiders Somateria mollissima Residing in Water. Polar Research 10: 579-84.

Jenssen, B. M. and M. Ekker, 1991b. Effects of Plumage Contamination with Crude Oil Dispersant Mixtures on Thermoregulation in Common Eiders and Mallards. Archives of Environmental Contamination and Toxicology 20: 398-403.

Jenssen, B.M., 1994. Review article: effects of oil pollution, chemically treated oil, and cleaning on thermal balance of birds. Environmental Pollution. 86(2):207-215.

Jones, R.K., 1997. A Simplified Pseudo-Component of Oil Evaporation Model. In Proceedings of the 20th Arctic and Marine Oil Spill Program (AMOP) Technical Seminar, Environment Canada, pp. 43-61.

King, K.A. and C.A. Lefever, 1979. Effects of Oil Transferred from Incubating Gulls to Their Eggs. Marine Pollution Bulletin 10: 319-321.

Kooijman, S.A.L.M., 1981. Parametric analysis of mortality rates in bioassays. Water Res. 15:107-119.

Lee. K, Nedwed, T., Prince, R.C. and D. Palandro, 2013. Lab tests on the biodegradation of chemically dispersed oil should consider the rapid dilution that occurs at sea. Marine Poll. Bull., 73 (1) (2013), pp. 314-318

Lehr, W.J., D. Wesley, D. Simecek-Beatty, R. Jones, G. Kachook, and J. Lankford, 2000. Algorithm and interface modifications of the NOAA oil spill behavior model. In Proceedings of the 23rd Arctic and Marine Oil Spill Program (AMOP) Technical Seminar, Vancouver, BC, Environmental Protection Service, Environment Canada, pp. 525-539.

Levitus, S. 1982. Climatological Atlas of the World Ocean, NOAA/ERL GFDL Professional Paper 13, Princeton, N.J., 173 pp. (NTISPB83-184093).

Levitus, S., T.P., Boyer, H.E. Garcia, R.A. Locarnini, M.M. Zweng, A.V. Mishonov, J.R. Reagan, J.I. Antonov, O.K. Baranova, M. Biddle, M. Hamilton, D.R. Johnson, C.R. Paver, and D. Seidov. 2014. World Ocean Atlas 2013 (NODC accession 0114815). National Oceanographic Data Center, NOAA.

Lewis, A. 2007. Current Status of the BAOAC; Bonn Agreement Oil Appearance Code. A report to the Netherlands North Sea Agency Directie Noordzee. Alan Lewis Oil Release Consultant, submitted January, 2007.

Mackay, D., H. Puig and L.S. McCarty, 1992. An equation describing the time course and variability in uptake and toxicity of narcotic chemicals to fish. Environ. Toxicol. Chemistry 11: 941-951.

Maine Department of Environmental Protection (MDEP). 2016. Releases and Site Cleanup: Maine Environmental Vulnerability Index Maps. Available: http://www.maine.gov/dep/releases/emergreleaseresp/evi/. Accessed: March 2017.

Malins, D.C. and H.O. Hodgins, 1981. Petroleum and marine fishes: a review of uptake, disposition, and effects. Environmental Science & Technology 15(11):1272-1280.

Marsh, R., M. J. Roberts, R. A. Wood, and A. L. New, 1996: An intercomparison of a Bryan-Cox-type ocean model and an isopycnic ocean model, part II: the subtropical gyre and meridional heat transport. J. Phys. Oceanogr., 26, 1528-1551.

McAuliffe, C.D., 1989. The Weathering of Volatile Hydrocarbons from Crude Oil Slicks on Water. In Proceedings of the 1989 Oil Spill Conference, San Antonio, Texas, American Petroleum Institute, Washington, D.C., pp. 357-364.

McCarty, L.S., 1986. The Relationship Between Aquatic Toxicity QSARs and Bioconcentration for Some Organic Chemicals. Journal of Environmental Toxicology Chemistry 5:1071-1080.

McCarty, L.S., D. Mackay, A.D. Smith, G.W. Ozburn, and D.G. Dixon, 1992a. Residue-based Interpretation of Toxicity and Bioconcentration QSARs from Aquatic Bioassays: Neutral Narcotic Organics. Journal of Environmental Toxicology and Chemistry 11:917-930.

McCarty, L.S., G.W. Ozburn, A. D. Smith, and D.G. Dixon, 1992. Toxicokinetic modeling of mixtures of organic chemicals. Environmental Toxicology and Chemistry 11: 1037-1047.

McCarty, L.S., and D. Mackay, 1993. Enhancing Ecotoxicological Modeling and Assessment. Journal of Environmental Science and Technology 27(9):1719-1728.

McAuliffe, C.D., 1987. Organism exposure to volatile/soluble hydrocarbons from crude oil releases –a field and laboratory comparison. Proceedings of the 1987 Oil Release Conference. Washington, D.C.: API. pp. 275-288.

Milton, S., P. Lutz, and G. Shigenaka, 2003. Oil Toxicity and Impacts on Sea Turtles. In Shigenaka, G. (ed.), Oil and Sea Turtles: Biology, Planning, and Response. National Oceanic and Atmospheric Administration, 116 p.

National Oceanic and Atmospheric Administration (NOAA), 2014. Can the ocean freeze? Available: http://oceanservice.noaa.gov/facts/oceanfreeze.html. Accessed: April 2017.

National Oceanic and Atmospheric Administration (NOAA), 2016a. Environmental Sensitivity Index (ESI) Maps. Available: http://response.restoration.noaa.gov/maps-and-spatial-data/environmental-sensitivity-index-esi-maps.html. Accessed: 2011 - 2012.

National Oceanic and Atmospheric Administration (NOAA). 2016b. Open water oil identification job aid for aerial observation. U.S. Department of Commerce, Office of Response and Restoration [http://response.restoration.noaa.gov/oil-and-chemical-releases/oil-releases/resources/open-water-oil-identification-job-aid.html]

National Research Council (NRC), 1985. Oil in the Sea: Inputs, Fates and Effects. National Academy Press, Washington, D.C. 601p.

National Research Council (NRC), 2003. Oil in the Sea III: Inputs, Fates and Effects. National Academy Press, Washington, D.C. 280p.

National Research Council (NRC), 2005. National Research Council: Understanding Oil Spill Dispersants: Efficacy and Effects. Washington, D.C.: National Academies Press.

Neff, J.M., J.W. Anderson, B.A. Cox, R.B. Laughlin, Jr., S.S. Rossi, and H.E. Tatem, 1976. Effects of petroleum on survival respiration, and growth of marine animals. In Sources, Effects and Sinks of Hydrocarbons in the Aquatic Environment. American Institute of Biological Sciences, Washington, D.C. 515-539p.

Neff, J.M. and J.W. Anderson, 1981. Response of Marine Animals to Petroleum and Specific Petroleum Hydrocarbons. Applied Science Publishers Ltd., London and Halsted Press Division, John Wiley & Sons, NY. 177p.

New, A. and R. Bleck, 1995: An isopycnic model of the North Atlantic, Part II: interdecadal variability of the subtropical gyre. J. Phys. Oceanogr., 25, 2700-2714.

New, A., R. Bleck, Y. Jia, R. Marsh, M. Huddleston, and S. Barnard, 1995: An isopycnic model of the North Atlantic, Part I: model experiments. J. Phys. Oceanogr., 25, 2667-2699.

New Brunswick Department of Natural Resources (NBDNR). 2013. New Brunswick Canada: Regulated Wetlands. Available: http://www.snb.ca/geonb1/e/DC/RW.asp. Accessed: March 2017.

Nirmalakhandan, N. and R.E. Speece, 1988. Structure-activity relationships, quantitative techniques for predicting the behavior of chemicals in the ecosystem. Environmental Science and Technology 22:606-615.

North, E.W., Adams, E.E., Thessen, A.E., Schlag, Z., He R., Socolofsky, S.A., Masutani, S.M., Peckham, S.D., 2015. The influence of droplet size and biodegradation on the transport of subsurface oil droplets during the Deepwater Horizon spill: A model sensitivity study, Environmental Research Letters, 10, 2, #24016.

Nova Scotia Department of Natural Resources (NSDNR). 2013. Nova Scotia Canada: DNR Ecosystems and Habitats Program Overview. Available: https://novascotia.ca/natr/wildlife/habitats/wetlands.asp. Accessed: March 2017.

Payne, J.R., B.E. Kirstein, G.D. McNabb, Jr., J.L. Lambach, R. Redding R.E. Jordan, W. Hom, C. deOliveria, G.S. Smith, D.M. Baxter, and R. Gaegel, 1984. Multivariate analysis of petroleum weathering in the marine environment – sub Arctic. Environmental Assessment of the Alaskan Continental Shelf, OCEAP, Final Report of Principal Investigators, Vol. 21 and 22, Feb. 1984, 690p.

Payne, J.R., B.E. Kirstein, J.R. Clayton, Jr., C. Clary, R. Redding, G.D. McNabb, Jr., and G. Farmer, 1987. Integration of suspended particulate matter and oil transportation study. Final Report. Minerals Management Service, Environmental Studies Branch, Anchorage, AK. Contract No. 14-12-0001-30146, 216 p.

Peakall, D.B., P.G. Wells and D. Mackay, 1985. A hazard assessment of chemically dispersed oil spills and seabirds a novel approach. In: Proc. 8th Tech. Sem. Annual Arctic Marine Oil Spill Program, 18 20 June 1985. Environmental Protection Service Environmental Canada. Edmonton, Alta., pp. 78 90.

Petrie, B. and Anderson, C., 1983. Circulation on the Newfoundland continental shelf. Atmosphere-Ocean, 21(2), pp.207-226.

Petrie, B. A. Isenor, 1985. The Near-Surface Circulation and Exchange in the Newfoundland Grand Banks Region. Atmosphere-Ocean, vol. 23, no. 3, pp. 209-227.

Prince R.C., K. M. McFarlin, J. D. Butler, E. J. Febbo, F. C.Y. Wang, T. J. Nedwed, 2013. The primary biodegradation of dispersed crude oil in the sea. Chemosphere 90(2):521–526.

Prince RC, Coolbaugh TS, Parkerton TF, 2016. Oil dispersants do facilitate biodegradation of spilled oil. Proc Natl Acad Sci USA 113:E1421.

Rice, S.D., J.W. Short, and J.F. Karinen, 1977. Comparative oil toxicity and comparative animal sensitivity, p. 78-94. In D.A. Wolfe (ed.). Fate and Effects of Petroleum Hydrocarbons in Marine Ecosystems and Organisms. Pergamon Press, NY.

Richardson, P.L., 1983. Eddy Kinetic Energy in the North Atlantic From Surface Drifters. Journal of Geophysical Research, vol. 88, no. C7, pp. 4355-4367.

Roberts, M. J., R. Marsh, A. L. New, and R. A. Wood, 1996: An intercomparison of a Bryan-Cox-type ocean model and an isopycnic ocean model, part I: the subpolar gyre and high latitude processes. J. Phys. Oceanogr., 26, 1495-1527.

RPS ASA, 2013. NRC categories and observations of oil releases.

Saha, S., et al. 2010. NCEP Climate Forecast System Reanalysis (CFSR) 6-hourly Products, January 1979 to December 2010. Research Data Archive at the National Center for Atmospheric Research, Computational and Information Systems Laboratory. http://dx.doi.org/10.5065/D69K487J.

Service New Brunswick (SNB). 2010. Geographic Data & Maps – Products & Services: Digital Topographic Data Base 1998. Available: http://www.snb.ca/gdam-igec/e/2900e_1.asp. Accessed: March 2017.

S.L. Ross Environmental Research Ltd., 2011. Oil Release Fate and Behavior Modelling in Support of Corridor Resources Old Harry Prospect Drilling EA. Prepared for Corridor Resources Inc. 40 pp. + Appendix.

S.L. Ross Environmental Research Ltd., 2008. The Fate and Behavior of Hypothetical Oil Releases form the StatoilHydro 2008 Mizzen Drilling Program. Prepared for StatoilHydro Canada E&P. January 2008.

S.L. Ross Environmental Research Ltd., 2016. Release-related Properties of BdNL-76Z Ti-3 DST Dead Oil. 30 pp. + Appendices.

Smith, R.D. Maltrud, M.E., 2000. Numerical simulations of the North Atlantic Ocean at 1/10. Journal of physical Oceanography, no. 30, pp.1532-1561.

Sprague, J.B., 1969. Measurement of pollutant toxicity to fish. I. Bioassay methods for acute toxicity. Water Research 3: 793-821.

Spies, R.B., S.D. Rice, D.A. Wolfe, and B.A. Wright, 1996. The Effects of the Exxon Valdez Oil Spill on the Alaskan Coastal Environment. In Proceedings of the Exxon Valdez Oil Spill Symposium 18, American Fisheries Society, Bethesda, MD, pp. 1-16.

Statoil 2016. Response to Comments – 2016 Drilling EA Amendment. SC-CNO-0122-16. December 15, 2016.

Swartz, R.C., D.W. Schults, R.J. Ozretich, J.O. Lamberson, F.A. Cole, T.H. DeWitt, M.S. Redmond, and S.P. Ferraro, 1995. ΣPAH: A Model to Predict the Toxicity of Polynuclear Aromatic Hydrocarbon Mixtures in Field-Collected Sediments. Journal of Environmental Toxicology and Chemistry 14(11): 1977-1987.

Tatem, H.E., B.A. Cox, and J.W. Anderson, 1978. The toxicity of oils and petroleum hydrocarbons to estuarine crustaceans. Estuarine and Coastal Marine Science 6:365-373.

Therrien, A., 2017. Shoreline Segmentation (SCAT Classification). Environment and Climate Change Canada.

Trudel, B.K., R.C. Belore, B.J. Jessiman and S.L. Ross., 1989. A micro-computer based release impact assessment system for untreated and chemically dispersed oil releases in the U.S. Gulf of Mexico. 1989 International Oil Release Conference.

United States Coast Guard (USCG). 2009. How do the Labrador and Gulf Stream Currents Affect Icebergs. Labrador and Gulf Stream currents affect icebergs in the North Atlantic Ocean. USCG Navigation Center. U.S. Department of Homeland Security. Available: https://navcen.uscg.gov/?pageName=iipHowDoTheLabradorAndGulfStreamCurrentsAffectIcebergsInTheNorthAtlanticOcean. Accessed: March 2017.

U.S. Environmental Protection Agency (US EPA), 2003. Procedures for the Derivation of Equilibrium Partitioning Sediment benchmarks (ESBs) for the Protection of Benthic Organisms (PDF). PAH Mixtures. EPA-600-R-02-013. Office of Research and Development. Washington, DC.

U.S. Environmental Protection Agency (US EPA), 2008. Procedures for the Derivation of Equilibrium Partitioning Sediment benchmarks (ESBs) for the Protection of Benthic Organisms (PDF). Compendium of Tier 2 Values for Nonionic Organics. U.S. Environmental Protection Agency, Office of Research and Development: Washington DC. EPA/600/R-02/016. PB2008-107282. March 2008.

U.S. Environmental Protection Agency (US EPA), 2016. ECOTOX User Guide: ECOTOXicology Database System. Version 4.0. Available: http:/www.epa.gov/ecotox/

Vargo, S., P. Lutz, D. Odell, E. Van Vleep, and G. Bossart, 1986. Final Report: Study of Effects of Oil on Marine Turtles. Technical Report OCS study MMS 86-0070. Vol. 2, 181 p.

Varhaar, H.J.M, C.J. VanLeeuwen, and J.L.M. Hermens, 1992. Classifying Environmental Pollutants, 1: Structure-activity Relationships for Prediction of Aquatic Toxicity. Chemosphere 25:471-491.

Varoujean, D.H., D.M. Baltz, B. Allen, D. Power, D.A. Schroeder, and K.M. Kempner, 1983. Seabird Oil Spill Behavior Study, Vol 1: Executive Summary, Volume 2: Technical Report, Volume 3: Appendices. Final Report to U.S. Dept. of the Interior, Minerals Management Service, Reston, VA, by Nero and Associates, Inc., Portland, OR, MMS QN TE 83 007, NTIS #PB84 17930, 365 p.

VLIZ (2014). Maritime Boundaries Geodatabase, version 8. Available online at http://www.marineregions.org/. Consulted on 2014-04-14.

Volkov, D.L., 2005. Interannual Variability of the Altimetry-Derived Eddy Field and Surface Circulation in the Extratropical North Atlantic Ocean in 1993-2001. Journal of Physical Oceanography, Vol. 35, pp. 405-426.

Wang, Z., P. Jokuty, M. Fingas, et al., 2001. Characterization of Federated Oil fractions used for the PTAC project to study the petroleum fraction-specific toxicity to soils. Proceedings of the 18th AMOP Conference, 2001. pp 79-98.

Wolfe, J.L. and R.J. Esher, 1981. Effects of Crude Oil on Swimming Behavior and Survival in the Rice Rat. Environmental Research 26: 486-489.

Zahed, M. A., Aziz, H.A., Isa, M.H., Mohajeri, L., Mohajeri, S. and Kutty, S.R.M. 2011. Kinetic modeling and half-life study on bioremediation of crude oil dispersed by Corexit 9500. Journal of Hazardous Materials 185(2-3):1027-1031.

Trajectory Modelling in Support of the Bay du Nord Development Project

Appendix A: SIMAP and OILMAPDeep Model Descriptions

Prepared for: Equinor Canada Ltd.

Project Number:
2018-P-22390

Version:
Final Report

Date Submitted:
06/23/2020

Project Manager
Matthew Horn, Ph.D.

RPS
55 Village Square Dr.
South Kingstown, RI USA
02879-8248

Release	File Name	Date Submitted	Notes
Revised Final	Equinor – RPS Technical Report_20200623_AppendixA.docx	06/23/2020	RPS final version of Appendix A
Revised Final	Equinor – RPS Technical Report_20190206_AppendixA.docx	02/06/2019	RPS final version of Appendix A
Revised Final	Equinor – RPS Technical Report_20181130_AppendixA.docx	11/30/2018	RPS final version of Appendix A
Final	Equinor – RPS Technical Report_20181019_AppendixA.docx	10/19/2018	RPS Draft final version of Appendix A following senior technical review

Summary

This Appendix A is provided as a reference to RPS Technical Report: Trajectory Modelling in Support of the Equinor Bay du Nord Development Project. Appendix A provides a detailed description of the SIMAP model and the fates processes and algorithms that were used, as well as a description of the theory and implementation of the OIMAP Deep model.

Table of Contents

List of Figures

1 SIMAP Model Description

The analysis was performed using the model system developed by Applied Science Associates (ASA) called SIMAP (Spill Impact Model Analysis Package). SIMAP originated from the oil fates and biological effects submodels in the Natural Resource Damage Assessment Models for Coastal and Marine Environments (NRDAM/CME) and Great Lakes Environments (NRDAM/GLE), which ASA developed in the early 1990s for the U.S. Department of the Interior for use in "type A" Natural Resource Damage Assessment (NRDA) regulations under the Comprehensive Environmental Response, Compensation and Liability Act of 1980 (CERCLA). The most recent version of the type A models, the NRDAM/CME (Version 2.4, April 1996) was published as part of the CERCLA type A NRDA Final Rule (Federal Register, May 7, 1996, Vol. 61, No. 89, p. 20559-20614). The technical documentation for the NRDAM/CME is in French et al. (1996 a-c). This technical development involved several in-depth peer reviews, as described in the Final Rule.

While the NRDAM/CME and NRDAM/GLE were developed for simplified natural resource damage assessments of small spills in the United States, SIMAP is designed to evaluate fates and effects of both real and hypothetical spills in marine, estuarine and freshwater environments worldwide. Additions and modifications to prepare SIMAP were made to increase model resolution, allow modification and site-specificity of input data, allow incorporation of temporally varying current data, evaluate subsurface releases and movements of subsurface oil, track multiple chemical components of the oil, enable stochastic modelling, and facilitate analysis of results.

Below are brief descriptions of the fates and effects models presented in SIMAP. Detailed descriptions of the algorithms and assumptions in the model are in published papers (French McCay, 2002; 2003; 2004; 2009). The model has been validated with more than 20 case histories, including the *Exxon Valdez* and other large spills (French and Rines, 1997; French McCay, 2003; 2004; French McCay and Rowe, 2004) as well as test spills designed to verify the model (French et al., 1997).

1.1 Physical Fates Model

The three-dimensional physical fates model estimates distribution (as mass and concentrations) of whole oil and oil components on the water surface, on shorelines, in the water column, and in sediments. Oil fate processes included are oil spreading (gravitational and by shearing), evaporation, transport, randomized dispersion, emulsification, entrainment (natural and facilitated by dispersant), dissolution, volatilization of dissolved hydrocarbons from the surface water, adherence of oil droplets to suspended sediments, adsorption of soluble and sparingly-soluble aromatics to suspended sediments, sedimentation, and degradation.

Oil is a mixture of hydrocarbons of varying physical, chemical, and toxicological characteristics. In the model, oil is represented by component categories, and the fate of each component is tracked separately. The "pseudo-component" approach (Payne et al., 1984; 1987; French et al., 1996a; Jones, 1997; Lehr et al., 2000) is used, where chemicals in the oil mixture are grouped by physical-chemical

properties, and the resulting component category behaves as if it were a single chemical with characteristics typical of the chemical group.

The most toxic components of oil to aquatic organisms are low molecular weight aromatic compounds (monoaromatic and polycyclic aromatic hydrocarbons, MAHs and PAHs), which are both volatile and soluble in water. Their acute toxic effects are caused by non-polar narcosis, where toxicity is related to the octanol-water partition coefficient (K_{ow}), a measure of hydrophobicity. The more hydrophobic the compound, the more toxic it is likely to be. However, as K_{ow} increases, the compound also becomes less soluble in water, and so there is less exposure to aquatic organisms. The toxicity of compounds having log(K_{ow}) values greater than about 5.6 is limited by their very low solubility in water, and consequent low bioavailability to aquatic biota (French McCay, 2002, Di Toro et al., 2000). Thus, the potential for acute effects is the result of a balance between bioavailability (exposure), toxicity once exposed, and duration of exposure. French McCay (2002) contains a full description of the oil toxicity model in SIMAP, and French McCay (2002) describes the implementation of the toxicity model in SIMAP.

Because of these considerations, the SIMAP fates model focuses on tracking the lower molecular weight aromatic components divided into chemical groups based on volatility, solubility, and hydrophobicity. In the model, the oil is treated as comprising eight components (defined in Table 1). Six of the components (i.e., all but the two non-volatile residual components representing non-volatile aromatics and aliphatics) evaporate at rates specific to the pseudo-component. Solubility is strongly correlated with volatility, and the solubility of aromatics is higher than aliphatics of the same volatility. The MAHs are the most soluble, the 2-ring PAHs are less soluble, and the 3-ring PAHs slightly soluble (Mackay et al., 1992). Both the solubility and toxicity of the non-aromatic hydrocarbons are much less than for the aromatics, and dissolution (and water concentrations) of non-aromatics is safely ignored. Thus, dissolved concentrations are calculated only for each of the three soluble aromatic pseudo-components.

Table 1. Definition of four distillation cuts and the eight pseudo-components in the model (Monoaromatic Hydrocarbons, MAHs; Benzene + Toluene + Ethylbenzene + Xylene, BTEX; Polycyclic Aromatic Hydrocarbons, PAHs).

Characteristic	Volatile and Highly Soluble	Semi-volatile and Soluble	Low Volatility and Slightly Soluble	Residual (non-volatile and very low solubility)
Distillation cut	1	2	3	4
Boiling Point (°C)	< 180	180 - 265	265 - 380	>380
Molecular Weight	50 - 125	125 - 168	152 - 215	> 215
Log(K_{ow})	2.1-3.7	3.7-4.4	3.9-5.6	>5.6
Aliphatic pseudo-components: Number of Carbons	volatile aliphatics: C4 – C10	semi-volatile aliphatics: C10 – C15	low-volatility aliphatics: C15 – C20	non-volatile aliphatics: > C20
Aromatic pseudo-component name: included compounds	MAHs: BTEX, MAHs to C3-benzenes	2 ring PAHs: C4-benzenes, naphthalene, C1-, C2-naphthalenes	3 ring PAHs: C3-, C4-naphthalenes, 3-4 ring PAHs with log(K_{ow}) < 5.6	≥4 ring aromatics: PAHs with log(K_{ow}) > 5.6 (very low solubility)

This number of components provides sufficient accuracy for the evaporation and dissolution calculations, particularly given the time frame (minutes) over which dissolution occurs from small droplets and the rapid resurfacing of large droplets (see discussion above). The alternative of treating oil as a single compound with empirically-derived rates (e.g., Mackay et al., 1980; Stiver and Mackay, 1984) does not provide sufficient accuracy for environmental effects analyses because the effects to water column organisms are caused by MAHs and PAHs, which have specific properties that differ from the other volatile and soluble compounds. The model has been validated both in predicting dissolved concentrations and resulting toxic effects, supporting the adequacy of the use of this number of pseudo-components (French McCay, 2003).

The lower molecular weight aromatics dissolve from the whole oil and are partitioned in the water column and sediments according to equilibrium partitioning theory (French et al., 1996a; French McCay, 2004). The residual fractions in the model are composed of non-volatile and insoluble compounds that remain in the “whole oil” that spreads, is transported on the water surface, strands on shorelines, and disperses into the water column as oil droplets or remains on the surface as tar balls. This is the fraction that composes black oil, mousse, and sheen.

1.2 Oil Fate Model Processes

The schematic in Figure 1 depicts oil fates processes simulated in open water conditions, while the schematic in Figure 2 depicts oil fates processes that are simulated at and near the shoreline. Because oil contains many chemicals with varying physical-chemical properties, and the environment is spatially and temporally variable, the oil rapidly separates into different phases or parts of the environment:

- Surface oil
- Emulsified oil (mousse) and tar balls
- Oil droplets suspended in the water column
- Oil adhering to suspended particulate matter in the water
- Dissolved lower molecular weight components (MAHs, PAHs, and other soluble components) in the water column
- Oil on and in the sediments
- Dissolved lower molecular weight components (MAHs, PAHs, and other soluble components) in the sediment pore water
- Oil on and in the shoreline sediments and surfaces

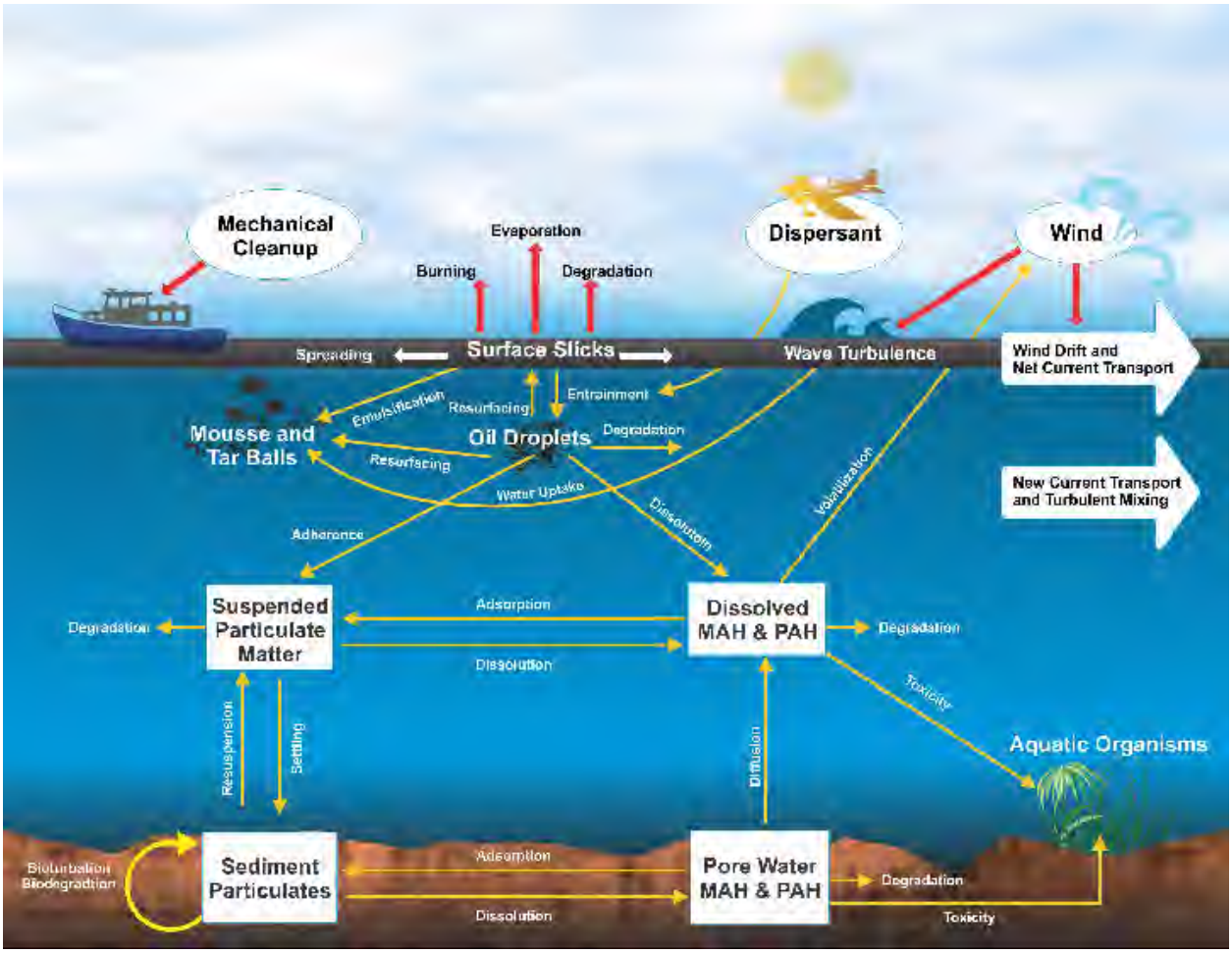

Figure 1. Simulated oil fates processes in open water in the SIMAP model.

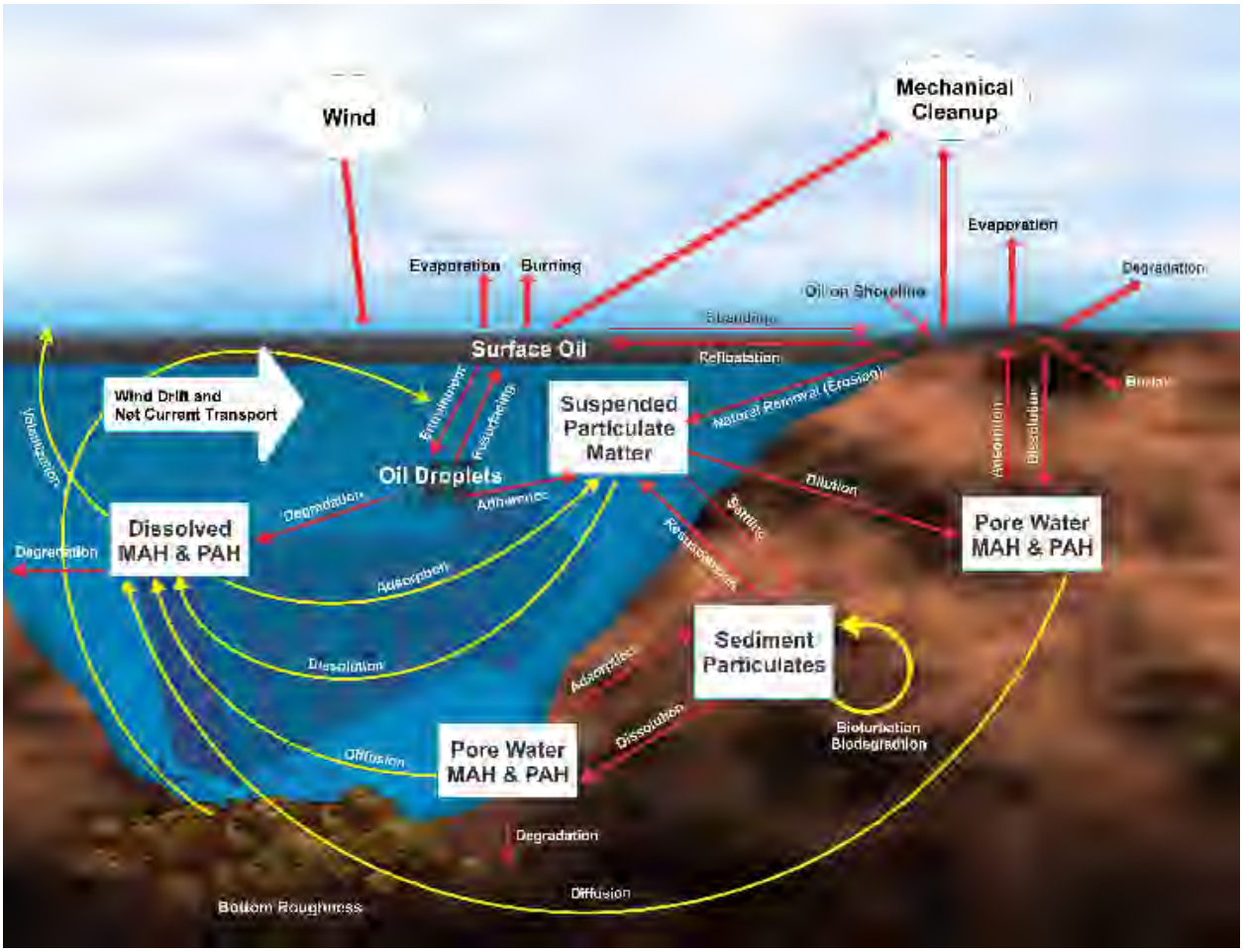

Figure 2. Simulated oil fates processes at the shoreline in the SIMAP model.

The schematics in Figure 1 and Figure 2 represent oil fates processes that are simulated in the model:

- Spreading is the thinning and broadening of surface slicks caused by gravitational forces and surface tension. This occurs rapidly after oil is spilled on the water surface. The rate of spreading is faster if oil viscosity is lower. Viscosity decreases as temperature increases. Viscosity increases as oil emulsifies.
- Transport is the process where oil is carried by currents.
- Turbulent dispersion: Typically there are also “sub-scale” currents (not included in the current data), better known as turbulence that move oil and mix it both in three dimensions. The process by which turbulence mixes and spreads oil components on the water surface and in the water is called turbulent dispersion.
- Evaporation is the process where volatile components of the oil diffuse from the oil and enter the gaseous phase (atmosphere). Evaporation from surface and shoreline oil increases as the oil

surface area, temperature, and wind speed increase. As lighter components evaporate off, the remaining “weathered” oil becomes more viscous.

- Emulsification is the process where water is mixed into the oil, such that the oil makes a matrix with embedded water droplets. The resulting mixture is commonly called mousse. It is technically referred to as a water-in-oil emulsion. The rate of emulsification increases with increasing wind speed and turbulence on the surface of the water. Viscosity increases as oil emulsifies.
- Entrainment is the process where waves break over surface oil and carry it as droplets into the water column. At higher wind speeds, or where currents and bottom roughness induce turbulence, wave heights may reach a threshold where they break. In open waters, waves break beginning at about 12 knots of wind speed and wave breaking increases as wind speed becomes higher. Thus, entrainment becomes increasingly important (higher rate of mass transfer to the water) the higher the wind speed. As turbulence from whatever source increases, the oil droplet sizes become smaller. Application of chemical dispersant increases the entrainment rate of oil and decreases droplet size at a given level of turbulence. Entrainment rate is slower, and droplet size is larger, as oil viscosity increases (by emulsification and evaporation loss of lighter volatile components). The droplet size determines how fast and whether the oil resurfaces.
- Resurfacing of entrained oil rapidly occurs for larger oil droplets. Smaller droplets resurface when the wave turbulence decreases. The smallest droplets do not resurface, as typical turbulence levels in the water keep them in suspension indefinitely. Local winds at the water surface can also prevent oil from surfacing. Resurfaced oil typically forms sheens. In open water where currents are relatively slow, surface slicks are usually blown down wind faster than the underlying water, resurfacing droplets come up behind the leading edge of the oil, effectively spreading the slicks in the down-wind direction.
- Dissolution is the process where water-soluble components diffuse out of the oil into the water. Dissolution rate increases the higher the surface area of the oil relative to its volume. As the surface area to volume ratio is higher for smaller spherical droplets, the smaller the droplets the higher the dissolution rate. The higher the wave turbulence, the smaller the droplets of entrained oil. Dissolution from entrained small droplets is much faster than from surface slicks in the shape of flat plates. The soluble components are also volatile, and evaporation from surface slicks is faster than dissolution into the underlying water. Thus, the processes of evaporation and dissolution are competitive, with evaporation the dominant process for surface oil.
- Volatilization of dissolved components from the water to the atmosphere occurs as they are mixed and diffuse to the water surface boundary and enter the gas phase. Volatilization rate increase with increasing air and water temperature.
- Adsorption of dissolved components to particulate matter in the water occurs because the soluble components are only sparingly so. These compounds (MAHs and PAHs) preferentially adsorb to particulates when the latter are present. The higher the concentration of suspended

particulates, the more adsorption. Also, the higher the molecular weight of the compound, the less soluble, and the more the compound adsorbs to particulate matter.

- Adherence is the process where oil droplets combine with particles in the water. If the particles are suspended sediments, the combined oil/suspended sediment agglomerate is heavier than the oil itself and than the water. If turbulence subsides sufficiently, the oil-sediment agglomerates will settle.
- Sedimentation (settling) is the process where oil-sediment agglomerates and particles with adsorbed sparingly-soluble components (MAHs and PAHs) settle to the bottom sediments. Adherence and sedimentation can be an important pathway of oil in near shore areas when waves are strong and subsequently subside. Generally, oil-sediment agglomerates transfer more PAH to the bottom than sediments with PAHs that were adsorbed from the dissolved phase in the water column.
- Resuspension of settled oil-sediment particles and particles with adsorbed sparingly-soluble components (MAHs and PAHs) may occur if current speeds and turbulence exceed threshold values where cohesive forces can be overcome.
- Diffusion is the process where dissolved compounds move from higher to lower concentration areas by random motion of molecules and micro-scale turbulence. Dissolved components in bottom and shoreline sediments can diffuse out to the water where concentrations are relatively low. Bioturbation, groundwater discharge and hyporheic flow of water through stream-bed sediments can greatly increase the rate of diffusion from sediments (see below).
- Dilution occurs when water of lower concentration is mixed into water with higher concentration by turbulence, currents, or shoreline groundwater.
- Bioturbation is the process where animals in the sediments mix the surface sediment layer while burrowing, feeding, or passing water over their gills. In open-water soft-bottom environments, bioturbation effectively mixes the surface sediment layer about 10 cm thick (in non-polluted areas).
- Degradation is the process where oil components are changed either chemically or biologically (biodegradation) to another compound. It includes breakdown to simpler organic carbon compounds by bacteria and other organisms, photo-oxidation by solar energy, and other chemical reactions. Higher temperature and higher light intensity (particularly ultraviolet wavelengths) increase the rate of degradation.
- Floating oil may strand on shorelines and refloat as water levels rise, allowing the oil to move further down current (downstream).

For a spill on the water surface, the gravitational spreading occurs very rapidly (within hours) to a minimum thickness. Thus, the area exposed to evaporation is high relative to the oil volume. Evaporation proceeds faster than dissolution. Thus, most of the volatiles and semi-volatiles evaporate, with a smaller fraction dissolving into the water. Degradation (photo-oxidation and biodegradation) also occurs at a relatively slow rate compared to these processes.

Evaporation is more rapid as the wind speed increases. However, above about 12 knots (6 m/s) of wind speed and in open water, white caps begin to form and the breaking waves entrain oil as droplets into the water column. Higher wind speeds (and turbulence) increase entrainment and results in smaller droplet sizes. From Stoke's Law, larger droplets resurface faster and form surface slicks. Thus, a dynamic balance evolves between entrainment and resurfacing. As high-wind events occur, the entrainment rate increases. When the winds subside to less than 12 knots, the larger oil droplets resurface and remain floating. Similar dynamics occur in turbulent streams.

The smallest oil droplets remain entrained in the water column for an indefinite period. Larger oil droplets rise to the surface at varying rates. While the droplets are under water, dissolution of the light and soluble components occurs. Dissolution rate is a function of the surface area available. Thus, most dissolution occurs from droplets, as opposed to from surface slicks, since droplets have a higher surface area to volume ratio, and they are not in contact with the atmosphere (and so the soluble components do not preferentially evaporate as they do from surface oil).

If oil is released or driven underwater, it forms droplets of varying sizes. More turbulent conditions result in smaller droplet sizes. From Stoke's Law, larger droplets rise faster, and surface if the water is shallow. Resurfaced oil behaves as surface oil after gravitational spreading has occurred. The surface oil may be re-entrained. The smallest droplets in most cases remain in the water permanently. As a result of the higher surface area per volume of small droplets, the dissolution rate is much higher from subsurface oil than from floating oil on the water surface.

Because of these interactions, the majority of dissolved constituents (which are of concern because of potential effects on aquatic organisms) are from droplets entrained in the water. For a given spill volume and oil type/composition, with increasing turbulence either at the water surface and/or at the stream bed: there is an increasing amount of oil entrained; the oil is increasingly broken up into smaller droplets; there is more likelihood of the oil remaining entrained rather than resurfacing; and the dissolved concentrations will be higher. Entrainment and dissolved concentrations increase with (1) higher wind speed, (2) increased turbulence from other sources of turbulence (waves on a beach, rapids, and waterfalls in rivers, etc.), (3) subsurface releases (especially under higher pressure and turbulence), and (4) application of chemical dispersants. Chemical dispersants both increase the amount of oil entrained and decrease the oil droplet size. Thus, chemical dispersants increase the dissolution rate of soluble components.

These processes that increase the rate of supply of dissolved constituents are balanced by loss terms in the model: (1) transport (dilution), (2) volatilization from the dissolved phase to the atmosphere, (3) adsorption to suspended particulate material (SPM) and sedimentation, and (4) degradation (photo-oxidation or biologically mediated). Also, other processes slow the entrainment rate: (1) emulsification increases viscosity and slows or eliminates entrainment; (2) adsorption of oil droplets to SPM and settling removes oil from the water; (3) stranding on shorelines removes oil from the water; and (4) mechanical cleanup and burning removes mass from the water surface and shorelines. Thus, the model-

predicted concentrations are the resulting balance of all these processes and the best estimates based on our quantitative understanding of the individual processes.

The algorithms used to model these processes are described in French McCay (2004). Lagrangian elements (spillets) are used to simulate the movements of oil components in three dimensions over time. Surface floating oil, subsurface droplets, and dissolved components are tracked in separate spillets. Transport is the sum of advective velocities by currents input to the model, surface wind drift, vertical movement according to buoyancy, and randomized turbulent diffusive velocities in three dimensions. The vertical diffusion coefficient is computed as a function of wind speed in the surface wave-mixed layer. The horizontal and deeper water vertical diffusion coefficients are model inputs.

The oil (whole and as pseudo-components) separates into different phases or parts of the environment, i.e., surface slicks; emulsified oil (mousse) and tar balls; oil droplets suspended in the water column; dissolved lower molecular weight components (MAHs and PAHs) in the water column; oil droplets adhered and hydrocarbons adsorbed to suspended particulate matter in the water; hydrocarbons on and in the sediments; dissolved MAHs and PAHs in the sediment pore water; and hydrocarbons on and in the shoreline sediments and surfaces.

1.3 Oil Fates Algorithms

1.3.1 Transport

Lagrangian particles (spillets) are moved in three dimensions over time. For each model time step, the new vector position of the spillet centre is calculated from the old plus the vector sum of east-west, north-south, and vertical components of advective and diffusive velocities:

$$X_t = X_{t-1} + \Delta t \, (U_t + D_t + R_t + W_t)$$

where X_t is the vector position at time t, X_{t-1} is the vector position the previous time step, Δt is the time step, U_t is the sum of all the advective (current) velocity components in three dimensions at time t, D_t is the sum of the randomized diffusive velocities in three dimensions at time t, R_t is the rise or sinking velocity of whole oil droplets in the water column, and W_t is the surface wind transport ("wind drift"). The magnitudes of the components of D_t are scaled by horizontal and vertical diffusion coefficients (Okubo and Ozmidov, 1970; Okubo, 1971). The vertical diffusion coefficient is computed as a function of wind speed in the surface wave-mixed layer (which ranges from centimeter scales in rivers and near lee shorelines to potentially meters in large water bodies away from shore when wind speeds are high), based on Thorpe (1984). R_t is computed by Stokes law, where velocity is related to the difference in density between the particle and the water, and to the particle diameter. The algorithm developed by Youssef and Spaulding (1993) is used for wind transport in the surface wave-mixed layer (W_t, described below).

1.3.2 Shoreline Stranding

The fate of spilled oil that reaches the shoreline depends on characteristics of the oil, the type of shoreline, and the energy environment. The stranding algorithm is based on work by CSE/ASA/BAT (1986), Gundlach (1987), and Reed and Gundlach (1989) in developing the COZOIL model for the U.S. Minerals Management Service. In SIMAP, deposition occurs when an oil spillet intersects shore surface. Deposition ceases when the volume holding capacity for the shore surface is reached. Subsequent oil coming ashore is not allowed to remain on the shore surface. It is refloated by rising water, and carried away by currents and wind drift. The remaining shoreline oil is then removed exponentially with time. Data for holding capacity and removal rate are taken from CSE/ABA/BAT (1986) and Gundlach (1987), and are a function of oil viscosity and shore type. The algorithm and data are in French et al. (1996a).

1.3.3 Spreading

Spreading determines the areal extent of the surface oil, which in turn influences its rates of evaporation, dissolution, dispersion (entrainment) and photo-oxidation, all of which are functions of surface area. Spreading results from the balance among the forces of gravity, inertia, viscosity, and surface tension (which increases the diameter of each spillet); turbulent diffusion (which spreads the spillets apart); and entrainment followed by resurfacing, which can spatially separate the leading edge of the oil from resurfaced oil transported in a different direction by subsurface currents.

For many years Fay's (1971) three-regime spreading theory was widely used in oil spill models (ASCE, 1996). Mackay et al. (1980; 1982) modified Fay's approach and described the oil as thin and thick slicks. Their approach used an empirical formulation based on Fay's (1971) terminal spreading behavior. They assumed the thick slick feeds the thin slick and that 80-90% of the total slick area is represented by the thin slick. In SIMAP, oil spillets on the water surface increase in diameter according to the spreading algorithm empirically-derived by Mackay et al. (1980; 1982). Sensitivity analyses of this algorithm led to the discovery that the solution was affected by the number of spillets used. Thus, a formulation was derived to normalize the solution under differing numbers of surface spillets (Kolluru et al., 1994). Spreading is stopped when an oil-specific terminal thickness is reached.

1.3.4 Evaporation

The rate of evaporation depends on surface area, thickness, vapor pressure and mass transport coefficient, which in turn are functions of the composition of the oil, wind speed and temperature (Fingas, 1996; 1997; 1998; 1999; Jones, 1997). As oil evaporates its composition changes, affecting its density and viscosity as well as subsequent evaporation. The most volatile hydrocarbons evaporate most rapidly, typically in less than a day and sometimes in under an hour (McAuliffe, 1989). As the oil continues to weather, and particularly if it forms a water-in-oil emulsion, evaporation will be significantly decreased.

The evaporation algorithm in SIMAP is based on accepted evaporation theory, which follows Raoult's Law that each component will evaporate with a rate proportional to the saturation vapor pressure and mole fraction present for that component. The pseudo-component approach (Payne et al., 1984; French et al., 1996a; Jones, 1997; Lehr et al., 2000) is used, such that each component evaporates according to its mean vapor pressure, solubility, and molecular weight (Table 2-3). The mass transfer coefficient is calculated using the methodology of Mackay and Matsugu (1973), as described in French et al. (1996a).

1.3.5 Entrainment

As oil on the water surface is exposed to wind and waves, or if oil moves into a turbulent area of a stream or river, it is entrained (or dispersed) into the water column. Entrainment is a physical process where globules of oil are transported from the water surface into the water column due to breaking waves or other turbulence. It has been observed that entrained oil is broken into droplets of varying sizes. Smaller droplets spread and diffuse in the water column, while larger ones rise back to the surface.

Entrainment by Breaking Surface Wave Action

In open waters, breaking waves created by the action of wind and waves on the water surface are the primary sources of energy for entrainment. Entrainment is strongly dependant on turbulence and is greater in areas of high wave energy (Delvigne and Sweeney, 1988).

Delvigne and Sweeney (1988), using laboratory and flume experimental observations, developed a relationship for entrainment rate and oil droplet size distribution as a function of turbulent energy level and oil viscosity. Entrained droplets in the water column rise according to Stokes law, where velocity is related to the difference in density between the particle and the water, and to the particle diameter. The data and relationships in Delvigne and Sweeney (1988) are used in SIMAP to calculate mass and particle size distribution of droplets entrained. Particle size decreases with higher turbulent energy level and lower oil viscosity. The natural dispersion particle sizes observed by Delvigne and Sweeney (1988) are confirmed by field observations by Lunel (1993a,b).

Use of chemical dispersants (not modelled in the scenarios examined here) decrease the median particle size, increasing the number of droplets in the <70 μm range (Daling et al., 1990; Lunel, 1993a,b). Particle size distributions for dispersed oil are available for several oils from these studies. When dispersant is applied, the model entrains surface oil, creating subsurface droplets in the appropriate size distribution for dispersant use. The median particle size for permanently dispersed droplets is set at 20 microns, the median size observed by Lunel (1993a,b). The fraction of oil permanently dispersed is set by the assumed dispersant efficiency. The IKU/SINTEF studies provide data on the viscosity range where oils may be dispersed chemically. Typically, dispersants are effective up to about 10,000 cP (Aamo et al., 1993; Daling and Brandvik, 1988; 1991; Daling et al., 1997). In the model, oil is dispersed up to 10,000 cp.

Entrained oil is well mixed in (i.e., mixed uniformly throughout) the wave-mixed zone. Vertical mixing is simulated by random placement of particles within the wave-mixed layer each time step. Settling of particles does not occur in water depths where waves reach the bottom (taken as 1.5 times wave height). Wave height is calculated from wind speed, duration and fetch (distance upwind to land), using the algorithms in CERC (1984). Wave height is on the scale of centimetres in small rivers and streams, and near lee shorelines; whereas it may increase to metres in open waters under windy conditions.

1.3.6 Emulsification (Mousse Formation)

The formation of water-in-oil emulsions, or mousse, depends on oil composition and turbulence level. Emulsified oil can contain as much as 80% water in the form of micrometre-sized droplets dispersed within a continuous phase of oil (Daling and Brandvik, 1988; Fingas et al., 1997). Viscosities are typically much higher than that of the parent oil. The incorporation of water also dramatically increases the oil/water mixture volume.

The Mackay and Zagorski (1982) emulsification scheme is implemented in SIMAP for floating oil. Water content increases exponentially, with the rate related to the square of wind speed and previous water incorporation. Viscosity is a function of water content. The change in viscosity feeds back in the model to the entrainment rate.

1.3.7 Dissolution

Dissolution is the process by which soluble hydrocarbons enter the water from a surface slick or from entrained oil droplets. The lower molecular weight hydrocarbons tend to be both more volatile and more soluble than those of higher molecular weight. For surface slicks, since the partial pressures tend to exceed the solubilities of these lower molecular weight compounds, evaporation accounts for a larger portion of the mass than dissolution (McAuliffe, 1989), except perhaps under ice. Dissolution and evaporation are competitive processes. The dissolved component concentration of hydrocarbons in water under a surface slick shows an initial increase followed by a rapid decrease after some hours due to the evaporative loss of components. Most soluble components are also volatile and direct evaporation (volatilization) from the water column depletes their concentrations in the water. Dissolution is particularly important where evaporation is low (dispersed oil droplets and ice-covered surfaces). Dissolution can be significant from entrained droplets because of the lack of atmospheric exposure and because of the higher surface area per unit of volume.

The model developed by Mackay and Leinonen (1977) is used in SIMAP for dissolution from a surface slick. The slick (spillet) is treated as a flat plate, with a mass flux (Hines and Maddox, 1985) related to solubility and temperature. It assumes a well-mixed layer with most of the resistance to mass transfer lying in a hypothetical stagnant region close to the oil. For subsurface oil, dissolution is treated as a mass flux across the surface area of a droplet (treated as a sphere) in a calculation analogous to the Mackay and Leinonen (1977) algorithm. The dissolution algorithm was developed in French et al. (1996a).

1.3.8 Volatilization from the Water column

The procedure outlined by Lyman et al. (1982), based on Henry's Law and mass flux (Hines and Maddox, 1985), is followed in the SIMAP fates model. The volatilization depth for dissolved substances is limited to the maximum of one half the wave height. Wave height is computed from the wind speed and fetch (CERC, 1984). The volatilization algorithm was developed in French et al. (1996a).

1.3.9 Adsorption and Sedimentation

Aromatics dissolved in the water column are carried to the sediments primarily by adsorption to suspended particulates, and subsequent settling. The ratio of adsorbed (C_a) to dissolved (C_{dis}) concentrations is computed from standard equilibrium partitioning theory as

$$C_a / C_{dis} = K_{oc} C_{ss}$$

K_{oc} is a dimensionless partition coefficient and C_{ss} is the concentration of suspended particulate matter (SPM) in the water column expressed as mass of particulate per volume of water. As a default, the model uses a mean value of total suspended solids of 10 mg/l (Kullenberg, 1982); alternatively, suspended sediment concentration is specified as model input.

Sedimentation of oil droplets occurs when the specific gravity of oil increases over that of the surrounding water. Several processes may act on entrained oil and surface slicks to increase density: weathering (evaporation, dissolution and emulsification), adhesion or sorption onto suspended particles or detrital material, and incorporation of sediment into oil during interaction with suspended particulates, bottom sediments, and shorelines. Rates of sedimentation depend on the concentration of suspended particulates and the rates of particulate flux into and out of an area. In areas with high suspended particulate concentrations, rapid dispersal and removal of oil is found due to sorption and adhesion (Payne and McNabb, 1984).

Kirstein et al. (1987) and Payne et al. (1987) used a reaction term to characterize the water column interactions of oil and suspended particulates. The reaction term represents the collision of oil droplets and suspended matter, and both oiled and unoiled particulates are accounted for. The model formulation developed by Kirstein et al. (1987) is used to calculate the volume of oil adhered to particles. In the case where the oil mass is larger than the adhered sediment (i.e., the sediment has been incorporated into the oil) the buoyancy of the oil droplet will control its settling or rise rate. The Stoke's law formulation is used to adjust vertical position of these particles. If the mass of adhered droplets is small relative to the mass of the sediment it has adhered to, the sediment settling velocity will control the fate of the combined particulate.

1.3.10 Degradation

Degradation may occur as the result of photolysis, which is a chemical process energized by ultraviolet light from the sun, and by biological (bacterial) breakdown, termed biodegradation. In the model, degradation occurs on the surface slick, deposited oil on the shore, the entrained oil and aromatics in the water column, and oil in the sediments. A first order decay algorithm is used, with a specified (total) degradation rate for each of surface oil, water column oil and sedimented oil (French et al., 1999).

1.4 Habitat Type

Ecological habitat types (Table 2) are broadly categorized into two zones within SIMAP: shoreline and submerged (or intertidal versus subtidal in estuarine and marine areas, where intertidal habitats are those above spring low water tide level, with subtidal being all water areas below that level). In modelled scenarios, the shoreline habitats may become oiled as surface oil makes contact with these cells. Submerged or subtidal cells are always underwater. Intertidal/shoreline areas may be extensive, such that they are wide enough to be represented by an entire grid cell at the resolution of the grid. These are typically either mud flats or wetlands, and are coded 20 (seaward mudflat), 21 (seaward wetland), 50 (landward mudflat), or 51 (landward wetland). All other intertidal/shoreline habitats are typically much narrower than the size of a grid cell. Thus, these fringing intertidal/shore types (indicated by F in Table 2) have typical (for the region, e.g., French et al., 1996a for estuarine and marine areas) widths associated with them in the model. Boundaries between land and water are fringing habitat types. On the waterside of fringing grid cells, there may be extensive intertidal/shoreline grid cells if the wetlands or mudflats are extensive. Otherwise, subtidal/submerged habitats border the fringing cells.

Table 2. Classification of habitats. seaward (Sw) and landward (Lw) system codes are listed. (fringing types indicated by (F) are only as wide as the intertidal zone or shoreline width where oiling might occur. Others (W = water) are a full grid cell wide and have a fringing type on the land side.)

Habitat Code (Sw,Lw)	Ecological Habitat	F or W
Intertidal / Shore		
1,31	Rocky Shore	F
2,32	Gravel Shore	F
3,33	Sand Beach or Shore	F
4,34	Fringing Mud Flat	F
5,35	Fringing Wetland (Emergent or Forested)	F
6,36	Macroalgal Bed	F

Habitat Code (Sw,Lw)	Ecological Habitat	F or W
7,37	Mollusk Reef	F
8,38	Coral Reef (marine only)	F
Subtidal / Submerged		
9,39	Rock Bottom	W
10,40	Gravel Bottom	W
11,41	Sand Bottom	W
12,42	Silt-mud Bottom	W
13,43	Wetland (submerged areas)	W
14,44	Macroalgal Bed	W
15,45	Mollusk Reef	W
16,46	Coral Reef (marine only)	W
17,47	Submerged Aquatic Vegetation Bed	W
Intertidal / Shore		
18,48	Man-made, Artificial	F
19,49	Ice Edge	F
20,50	Extensive Mud Flat	W
21,51	Extensive Wetland (Emergent or Forested)	W

1.5 References

Aamo, O.M., M. Reed and P. Daling, 1993. A laboratory based weathering model: PC version for coupling to transport models. In Proceedings of the 16th Arctic and Marine Oil Spill Program (AMOP) Technical Seminar, Environmental Protection Service, Emergencies Science Division, Environment Canada, Ottawa, ON, Canada, pp. 617-626.

ASCE Task Committee on Modeling Oil Spills, 1996. State-of-the-art Review of Modeling Transport and Fate of Oil Spills, Water Resources Engineering Division, ASCE, Journal of Hydraulic Engineering 122(11): 594-609.

Coastal Engineering Research Center (CERC), 1984. Shore Protection Manual, Vol. I. Coastal Engineering Research Center, Department of the Army, Waterways Experiment Station, U.S. Army Corps of Engineers, Vicksburg, Mississippi, 1,105p. plus 134p. in appendices.

CSE/ASA/BAT, 1986. Development of a Coastal Oil Spill Smear Model. Phase 1: Analysis of Available and Proposed Models, Prepared for Minerals Management Service by Coastal Science & Engineering, Inc. (CSE) with Applied Science Associates, Inc. (ASA) and Battelle New England Research Laboratory (BAT), 121p.

Daling, P.S. and P.J. Brandvik, 1988. A Study of the Formation and Stability of Water-in-Oil Emulsions. In Proceedings of the 11th Arctic and Marine Oil Spill Program Technical Seminar. Emergencies Science Division, Environment Canada, Ottawa, ON, Canada, pp.153-170.

Daling, P.S., D. Mackay, N. Mackay, and P.J. Brandvik, 1990. Droplet size distributions in chemical dispersion of oil spills: Towards a mathematical model. Oil and Chemical Pollution 7: 173-198.

Daling, P.S. and P.J. Brandvik, 1991. Characterization and prediction of the weathering properties of oils at sea – A manual for the oils investigated in the DIWO project. IKU SINTEF Group report 91.037, DIWO report no. 16 02.0786.00/16/91, 29 May 1991, 140p.

Daling, P.S., O.M. Aamo, A. Lewis, and T. Strom-Kritiansen, 1997. SINTEF/IKU Oil-Weathering Model: Predicting Oil's Properties at Sea. In Proceedings 1997 Oil Spill Conference, Publication No. 4651, American Petroleum Institute, Washington, D.C., pp. 297-307.

Daling, P.S. A.Lewis, S. Ramstad. 1999. The use of colour as a guide to oil film thickness – Main report. SINTEF Report STF66 F99082. 48p., SINTEF, Trondheim, Norway.

Delvigne, G.A.L. and C.E. Sweeney, 1988. Natural Dispersion of Oil. Oil and Chemical Pollution 4: 281-310.

Di Toro, D.M., J.A. McGrath and D.J. Hansen, 2000. Technical basis for narcotic chemicals and polycyclic aromatic hydrocarbon criteria. I. Water and tissue. Environmental Toxicology and Chemistry 19(8): 1951-1970.

Fay, J.A., 1971. Physical processes in the spread of oil on a water surface. In Proceedings, Conference on Prevention and Control of Oil Spills, sponsored by API, EPA, and US Coast Guard, American Petroleum Institute, Washington, D.C., June 15-17, 1971, pp. 463-467.

Fingas, M., 1996. The Evaporation of Crude Oil and Petroleum Products. PhD Dissertation, McGill University, Montreal, Canada, 181p.

Fingas, M., B. Fieldhouse, and J.V. Mullin, 1997. Studies of Water-in-Oil Emulsions: Stability Studies. In Proceedings of 20th Arctic and Marine Oil Spill Program (AMOP) Technical Seminar, Emergencies Science Division, Environment Canada, Ottawa, ON, Canada, pp. 21-42.

Fingas, M., 1997. The Evaporation of Oil Spills: Prediction of Equations Using Distillation Data. In Proceedings of the 20th Arctic and Marine Oil Spill Program (AMOP) Technical Seminar, Emergencies Science Division, Environment Canada, Ottawa, ON, Canada, pp. 1-20.

Fingas, M.F., 1998. Studies on the Evaporation of Crude Oil and Petroleum Products: II. Boundary Layer Regulation. Journal of Hazardous Materials, Vol. 57, pp.41-58.

Fingas, M.F., 1999. The Evaporation of Oil Spills: Development and Implementation of New Prediction Methodology. In Proceedings of the 1999 International Oil Spill Conference, American Petroleum Institute, Washington, D.C., pp. 281-287.

Fingas, M., B. Fieldhouse, and J.V. Mullin, 1997. Studies of Water-in-Oil Emulsions: Stability Studies. In: Proceedings of 20th Arctic and Marine Oil Spill Program (AMOP) Technical Seminar, Emergencies Science Division, Environment Canada, Ottawa, ON, Canada, pp. 21-42.

French, D., M. Reed, K. Jayko, S. Feng, H. Rines, S. Pavignano, T. Isaji, S. Puckett, A. Keller, F. W. French III, D. Gifford, J. McCue, G. Brown, E. MacDonald, J. Quirk, S. Natzke, R. Bishop, M. Welsh, M. Phillips and B.S. Ingram, 1996a. The CERCLA type A natural resource damage assessment model for coastal and marine environments (NRDAM/CME), Technical Documentation, Vol. I - Model Description. Final Report, submitted to the Office of Environmental Policy and Compliance, U.S. Dept. of the Interior, Washington, DC, April, 1996, Contract No. 14-0001-91-C-11.

French, D., M. Reed, S. Feng and S. Pavignano, 1996b. The CERCLA type A natural resource damage assessment model for coastal and marine environments (NRDAM/CME), Technical Documentation, Vol. III - Chemical and Environmental Databases. Final Report, Submitted to the Office of Environmental Policy and Compliance, U.S. Dept. of the Interior, Washington, DC, April, 1996, Contract No. 14-01-0001-91-C-11.

French, D., S. Pavignano, H. Rines, A. Keller, F.W. French III and D. Gifford, 1996c. The CERCLA type A natural resource damage assessment model for coastal and marine environments (NRDAM/CME), Technical Documentation, Vol.IV - Biological Databases. Final Report, Submitted to the Office of Environmental Policy and Compliance, U.S. Dept. of the Interior, Washington, DC, April, 1996, Contract No. 14-01-0001-91-C-11.

French, D.P. and H. Rines, 1997. Validation and use of spill impact modeling for impact assessment. Proceedings, 1997 International Oil Spill Conference, Fort Lauderdale, Florida, American Petroleum Institute Publication No. 4651, Washington, DC, pp-829-834.

French, D.P., H. Rines and P. Masciangioli, 1997. Validation of an Orimulsion spill fates model using observations from field test spills. Proceedings, Twentieth Arctic and Marine Oil Spill Program Technical Seminar, Vancouver, Canada, June 10-13, 1997.

French, D., H. Schuttenberg, and T. Isaji, 1999. Probabilities of Oil Exceeding Thresholds of Concern: Examples from an Evaluation for Florida Power and Light. In Proceedings of the 22nd Arctic and

Marine Oil Spill Program (AMOP) Technical Seminar, June 2-4, 1999, Calgary, Alberta, Environment Canada, pp.243-270.

French McCay, D. and J.R. Payne, 2001. Model of Oil Fate and Water concentrations with and without application of dispersants. In Proceedings of the 24th Arctic and Marine Oil Spill Program (AMOP) Technical Seminar, Emergencies Science Division, Environment Canada, Ottawa, ON, Canada, pp. 601-653.

French McCay, D.P., 2002. Development and Application of an Oil Toxicity and Exposure Model, OilToxEx. Environmental Toxicology and Chemistry 21(10): 2080-2094.

French McCay, D.P., 2003. Development and Application of Damage Assessment Modeling: Example Assessment for the North Cape Oil Spill. Marine Pollution Bulletin, Volume 47, Issues 9-12, September-December 2003, pp. 341-359.

French McCay, D.P., 2004. Oil spill impact modeling: Development and validation. Environmental Toxicology and Chemistry 23(10): 2441-2456.

French McCay, D.P., and J.J. Rowe, 2004. Evaluation of Bird Impacts in Historical Oil Spill Cases Using the SIMAP Oil Spill Model. In Proceedings of the 27th Arctic and Marine Oil Spill Program (AMOP) Technical Seminar, Emergencies Science Division, Environment Canada, Ottawa, ON, Canada, pp. 421-452.

Gundlach, E.R., 1987. Oil Holding Capacities and Removal Coefficients for Different Shoreline Types to Computer Simulate Spills in Coastal Waters. In Proceedings of the 1987 Oil Spill Conference, pp. 451-457.

Hines, A.L. and R.N. Maddox, 1985. Mass Transfer Fundamentals and Application. Prentice-Hall, Inc., Englewood Cliffs, New Jersey, 542p.

Jones, R.K., 1997. A Simplified Pseudo-Component of Oil Evaporation Model. In Proceedings of the 20th Arctic and Marine Oil Spill Program (AMOP) Technical Seminar, Environment Canada, pp. 43-61.

Kirstein, B.E., J.R. Clayton, C. Clary, J.R. Payne, D. McNabb, Jr., G. Fauna and R. Redding, 1987. Integration of Suspended Particulate Matter and Oil Transportation Study. Minerals Management Service, OCS Study MMS87-0083, Anchorage, Alaska, 216p.

Kolluru, V., M.L. Spaulding and E. Anderson, 1994. A three dimensional subsurface oil dispersion model using a particle based approach. In Proceedings of 17th Arctic and Marine Oil Spill Program (AMOP) Technical Seminar, Vancouver, British Columbia, June 8-10, 1994, Emergencies Science Division, Environment Canada, Ottawa, ON, Canada, pp. 867-893.

Kullenberg, G. (ed.), 1982. Pollutant transfer and transport in the sea. Volume I. CRC Press, Boca Raton, Florida. 227 p.

Lehr, W.J., D. Wesley, D. Simecek-Beatty, R. Jones, G. Kachook and J. Lankford, 2000. Algorithm and interface modifications of the NOAA oil spill behavior model. In Proceedings of the 23rd Arctic and

Marine Oil Spill Program (AMOP) Technical Seminar, Vancouver, BC, Environmental Protection Service, Environment Canada, pp. 525-539.

Lunel, T., 1993a. Dispersion: Oil droplet size measurements at sea. In Proceedings of the 16th Arctic Marine Oilspill Program (AMOP) Technical Seminar, Environment Canada, Calgary, Alberta, June 7-9, 1993, pp. 1023-1056.

Lunel, T., 1993b. Dispersion: Oil droplet size measurements at sea. In Proceedings of the 1993 Oil Spill Conference, pp. 794-795.

Lyman, C.J., W.F. Reehl, and D.H. Rosenblatt, 1982. Handbook of Chemical Property Estimation Methods. McGraw-Hill Book Co., New York, 960p.

Mackay, D. and R.M. Matsugu, 1973. Evaporation rates of liquid hydrocarbon spills on land and water. Canadian Journal of Chemical Engineering 51: 434-439.

Mackay, D. and P.J. Leinonen, 1977. Mathematical model of the behavior of oil spills on water with natural and chemical dispersion. Prepared for Fisheries and Environment Canada. Economic and Technical Review Report EPS-3-EC-77-19, 39p.

Mackay, D., S. Paterson and K. Trudel, 1980. A mathematical model of oil spill behavior. Department of Chemical and Applied Chemistry, University of Toronto, Canada, 39p.

Mackay, D., and W. Zagorski, 1982. Water-In-Oil Emulsions. Environment Canada Manuscript Report EE-34, Ottawa, Ontario, Canada, 93p.

Mackay, D, W.Y. Shiu, K. Hossain, W. Stiver, D. McCurdy and S. Peterson, 1982. Development and calibration of an oil spill behavior model. Report No. CG-D-27-83, U.S. Coast Guard, Research and Development Center, Groton, Connecticut, 83p.

Mackay, D., W.Y. Shiu, and K.C. Ma, 1992. Illustrated Handbook of Physical-Chemical Properties and Environmental Fate for Organic Chemicals, Vol. I-IV. Lewis Publishers, Inc, Chelsea, Michigan.

McAuliffe, C.D., 1987. Organism exposure to volatile/soluble hydrocarbons from crude oil spills –a field and laboratory comparison. Proceedings of the 1987 Oil Spill Conference. Washington, D.C.: API. pp. 275-288.

McAuliffe, C.D., 1989. The Weathering of Volatile Hydrocarbons from Crude Oil Slicks on Water. In Proceedings of the 1989 Oil Spill Conference, San Antonio, Texas, American Petroleum Institute, Washington, D.C., pp. 357-364.

Okubo, A. and R.V. Ozmidov, 1970. Empirical dependence of the coefficient of horizontal turbulent diffusion in the ocean on the scale of the phenomenon in question. Atmospheric and Ocean Physics 6(5):534-536.

Okubo, A., 1971. Oceanic diffusion diagrams. Deep-Sea Research 8:789-802.

Payne, J.R. and G.D. McNabb Jr., 1984. Weathering of Petroleum in the Marine Environment. Marine Technology Society Journal 18(3):24-42.

Payne, J.R., B.E. Kirstein, G.D. McNabb, Jr., J.L. Lambach, R. Redding R.E. Jordan, W. Hom, C. deOliveria, G.S. Smith, D.M. Baxter, and R. Gaegel, 1984. Multivariate analysis of petroleum weathering in the marine environment – sub Arctic. Environmental Assessment of the Alaskan Continental Shelf, OCEAP, Final Report of Principal Investigators, Vol. 21 and 22, Feb. 1984, 690p.

Payne, J.R., B.E. Kirstein, J.R. Clayton, Jr., C. Clary, R. Redding, G.D. McNabb, Jr., and G. Farmer, 1987. Integration of suspended particulate matter and oil transportation study. Final Report. Minerals Management Service, Environmental Studies Branch, Anchorage, AK. Contract No. 14-12-0001-30146, 216 p.

Reed, M. and E. Gundlach, 1989. Hindcast of the *Amoco Cadiz* event with a coastal zone oil spill model. Oil and Chemical Pollution. Vol. 5. Iss. 6. Pp. 451-476.

Stiver, W. and D. Mackay, 1984. Evaporation rate of oil spills of hydrocarbons and petroleum mixtures. Environmental Science and Technology 18: 834-840.

Thorpe, S.A., 1984. On the Determination of K in the Near Surface Ocean from Acoustic Measurements of Bubbles. Journal of Physical Oceanography 14: 855-863.

Youssef, M. and M.L. Spaulding, 1993. Drift current under the action of wind waves, Proceedings of the 16th Arctic and Marine Oil Spill Program Technical Seminar, Calgary, Alberta, Canada, pp. 587-615.

1.6 References – SIMAP Example Applications and Validations

Copies of these papers can be provided by sending a request to matt.horn@rpsgroup.com and requesting one or more specific papers.

French, D.P., and H. Rines, 1997. Validation and use of spill impact modeling for impact assessment. In Proceedings, 1997 International Oil Spill Conference, Fort Lauderdale, Florida, American Petroleum Institute Publication No. 4651, Washington, DC, pp-829-834.

French, D. P., 1998a. Estimate of Injuries to Marine Communities Resulting from the North Cape Oil Spill Based on Modeling of Fates and Effects. Report to US Department of

14 Commerce, National Oceanic and Atmospheric Administration (NOAA), Damage Assessment Center, Silver Spring, MD, January 1998.

French, D. P., 1998b. Updated Estimate of Injuries to Marine Communities Resulting from the North Cape Oil Spill Based on Modeling of Fates and Effects. Report to US Department of Commerce, National Oceanic and Atmospheric Administration (NOAA), Damage Assessment Center, Silver Spring, MD, December 1998.

French, D.P., 1998c. Modeling the Impacts of the North Cape, p. 387-430.In Proceedings, 21st Arctic and Marine Oilspill Program (AMOP) Technical Seminar, June 10-12, 1998, West Edmonton Mall Hotel Edmonton, Alberta, Canada, Emergencies Science Division, Environment Canada, Ottawa, ON, Canada.

French McCay, D. and James R. Payne, 2001.Model of Oil Fate and Water concentrations with and with out application of dispersants. In Proceedings of the 2001 24th Arctic and Marine Oil spill Program (AMOP) Technical Seminar, June 12-14, 2001, Environment Canada, pp.611-645.

French, D. P., Jones, M. A., and Coakley, L., 2001. Use of Oil Spill Modeling for Contingency Planning and Impact Assessment: Application for Florida Power and Light. In Proceedings of the 2001 International Oil Spill Conference & Exposition, American Petroleum Institute, March 26-29, 2001, Tampa, Florida.

French, D.P. and H. Schuttenberg, 1999.Evaluation of net environmental benefit using fates and effects modeling. Paper ID #321. In Proceedings, 1999 International Oil Spill Conference, American Petroleum Institute.

French McCay, D. 2002. Modeling Evaluation of Water Concentrations and Impacts Resulting from Oil Spills With and Without the Application of Dispersants. International Marine Environmental Seminar 2001, Journal of Marine Systems, Special Issue 2002.

French McCay, D., N. Whittier, S. Sankaranarayanan, J. Jennings, and D. S. Etkin, 2002.Modeling Fates and Impacts for Bio-Economic Analysis of Hypothetical Oil Spill Scenarios in San Francisco Bay. In Proceedings of the Twenty Fifth Arctic and Marine Oil Spill Program (AMOP) Technical Seminar, Environment Canada, Calgary, AB, Canada, 2002, p. 1051-1074.

French McCay, D., N. Whittier, T. Isaji, and W.Saunders, 2003. Assessment of the Potential Impacts of Oil Spills in the James River, Virginia. In Proceedings of the 26th Arctic and Marine Oil Spill Program (AMOP) Technical Seminar, Emergencies Science Division, Environment Canada, Ottawa, ON, Canada, p. 857-878.

French McCay, D., N. Whittier, S. Sankaranarayanan, J. Jennings, and D. S. Etkin, 2003.Estimation of Potential Impacts and Natural Resource Damages of Oil. J. Hazardous Materials (in press).

French McCay, D. and N. Whittier, 2003.Modeling Assessment of Potential Fates and Exposure for Orimulsion and Heavy Fuel Oil Spills. In: Proceedings, International Oil Spill Conference, April 2003, Paper 157, American Petroleum Institute, Washington, DC.

French McCay, D.P., 2003. Development and Application of Damage Assessment Modeling: Example Assessment for the North Cape Oil Spill. Marine Pollution Bulletin, Volume 47, Issues 9-12, September-December 2003, pp. 341-359.

French McCay, D.P., and J.J. Rowe, 2004.Evaluation of Bird Impacts in Historical Oil Spill Cases Using the SIMAP Oil Spill Model. In Proceedings of the 27th Arctic and Marine Oil Spill Program (AMOP) Technical Seminar, Emergencies Science Division, Environment Canada, Ottawa, ON, Canada, pp. 421-452.

French-McCay, D.P., J.J. Rowe, N. Whittier, S. Sankaranarayanan, D. S. Etkin, and L. Pilkey- Jarvis, 2005. Evaluation of the Consequences of Various Response Options Using Modeling of Fate, Effects and NRDA Costs of Oil Spills into Washington Waters. In: Proceedings, International Oil Spill Conference, May 2005, Paper 395, American Petroleum Institute, Washington, DC.

French-McCay, D.P., N. Whittier, C. Dalton, J.J. Rowe, and S. Sankaranarayanan, 2005.Modeling fates and impacts of hypothetical oil spills in Delaware, Florida, Texas, California, and Alaska waters, varying response options including use of dispersants. In: Proceedings, International Oil Spill Conference, May 2005, Paper 399, American Petroleum Institute, Washington, DC.

French McCay, D., N. Whittier, J.J. Rowe, S. Sankaranarayanan and H.-S.Kim, 2005. Use of Probabilistic Trajectory and Impact Modeling to Assess Consequences of Oil Spills with Various Response Strategies. In Proceedings of the 28th Arctic and Marine Oil Spill Program (AMOP) Technical Seminar, Emergencies Science Division, Environment Canada, Ottawa, ON, Canada, pp. 253-271, 2005.

French-McCay, D.P., M. Horn, Z. Li, K. Jayko, M. Spaulding, D. Crowley, and D. Mendelsohn. 2017. Modeling Distribution, Fate, and Concentrations of Deepwater Horizon Oil in Subsurface Waters of the Gulf of Mexico. In: S.A. Stout and Z. Wang (eds.) Case Studies in Oil Spill Environmental Forensics. Elsevier.

2 OILMAP Deep Model Description

OILMAP Deep was used to characterize the near field blowout conditions for use in the SIMAP model, which characterized the far field effects. OILMAP Deep contains two sub-models, a plume model and a droplet size model. The plume model predicts the evolution of plume position, geometry, centerline velocity, and oil and gas concentrations until the plume either surfaces or reaches a terminal height at which point the plume is trapped (Figure 3). The droplet model predicts the size and volume (mass) distribution of the oil droplets. Provided below is an overview of blowout theory and modeling implementation.

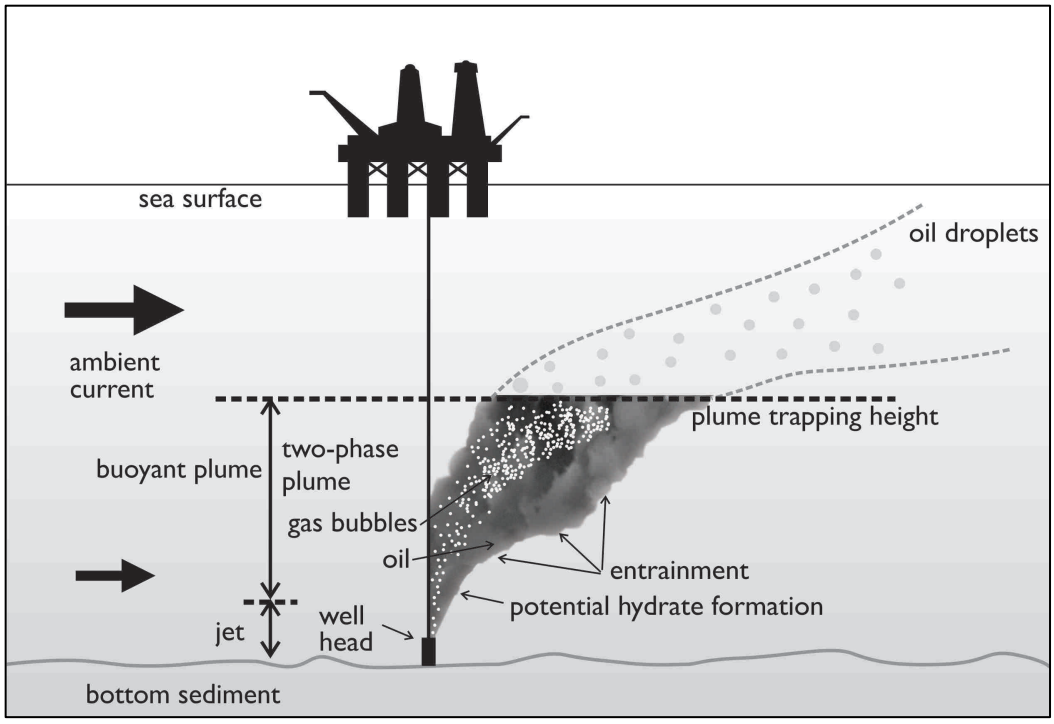

Figure 3. Modelled processes for a subsea blowout in OILMAP Deep.

2.1 Blowout Model Theory

RPS ASA's oil blowout model is based on the work of McDougall (gas plume model, 1978), Fanneløp and Sjøen (1980a, plume/free surface interaction), Spaulding (1982, oil concentration model), Kolluru, (1994, World Oil Spill Model implementation), Spaulding et.al. (2000, hydrate formation) and Zheng et.al. (2002, 2003, gas dissolution). A simplified integral jet theory is employed for the vertical as well as for the horizontal motions of the gas-oil plume. The necessary model parameters defining the rates of entrainment and spreading of the jet are obtained from laboratory studies (Fanneløp and Sjøen 1980a). The gas plume analysis is described in McDougall (1978), Spaulding (1982), and Fanneløp and Sjøen

(1980a). The hydrate formation and dissociation is formulated based on a unique equilibrium kinetics model developed by R. Bishnoi and colleagues at the University of Calgary. A brief description of the governing equations used in RPS ASA's blowout model and the solution methodology are described in Spaulding et al., 2000. The core components of this model are conservation of water mass, conservation of oil mass, conservation of momentum, and conservation of buoyancy.

Oil droplet size distribution calculations are based on the methodology presented by Yapa and Zheng (2001a&b) and Chen and Yapa (2007), which uses a maximum diameter calculation and the associated volumetric droplet size distribution. The maximum diameter can is determined using Hinze (1955) and coefficients consistent with Chen and Yapa (2007). The droplet size distribution is defined using a Rosin-Rammler (1933) function.

2.2 Blowout Model Implementation

The results of the near-field blowout model provide information to the far field fates model about the plume (the three-dimensional extent of the mixture of gas/oil/water) and a characterization of the initial dispersion/mixing of the oil discharged during the blowout. Key factors in this analysis are the volume flux of oil and gas, gas to oil ratio (GOR), depth, exit flow velocity and environmental water column conditions (the profile of water temperature and density), which affect both the trap height and the potential for hydrate formation. Other factors such as duration of the blowout and ambient currents are also included but are less important.

The OILMAP Deep blowout model implementation is done in two parts; the first is the plume model described in the previous section, based on the McDougall bubble plume model; the second is the oil droplet size distribution and volume fraction calculation. While they are based on the same scenario blowout specifications (e.g. oil type and flow rate, gas oil ratio and depth), the model predictions are treated separately and do not interact. The two parts of the model predictions only come together at the collapse of the near field plume, at the trap height, where the depth and droplet distribution predictions are used for initialization of the far field particle model simulation.

The blowout plume model solves equations for conservation of water mass, momentum, buoyancy, and gas mass as described in Section 2.1 of the OILMAP Deep Technical Documentation, using integral plume theory. An additional equation for the conservation of oil at the plume centerline is also solved.

The plume model prediction is defined externally by a small set of parameters including:

- Blowout release depth
- Oil discharge rate
- Oil density
- Gas: oil ratio (GOR) at the surface
- Atmospheric pressure
- Ambient seawater density profile
- Plume spreading coefficient

- Entrainment parameter (α)
- Slip velocity of gas bubbles in the oil plume
- Ambient current velocity
- Water column profile of temperature and density

The blowout plume models the evolution of the plume within the water column, solving for the position, radius, velocity and oil and gas concentrations along the centerline. The blowout droplet model solves for the distribution of mass within droplet sizes associated with the turbulence of the release. Typically, the near-field model is on the timescale of seconds and length scale of hundreds of meters, where the far-field model is on the scales of hours/days and kilometers. The details of the near field modelling that are passed along to the far field model include the distribution of the release mass in different droplet sizes at the appropriate initial position in the water column.

2.3 References

Chen, F.H. and P.D. Yapa. 2007. Estimating the Oil Droplet Size Distributions in Deepwater Oil Spills. Journal of Hydraulic Engineering, Vol. 133, No. 2, pp. 197-207.

Fanneløp, T.K. and K. Sjoen , 1980a. Hydrodynamics of underwater blowouts, AIAA 8th Aerospace Sciences Meeting, January 14-16, Pasadena, California, AIAA paper, pp. 80- 0219.

Fanneløp, T. K. and K. Sjoen, 1980b. Hydrodynamics of underwater blowouts, Norwegian Maritime Research, No. 4, pp. 17-33.

Hinze, J. O. 1955 Fundamentals of the hydrodynamics mechanisms of splitting in dispersion process. AIChE J. 1, 289–295.

Kolluru, V., M.L. Spaulding and E. Anderson, 1994. A three dimensional subsurface oil dispersion model using a particle based approach. In Proceedings of 17th Arctic and Marine Oil Spill Program (AMOP) Technical Seminar, Vancouver, British Columbia, June 8-10, 1994, Emergencies Science Division, Environment Canada, Ottawa, ON, Canada, pp. 867-893.

McDougall, T.J., 1978. Bubble plumes in stratified environments, Journal of Fluid Mechanics, Vol. 85, Part 4, pp. 655-672.

Rosin, P. and E. Rammler, 1933. The Laws Governing the Fineness of Powdered Coal, Journal of the Institute of Fuel 7: 29–36Seo, I.W. and K.O. Baek, 2004. Estimation of the Longitudinal Dispersion Coefficient Using the Velocity Profile in Natural Streams. Journal of Hydraulic Engineering. March 2004.

Spaulding, M.L., 1982. User's manual for a simple gas blowout plume model, Continental Shelf Institute, Trondheim, Norway.

Spaulding, M.L., 1984. A vertically averaged circulation model using boundary-fitted coordinates. Journal of Physical Oceanography 14: 973-982.

Spaulding, M.L., P.R. Bishnoi, E. Anderson, and T. Isaji, 2000, An Integrated Model for Prediction of Oil Transport from a Deep Water Blowout.

Yapa, P. D., Zheng, L., and Chen, F. H. 2001a. A model for deepwater oil/gas blowouts. Mar. Pollution Bull., 43, 234–241.

Yapa, P. D., Zheng, L., and Chen, F. H. 2001b. Clarkson deepwater oil & gas ~CDOG model. Rep. No. 01–10, Dept. of Civil and Environmental Engineering, Clarkson Univ., Potsdam, N.Y.

Zheng, L. and Yapa, P.D., 2002. Modelling Gas Dissolution in Deepwater Oil/Gas Spills, Journal of Marine Systems, Elsevier, the Netherlands, March, 299-309

Zheng, L., Yapa, P.D. and Chen, F.H., 2003. A Model for Simulating Deepwater Oil and Gas Blowouts - Part I: Theory and Model Formulation, Journal of Hydraulic Research, IAHR, August, Vol. 41(4), 339-351

Trajectory Modelling in Support of the Bay du Nord Development Project
Appendix B: Modeling Oil Interactions in Ice

Prepared for: Equinor Canada Ltd.

Project Number:
2018-P-22390

Version:
Final Report

Date Submitted:
06/23/2020

Project Manager
Matthew Horn, Ph.D.

RPS
55 Village Square Dr.
South Kingstown, RI USA
02879-8248

Release	File Name	Date Submitted	Notes
Revised Final	Equinor – RPS Technical Report_20200623_AppendixA.docx	06/23/2020	RPS final version of Appendix A
Revised Final	Equinor – RPS Technical Report_20190206_AppendixA.docx	02/06/2019	RPS final version of Appendix A
Revised Final	Equinor – RPS Technical Report_20181130_AppendixA.docx	11/30/2018	RPS final version of Appendix A
Final	Equinor – RPS Technical Report_20181019_AppendixB.docx	10/19/2018	RPS Final version of Appendix B following senior technical review

Summary

This Appendix B is provided as a reference to RPS Technical Report: Trajectory Modelling in Support of the Equinor Bay du Nord Development Project. Appendix B provides a detailed description of modeling oil interactions in ice.

Table of Contents

List of Figures

1 Introduction

Oil interactions with mobile sea ice or immobile landfast ice, or the ice that is attached to or grounded on shore or land, involve several processes that affect transport and fate of the oil. If oil is released at or above the water surface, it may spill into water and/or onto the surface of the ice. Oil deposited on ice may absorb into surface snow, run off and become trapped between cracks or in open water fields between floes, and/or become encapsulated in the ice. Oil released into and under water may become trapped under the ice in ridges and keels, or build up along and become trapped in sea or landfast ice edges (Figure 1; Drozdowski et al., 2011). Many of these interactions and processes are at a finer scale than can be captured in oil spill models using inputs from large scale meteorological, hydrodynamic and coupled ocean-ice models. However, the influence of ice on net transport and fate processes is simulated by considering potential reduction in surface area of the oil and the water in contact with the atmosphere, which changes the wave environment, spreading, movements, volatilization, and mixing.

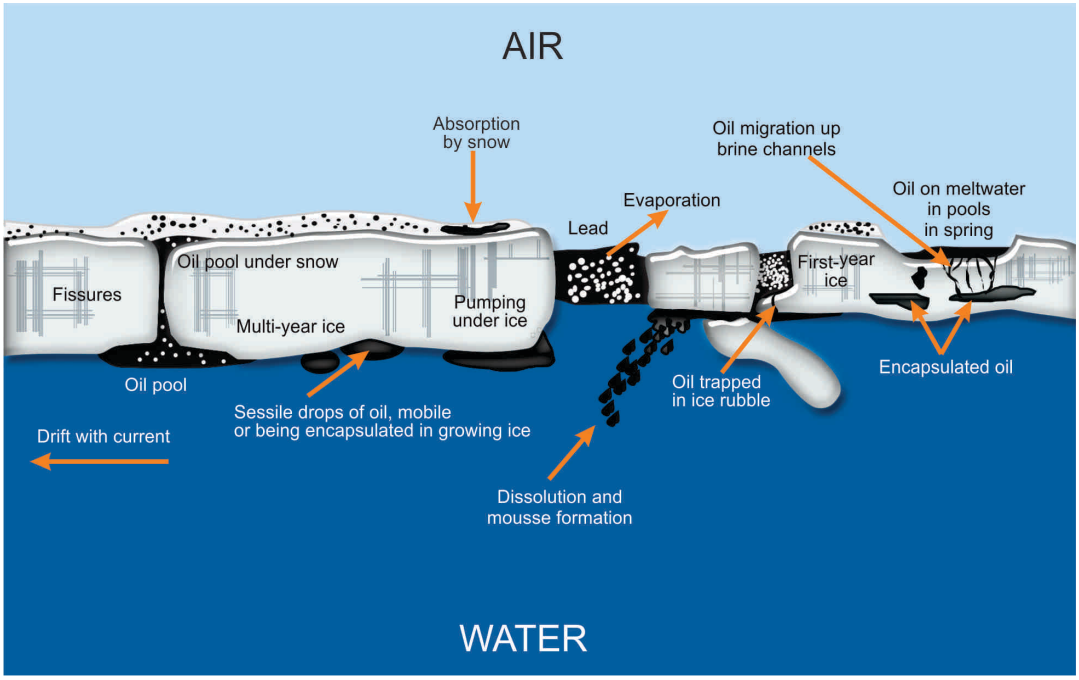

Figure 1. General Schematic Showing Dynamics and Characteristics of Sea Ice and Oil Interaction at the Sea Surface (Source: Original Figure by Alan A. Allen)

2 Oil Transport in Sea Ice

When oil interacts with mobile sea ice, some fraction of that oil will become contained (either on top, in, or underneath the ice) and will then travel with the ice floe (Drozdowski et al., 2011). Sea ice fields can drift rapidly and over great distances in the Arctic (Peterson et al., 2008). The fraction of oil moving with the ice verses in open water depends on conditions and specifics of the release. In some cases, all of the oil becomes completely frozen in the ice and remains there until it melts. This scenario is readily modeled (i.e., 100% of oil drifts with ice). However, in most cases since sea ice can be patchy, only partial amounts may become either encapsulated or trapped (e.g., between ice fragments or under ice sheet in small cavities) (Drozdowski et al., 2011), depending on ice coverage, subsurface roughness, winds and currents, and ice formation/melting dynamics.

To simplify the problem, the ice coverage or concentration information provided by ice data or an ice model can be used as an indicator of whether oil follows the surface currents or the ice currents. Ice coverage information available in coupled hydrodynamics and ice models typically is based on or calibrated to remotely sensed satellite data. A rule of thumb followed by past modeling studies is oil will generally drift with ice when ice coverage is greater than 30% (Drozdowski et al., 2011; Venkatesh et al., 1990). For more description of the ice coverage information and ice currents utilized in this modeling study refer to Appendix D.

When a coupled ocean-ice model is available and can provide water currents and ice velocities, the SIMAP^{TM} model uses the ice coverage data to determine whether floating (or ice-trapped) oil moves with the surface water currents or the ice. If the ice coverage is <30%, the oil is assumed not to be trapped and moves with surface water currents. If ice coverage exceeds this threshold, the ice is assumed to have ample spatial coverage to trap the oil in it or between floes, and oil is transported along with the ice using the ice velocities from the ocean-ice model.

In areas and at times where ice cover <30%, floating oil is transported with surface water currents and a wind drift algorithm to account for wind-induced drift current not resolved by the hydrodynamic model plus Stokes drift caused by wave motions. Wind drift is predicted in SIMAP based on the modeling analysis of Stokes drift and Ekman flow by Youssef (1993) and Youssef and Spaulding (1993, 1994). According to this algorithm, at moderate wind speeds, floating oil drifts 20° to the right of downwind at about 3.5% of wind speed. Alternatively, a constant drift speed percentage and angle may be used in simulations; however, the modeled drift is used in the examples herein. In areas where ice exceeds 30%, and an ice drift model provides transport velocities, the ice drift model has accounted for wind drift, and so no additional wind drift is added in SIMAP.

To simulate oil transport in this study, the SIMAP model used the ice coverage variable, and both the regular water currents and the ice currents or ice velocities available in the hydrodynamics and ice model TOPAZ4 (Appendix D).

3 Oil Transport and Interaction with Landfast Ice

Immobile or fixed landfast ice which seasonally extends out from the coast may act as a natural barrier where oil collects. The ice edge is complex with ridges, keels, cracks, and crevices where oil can become trapped. During landfast ice melt, oil that has been stored along the edge may either release back into open water, or may retreat back with the ice towards the coast (Drozdowski et al., 2011).

In the model, when oil encounters landfast ice at the surface of the ocean it is assumed to trap along the ice edge and remain immobile until ice retreats. When landfast ice is no longer present at trapped oil's location, the oil is released back into the water as floating oil. In areas deep enough for landfast ice to have subsurface open channels (i.e., where the ice sheet may not extend completely to the seabed in all areas), entrained oil is allowed to circulate underneath the surface ice using subsurface current data for transport. The thickness of landfast ice is typically about 2 m in the Beaufort Sea; thus, in deeper waters subsurface oil spillets continue to move with currents, whereas in shallower areas, subsurface oil spillets remain stationary for the time where landfast ice is present. Monthly representations of the landfast edge along the entire coast (capturing average growth and retreat patterns) were prepared as data inputs, as described in Section C.4.

4 Effects of Ice on Oil Fates and Behavior Process

The presence of ice can shelter oil from the wind and waves (Drozdowski et al., 2011). Thus, weathering processes such as evaporation and emulsification, and behavior s such as spreading and entrainment are slowed (Spaulding, 1988). Field data show evaporation, dispersion, and emulsification significantly slowed in ice leads. Wave-damping, the limitations on spreading dictated by the presence of sea ice, and temperature appear to be the primary factors governing observed spreading and weathering rates (Sørstrøm et al., 2010).

As with transport, the ice coverage or concentration variable provided in the ice model is used as an index to control oil weathering and behavior processes (Table 1). Oil behaves as it would in open water in <30% ice coverage. Ice coverage exceeding 80% is assumed fast ice and effectively continuous ice cover. Evaporation and volatilization of oil under/in ice, as well as spreading, emulsification, and entrainment into the surface water are zeroed in fast ice. Oil spilled on top of fast ice is allowed to evaporate, but does not spread from the initial condition of the release. Degradation of subsurface and

ice-bound oil occurs during all ice conditions, at rates occurring at the location (i.e., floating versus subsurface) without ice present. Dissolution of soluble aromatics proceeds for subsurface oil and oil under ice using the normal open-water algorithm (French McCay, 2004).

In ice coverage between 30% and 80%, a linear reduction in wind speed from the open-water value (used in <30% ice) to zero in fast ice (>80% ice coverage) is applied to simulate shielding from wind effects. This reduces the evaporation, volatilization, emulsification, and entrainment rates due to reduced wind and wave energy. Terminal thickness of oil is increased in proportion to ice coverage in this range (i.e., oil is thickest at >80% ice coverage).

Table 1. Percent Ice Coverage Thresholds for Oil Fates and Behavior Processes Applied in the SIMAP Model

Ice Cover (Percent)	Advection	Evaporation & Emulsification	Entrainment	Spreading
0 - 30 (Drift Ice)	Surface oil moves as in open water	As in open water	As in open water	As in open water
30 - 80 (Ice Patches and Leads)	Surface oil moves with the ice	Linear reduction with ice cover (i.e., none at 80% ice cover)	Linear reduction with ice cover (i.e., none at 80% ice cover)	Terminal thickness increased in proportion to ice coverage
80 - 100 (Pack Ice)	Surface oil moves with the ice	None	None	None

Assumptions applied to fates and behavior processes are not well quantified by field experiments or other studies. In addition, the coupled ocean-ice models available to date do not resolve the details of leads, fractures, and ice roughness. The applied thresholds, or the discrete bands of 0 to 30, 30 to 80, and 80 to 100%, may not reflect the fate of oil in real ice cover at fine scales.

5 Landfast Ice for Arctic

Numerous general definitions of landfast ice can be found in the literature (see review in Eicken et al., 2006). Barry et al. (1979) provides a clear list of criteria to distinguish landfast ice from other forms of sea ice: "(i) the ice remains relatively immobile near the shore for a specified time interval; (ii) the ice extends from the coast as a continuous sheet; (iii) the ice is grounded or forms a continuous sheet which is bounded at the seaward edge by an intermittent or nearly continuous zone of grounded ridges." Though this definition thoroughly describes the attributes of landfast ice, for the purposes of this modelling study a more concrete definition of landfast was required. In the interest of accurately and

consistently identifying landfast ice, Eicken et al. (2006) define landfast ice as sea ice contiguous with the shoreline and lacking motion detectable in satellite imagery for approximately 20 days. Using this definition, Mahoney et al. (2012) quantified the coverage of landfast ice along the Alaskan Arctic coast.

A BOEM study (Mahoney et al., 2012) quantified the extent of landfast ice along the Arctic coast of Alaska including the Chukchi and Beaufort Seas. Publically available shapefiles were extracted from the project website (http://boemre-new.gina.alaska.edu/beaufort-sea/landfast-summary). Monthly averaged means (1996-2008) were utilized as baseline data for the Arctic landfast ice coverage.

Landfast ice coverage was available for more eastern portions (east of the Mackenzie River delta) of the modelling zone through the National Snow and Ice Data Center (NSIDC) (Konig Beatty, 2012). Monthly data from the years 1991 through 1998 were composited into mean monthly landfast ice coverage. This dataset included ice concentration percentages for each raster cell. Cells with a concentration of greater than 15% were considered to have landfast ice. This concentration level most strongly corresponded with the higher resolution shapefile data available through BOEM (Mahoney et al., 2012). These mean raster datasets were converted into shapefile extents.

These two datasets (BOEM and NSIDC) were then merged to create continuous landfast ice coverage (monthly average) for the entire area of interest. The BOEM dataset (1996-2008) provided higher resolution and more recent years than the NSIDC dataset (1991-1998). Therefore, the BOEM dataset served as the reference dataset for merging. Figure 2, Figure **3** and Figure 4 show the composited monthly average landfast ice coverage used in this modeling study.

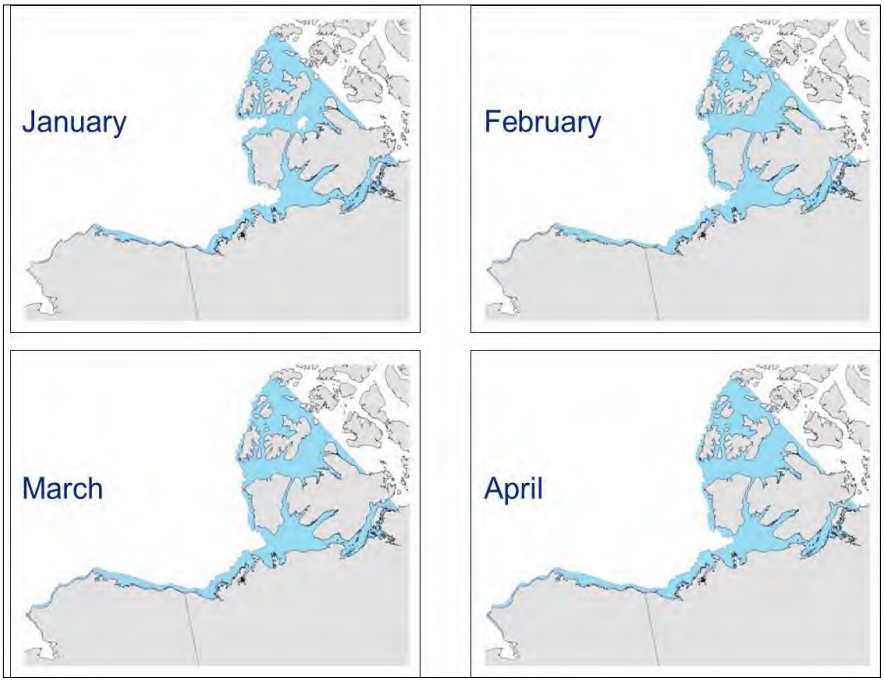

Figure 2. U.S. Chukchi and U.S/Canada Beaufort January-April Monthly Average Landfast Ice Coverage

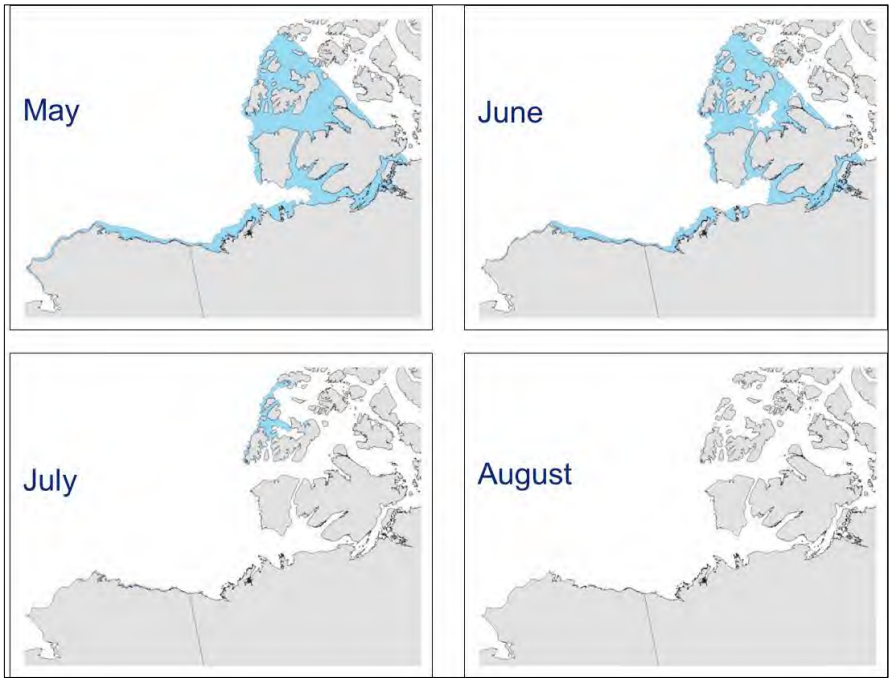

Figure 3. **U.S. Chukchi and U.S/Canada Beaufort May-August Monthly Average Landfast Ice Coverage**

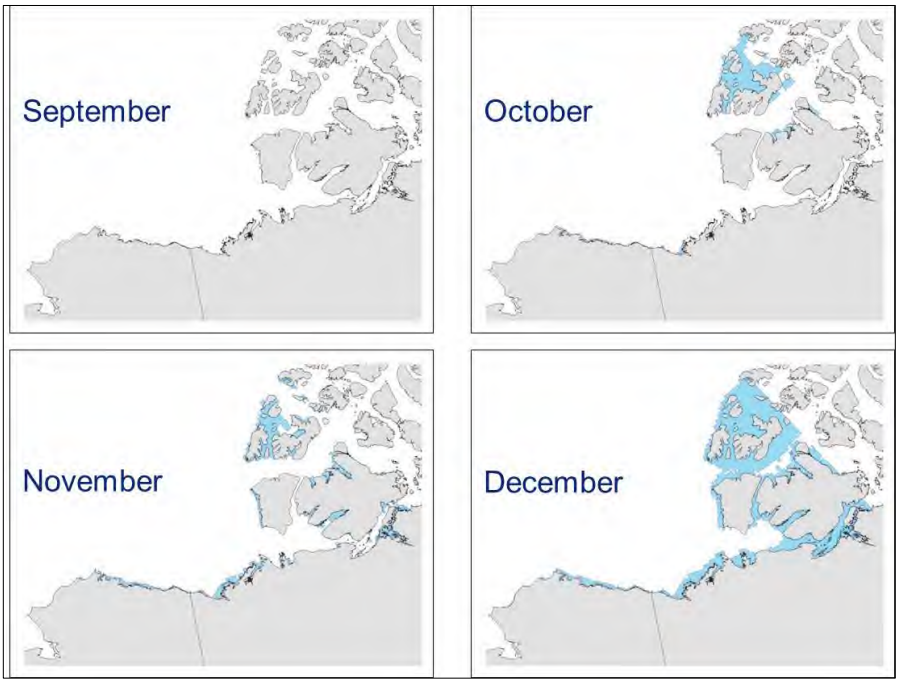

Figure 4. U.S. Chukchi and U.S/Canada Beaufort September-December Monthly Average Landfast Ice Coverage

6 References

Barry, R.G., Moritz, R.E., and Rogers, J.C., (1979). The fast ice regimes of the Beaufort and Chukchi Sea coasts, Alaska. *Cold Regions Science and Technology* (1) 129-152.

Drozdowski, A., Nudds, S., Hannah, C. G., Niu, H., Peterson, I., and Perrie, W. 2011. Review of Oil Spill Trajectory Modelling in the Presence of Ice. Can. Tech. Rep. Hydrogr. Ocean Sci. 274: vi + 84 pp.

Eicken, H., Shapiro, L.H., Gens, R., Meyer, F., Heninrichs, T., Mahoney, A.R., Gaylord, A., and P. W. Cotter 2006. Mapping and Characterization of Recurring Spring Leads and Landfast Ice in the Beaufort and Chukchi Seas. U.S. Department of the Interior, Minerals Management Service (MMS), Alaska Outer Continental Shelf Region, Anchorage, AK. Final Report, OCS Study MMS 2005-068.

French McCay, D.P., 2004. Oil spill impact modeling: development and validation. *Environmental Toxicology and Chemistry* 23(10): 2441-2456.

Konig Beatty, C. S. 2012. Arctic Landfast Sea Ice 1953-1998. Boulder, Colorado USA: National Snow and Ice Data Center. http://dx.doi.org/10.7265/N5ZW1HV4.

Mahoney, A.R., H. Eicken, L.H. Shapiro, R. Gens, T. Heinrichs, F. Meyer, and A.G. Gaylord. 2012. Mapping and Characterization of Recurring Spring Leads and Landfast Ice in the Beaufort and Chukchi Seas. USDOI, BOEM OCS Study 2012-0069. Anchorage, AK: USDOI, BOEM. 154 pp.

Peterson, I.K., Prinsenberg, S., and Holladay, J.S. 2008. Observations of sea ice thickness, surface roughness and ice motion in Amundsen Gulf. *Journal of Geophysical Research* (113) doi: 10.1029/2007JC004456.

Sørstrøm, S.E., Brandvik, P.J., Buist, I., Daling, P., Dickins, D., Faksness, L.G., Potter, S., Fritt-Rasmussen, J., Singsaas, I., 2010. Joint industry program on oil contingency for Arctic and ice-covered waters. Summary report. SINTEF A14181, ISBN-No. 978-82-14-04759-2.

Spaulding, M.L. 1988. A state-of-the-art review of oil spill trajectory and fate modelling. *Oil and Chemical Pollution (*4): 39-55.

Venkatesh, S., H. El-Tahan, G. Comfort, and Abdelnour, R. 1990. Modelling the Behavior of Oil Spills in Ice-Infested Waters. *Atmosphere-Ocean*. Canadian Meteorological and Oceanographic Society (28:3) 303-329.

Youssef, M. 1993. The behavior of the near ocean surface under the combined action of waves and currents in shallow water. PhD Dissertation, Department of Ocean Engineering, University of Rhode Island, Narragansett, RI.

Youssef, M. and Spaulding, M. L. 1993. Drift current under the action of wind waves, in *Proceedings of the 16th Arctic and Marine Oil Spill Program Technical Seminar*, Calgary, Alberta, Canada, 587-615.

Youssef, M. and Spaulding, M.L. 1994. Drift Current under the Combined Action of Wind and Waves in Shallow Water, in *Proceedings of the 17th AMOP Technical Seminar*, Vancouver, British Columbia, 767-784.